UNIVERSITY OF SOUTHAMPTON

Factors Controlling the Mobility of Shingle Beaches, with Particular Reference to the North Kent Coast

Stephen M McFarland

Thesis submitted to the University of Southampton for the Degree of Doctor of Philosophy in the Department of Oceanography

September 1999

University of Southampton

ABSTRACT

FACULTY OF SCIENCE
OCEANOGRAPHY

Doctor of Philosophy

Factors Controlling the Mobility of Shingle Beaches,
With Particular Reference to the North Kent Coast.
by Stephen M McFarland

Despite their scarcity on a global scale, shingle beaches are a common feature of the coastline of the UK, in particular southern England. Shingle beaches have the ability to dissipate large amounts of wave energy over short distances. As a result of this ability, shingle beaches have become a popular 'soft' engineering option for providing protection to coastal regions from the effects of sea flooding and erosion.

Shingle beaches are mobile features and, as a result, are subjected to transport under the action of waves and currents. Whilst this mobility allows shingle beaches to respond rapidly to changing environmental conditions, it often also results in localised erosion. This leads to the lowering of beach levels and a subsequent reduction in the level of protection afforded to the shoreline.

Numerical modelling techniques have been used in conjunction with archived wind, water level, wave and beach profile data to assess the factors which influence the mobility and stability of the shingle beaches on the coastline of north Kent in the southeast of England.

Shingle beaches which become eroded are commonly replenished using offshore gravel deposits. Frequently, it has been found that the replenishment material contains a higher percentage of fine-grained material than occurred on the natural shingle beach. These replenished beaches are more reflective than their natural counterparts; this has important implications for the estimated life expectancy of replenishment schemes and for the performance of replenished beaches under storm conditions.

Contents

	Page
Abstract	i
Contents	ii
List of Tables	viii
List of Figures	xi
List of Plates	xvii
Acknowledgements	xviii
List of Symbols and Abbreviations	xix
Introduction	1
Chapter 1: Review of Published Literature	5
1.1 Occurrence and Composition of Shingle Beaches	5
1.1.1 Terminology	5
1.1.2 World-wide Occurrence	5
1.1.3 British Isles Occurrences	5
1.1.4 Beach Composition	7
1.1.5 Beach Structure	8
1.1.6 Mixed Beaches	9
1.2 Shingle Beach Profile Characteristics	10
1.2.1 Beach Terminology	10
1.2.2 Beach Profile Response to Hydrodynamic Forces	11
1.2.3 Effects of Beach and Sediment Characteristics on Beach Profile Development	12
1.3 Hydrodynamic Factors Acting as Process Controls	14
1.3.1 Terminology	14
1.3.2 Waves and Wave - Beach Interaction	15

1.4 Shingle Mobility and Transport 19
1.4.1 Shingle Threshold and Transport 19
1.4.2 Longshore Sediment Transport Formulae 21

1.5 Field Measurement of Longshore Transport 25
1.5.1 Trapping 25
1.5.2 Tracers 26
1.5.3 Impoundment 27

1.6 Regional Sediment Budgets 28

Chapter 2: Area Under Investigation 35

2.1 Location and Geographical Setting 35
2.1.1 A Brief Description of the Coastline 35
2.1.2 Slope stabilities 35
2.1.3 Low-Lying Coastline 35

2.2 Geology of the Study Area 36
2.2.1 Nature of the Coastal Outcrops 36
2.2.2 Evolution of the Thames Estuary 38

2.3 Oceanographic Setting 40
2.3.1 Bathymetry 40
2.3.2 Sea Level Changes 40
2.3.3 Tides 41
2.3.4 Extreme water levels 42
2.3.5 Wind conditions 42
2.3.6 Wave conditions 42

2.4 Sediment Distribution and Mobility 43
2.4.1 Offshore sediment distribution 43

2.4.2 Beach and Nearshore Sediment Distribution 43
2.4.4 Beach and Nearshore Sediment Mobility 45

CHAPTER 3: Methods and Analytical Techniques 64

3.1 Introduction 64

3.2 Long-term data sets 64
3.2.1 Manston Airport (wind speed and direction) 65
3.2.2 Borstal Hill, Whitstable (wind speed and direction) 65
3.2.3 Port of Sheerness (water level data) 65
3.2.4 Whitstable Harbour (water level data) 66
3.2.5 Whitstable Harbour (wave records) 66
3.2.6 Beach Profile Data 67

3.3 Numerical modelling 67

3.4 Offshore Wave Generation Model (Stage 1) 68
3.4.1 Model Description 68
3.4.2 Directional Sectors and Coastal Units 71

3.5 Nearshore Wave Conditions (Stage 2) 71

3.6 Calibration of Nearshore Wave Conditions 75

3.7 Nearshore Wave Climate (Stage 3) 76

3.8 Longshore Transport Calculations 77

3.9 Calibration of the longshore transport formulae 79
3.9.1 Electronic tracer pebble development 79
3.9.2 Sediment Dynamics Experiments (Long Beach, Whitstable) 79

3.10 Sediment Budget 82
3.10.1 Introduction 82
3.10.2 Beach management units and beach volume calculations 82

CHAPTER 4: Results - Coastal Hydrodynamics Model 92

4.1 Introduction 92

4.2 Offshore Wave Conditions 92

4.3 Nearshore Wave Conditions 93
4.3.1 Sensitivity Analysis 93
4.3.2 Nearshore Wave Model Results 94

4.4 Recorded Wave Data 95
4.4.1 Wave record analysis (Whitstable Harbour) 95
4.4.2 Calibration of Wave Conditions with Recorded Wave Data 97

4.4.3 The Correlation between Predicted and Recorded Nearshore Wave Conditions 100
4.5 Derivation of the Wave Climate 104
4.5.1 Wind Climate 104
4.5.2. Water Level Climate 105
4.5.3 Offshore Wave Climate 105
4.5.4 Nearshore Wave Climate 106

4.6 Extreme Events 107
4.6.1 Extreme Wind Conditions 107
4.6.2 Extreme Water Levels 108
4.6.3 Extreme Wave Conditions 109
4.6.4 Interdependence of Water Level - Wind / Wave Conditions 110

Chapter 5: Results - Sediment Transport Studies 137

5.1 Introduction 137

5.2. A Description of the Long Beach Study Site 137
5.2.1 Initial Field Study At Long Beach (16th to 18th March, 1992) 140

5.3 Main Field Study At Long Beach (23rd to 26th January, 1993) 142
5.3.1 Weather Conditions, 23rd to 26th January, 1993 143
5.3.2 Water Levels, 23rd to 26th January, 1993 143

5.3.3 Wave Conditions derived from the Whitstable Harbour Wave Recorder 143
5.3.4 Visual Observations of Wave Conditions at Long Beach, Whitstable 144
5.3.5 Data obtained from the Long Beach Array 145
5.3.6 Wave Conditions from Model and Comparison with Wave Records 149
5.3.7 Transport Rate Calculations from Wave Conditions 151

5.4 Transport Rate Calculations based on Tracer Pebbles 153
5.4.1. Tracer pebble deployment 154
5.4.2 Tracer Search and Recovery 155
5.4.3 Tracer Displacement 157
5.4.4 Mobile Layer Calculations 161
5.4.5 Transport rates based upon tracer movement 165

5.5 Beach survey and analysis 166

5.6. Comparison of Transport Rate Calculations 168
5.6.1 Summary of Data Collected 168
5.6.2 Summary of Results 169
5.6.3 Comparison of Longshore Transport Rates: 23rd to 26th January 1993 170

5.7 Calculation of Potential Annual Net Longshore Transport Rates 172

5.8 Seasonal Variations in Potential Net Longshore Transport Rates 174

5.9 Impact of Climatic Anomalies on Potential Net Longshore Transport Rates 175

Chapter 6: Results - Sediment Transport Studies 229

6.1 Introduction 229

6.2 Discussion of Results for Individual Coastal Section 230
6.2.1 Unit 1: Seasalter 230
6.2.2 Unit 1B: Whitstable 231
6.2.3 Unit 2: Tankerton 232
6.2.4 Unit 3: Studd Hill 233
6.2.5 Unit 4B: Herne Bay 233
6.2.6 Unit 5: East Cliff 234
6.2.7 Unit 6(A to C): Reculver, Northern Sea Wall and Minnis Bay 235

6.3 Sediment Budget Analysis for Specific Coastal Sections 237
6.3.1 Whitstable, Central 237
6.3.2 Herne Bay, West 239
6.3.3 Tankerton 244

7. Discussion 276

7.1. Introduction 276

7.2. Hydrodynamics of the Study Area 276

7.2.1. General points 276
7.2.2. Coastal hydrodynamics model 277
7.2.3. Hydrodymamic characteristic of the study area 280

7.3. Sediment Dynamics of the Study Area 283

7.3.1. General points 283
7.3.2. Longshore transport model 284
7.3.3. Sediment dynamic characteristics of the study area 287

8. Conclusions and Recommendations for Further Research 290

8.1. Conclusions 290

8.2. Recommendations for Further Research 291

References 293

List of Tables

Table 1.1 Particle Size Classification after Wentworth (1922) and Krumbein (1934) 29
Table 1.2 Linear, Airy Wave Theory Equations, after Carter 1989 30
Table 2.1 Tidal Parameters for Coastal Locations Within the Study Area 47

Table 3.1 Tidal Relationship Between Principal Ports and the Coastal Units within the Study Area 84
Table 3.2 Sedimentological Characteristics of: (a) Transmitting; and (b) Aluminium Tracer Pebbles 85

Table 4.1 Summary of Fetch Water Depths Used in the Offshore Wave Model 114
Table 4.2 Example of SHALLPRE Output: Unit 6; Sector 4 114
Table 4.3 Example of Endec Results for Unit 1B; Sector 5 115
Table 4.4 Correlation Statistics of Predicted / Recorded Wave Heights and Periods 116
Table 4.5 Calibration Coefficients to be used with the Nearshore Wave Model 117
Table 4.6 Still Water Level Frequency Distribution for the Study Area 117
Table 4.7 Occurrence of Extreme Wind Conditions at the Coastline in the Study Area 118
Table 4.8 Frequency Distribution of Predicted High Water Levels and High Water Surge Residuals At Sheerness, (1978, 1981-1985) 118
Table 4.9 Extreme Water Levels Recorded At Whitstable Harbour 119
Table 4.10 Theoretical Accuracy of Extreme Wave Predictions 119
Table 4.11 Extreme Wave Conditions at Whitstable based on Statistically Extrapolated Recorded Data 120
Table 4.12(a) Percentage Occurrence of High Water Surge Residuals (Southend) by Wind Direction (after Ackers, 1972) 121
Table 4.12(b) Percentage Occurrence of High Water Surge Residuals (Southend) by Wind Speed (after Ackers, 1972) 121
Table 4.13 Recorded Maximum Still Water Levels and Wind / Wave Conditions for Storm Events at Whitstable 122
Table 4.14 Extreme Event Criteria derived for the Whitstable Wave Recorder Site for Northwesterly, Northerly and Northeasterly Winds 123

Table 5.1. Aluminium Tracer Displacements at Long Beach, Whitstable, 16/03/92 to 31/03/92 180
Table 5.2 Visual Observations of Wave Conditions at Long Beach, Whitstable: 23/01/93 to 25/ 01/93 181
Table 5.3 Analysis of wave data, (time and frequency domain), Long Beach, Whitstable: 23/01/93 to 26/01/93 182
Table 5.4 Longshore Transport Rates calculated using the "Delft" formula and wave model output 183
Table 5.5 Recovery Rates of Tracers, Long Beach, Whitstable: 23/01/93 to 26/01/93 183
Table 5.6 Displacement of tracer pebbles, Long Beach, Whitstable: 23/01/93 to 26/01/93 184
Table 5.7 Estimation of extent of mobile layer, Long Beach, Whitstable: 23/01/93 to 26/01/93 184
Table 5.8 Longshore transport rates based on displacement of tracer pebbles, Long Beach, Whitstable: 23/01/93 to 26/01/93 184
Table 5.9 Beach Profile Cross Section Areas and Volumetric Changes, Long Beach, Whitstable: 23/01/93 to 26/01/93 185
Table 5.10 Longshore Transport rates based on beach volumetric changes, Long Beach, Whitstable: 23/01/93 to 26/01/93 185
Table 5.11 Summary of Data collected during field experiment at Long Beach, Whitstable: 23/01/93 to 26/01/93 186
Table 5.12 Comparison of longshore transport rates determined for Long Beach, Whitstable: 23/01/93 to 26/01/93 187
Table 5.13 Summary of longshore transport rates determined for Long Beach, Whitstable: 23/01/93 to 26/01/93 188
Table 5.14 Average annual potential net longshore transport rates for the Study Area 189
Table 5.15 Transport Equilibrium Orientations for beaches in the Study Area 190
Table 5.16 Longshore transport rates for extreme events at Long Beach, Whitstable: (a) 1st February 1953; (b) 12th December 1990, and (c) 20th February 1996 191
Table 5.17 Wind Speed and Direction Occurrences at Manston Airport: (a) September 1995; (b) October 1995, and; (c) November 1995 192
Table 5.17(cont) Wind Speed and Direction Occurrences at Manston Airport: (d) December 1995; (e) January 1996, and; (f) February 1996 193
Table 5.17(cont) Wind Speed and Direction Occurrences (%) at Manston Airport: (g) March 1996; (h)April 1996, and; (i) summation of winter months (October 1995 - March 1996) 194

Table 5.18 Monthly Variation in Longshore Transport Rates, September 1995 to April 1996 at Long Beach Whitstable 195

Table 6.1 Details of Beach Monitoring Stations at Whitstable Central and results of regression analysis 249
Table 6.2 Details of Beach Management Units at Whitstable Central and results of regression analysis 249
Table 6.3 (a) Details of beach replenishments carried out at Herne Bay West: 1975 - 1994 250
Table 6.3 (b) Annually-averaged replenishment, added to each Beach Management Unit at Herne Bay West: 1975 - 1994 250
Table 6.4 Details of Beach Monitoring Stations at Herne Bay West and results of regression analysis for data collected between 1975 and 1994 251
Table 6.5 Details of Beach Management Units at Herne Bay West and results of regression analysis for data collected between 1975 and 1994 251
Table 6.6 Annual-averaged sediment budget for Herne Bay Central showing situation: (a) pre-breakwater construction (1975 - 1991); and (b) post-breakwater construction (predicted) 252
Table 6.7 Beach Replenishments carried out at Tankerton: 1980 - 1994 253
Table 6.8 Details of regression analysis (1980 to 1994) for: (a) profile data collected from Beach Monitoring Stations at Tankerton; and (b) Beach Management Units at Tankerton 254
Table 6.9 Sediment budget for Tankerton based upon beach profile data collected between 1980 and 1994, assuming: (a) offshore losses of 0.5 $m^3 m^{-1} yr^{-1}$; (b) no net offshore losses 255
Table 6.9 (cont) Sediment budget for Tankerton based upon beach profile data collected between 1980 and 1994, assuming: (c) offshore losses of 0.5 $m^3 m^{-1} yr^{-1}$, and additional losses of 0.5 $m^3 m^{-1} yr^{-1}$ to the Street from BMU B; (d) offshore losses of 0.5 $m^3 m^{-1} yr^{-1}$, and additional losses of 1.5 $m^3 m^{-1} yr^{-1}$ to the Street from BMU B 256

List of Figures

Figure 1.1 Shingle Beach Structure, in terms of shingle size and shape, (Bluck, 1967) 31
Figure 1.2 Shingle Beach Terminology 32
Figure 1.3 Beach Hydrodynamics Terminology 32
Figure 1.4 Influence of Particle Position on Threshold of Movement 33
Figure 1.5 Example of Sediment Budget Approach (after Bray 1990) 34

Figure 2.1 Location of the Study Area 48
Figure 2.2 General layout of the study area 49
Figure 2.3 Geological Map of the Study Area, after Holmes (1981) 50
Figure 2.4 Pleistocene Development of River Systems in the Thames Estuary and southern North Sea, after BGS (1990) 51
Figure 2.5 Simplified Bathymetry of the Study Area, 52
Figure 2.6 Location of Amphodromic Points and Tidal Ranges in the Study Area, after Pugh 1980 53

Figure 3.1 Relationship Between Primary Controls and the Hydraulic / Sediment Responses 86
Figure 3.2 Location of Oceanographic Instrument Sites for the Data Sets Used in Study Area 87
Figure 3.3 Stages Involved in the Development of a Numerical Model for the Study Area 88
Figure 3.4 Subdivision of the Coastline into Coastal Units and Wind Directional Sectors, (see Section 3.4.2. for Explanation) 89
Figure 3.5 Experimental Setup for the Beach Process Field Study at Long Beach, Whitstable 90
Figure 3.6 Particle Size Distribution Curve Showing Relationship Between Tracers and the Indigenous Beach Sediments 91

Figure 4.1(a) Comparison of Offshore Wave Heights for the Various Directional Sectors 124
Figure 4.1(b) Comparison of Offshore Wave Heights for the Various Coastal Units 124

Figure 4.2 Example of Nearshore Wave Conditions from the Wave Model Showing Variation in (a) Wave Height (Hs, m); (b) Wave Period (Tz, s); and (c) Wave Angle (∝, °) 125
Figure 4.3(a) Wave Height / Period Scattergraph based on Records from Whitstable Harbour (1978 - 1990) 126
Figure 4.3(b) Wave Height / Period Scattergraph based on Records from Whitstable Harbour (1978 - 1990, Winter Months) 127
Figure 4.3(c) Wave Height / Period Scattergraph based on Records from Whitstable Harbour (1978 - 1990, Summer Months) 128
Figure 4.4(a) Monthly Variation in the Exceedence of Recorded Wave Heights at Whitstable Harbour, (1978 - 1990) 129
Figure 4.4(b) Yearly Variation in the Exceedence of Recorded Wave Heights at Whitstable Harbour, (1978 - 1990) 129
Figure 4.5(a) Predicted Wave Height (Hs, m), versus Recorded Wave Height (Hs, m), at the Whitstable Harbour Recorder (for Sector 1), Showing the Effects of Water Level 130
Figure 4.5(b) Predicted Wave Period (Tz, s), versus Recorded Wave Period (Tp, s), at the Whitstable Harbour Recorder (for Sector 1), Showing the Effects of Water Level 130
Figure 4.6 Depth Attenuation of Surface Waves with Wave Period and Water Depth 131
Figure 4.7(a) Annual Wind Climate At Manston Airport (1979 to 1989) 131
Figure 4.7(b) Winter Wind Climate At Manston Airport (1979 to 1989) 132
Figure 4.7(c) Summer Wind Climate At Manston Airport (1979 to 1989) 132
Figure 4.8(a) Offshore Wave Climate for Seasalter / Whitstable (Unit 1), (1979 to 1989) 133
Figure 4.8(b) Offshore Wave Climate for Reculver / Minnis Bay (Unit 6), (1979 to 1989) 133
Figure 4.9(a) Nearshore Wave Climate for Whitstable (Unit 1A), (1979 to 1989) 134
Figure 4.9(b) Nearshore Wave Climate for Reculver (Unit 6A), (1979 to 1989) 134
Figure 4.10 Distribution of Large Positive Surges (>0.6m) at Southend (dates), Relative to the Time of Predicted High Water, (after Pugh 1987) 135
Figure 4.11 Extreme Still Water Level Distributions in the Study Area (Based on Data From Hydraulics Research (1981, 1985) 135
Figure 4.12 Probability of Exceedence of Wave Height at Whitstable, (Based Upon Recorded Data from Whitstable Harbour (1978 to 1990) 136
Figure 4.13 Dependency Between the Return Period of Extreme Still Water Levels on Wind Direction (Based on Data From Hydraulics Research (1981, 1985) 136

Figure 5.1 Location of Long Beach Whitstable, site of the shingle transport field studies: 23/01/93 to 26/01/93 196
Figure 5.2 Particle size distribution variation along a "Typical" beach profile, Long Beach, Whitstable, 23/01/93 197
Figure 5.3 Details of Experimental Set-up, Long Beach, Whitstable: 2301/93 to 26/01/93 198
Figure 5.4 (a) Wave Height (Hs) and (b) Wave Period (Tp) data from the Whitstable Harbour wave recorder (see Figure 3.2 for location): 16/03/92 to 31/03/92 199
Figure 5.5 Recorded (a) Wind Direction and (b) Wind Speed data collected from Borstal Hill, Whitstable: 22/01/93 to 26/01/93 200
Figure 5.6 Recorded water levels, predicted water levels and the surge residual at Whitstable Harbour: 22/01/93 to 26/01/93 201
Figure 5.7 Wave Height (Hs) and Wave Period (Tp) data from Whitstable Harbour recorder (see Figure 3.2 for location): 22/01/93 to 26/01/93 201
Figure 5.8(a) Time series wave conditions recorded at Long Beach Whitstable: 23/01/93 (am) 202
Figure 5.8(b) Time series wave conditions recorded at Long Beach Whitstable: 23/01/93 (pm) 202
Figure 5.8(c) Time series wave conditions recorded at Long Beach Whitstable: 24/01/93 (am) 203
Figure 5.8(d) Time series wave conditions recorded at Long Beach Whitstable: 24/01/93 (pm) 203
Figure 5.8(e) Time series wave conditions recorded at Long Beach Whitstable: 25/01/93 (am) 204
Figure 5.9(a-f) Spectral energy density for wave conditions recorded at Long Beach Whitstable: 23/01/93 (am) (vertical scale exaggerated compared to succeeding graphs) 205
Figure 5.9(g-k) Spectral energy density for wave conditions recorded at Long Beach Whitstable: 23/01/93 (pm) 206
Figure 5.9(l-q) Spectral energy density for wave conditions recorded at Long Beach Whitstable: 24/01/93 (am) 207
Figure 5.9(r-t) Spectral energy density for wave conditions recorded at Long Beach Whitstable: 24/01/93 (pm) 208
Figure 5.9(u-z) Spectral energy density for wave conditions recorded at Long Beach Whitstable: 25/01/93 (am) 209
Figure 5.10(a) Comparison of recorded and hindcast significant wave height (Hs, m) at Whitstable Harbour: 23/01/93 to 26/01/93 210
Figure 5.10(b) Comparison of recorded and hindcast significant wave height (Hs, m) at Long

Beach, Whitstable: 23/01/93 to 26/01/93 210
Figure 5.10(c) Comparison of recorded and hindcast significant wave height (Hs, m) at Long Beach, Whitstable: 23/01/93 to 26/01/93 (pm recordings temperature corrected) 211
Figure 5.10(d) Comparison of recorded and hindcast wave period (T, s) at Long Beach, Whitstable: 23/01/93 to 26/01/93 211
Figure 5.10(e) Comparison of hindcast wave angle ($\propto$,°) at Long Beach, Whitstable and at the wave recorder site: 23/01/93 to 26/01/93 212
Figure 5.11(a) Location of electronic tracer pebbles at Long Beach, Whitstable: 23/01/93 (am) 213
Figure 5.11(b) Location of electronic tracer pebbles at Long Beach, Whitstable: 24/01/93 (am) 214
Figure 5.11(c) Location of electronic tracer pebbles at Long Beach, Whitstable: 24/01/93 (pm) 215
Figure 5.11(d) Location of electronic tracer pebbles at Long Beach, Whitstable: 25/01/93 (am) 216
Figure 5.11(e) Location of electronic tracer pebbles at Long Beach, Whitstable: 25/01/93 (pm) 217
Figure 5.11(f) Location of electronic tracer pebbles at Long Beach, Whitstable: 26/01/93 (am) 218
Figure 5.12(a) Beach changes at Profile 1: Long Beach, Whitstable: 23/01/93 to 26/01/93 219
Figure 5.12(b) Beach changes at Profile 2: Long Beach, Whitstable: 23/01/93 to 26/01/93 219
Figure 5.12(c) Beach changes at Profile 3: Long Beach, Whitstable: 23/01/93 to 26/01/93 220
Figure 5.12(d) Beach changes at Profile 4: Long Beach, Whitstable: 23/01/93 to 26/01/93 220
Figure 5.12(e) Beach changes at Profile 5: Long Beach, Whitstable: 23/01/93 to 26/01/93 221
Figure 5.12(f) Beach changes at Profile 6: Long Beach, Whitstable: 23/01/93 to 26/01/93 221
Figure 5.12(g) Beach changes at Profile 7: Long Beach, Whitstable: 23/01/93 to 26/01/93 222
Figure 5.12(h) Beach changes at Profile 8: Long Beach, Whitstable: 23/01/93 to 26/01/93 222
Figure 5.13 Volumetric changes for Long Beach, Whitstable: 23/01/93 to 26/01/93 (see Section 5.5 for details) 223
Figure 5.14 Longshore transport rates calculated from beach volumetric changes, Long Beach,

Whitstable: 23/01/93 to 26/01/93 (see Section 5.5 for details) 223
Figure 5.15 Examples of variation in average annual potential net longshore transport rates due to coastal orientation 224
Figure 5.16 Seasonal variation in average annual potential net longshore transport rates at Long Beach, Whitstable 224
Figure 5.17 Comparison of wind speed and direction occurrences for the 'winter' period 1995/1996, and the average of 'winter' periods between 1979 to 1989: (data obtained from Manston Airport) 225

Figure 6.1 Location of sites where the sediment budget has been assessed 257
Figure 6.2 Net annual potential longshore transport rates for the study area 258
Figure 6.2 (cont) Net annual potential longshore transport rates for the study area 259
Figure 6.2 (cont) Net annual potential longshore transport rates for the study area 260
Figure 6.2 (cont) Net annual potential longshore transport rates for the study area 261
Figure 6.2 (cont) Net annual potential longshore transport rates for the study area 262
Figure 6.3 Variation in net annual potential longshore transport rates for beaches in Whitstable Central (based upon coastal model, see section 6.2.2 263
Figure 6.4 Extent of sediment budget study at Whitstable Central, showing location of Beach Monitoring Stations and Beach Management Units 264
Figure 6.5(a) Variation in cross-sectional area of beach, BMS 9.2 (Whitstable): 1989 - 1994 265
Figure 6.5(b) Variation in cross-sectional area of beach, BMS 9.5 (Whitstable): 1989 - 1994 265
Figure 6.5(c) Variation in cross-sectional area of beach, BMS 9.9 (Whitstable): 1989 - 1994 266
Figure 6.5(d) Variation in cross-sectional area of beach, BMS 10.5 (Whitstable): 1989 - 1994 266
Figure 6.5(e) Variation in cross-sectional area of beach, BMS 11.5 (Whitstable): 1989 - 1994 267
Figure 6.5(f) Variation in cross-sectional area of beach, BMS 12.1 (Whitstable): 1989 - 1994 267
Figure 6.5(g) Variation in cross-sectional area of beach, BMS 12.2 (Whitstable): 1989 - 1994 268
Figure 6.5(h) Variation in cross-sectional area of beach, BMS 12.3 (Whitstable): 1989 - 1994 268
Figure 6.6 Variation in the total volume of beach material at Whitstable Central: 1989 - 1994 269
Figure 6.7 Extent of sediment budget study at Herne Bay West, showing location of Beach

Monitoring Stations and Beach Management Units 270

Figure 6.8(a) Variation in cross-sectional area of beach, BMS 33 (Herne Bay): 1975 - 1994 271

Figure 6.8(b) Variation in cross-sectional area of beach, BMS 34 (Herne Bay): 1975 - 1994 271

Figure 6.8(c) Variation in cross-sectional area of beach, BMS 35 (Herne Bay): 1975 - 1994 272

Figure 6.8(d) Variation in cross-sectional area of beach, BMS 36 (Herne Bay): 1975 - 1994 272

Figure 6.8(e) Variation in cross-sectional area of beach, BMS 37 (Herne Bay): 1975 - 1994 273

Figure 6.9 Extent of sediment budget study at Tankerton, showing location of Beach Monitoring Stations and Beach Management Units 274

Figure 6.10 Sediment Budget for Tankerton based on beach profile data, 1980 - 1994, after Delft Hydraulics (1995) 275

List of Plates

Plate 2.1(a) Aerial view of the coastline to the west of Whitstable, 1991; looking west towards Seasalter, (see Figure 2.2 for location) 54
Plate 2.1(b) Aerial view of the coastline around Whitstable Harbour, 1991; showing "the Street" in the foreground, (see Figure 2.2 for location) 55
Plate 2.1(c) Aerial view of the coastline around Tankerton, 1991; showing "Long Rock" in the foreground, (see Figure 2.2 for location) 56
Plate 2.1(d) Aerial view of the coastline around Studd Hill, 1993, (see Figure 2.2 for location) 57
Plate 2.1(e) Aerial view of the coastline around Herne Bay, 1991; prior to the construction of the breakwater, (see section 6.3 for details of breakwater, and Figure 2.2 for location) 58
Plate 2.1(f) Aerial view of the coastline to the east of Herne Bay; (see Figure 2.2 for location) 59
Plate 2.1(g) Aerial view of the coastline around Reculver, 1991; (see Figure 2.2 for location) 60
Plate 2.2 Wave Overtopping of Coastal Defences at Whitstable, 1949 61
Plate 2.3 Flooding to Central Whitstable, 1953 61
Plate 2.4 Outcrop of "Doggers" in the Thanet Sands, Reculver 62
Plate 2.5 Black pebble beds in the Herne Bay Member / Bishopstone Glen 62
Plate 2.6 Intermediate Head Gravels, near Bishopstone Glen 63
Plate 2.7 Typical Beach in the Study Area, (seafront, Herne Bay) 63

Plate 5.1 Aerial view of the field study site, Long Beach, Whitstable 226
Plate 5.2 Movement of painted tracer pebbles across the 'sand run' under very low energy conditions at Long Beach, Whitstable: 16/03/92 227
Plate 5.3 Pressure transducer and EM current meter, Long Beach, Whitstable: 23/01/93 227
Plate 5.4 Typical wave conditions, Long Beach, Whitstable: 25/01/93 (am) 228

Acknowledgements

First I would like to say thank you to Professor Collins for his supervision and his guidance in the completion of the research involved in this investigation. Thanks also to Canterbury City Council for their sponsorship, especially to Andrew Roberts, Viv Pritchard, Ted Edwards and Peter Brookes for their encouragement. Finally thank you to Les Whitcombe and Travis Mason for their help along the way.

List of Symbols and Abbreviations

a	Wave amplitude
C	Phase velocity
Cg	Group velocity
d	Water depth
D	Grain diameter
D_{50}	Median grain diameter
Dn_{50}	Nominal median grain size
E	Wave energy flux
f	Frequency interval
fw	Wave friction factor
g	Gravity
H	Wave height
H_{rms}	Root mean square wave height
H_s	Significant wave height
H_b	Significant wave height at breaking
I_{ls}	Immersed-weight longshore transport rate
k	Wavenumber
K	Dimensionless longshore transport coefficient
$m_{0,1}$	Spectral moments
Q_{ls}	Longshore Sediment transport rate
t	Duration
T	Wave period (s)
Tz	Zero-crossing wave period (s)
Tp	Peak wave period (s)
U	Mean current velocity (ms^{-1})
z_o	Still water level (m)
α	wave approach angle
λ	Wavelength (m)
π	Pi
σ	Angular frequency
ρ	Fluid density ($kg\ m^{-3}$)
ρ_s	Sediment density ($kg\ m^{-3}$)
τ	Shear stress
Δ	Relative density

AOD	Above Ordnance Datum (Newlyn)
CCC	Canterbury City Council
CD	Chart Datum
HAT	Highest Astronomical Tide
LAT	Lowest Astromonical Tide
MHWN	Mean High Water Neaps
MHWS	Mean High Water Springs
MLWN	Mean Low Water Neaps
MLWS	Mean Low Water Springs
MSL	Mean Sea Level
OD	Ordnance Datum

Introduction

Beaches are a common feature on coastlines around the world; they are accumulations of sediment on the land - water interface, which display a variety of forms (Carter, 1989). Well cited beaches occur on the eastern coastline of the USA, and the south coast of England. It is on one of the latter sites that the present research project is to be undertaken.

Beaches are of interest to geologists in the reconstruction of ancient environments (Hart & Plint, 1989), coastal geomorphologists on the development and evolution of landforms (King, 1972), oceanographers for the examination of physical processes (Open University, 1994), and coastal engineers involved with the design of sea defences and construction in the beach / nearshore region (Muir Wood and Fleming, 1981).

Coastal zones and beaches are areas of wave and tidal energy dissipation. An understanding of the processes of sediment transport in response to hydrodynamic forces is important in the understanding and effective management of the nearshore and coastal regions (Dyer, 1986).

Shingle beaches are characterised by their steep gradients and stepped profiles (Nicholls and Webber, 1988). Such features are subject to rapid morphological changes under wave action, having the ability to dissipate large amounts of wave energy within a relatively narrow zone (Powell, 1990; Diserens and Coates, 1993). Consequently, understanding the mobility of shingle beaches in response to hydrodynamic forces and local geomorphological controls is of extreme importance, both scientifically (Carr, 1983) and in the design of coastal protection schemes and structures, (MAFF, 1993).

Hydrodynamic controls on shingle mobility include: variation in water level (tidal height variations, including superimposed surges); wave energy, (temporal variations in wave height, period and angle of approach); longshore currents; and climatic changes (global sea level rise and changes in storm patterns), (Bird, 1996).

Geological controls include the source and the nature of the material composing the beach, (Bluck, 1967). Sources may include the reworking of offshore deposits, longshore transport from adjacent areas and the erosion of cliffs.

The type of material comprising the beaches range from flints and cherts to biogenic material, such as fragments of coral reefs. Morphological controls include the presence of headlands or any local changes in the coastal configuration (Muir Wood and Fleming, 1981). Also, bathymetric controls can influence and modify wave patterns as they approach the shoreline. The modification of waves will, in turn, be reflected in the patterns of beach sedimentation (Carter, 1989).

It has been estimated that one third of the UK coastline is protected by shingle beaches (Fuller & Randall, 1988). When these beaches become depleted by erosion, replenishment has often been undertaken, using marine dredged gravels (Fairgrieve, 1994). In some cases, coarser material derived from land-based quarries, has been added to the marine dredged replenishment (McFarland et al, 1994); this was undertaken to increase the mean grain size of the replenished beach.

As the local Coast Protection Authority, Canterbury City Council (CCC), are responsible for the provision and maintenance of coastal defences within the bulk of the study area; these defences have an estimated replacement value of £100 million (Canterbury City Council, 1988).

Previous work carried out within the study area has been limited to engineering-based investigations, directed at specific coastal locations, (for example, Delft Hydraulics 1990a). Prior to the present investigation, little effort has been made to develop a regional understanding of coastal hydrodynamic processes along the north Kent coastline. The lack of understanding of processes affecting shingle beaches (on both a global scientific basis, and a regional coastal engineering basis) was of particular concern to the local coast protection Authority, who have supported the present study.

Within the context of the framework which has been discussed, a research programme has been undertaken along the north Kent coast, with the purpose of developing an understanding of stability of beaches, with particular reference to shingle-sized material. The research objectives include:

- derivation of a wave climate for the study area, based upon numerical modelling and, calibration of the model using recorded data;

- evaluation of a formula for the longshore transport of shingle within the study area, based upon measurements of the hydrodynamic controls and, the resulting sediment response;

- establishing the regional patterns of shingle movement, based upon the numerically modelled wave climate and longshore transport calculations;

- examination of improved techniques for the determination of longshore transport rates, through the use of tracer pebbles;

- evaluation of a sediment budgetary approach to determining long term patterns of shingle movement;

- assessment of the impact of extreme events upon beach stability and patterns of longshore transport; and

- consideration of the various advantages and disadvantages associated with beach replenishment schemes.

Data already collected by Canterbury City Council, has been used in conjunction with intensive field monitoring to achieve the research objectives.

The present report is structured as follows:

- an examination of those aspects of the published literature relevant to the present study (Chapter 1);

- a description of the study area, including the state of knowledge on regional coastal processes, at the outset of the present investigations (Chapter 2);

- an outline of the existing data availability, and the methodologies adopted for; (i) obtaining additional data, and (ii) carrying out the analysis required to meet the study objectives (Chapter 3);

- the derivation of the numerical wave model, its calibration using recorded wave data, and its application to the determination of a wave climate for the study area (Chapter 4);

- details of the intensive field investigations carried out to evaluate the existing shingle transport formula, and the development of the longshore transport numerical model for the study area (Chapter 5);

- application of the longshore transport model to beaches within the study area, and comparison with assessments of shingle mobility undertaken using archive beach profile data (Chapter 6)

- discussion on the findings of the present investigation on beach stability, within the context of regional coastal management and, the wider applicability of the findings to the understanding of the hydrodynamics of coarse-grained and mixed sediment beaches (Chapter 7)

- Finally, recommendations for further research are presented (Chapter 8).

In addition to the present document, the findings of these studies are presented as a series of reports, compiled by the author, for the local coast protection Authority (Canterbury City Council, 1990; 1991; 1992a; 1993a; 1993b; 1994). The results have also been used for the investigation and design of coastal defence works within the study area (Canterbury City Council, 1992b; 1994b, 1995; 1997; Robert West & Partners, 1993; Halcrow, 1996).

Chapter 1: Review of Published Literature

1.1. Occurrence and Composition of Shingle Beaches

1.1.1. Terminology

Terminology for use in the description of coarse-grained beaches is fraught with ambiguities (Carter and Orford, 1993). In the present investigation, the term "shingle" is used to describe rounded or sub-rounded stones, having a long axis of between 4 and 256mm. This range corresponds to the pebble and cobble ranges of the Wentworth scale (Table 1.1).

Beaches which have a significant proportion of sand are described as "mixed" (sand-shingle) beaches (Kirk, 1980). The sand may lie in the interstices of the shingle, or it may be present as a fringing sand apron. However, no fixed terminology exists to define the percentage of sand-sized material, which needs to be present to merit its description as a mixed beach.

1.1.2. World-wide Occurrence.

Shingle beaches are common in northern latitudes where glaciation has had a marked influence on the Recent geomorphology (Whitcombe, 1995); they occur where the erosion of cliffs or nearshore outcrops yield pebble or cobble sized material. In tropical regions, such coarse sediments may be transported to the coastline by torrential rivers; eventually, they are reworked as beaches. Shingle beaches are also common in Canada, New Zealand, Ireland, and along stretches of the pacific coast of the USA (Carter, 1989).

1.1.3. British Isles Occurrences.

The British Isles and, in particular the south coast of England, exhibit a wide range of shingle features. It has been estimated that one third of the UK coastline is protected by shingle beaches (Fuller and Randall, 1988). A well known and extensively studied shingle feature is Chesil Beach, in Dorset (Carr, 1983); this beach stretches from Bridport (in the west) to the Isle of Portland (in the east). At either end of the system the beach is attached to the land; over its central part however, it is detached and encloses a narrow stretch of water called "The

Fleet". The height of the bank and the mean size of the shingle increases gradually from west to east, representing a corresponding increase in exposure to wave action (Carr, 1983).

Dungeness (Kent) is an example of a constructional shingle feature; it has been formed as a series of abandoned storm crests, as shingle has built up in response to longshore supply from both the west and the north-east. Elsewhere along the coastline of south-east England, there are numerous smaller shingle accumulations, examples of which are to be found in Christchurch Bay (including Hurst Spit, Nicholls and Webber, 1988), at Hayling Island (Harlow, 1980), and along the north Kent coast, (the present investigation).

Elsewhere in the British Isles, shingle is found in pocket beaches along indented coastlines of Dorset (Bray 1990), South Wales (Bluck, 1967), and as accumulations at the head of flooded rivers or glacial valleys (for example, Arran Island in Western Scotland).

The abundant occurrence of shingle beaches around the British Isles and in particular, south-east England has been attributed to a number of geological and hydrodynamic factors:

- the availability and durability of suitably sized source material;
- the effects of post-glacial sea level rise;
- and the characteristics of the wave climate.

Flint deposits occur as nodules (often in bands), within the Cretaceous Chalk of the British Isles. A large proportion of these flint nodules have been released into rivers or the sea, where the Chalk has been eroded. In addition, Jurassic strata commonly contain bands of siliceous chert rock in association with softer rocks such as clay, marl and limestone. The more durable flint and chert material is reworked by rivers or by the sea to form substantial accumulations of shingle-sized material.

In the central and northern parts of the British Isles, glacial moraines contain a range of particle sizes from fine silts to large boulders; these have been eroded from hard igneous or metamorphic rocks. Erosion of these glacial deposits yield suitable source materials for shingle beaches to accumulate at coastlines (common in Scotland, Wales and the northern parts of Ireland). Cliff erosion may supply shingle sized material if either the pebbles or cobbles are

already present in a softer matrix, or the exposed rock is heavily jointed or fractured. The latter is commonly found in fine grained metamorphic rocks.

Following a period of Recent glaciation in the northern latitudes, extensive sand and gravel deposits covered what was to become the southern North Sea and the south-east of England. Many of these deposits had been extensively reworked by ancient river systems (D'Olier, 1975). As the ice retreated, accompanied by a rise in sea levels, large amounts of gravel were eroded and moved landwards. As the gravels were transported progressively inland, in response to the rising sea level, they formed shingle barriers; for example Chesil Beach and Slapton Beach (Carr, 1983). It is considered that the majority of beaches in the south of England were formed by such a mechanism and nowadays receive little or no natural replenishment. Beaches formed in this way are referred to as fossil or relict beaches.

Within the British Isles, there is a large potential supply of shingle-sized material (as described above). However, the supply of finer-grained sediment, such as sand, is significantly greater than that of shingle, therefore, most beaches should be dominated by sand-sized material. The reason why this does not occur extensively and why shingle dominates has been attributed to the nature of the wave climate (Vincent, 1979). Swell waves (ie of low amplitude and long period), occur commonly on oceanic coastlines and tend to move sand inshore to accumulate on the beaches. With storm waves (locally-generated with a short wave period); sand is carried offshore and accumulates in banks or bars. Shingle tends to move onshore, however, as a constructional response to storm waves.

The high storm / swell wave ratio experienced around the British Isles means that sand moves offshore easily, leaving the shingle behind on the beach and in the nearshore regions. A tendency for the sand eroded from cliffs to move offshore at the ness sites in East Anglia has also been observed by Vincent (1979); this was seen as a means of maintaining a high shingle to sand content on the beaches in this region.

1.1.4. Beach Composition.

The composition of shingle beaches, in terms of lithology and size-shape parameters, depends upon: the composition of the supply; the durability of the clasts; and exposure to wave activity.

Geological materials which have a low durability, such as limestones, are common in some areas; they are usually restricted to the proximity of their source, due to their short life-span. Flints and cherts are highly durable, forming a disproportionate percentage of clasts on many beaches (for example, 98.5% on Chesil Beach (Carr, 1971)).

The size and shape of clasts on the beach differ from their source, due to the process of abrasion. Clast size may be very gradually reduced by abrasion, or more rapidly reduced by fracturing. The shape of the clasts should, in theory, approach spheres with increasing maturity; however, there is conflicting evidence as to whether or not this modification of shape actually occurs (Carr, 1983). Pebble shape may be controlled by lithology; for example, the greywackes described by Bluck (1967) tend to fracture to form discs and blades. Likewise, large cobbles have been shown to display a higher sphericity than smaller pebbles (Bray, 1990).

Regarding the angularity of the clast, there is little doubt from the published literature that beach clasts become more rounded with time; however, periodic breakage will have the opposite effect. Larger pebbles and cobbles display a greater degree of roundness than their smaller counterparts (Carr, 1983).

Mixed beaches are of two types. The first is a composite structure, consisting of a ridge of shingle or mixed sand and shingle, to seaward of which there is a wide sandy lower foreshore. The second mixed beach type consists of fairly equal proportions of sand and shingle, which vary in concentration both in the longshore and the cross-shore directions.

1.1.5. Beach Structure.

The internal structure of shingle beaches is difficult to study because, unlike sandy beaches, trenches excavated for investigation purposes cannot stand up vertically. Shingle beaches preserved in the geological record display a coarsening upwards cycle together with trough cross bedding. Examples of ancient beaches are found in the Upper Cretaceous of Alberta (Hart and Plint, 1989).

The changes in beach structure, in terms of clast size and shape, is an important part of beach development, (Bluck, 1967). Sorting of clasts by shape occurs due to the different hydraulic

response of discs and blades, to spheres and rods, on the beach. Discs and blades tend to be pushed up the beach by swash where they remain; this is in contrast to the spheres and rods, which are rolled back down the beach under the action of the backwash. The ability of different pebble shapes and sizes to migrate within and across the beach face is seen also as an important size-shape sorting mechanism. On the basis of studies undertaken on the shingle beaches of South Wales, Bluck (1967) has defined four distinct zones: to the seaward side, an outer frame of spherical cobbles; adjacent to an infill zone of spherical cobbles, with rod-shaped pebbles; an imbricate zone of mainly disc-shaped pebbles; and a large disc zone on the landward side (Figure 1.1). Bluck (op cit.), identified also the "sand run", which separates the landward zone of imbricated disc-shaped particles from the seaward large cobble frame.

1.1.6. Mixed Beaches.

Mixed beaches show a strong bimodal character in their grain size distributions (Kirk, 1980), which may represent mixing of two end members of the sediment population (Folk and Ward, 1957). Alternatively, the distribution of sand and shingle, within a mixed beach, may result from a combination of bed roughness, settling velocity and thresholds for sediment transport (Inman, 1949; McLean and Kirk, 1969).

The internal structure of a mixed beach is more complex than that observed for shingle structures. Below the surface layer of mobile pebbles, a mixed beach becomes less permeable, as the interstices between the pebbles and cobbles is filled with sand-sized material (Petrov, 1989). Distinct layers of sand may also be present (McFarland et al, 1994).

The degree of interdependence exhibited by the separate fractions on a mixed beach is not well understood. Some degree of hybridisation of the material occurs: this is exhibited most commonly as a spatial and temporal variation in the beach surface, between rough shingle and smooth sand.

1.2. Shingle Beach Profile Characteristics.

1.2.1. Beach Terminology.

The basic terminology for a shingle beach profile is shown in Figure 1.2. The definitions presented below are based upon those given in the Shore Protection Manual, (CERC 1984).

Backshore: That zone of the shore or beach lying between the foreshore and the coastline which only experiences wave action during severe storms.

Bar: An embankment of sand or gravel build seaward of, but as an integral part of, the main shingle beach.

Beach Face: The section of the beach normally exposed to the action of the wave uprush.

Beach Ridge or crest: An accumulation of beach material above high water mark, with a steep seaward face and a horizontal or landward dipping backshore. Several ridges may occur on the same beach, representing different high water levels.

Foreshore: The area of beach between the ordinary low water mark and the seaward side of the main beach crest.

Littoral Zone: The area between the base of the sea cliffs (or seawall) across the beach and to a water depth where the ability of waves to cause sediment transport is limited (generally taken as 18m, for shingle).

Offshore: The area extending to seaward of the breaker zone to the edge of the continental shelf.

Step: A submerged ridge occurring at the point of wave breaking (also known as the break point step).

1.2.2. Beach Profile Response to Hydrodynamic Forces

Shingle beaches respond rapidly to wave action by altering their profile, as they attempt to reach an equilibrium in which offshore and onshore transport rates are equal. On the basis of model studies, two basic profile shapes have been shown to exist (Powell, 1990) (as outlined below).

- A step profile, formed by waves of low steepness and associated with accretion (synonymous with summer, swell and accretional profile);
- and, a bar profile, formed by waves of high steepness and associated with erosion (synonymous with winter, storm or erosional profile).

In the natural environment, waves occur randomly and the beach is unable to reach an equilibrium profile. Profile formation is further complicated by changing water levels, in response to tides. Some doubt exists as to whether the bar profile can fully develop on natural beaches (Powell, 1990).

The following hydrodynamic factors have been shown to be important characteristics which influence the profile development of shingle beaches: (i) wave height; (ii) wave period; (iii) wave duration; (iv) water level; (v) angle of wave attack; and (vi) spectral shape of the wave energy distribution.

Wave height and period significantly influence the development of the profile (van der Meer, 1988; Powell, 1990). An increase in the wave height appears to have the effect of lengthening the surf zone, where the wave energy is dissipated. Increasing the wave period seems to have the effect of moving more material above the still water level, raising the elevation of the main crest. A compensatory reduction in the volume of material is found below the step point of the profile (Powell, 1990).

In model tests, it has been shown that the profile evolves rapidly, approaching its equilibrium profile at an early stage. Longer durations of wave attack allow only minor adjustments to the final profile (Powell, 1990). This pattern is manifested on a natural beach, which may alter in response to individual waves within a train.

Varying water levels influence the beach, by moving the profile up and down along the still water level; they do not, however, alter the dimensions of the profile (Kemp, 1963). In nature, the potential exists for water levels to indirectly affect the profile formed, by modifying the waves incident to the shoreline.

1.2.3. Effects of Beach and Sediment Characteristics on Beach Profile Development.

In addition to the hydrodynamic controls on profile development, the following parameters may influence the equilibrium profile: (i) initial beach profile or slope; (ii) beach material size; (iii) beach material grading; (iv) shape of beach material (v) effective depth of beach material and; (vi) foreshore levels.

Conflicting evidence exists as to whether the initial slope influences the final profile or not. Van der Meer (1988) is amongst those who found that the slope had no effect; however, Sunamura and Horikawa (1974), found that the final profile shape did depend on the initial slope. A possible explanation for such contradictions is that the initial slope may influence the mode of wave breaking (ie spilling or plunging); hence, the critical value which determines whether or not the beach is erosional or accretional is bridged (King, 1972). Powell (1990) has suggested that whilst the initial slope may affect the mode of formation of the equilibrium profile, along its active length, the final shape would be the same.

Beach material has been shown to control the angle of repose, or gradient, of the beach. Investigations undertaken by Bagnold (1940), Meyers (1933) and Bascom (1952), all confirm that coarser-grained material forms a steeper slope. Model experiments have examined the response of the entire profile to differences in the mean grain size (van Hijum, 1974; van der Meer, 1988; and Powell, 1990). The results of the model experiments have demonstrated that mean grain size influenced the slope of the beach face and the horizontal position of the main features (for example, the crest-line). The crest height seems to depend more upon wave run-up than on mean sediment diameter (van der Meer, 1988). The differing effects of the mean grain size on the profile also seem to be influenced by the wave steepness (Powell, 1990).

The equilibrium profile of a shingle beach is steeper than on sandy beaches, typically with a

slope of 1:7 to 1:10. Incoming waves and swash percolate into the beach to a much higher degree than on sand beaches; the result is that the backwash is weakened and shingle tends to be pushed onshore by wave action. However, due to the low water retention exhibited by shingle beaches, there can be a higher exfiltration during the backwash; this enhances the offshore transport of spherical and rod-shaped particles (Bluck, 1967).

Because shingle beaches form steeper profiles, waves tend to propogate further inshore before breaking; consequently, breaking is then confined to a narrow zone on the beach. Further, due to the rapid decrease in water depth experienced on shingle beaches, refraction of waves may be incomplete at the point of breaking; breaking wave angles are, therefore, greater than those experienced on sandy beaches where refraction occurs over a longer distance.

Shingle beaches rely on their permeability to maintain their profile shape (Nicholls and Webber, 1988). The presence of impermeable layers within the beach, can lead to destabilisation of the beach; an extreme example of this being where a shingle beach overlies a sloping concrete or stone apron.

Powell (1990) divided beaches into three categories, depending upon the ratio of the mean sediment size (D_{50}) to the effective depth of beach (D_B), as follows;

- $D_B/D_{50} \geq 100$ (1.1 (a))
- $30 < D_B/D_{50} < 100$ (1.1 (b))
- $D_B / D_{50} < 30$ (1.1 (c))

In case 1.1(a), the effective thickness of the beach is sufficient to have no influence on the profile development, whilst in case 1.1(c) the beach structure will break down and the upper beach layers will be eroded. In case 1.1(b), the crest is displaced horizontally in the landward direction, depending upon the wave steepness (Powell, op cit).

Mixed beaches, due to the presence of sand infilling the voids between the shingle particles, exhibit a lower permeability than their pure shingle counterparts. Reflection of wave energy from a beach increases with beach slope, but decreases with increasing permeability (Kobayashi et al, 1992). Hence, mixed beaches should be associated with a high level of

reflected wave energy as they are both steep and have a lower permeability (Davidson et al, 1994). Powell (1988) found that reflection from shingle beaches was around 10%, regardless of the grain size. This investigation concluded that the main cause of energy dissipation on shingle beaches was frictional energy loss on the beach surface rather than by percolation.

1.3. Hydrodynamic Factors Acting as Process Controls.

1.3.1. Terminology.

The terminology used here to describe tidal and wave activity on a shingle beach, is shown in Figure 1.3. The accompanying definitions are based upon those presented in the Shore Protection Manual (CERC, 1984) and the Admiralty Tide Tables (1991).

Breaker zone: the position in the nearshore, where incoming waves become unstable and break - if the waves are of a uniform height and period, so that the waves break in the same place, a breaker line or point is defined.

Highest Astronomical Tide, (HAT): the highest water level which can be predicted to occur under any combination of astronomical conditions and average meteorological conditions.

Lowest Astronomical Tide, (LAT): the lowest water level which can be predicted to occur under any combination of astronomical conditions and average meteorological conditions.

Mean High Water Springs-Neaps (MHWS-MHWN): the average throughout the year of the two highest tides occurring within a 24hr period, when the tidal range is at its highest / lowest.

Mean Low Water Springs-Neaps, (MLWS-MLWN): the average throughout the year of the two lowest tides occurring within a 24hr period, when the tidal range is at its highest / lowest.

Mean Sea Level, (MSL): is the average level of the sea surface over a period of time.

Nearshore Zone: an indefinite zone extending seaward from the shoreline, to well beyond the breaker zone.

Offshore: the area extending to seaward of the nearshore zone, to the edge of the continental shelf.

Surf Zone: part of the nearshore zone between the landward side of the breaker zone and the seaward side of the swash zone - on a steep shingle beach, the breaker zone and the swash zone lie beside each other and the surf zone is eliminated.

Swash Zone: part of the nearshore region, where the beach is alternately covered by wave run-up and exposed by backwash.

The zones which refer to wave activity are not fixed and will vary, depending upon wave conditions, tidal state and water level.

1.3.2. Waves and Wave - Beach Interaction

Wave Generation and Deep Water Processes

Wind blowing over a water body transfers energy across the air-water interface, which is manifest in the generation of waves and surface currents. The waves, in turn, transfer energy to the beach and nearshore areas inducing sediment movement. An understanding of the processes of wave generation, propagation, and the breaking of waves; within the present study is a necessary precursor to the examination of regional beach and nearshore morphological changes.

The turbulent nature of the wind, as it blows over the water surface, causes random stresses and, hence, random pressure fluctuations on the surface of the water. The movement of these pressure fluctuations over the surface is responsible for the early generation and growth of waves (Phillips, 1957). Subsequent wave growth and movement is facilitated by an induced pressure reduction at the top of, and on the downwind side of, the wave crest (Miles, 1965; Miles, 1967). The mechanisms of wave growth are comprehensively summarised elsewhere (King, 1972; Silvester, 1979; CERC, 1984).

In a developing sea (ie within the area of wave generation), there are a range of wave

frequencies, heights and directions generated. The culmination of this interaction is represented in terms of a wave spectrum. Short waves receive proportionally more energy than long waves, because they travel more slowly and offer more resistance to the wind. Long waves derive energy by scavenging the energy of shorter waves, in a variety of complex non-linear processes (Longuet-Higgins, 1969; Hasselmann et al, 1973).

Waves within the proximity of their area of generation are referred to as sea, or as storm waves if on the coastline (King, 1972). As waves propagate outside the generation area, the wave front spreads out both radially and circumferentially; hence, the amount of energy per unit width of the wave crest declines, in both space and time (Carter, 1989). As the wave field develops, the nature of the wave spectrum changes in response to various wave-wave and wave-current interactions. Long waves travel faster than short waves in deep water, so that the various components of the spectrum begin to separate out along the line of propagation. Short waves use proportionally more energy to overcome viscosity effects and decay more quickly. On a coastline which is some distance from the generating site, only the long period low amplitude waves are experienced. Waves of this nature are referred to as swell, (King, op cit).

Shallow Water Effects

As waves move from deep water into shallow water, they undergo a number of changes induced by interaction with the bottom. This modification may be such that the wave conditions experienced on the beach bear little resemblance to the deep water waves from which they were derived. It is important to understand shallow water wave transformations: it is the products of these which ultimately transport sediment in the nearshore and beach environments.

Deep, intermediate and shallow water waves are defined in terms of the ratio of water depth to wavelength, as shown in equations 1.2 - 1.4.

- deep water, $d/L > 0.5$ (1.2)
- intermediate water, $0.5 < d/L > 0.05$ (1.3)
- shallow water, $d/L < 0.05$ (1.4)

Equations to determine wavelength and wave speed (phase velocity), derived from linear wave theory (Airy, 1845), are presented in Table 1.2.

In intermediate and shallow water depths, interaction between wave-induced orbital velocities and the sea bed lead to a transfer of energy from the waves to the bed. Shoaling of waves is the change in wave height, due to the conservation of energy flux. The wave height decreases slightly at first, then continues to increase until the point of breaking. Refraction is the bending of the wave crests parallel with the bottom contours, occurring as the wave crest passes obliquely over the sea bed contours. Morphological changes on the beach and nearshore areas are related to: the effects of wave caustics, areas of crossed orthogonals which are indicative of high wave convergence (Chao, 1970); wave diffraction, the lateral transfer of energy along a wave crest; and wave reflection; the seaward return of a wave caused by a structure or a sharp reduction in bathymetry. All of these factors are summarised by Carter (1989).

Wave Breaking

Wave breaking occurs when the horizontal water velocity at the crest exceeds the wave group velocity (Carter, 1989). The criterion for breaking has been calculated from solitary wave theory (McCowan, 1894), when the ratio of breaking wave height to water depth is 0.78.

ie. $H_b / d_b = 0.78$ (1.5)

In practice, waves are found to break at a wide range of values, depending upon factors such as the wavelength at breaking and the beach slope. The mode of wave breaking depends upon wave height, wavelength and beach slope.

There are two parameters used to describe wave types; these are the surf similarity parameter (Σ), (Iribarren and Nogales, 1949) and the surf scaling parameter (ϵ) (Carrier and Greenspan, 1958). The parameters are defined as follows (after Battjes, 1974) and (Guza and Inman, 1975), respectively:

$$\Sigma = \tan \beta / (H_o / L_o) \quad (1.6)$$

$$\epsilon = (Hb / 2 . \sigma^2) / (g \tan^2 \beta) \quad (1.7)$$

where β is beach slope and σ is the wave radian frequency.

Using the surf similarity index at the point of breaking (ϵ_b), a number of classes of breaking waves can be defined.

$\epsilon_b < 0.64$ = spilling breakers

$0.64 > \epsilon_b < 5.0$ = plunging breakers

$\epsilon_b > 5.0$ = surging breakers

A particular type of plunging breaker occurs when the front face of the wave breaks at a point below its maximum elevation; this is referred to as a collapsing breaker.

The characteristics of breaker types has been described by Galvin, (1972), as summarised below.

Spilling: Foam, bubbles, and turbulent water appear at the wave crest and eventually cover the front face of the wave. Spilling starts at the crest, when a small tongue of water moves forward faster than the wave form as a whole. In its final stages, the spilling wave evolves into a bore or an undulatory bore.

Plunging: The whole front face of the wave steepens until vertical; the crest curls over the front face and falls into the base of the wave; and a large sheet-like splash arises from the point where the crest touches down.

Collapsing: The lower part of the front face of the wave steepens until vertical; this front face curls over as an abbreviated plunging wave. The point where the front face begins to curl over is landward of, and lower than, the point of maximum elevation on the wave.

Surging: The front face and crest of the wave remains relatively smooth and the wave slides

up the beach, with only minor production of foam and bubbles; this resembles a standing wave.

After breaking, waves usually continue to the shoreline as small-scale surges or bores, within the swash zone. Final energy dissipation is achieved by the run-up of the wave swash, combined with percolation through the beach sediments.

Wave breaking on shingle beaches is confined to a narrow zone close to the shoreline; this is due to the sharp change in slope which occurs between the steep shingle beach and the relative flat lower foreshore. It is normal on a shingle beach to have a single line of plunging breakers. Because of the narrowness of the breaker zone, large amounts of wave energy are expended over relatively short distances, resulting in a very dynamic environment.

1.4. Shingle Mobility and Transport

1.4.1. Shingle Threshold and Transport

Sediment transport can be divided into two modes: bed-load transport; and suspended-load transport (McDowell, 1989). In the case of shingle, such transport is restricted to sliding and rolling of pebbles and cobbles along the bottom, as bed-load.

The minimum velocity required to dislodge and move a sediment particle is called the threshold velocity. Early studies undertaken on the threshold of sediment transport were by Hjulstrom (1935) and Shields (1936).

Shingle movement is initiated when the stresses applied by the movement of water over the bed exceed the forces of friction and gravity, which resist movement. The threshold of shingle movement has been shown to depend upon the size and shape of the individual clasts, their relationship to the neighbouring clasts and the flow characteristics (Muir Wood, 1970; Dyer 1986; and Evans and Hardisty, 1989). For a given current velocity, particles of the same shape and size may or may not move, depending on their orientation and relative position. For example, consider a clast resting on top of a bed of shingle. If the clast is larger than its neighbours, it presents more surface area to the flow of water and a large drag force is applied. The clast will tend to roll over easily, if the centre of gravity is located above the pivot about

which the clast would rotate (Figure 1.4(a)).

If the clast is resting in a position where the neighbouring grains afford a high degree of shelter, the drag on the clast is less. Moreover, if the clast pivot is above its centre of gravity, stresses are transferred to neighbouring grains through the points of contact (Figure 1.4(b)).

The threshold of shingle movement, with respect to grain pivot angle and bed-slope, has been investigated by Evans and Hardisty (1989). These experiments have shown that, prior to the initiation of movement of a clast, instability is indicated by a high speed vibration of the grain within its bed pocket.

'In-situ' acoustic measurements of marine gravel movement in the Solent has been undertaken by Thorne et al (1989) and Williams et al (1989), in association with the analysis of current data. The results of these experiments were used to demonstrate that shingle transport could occur in deep water (20 m), under the influence of tidal currents alone.

Flow over the shingle bed was seen to be turbulent, with the intermittent development of: sweeps (inrushes of high velocity fluid directed towards the bed); and ejections (upwelling of lower velocity fluid, from the near-bed region). Sweeps were shown to raise the localised shear stress on the sea bed, to a value which was sufficient to overcome the threshold value and initiate particle movement. Ejections were found to have little or no effect on the shingle; they did not normally result in an exceedence of the threshold value.

The effects of waves on offshore shingle accumulations may combine with tidal currents to exceed the threshold values (Dyer, 1986). Wave action alone is not thought to cause any significant movement below a water depth of 18 m. In water depths less than 18 m, the asymmetrical nature of the wave orbits may induce a shoreward migration of shingle (Muir Wood, 1970).

The mechanisms of shingle transport on beaches are likely to differ from those operating offshore. The driving forces (breaking waves, swash and backwash) are processes in which large amounts of energy are transferred to the beach, in a series of highly turbulent interactions. In the case of plunging breakers, large amounts of wave energy are expended at

the point of breaking. Some of this energy may be used to disturb or lift shingle-sized material momentarily off the bottom, displacing it in the direction of the applied force. A similar situation exists in the swash zone, where the uprush of water transports material landward and backwash returns the material seawards. Net shingle transport in the breaker and swash zones is related, therefore, to the direction of the highest velocities achieved which initiate movement i.e. not in the direction of the vector, which represents the residual wave velocity combined with the tidal current velocity (Muir Wood, 1970).

The mode of transport of shingle under wave action may take the form of a rolling, shuffling or sliding of clasts (Muir Wood, op cit.). A situation in which the whole surface layer of the beach is mobilised and creeps seaward has been identified, by Bluck (1967). Such motion is controlled by water percolation and the subsequent backwash of waves.

1.4.2. Longshore Sediment Transport Formulae.

The majority of longshore transport studies have been conducted for sand-sized material (Caldwell, 1956; Inman and Bagnold, 1963). On the basis of these studies, a variety of longshore transport equations have been proposed, (CERC, 1984; Kamphius et al, 1986). Van der Graaf and van Overeem (1979), have compared a number of these longshore transport formulae, finding considerable discrepancies between the various calculations.

Transport mechanisms on shingle beaches are less well understood than their sand equivalents, due to: (i) the rarity of shingle beaches in those countries, where the majority of beach research has been carried out (for example, the USA and Holland); and (ii) the difficulty involved in collecting field data on the bed-load transport of shingle in a high energy beach environment. The measurements which exist, tend to be have been undertaken over the medium-term (single tidal cycle), or the long-term (annual accumulation rates); there is, as yet, no means of readily recording the short-term response of shingle to wave action on beaches.

Processes on shingle beaches are very different from those which are associated with sand beaches. For example, sediment transport is restricted to a narrow band, comprising the breaker and swash zones; within this zone, processes are likely to be highly turbulent. In addition, shingle transport occurs primarily as bed-load, compared to a combination of bed-

load and suspended sediment load, typical of sandy beaches (Komar, 1978). Transport formulae which have been derived specifically for sand beaches may not therefore, perform well on shingle beaches.

Formulae used for estimating the longshore transport of shingle

(1) CERC Formula

Despite the differences in processes between sand and shingle beaches, one of the most widely-used transport formula for shingle has been the CERC formula (Chadwick, 1987) (the CERC formula is described in the Shore Protection Manual (CERC, 1984)). The CERC formula is based upon the calculation of the empirical relationship between the amount of available energy, from waves approaching at an angle (α) to the shoreline, and the resulting amount of longshore movement.

The volume of material transport alongshore (Q_{ls}) is given by:

$$Q_{ls} = K_1 P_{ls} \tag{1.8}$$

where the longshore component of wave energy flux P_{ls} is;

$$P_{ls} = (EC)_b (\sin 2\alpha_b / 2) \tag{1.9}$$

E is the wave energy flux in the surf zone,

$$E = \rho g H^2 C / 8 \tag{1.10}$$

Therefore,

$$P_{ls} = (\rho g H^2 C^2 \sin 2\alpha_b) / 16 \tag{1.11}$$

Alternatively, the wave energy flux can be related to the immersed-weight transport rate of sediment (I_s):

$$I_{ls} = K_2 P_{ls} \quad (1.12)$$

where K_2 is a dimensionless coefficient. I_{ls} can be related to the volume of material transported Q_{ls} by,

$$I_{ls} = (\rho_s - \rho) g a' Q_{ls} \quad (1.13)$$

where a' is the pore space factor, often taken as being equal to 0.6 (Muir Wood and Fleming, 1981).

A value for $K_2 = 0.29$ is given by Komar (1989), as being typical of sand beaches. Analytical studies (del Valle et al, 1993), have shown that calculated values of K_2 decrease with increasing grain size for material with a $D_{50} > 0.5$mm.

These studies are supported by the results of two tracer studies using aluminium pebbles, undertaken at Hengistbury Head (Wright, 1982) and at Hurst Spit (Nicholls, 1985). For these studies K_2 values of between 0.003 and 0.044 were obtained (Nicholls and Wright, 1991); ie K_2 are 1 to 2 orders of magnitude lower that the value used on sandy beaches. Whitcombe (1995) obtained K_2 values of 0.033 to 0.056 using aluminium pebbles on beaches in Hayling Island. Comparable K_2 values of between 0.021 and 0.061 were obtained at Shoreham (Chadwick, 1989). The recorded values for K_2 on shingle beaches compare well with the starting value of K_2 (0.02), used prior to calibration in model studies (Brampton and Motyka, 1987). More recently however, van Wellan et al (1999) obtained a value of K_2 equal to 0.35 on a mixed sand and shingle beach at Shoreham on the south coast of England. These latter results were based on a small tracer sample (15).

Various modifications have been made to the basic CERC formula to take account of particle size (Brampton and Motyka, op cit; Chadwick, 1989).

(2) Kamphuis formula

Kamphuis et al (1986) have derived a formula for calculating sediment transport (Q_{ls}), in terms of: beach slope (β); significant breaking wave height (Hb_s); grain diameter, (D); and breaking wave angle (α_b).

$$Q_{ls} = 1.28 ((\tan \beta \ Hb_s^{3.5}) / D) \sin 2 \alpha_b \qquad (kg / s) \qquad (1.14)$$

Whilst the formulae was derived for quartz sand transport, Kamphuis (1992) has suggested that it could also be applied to coarse-grained beaches as it contained both beach slope and grain size terms.

(3) Morfett Virtual Power Formula

Morfett (1989) has derived a shingle transport formula, based upon tracer and sediment trap experiments undertaken on beaches in Sussex. The formula consists of two parts, the threshold criterion and the transport equation; these are described below.

The threshold criterion, which depends upon water depth (d) and particle size (D_{50}) was derived from the laboratory data of van Hijum and Pilarczyk (1982).

$$H_{cr} = 2.0 D_{50} + (0.087 d_{cr} \log (1000 D_{50})) \qquad (1.15)$$

where H_{Cr} is the critical wave height.

Morfett's transport equation was based upon the laboratory data of van Hijum and Pilarczyk (1982) and the Shoreham trap data, Chadwick (1989):

$$Q = K \ ((pu_+^3 - pu_{+cr}^3)^{1.5} (\sin \theta)^{0.75}) / (g (\rho_s - \rho) D_{90}^2) \qquad (1.16)$$

where K is a calibration coefficient of the order of 2.84×10^{-5} and; the expression $(pu_+^3 - pu_{+cr}^3)$ is termed the virtual power (P_+).

and (u_+) is given as;

$$u_+ = (((\rho g^{1.5} H^3) / (4 H^{0.5} L)) / \rho)^{1/3} \qquad (1.17)$$

The equation is solved for all wave types present in the spectrum and, subsequently, the resulting transport rate can be calculated.

4. Delft Formula

The original Delft formula was derived on the basis of the dimensional analysis of laboratory experiments using random waves (van Hijum and Pilarczyk, 1982). However, the original form of the equation was difficult to apply (Chadwick, 1989). The results were reanalysed by both Chadwick (1989), and van der Meer (1990). Whilst the versions of the Delft equation produced by Chadwick (op cit), and van der Meer (op cit) are very similar, it has been the latter version which has been used most widely:

$$Q_{ls} = 0.0012\ g\ D_{n50}\ T_p\ (H_s . \sqrt{\text{Cos}\ \beta} / D_{n50}) . ((H_s . \sqrt{\text{Cos}\ \beta} / D_{n50}) - 11) . \sin \beta \qquad (1.18)$$

where

$$D_{n50} = (M_{50} / \rho_s)^{1/3} \qquad (1.19)$$

and Q_{ls} is in (m^3 / s).

1.5. Field Measurement of Longshore Transport

1.5.1. Trapping

The principle behind trapping techniques is to collect material moving in a longshore direction. Since relatively large robust traps are required for shingle entrapment, the trap is likely to interfere with the prevailing hydrodynamics in the area where material is being collected. Further, because the longshore transport component of shingle movement is small compared to the gross component of onshore - offshore transport (Quick, 1991), the efficiency of traps is reduced.

Since each trap can only sample at a single location, the interpretation of trap data (in terms of the full extent of the beach) is difficult.

1.5.2. Tracers

Tracers used in beach experiments are either natural or artificial materials; these can be distinguished from the native beach in the experimental area. The principal of the technique is that the tracer material can be identified after a specific period on the beach; its displacement from the injection point is recorded, then related to wave and tidal action. By assuming that the displacement of the tracer is representative of the displacement of the mobile beach, sediment transport rates and directions (at least, for the duration of the experiment) can be assessed.

In order to achieve acceptable results in such studies, a tracer should satisfy the following criteria:

- represent the indigenous beach material as closely as possible - including the size and grading, the shape, specific gravity and surface roughness of the beach material;

- be identifiable at low concentrations within the background beach sediments; and

- be resistant to impact and chemical reaction.

It is extremely difficult to identify a tracer method which fulfils all of the above criteria: the final selection is dictated often by the nature and duration of the experiment (and financial considerations).

Painted pebbles and resins are probably the simplest and most economical method of marking pebbles, for tracing on shingle beaches (Zenkovich, 1967; Kidson and Carr, 1959; and Caldwell, 1983). The main problems associated with the use of painted pebbles is the durability of the paint or resin, together with the likelihood of interference from the public.

Radioactive tracers are inconspicuous and can be treated with an isotope, whose half life is suited to the duration of the experiment. The method is best suited to sand and silt-sized material, although Kidson and Smith (1956) have used radioactive plugs in pebbles with some success. The main problems which arise are costs, combined with public concern over the use

of radioactive materials.

Fluorescent pebble tracers were used originally by Reid and Jolliffe (1961). Dye was incorporated into artificial pebbles, made of concrete and dolerite aggregate. Natural pebbles coated with fluorescent resins were used later by Kidson and Carr (1971).

Foreign rocks and materials may be added to the natural beach; examples include broken bricks and fireclay markers (Richardson, 1902) and natural rock of a different lithology (Carr, 1971). The material added may be difficult to identify and problems of inadequate mixing with the background beach material are difficult to overcome.

The most successful use of tracers have involved the use of aluminium pebbles (Wright et al, 1978; Nicholls and Webber, 1987; and Bray, 1990). The pebbles can be made to replicate the natural beach material, in terms of their size, shape and specific gravity. As a result, good mixing with the indigenous beach material can be achieved. Recovery of tracers, using metal detectors, allows high recovery rates to be achieved and the vertical distribution of tracers to be established. In addition, apart from radioactive tracers, no other tracing technique exists which allows detection of tracers below the surface of the beach.

1.5.3. Impoundment.

Beach plan surveys can be used to calculate the volumetric changes which occur within a specified area. In order to obtained estimates of longshore transport, it is necessary to impound the beach material against a substantial structure, for example a pier. If there is an exchange of sediment to / from the offshore area, then some idea of the volumes involved is required.

Beach plan surveys, carried out by experienced surveyors using electronic distance measuring (EDM) techniques, can be carried out to a high degree of accuracy. On the other hand, simplified techniques using measuring tapes to record distances on the beach can be fraught with inaccuracy. Over the longer term, aerial photograph can be used to estimate volumetric changes, Chadwick (1989).

1.6. Regional Sediment Budgets.

A sediment budget is a sediment transport volume balance for a particular section of coastline. Inputs or supplies to the system include: erosion of coastal cliffs or the foreshore; artificial renourishment; and from onshore or longshore transport. Outputs or sinks include the latter two mechanisms, along with attrition or artificial removal of sediment (CERC, 1984).

Coastal sediment budgets have been a means of studying coastal changes, since the original work of Johnson (1959).

Further examples include the approaches adopted by Inman and Frautschy (1965), Stapor (1971, 1983), Vincent (1979) and Reynolds (1987). The majority of these examples are from the USA, based upon the transport of sand-sized material. A shingle budget has been developed by Bray (1990), for beaches in South Dorset (Figure 1.5).

Sediment budget diagrams rely on the continuity of physical processes, over time. Secular changes and perhaps severe storm activity can affect the derivation of any sediment budget. Likewise, human interference, such as groyne building or the construction of sea defences, and beach replenishment / removal can all radically alter regional sediment budgets.

Particle	Wentworth (mm)	Krumbein (ϕ)
Boulder	> 256	> -8.0
Cobble	64 to 256	-8.0 to -6.0
Pebble	4 to 64	-6.0 to -2.0
Gravel	2 to 4	-2.0 to -1.0
Sand	1/16 - 2	-1.0 to 4.0
Silt	1/256 - 1/16	4.0 to 8.0
Clay	<1/256	>8.0

Table 1.1. Particle Size Classification after Wentworth (1922) and Krumbein (1934).

Deep Water (d/L >0.05)	Transitional Water Depth (0.05 > d/L > 0.5)	Shallow Water (d/L <0.5)
$C = gT / 2\pi$	$C = (gT / 2\pi) \tanh (2\pi / L)$	$C = (gd)^{0.5}$
$L = gT^2 / 2\pi$	$L = (gT^2 / 2\pi) \tanh (2\pi / L)$	$L = T (gd)^{0.5}$
$C_g = (gT / 2\pi)^{0.5}$	$C_g = (gT / 2\pi) ((1+(2\sigma d / \sinh 2\sigma d^{0.5}$	$C_g = (gd)^{0.5}$

Table 1.2. Examples of Linear Airy Wave Theory Equations, after (Carter 1989).

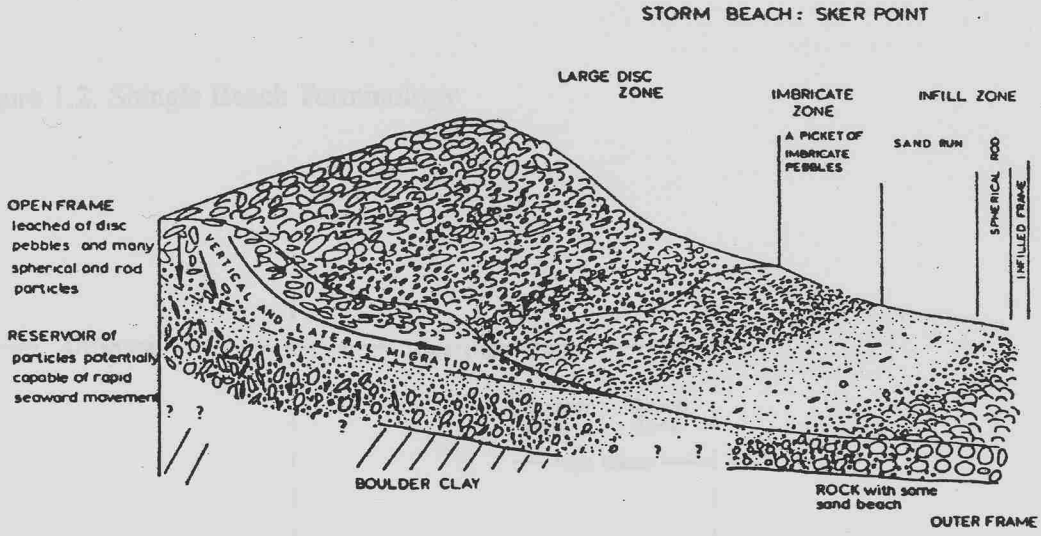

Figure 1.1. Shingle Beach Structure, in terms of shingle size and shape, (Bluck, 1967).

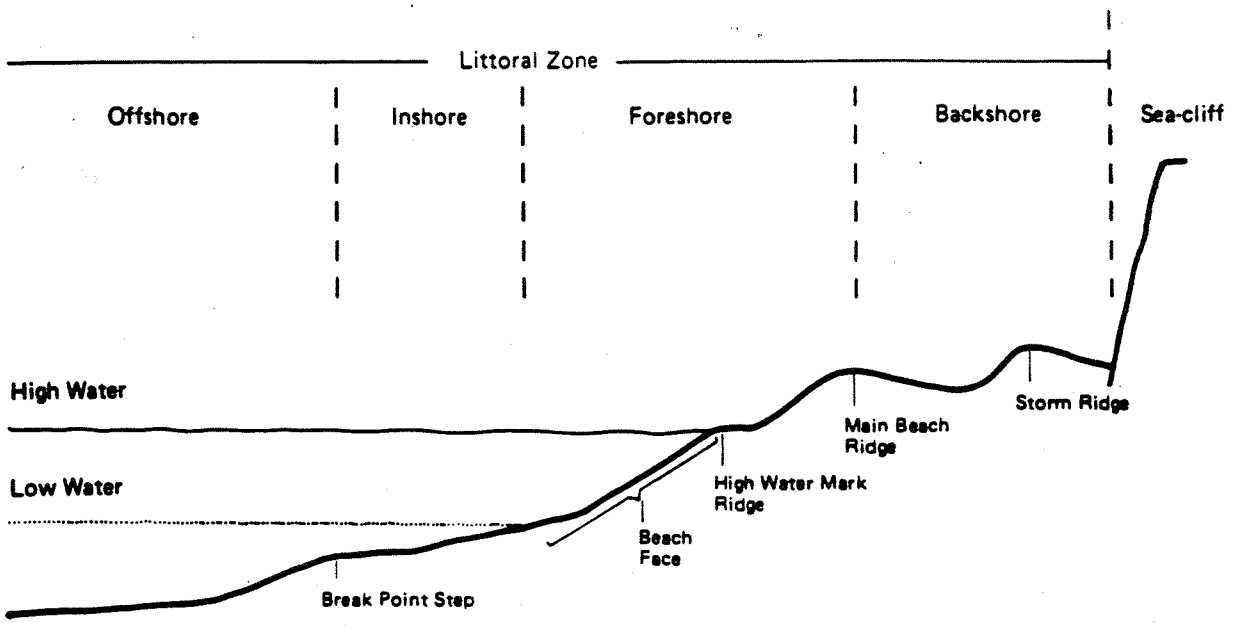

Figure 1.2. Shingle Beach Terminology

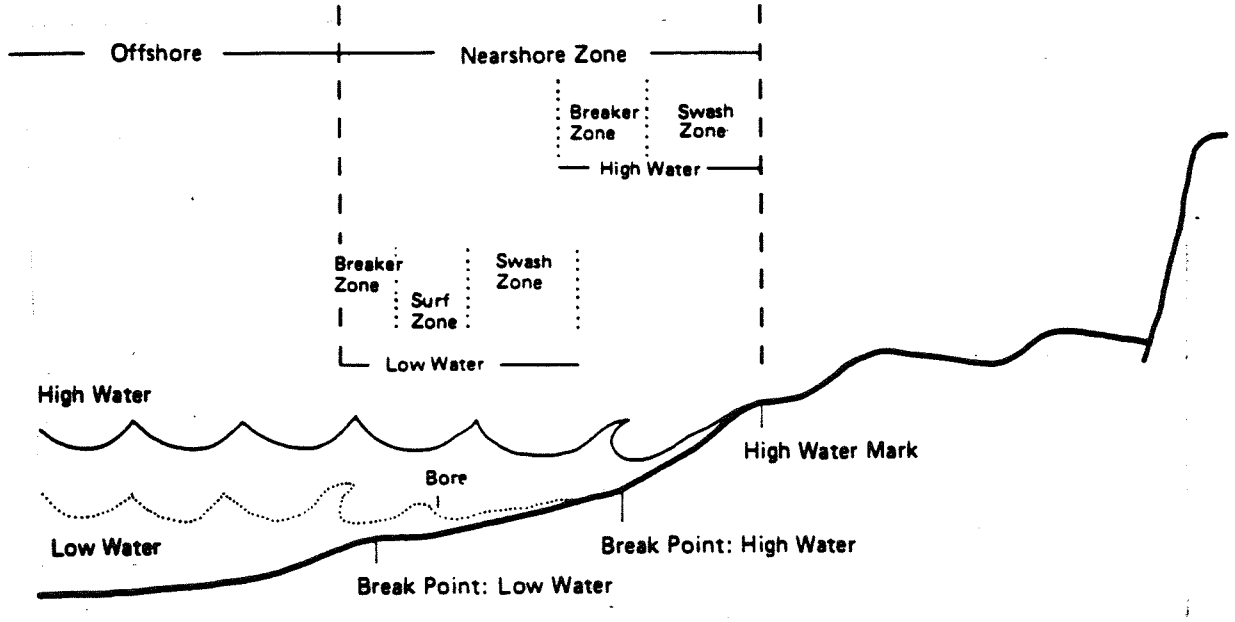

Figure 1.3. Terminology for Hydrodynamics on Shingle Beaches

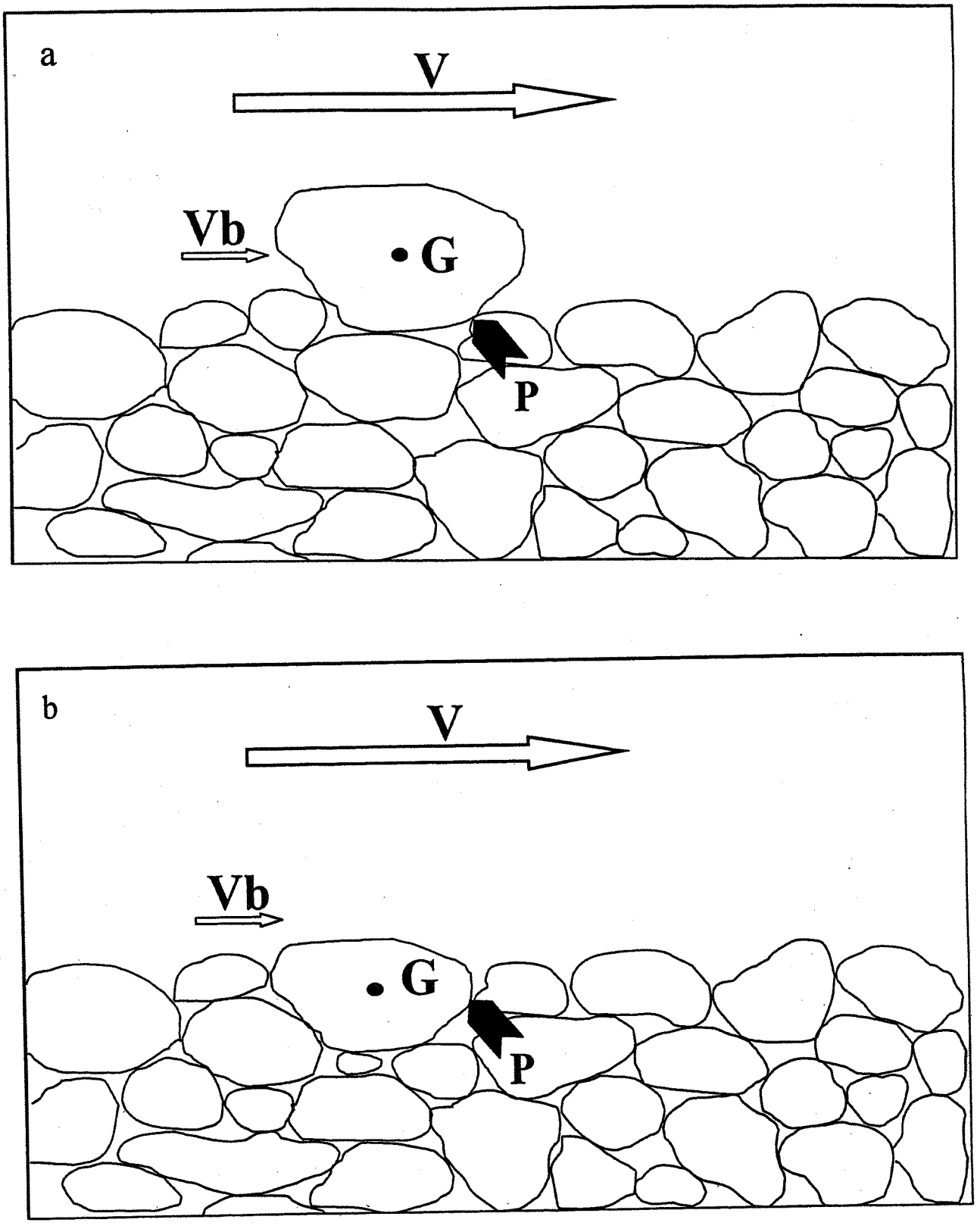

Figure 1.4. Influence of Particle Size and Position on Threshold of Movement: (a) large particle protuding from the surface of the bed, subject to overturning ; (b) uniform surface layer of particles with transfer of stresses to neigbouring grains. where G is the centre of gravity of the particle, P is the particle pivot point and Vb is the current velocity near the bed.

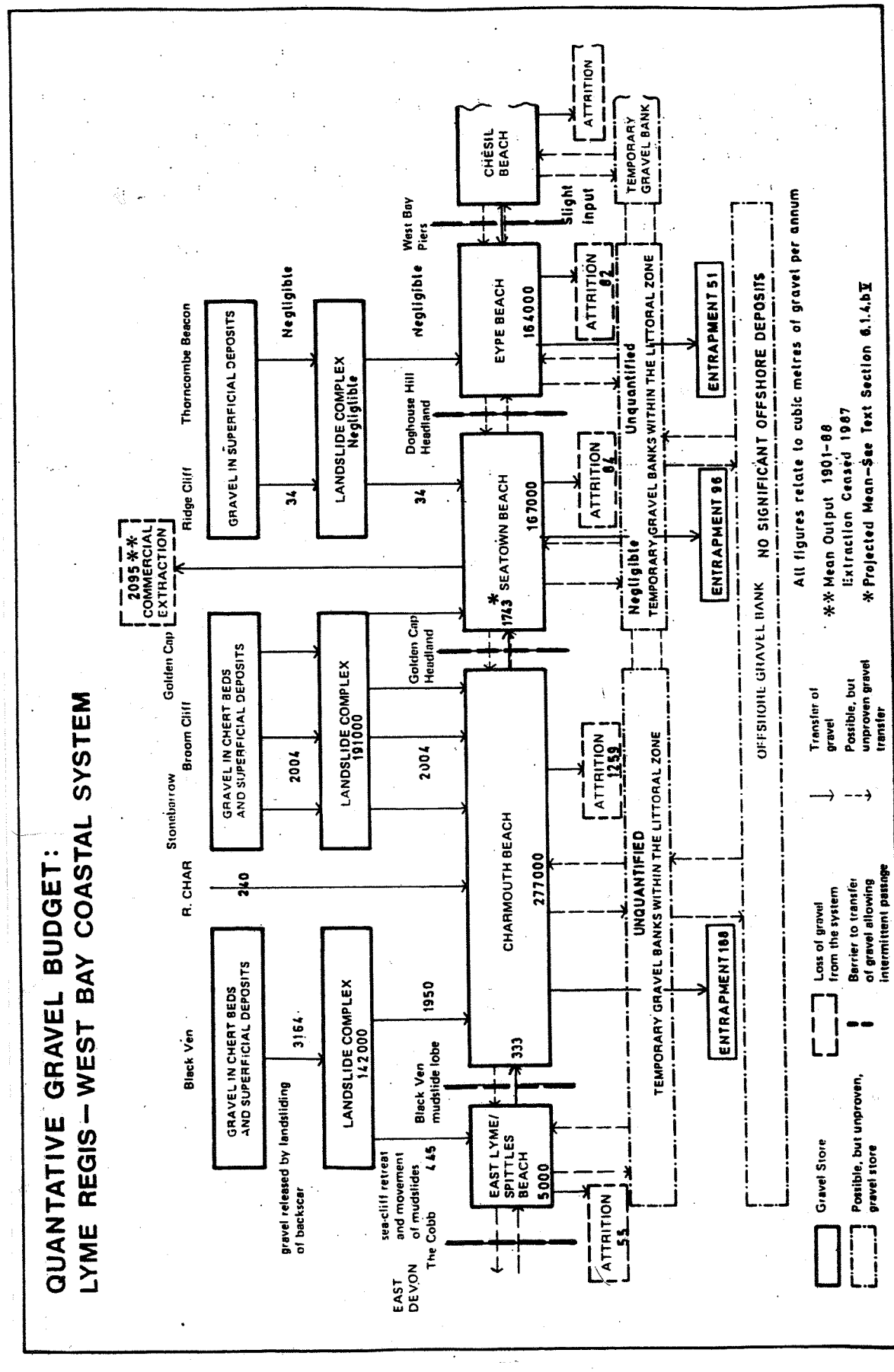

Figure 1.5. Typical Sediment Budget (after Bray, 1990)

Chapter 2. Area Under Investigation

2.1. Location and Geographical Setting

2.1.1. A Brief Description of the Coastline

The study area (Figure 2.1), is located on the northern coastline of Kent in the south-east of England. Like much of the rest of south-east England, the area is prone to coastal erosion due to the exposure of soft rocks along the coastline and a sea level which is rising relative to the land. Since Roman times it is estimated that a strip of land, up to 3 kilometres in width, has been lost to erosion, over the study area, So (1967).

The coastal zone shows a variety of topographies and land uses, Plates 2.1 ((a) to (g)). Herne Bay and Whitstable (Figure 2.2), are the main population centres at 35000 and 30000 respectively. The rest of the coastal zone within the study area is residential with the exception of the east and west ends which are characterised by low-lying farmland. The central section of the study area consists of graded clay slopes up to 30 metres in height, together with intervening low-lying areas. Apart from a short section of coastline, 3 km to the east of Herne Bay, the shoreline has been "fixed" by the construction of sea defences.

2.1.2. Slope stabilities

Instability of the coastal slopes has historically been a major problem along this particular section of coastline (Roberts and McGown, 1987). Details of failure mechanisms, a history of slope failures and the measures which have been undertaken to counteract slope instability are given by Canterbury City Council, (1984). Stabilisation of the coastal slopes has a direct impact on the coastal process in the study area as it has removed a major source of sediment supply, Canterbury City Council, (1993a)

2.1.3. Low-Lying Coastline

Within the study area there are sections of coastline comprised of low-lying land which has in the past been subject to erosion and flooding. These areas are protected now by seawalls and

beaches restrained by timber groynes. The predominantly shingle beaches themselves may be subject to erosion in response to variable longshore transport rates or beach draw down under wave attack however, to date there have been no investigations specifically carried out to determine shingle beach processes in the study area. As a result of localised beach erosion, shingle replenishment has been carried out on a regular basis.

Over the past 50 years there have been three storms which have caused severe flooding in the low-lying areas. These occurred in 1949, 1953 and 1978. The 1953 event was the most destructive of the three, causing widespread flooding to the commercial centres of Herne Bay and Whitstable, where flooding up to 2 m in depth was experienced (Plate 2.2, 2.3). To the east of Reculver, over 2000 hectares of farmland were flooded, (resulting in loss of livestock and crops), and the main road and rail links between London and East Kent were severed, McFarland and Edwards, (1998a).

2.2. Geology of the Study Area

The North Kent coastal zone has been recognised as a site of particular interest to geologists, since the mid-nineteenth century. The underlying and coastal geology is also important in coastal process studies as it controls the rates and patterns of coastal erosion, the coastal morphology and the supply of sediment to the beaches; these, in turn, provide subsequent controls on the regional and localised patterns of sediment transport. The geology of the area is summarised in Figure 2.3.

2.2.1. Nature of the Coastal Outcrops

(a). Upper Cretaceous Chalk

The Upper Cretaceous Chalk (100ma to 65ma) is exposed on the foreshore approximately 100 m to the east of the study area. Whilst there are no occurrences of chalk within the study area itself, these rocks are of great importance because they are the source of the flints, which dominate the shingle beaches in the south of England, Whitcombe (1995).

(b). Lower Tertiary - Sandstones

Overlying the chalks are the oldest Tertiary rocks exposed on the coastline. These deposits consist of fossiliferous sandstones and silty sandstones of the Thanet Sands (65ma to 56ma), the Woolwich Beds and the Oldhaven Beds (56ma to 53.5ma).

To the west of Reculver (Figure 2.2), the upper 8m of the Thanet Sands are exposed in the cliff section and on the foreshore. The exposure is typically a fine-grained clayey sandstone which becomes glauconitic (indicative of a marine origin) towards its upper part. A prominent layer of calcareous cemented sandstone (Plate 2.4), provides an important marker horizon; this lies some 4.8 m below the top of the Thanet Sands. The calcareous cemented layer is harder than the surrounding rocks and once undermined by erosion of the softer sands, breaks up to form large tabular blocks, typically 1 m across, which litter the foreshore west of Reculver.

Overlying the Thanet Sands are the Woolwich Beds, a sequence of fine-grained clayey sands and coarser shelly sands which are commonly glauconitic. The sands show cross-bedding indicative of shallow coastal environments, possibly with a deltaic or estuarine influence. The maximum thickness of the Woolwich Beds, at the coast is 7.5 m, Holmes (1981).

The Herne Bay member of the Oldhaven Beds is 6 m in thickness and has an erosive contact with the underlying Woolwich Beds. The basal layer consists of well-rounded black flints (Plate 2.5). Above the pebble beds are coarse sands showing strong cross-bedding; these grade into fine sands and, eventually, the silty clays which mark the base of the London Clay. Within the sandstones and silty clays, there are a variety of fossil shells, sharks teeth, fish bones as well as concretions of iron, gypsum and barite.

c. Upper Tertiary - London Clay

The coastline from Herne Bay to Seasalter is comprised of London Clay (53.5ma to 40ma), which has been drained, graded and provided with toe protection to prevent erosion and slippage. London Clay is exposed on the foreshore across the study area. The clay is uniform, steel blue - grey and very stiff (where fresh). Where weathered the rock is softer and light

brown in colour. Within the clay there are bands of calcareous concretions (septarian nodules). Pieces of septarian nodules, which have been eroded from the clay, are often seen scattered across the foreshore.

d. Quaternary - Glacial Deposits

Glacial deposits (1.8ma to 10,000 BP) are found at many locations along the coastline; they are important as a potential source of sediment supply to the coastal system.

Intermediate head gravels (Wolstonian) are found in the cliffs at west of Reculver, where the deposit is 2.5 m thick (Plate 2.6). The head gravels consists of broken angular flints, black flint pebbles and pieces of sandstone set in a matrix of coarse sand. The deposits frequently contain lenses of clay. Samples of head gravels from Beltinge have a coarse (shingle-sized) content of between 5% and 35%, Canterbury City Council, (1993a).

Head Brickearths are present in the coastal sections from the 2nd and 3rd stages; these represent deposition in the Early and Late Ipswichian interglacial period respectively (Holmes, 1981). Brickearth of the second stage is found to the west of Reculver, where it is associated intimately with the deposits of head gravels described previously; it is typically a dense loam with a variable content of sand and pebbles.

The Brickearths of the 3rd stage are widespread along the coast, where they tend to exist as infill to old river channels and other shallow depressions. These Brickearths are compact yellow loams which commonly contain small pockets of gravel and sand (Holmes, 1981).

2.2.2. Evolution of the Thames Estuary

The North Sea is a shallow sea formed by the inundation of part of the continental shelf of North West Europe: the Thames Estuary is an extension of this sea.

Tectonic movements in the Miocene (22.5 - 5.0 ma), resulted in the uplift of the Wealden area of Kent, creating a system of rivers which drained off the higher ground north and east into the present-day Thames Estuary and southern North Sea. In Kent the main rivers were the

Medway, the Stour and farthest to the east, the Lobourg, Figure 2.4(a). The Thames flowed further to the north. These river systems and their courses (as they existed in the Early to mid Pleistocene, 2.5ma to 600,000 BP are shown in Figure 2.4(a).

During the Anglian glaciation (500,000 BP) the route of the River Thames was diverted to the south and east by an ice sheet, to such an extent that it joined with the River Medway (D'Olier 1975). The lower reaches of the Medway river were also deflected to the south, probably by the same ice sheet, Figure 2.4(b).

By the Late Pleistocene (100,000 - 10,000 BP) the River Medway was captured by a tributary of the River Stour, causing the abandonment of the river systems farther to the north, (Figure 2.4(c)). The remains of the old Thames, Medway and Stour rivers have been located by geophysical surveying (D'Olier, 1975) at the positions shown in Figure 2.4(c). These river courses have since been buried beneath more recent estuarine deposits. River terraces have also been located in the present Thames Estuary and southern North Sea, confirming the proposed river system development.

Throughout this latter period, the rivers would have been eroding the bed rock. Such erosion of the Upper Cretaceous Chalks (and the Lower Tertiary sands to a lesser extent), provided a great deal of coarse (predominantly flint) clasts which are seen in the various river gravel deposits, both on the present land surface and on what is now the seabed of the Thames Estuary and southern North Sea; for example the sand and gravel deposits of Long Sand and Margate Sand to the north-east of the study area, Figure 2.5.

Sea level rise, commencing in the Flandrian (8900 BP), resulted in the progressive flooding of the southern North Sea and the ancient river valleys. At around 7800 BP the North Sea and English Channel became connected as the ridge of chalk which had separated them was overtopped and eroded. The connection of the southern North Sea and the English Channel allowed the establishment of a new and stronger system of tides; these swept up the sediments into large sandbanks around the mouth of the Thames Estuary, leaving the remainder of the seabed covered by a thin layer of lag deposits.

2.3. Oceanographic Setting

2.3.1. Bathymetry

The Thames Estuary (Figure 2.5), is broadly funnel shaped-opening into the southern North Sea at its eastern end. The estuary becomes shallower towards the west. Two main oceanographic consequences arise from this shape;

(i) tidal and surge waves are amplified up the estuary,
(ii) exposure to waves is likely to increase along the coast towards the east, due to the greater fetch and water depth (see section 2.3.6).

The southern North Sea is relatively shallow, typically 20 to 25m below Chart Datum (Figure 2.5) The remnants of the Lobourg river remain as a deep channel running approximately north - south, to the east of the present coast of Kent. The main features of the sea bed in the Southern North Sea, are a series of long NNE - SSW orientated sandbanks.

Other long sandbanks, separated by narrow scoured channels are located towards both the north and south banks at the mouth of the Thames Estuary. Farther into the Thames Estuary, there is a deep channel running east - west, approximately through the middle of the estuary.

Due to the shallow bathymetry of the region and a large tidal range (see section 2.3.3), extensive areas of the sand banks are exposed during low water. Wide stretches of intertidal flats on both the north and south banks of the Estuary are also exposed at low water.

2.3.2. Sea Level Changes

Across the south-east of England, an underlying trend of mean sea level rise with time has been identified, (MAFF, 1989). Pugh and Faull (1982), utilised data collected from the ports of Sheerness and Southend, (located just to the west of the study area), to study temporal changes in mean sea level. They concluded that mean sea level increased by 1.5 mm yr^{-1}, over a period of 50 years (Canterbury City Council, 1993b).These changes are consistent with estimates of epeirogenic movements (vertical land movements) associated with glacial

rebound. No conclusive evidence of eustatic changes (changes in global mean sea level) has yet been identified however, MAFF (1989), recommend that an additional 4.5 mm yr^{-1} rise in mean sea level should be allowed for in coastal management studies.

2.3.3. Tides

(a). Tidal height

The main tidal influence in the Thames Estuary is linked to the North Sea tidal system, although some additional tidal energy may enter from the English Channel through the Straits of Dover. The tidal wave propagates in an anticlockwise manner (under the influence of the Coriolis Force), moving down the east coast of Great Britain into the Thames Estuary and along the coast of France, Holland, Denmark and Scandinavia. Within the North Sea there are three amphidromic points around which the tidal wave moves. These "zero tidal range" locations control the patterns of tides in the North Sea and in the Thames Estuary, Figure 2.6.

Tidal parameters for the study area have been derived by interpolation between the principal ports of Sheerness (15 km to the west of the study area) and Margate (10 km to the east). The results are presented in Table 2.1. This shows that there is an increase in tidal range up Estuary. Predicted water levels display a simple diurnal cycle. The frequency distribution of water levels in the study area is discussed in section 4.5.2.

(b). Tidal currents

Current velocities vary between springs and neaps and with proximity to the coast. Within the Thames Estuary maximum spring and neap velocities are 1.0 m s^{-1} and 0.8 m s^{-1} respectively. Closer to the coast the velocities drop to 0.55 m s^{-1} for spring tides and 0.45 m s^{-1} for neaps. In the vicinity of protrusions at the coast, Hampton Pier for example, current velocities can reach 1.0 m s^{-1}. Within the study area, the flood tide tends to be stronger than the ebb but is shorter.

2.3.4. Extreme water levels

Water levels at a particular coastal site may vary from the values predicted on the basis of astromonical tide-generating forces alone due to meteorological effects. These include surges generated in the Atlantic Ocean and transmitted into the North Sea; and seiches generated within the North Sea, by strong northerly winds, the inverse barometer effect and wave set-up. These are discussed in detailed in section 4.6.

2.3.5. Wind conditions

The prevailing wind direction in the study area is from the south-west. Unlike most sites on the south coast of England however, south-westerly winds do not contribute much to the wave climate along the study coastline. Wind conditions in the study area are described in section 4.5.1.

2.3.6. Wave conditions

Wave activity which is controlled principally by wind speed and direction, wind duration, geographical fetch, bathymetry and tidal state. In general, the stronger winds produce the greater wave heights and the longer wave periods. The relationship between wave height, period and the wind speed is complicated in the study area by the presence of wide areas of shallow water, Figure 2.5.

Water depth is likely to be important within the context of wave generation processes, in that it limits the maximum wave height and the period which can exist for a given wind speed and direction. The water depth also controls the "nearshore" processes of wave refraction and wave shoaling which alter waves generated in deeper water as they approach the shoreline.

There has been little research into wave conditions in the study area however, the local coast protection Authority, have been recording waves at a site near Whitstable since 1979, see section 3.2.5. Preliminary analysis of this wave data suggest that wave conditions are typified by modest wave heights (generally Hs < 1m) and short periods (Tz = 2 to 5 s), Canterbury City Council, (1988). An investigation of wave conditions in the study area forms a major part of

the research. The results are reported in Chapter 4.

2.4. Sediment Distribution and Mobility

2.4.1. Offshore sediment distribution.

The sediment cover over the bed of the Thames Estuary has been investigated by the British Geological Survey and their findings have been published in terms of a sediment distribution map (BGS, 1990). Most of the sediments in the southern North Sea and Thames Estuary are believed to have been eroded and deposited by the major river systems, prior to the area being inundated as sea level rose (Greensmith and Tucker 1973). The majority of the surficial sediment is concentrated in the large sand banks distributed over the region. These sediments are dominated by sand-sized material although coarser material also exists.

The remainder of the sea bed is covered in a thin layer of lag deposits; these are a combination of gravels, sands and muds. Localised erosion of the sea bed provides small quantities of gravel-sized material, consisting of: flints from the Upper Cretaceous Chalk; rounded black pebbles, from the Oldhaven Beds; and irregular clasts of calcite cemented sandstones, from the Lower Tertiary outcrops. Locally, large cobbles and pebbles of calcareous mudstone are found on the sea bed. These are derived by the breakup of septarian concretions. Sand sized material is released due to the erosion of the Tertiary Sandstones, principally along the coasts of Essex and Suffolk (on the north side of the Thames Estuary).

2.4.2. Beach and Nearshore Sediment Distribution

A typical beach located within the study area is shown in Plate 2.7. The beach consists of a mixture of sand and shingle sediment, typically with a series of shingle beach ridges around high water mark and a mixed sand and shingle beach face. Ridges are comprised exclusively of pebbles having shapes comparable with the imbricated discs described by Bluck (1967). The D_{50} of the ridges varies from about 5 mm to 20 mm depending on location on the beach, Canterbury City Council, (1993a).

Seaward of the beach ridges the beach face is planar, typically with a slope of 1 in 9 to the toe

of the shingle beach. Surface layers of the beach face ranges from patches which are exclusively pebbles to patches which are exclusively sand; subsurface layers always comprising a mixture of both sand and shingle. Apart from a general trend where the surface of the beach immediately seaward of the ridges is more likely to be sandy (the sand run), the proportion of sand and shingle in the surface layers appears to vary in both a longshore as well as in a more obvious onshore / offshore direction, Canterbury City Council, (1993a).

The toe of the shingle beach comprises spherical and rod shaped cobbles and pebbles infilled with sand and some coarser material. This part of the beach broadly corresponds to the large cobble frame and infill of Bluck, (1967). Beyond the shingle toe there is a sharp transition to a gently sloping ($\approx$1 in 500) lower foreshore comprising a thin layer of sand and silt over weathered London Clay bedrock.

The total volume of shingle contained in the beaches of the study area has been estimated to be in the order of 1×10^6 m^3 (Canterbury City Council (1988)). Between 1974 and 1992 approximately 0.5×10^6 m^3 of aggregate (from both offshore and land-based sources) has been added to these beaches, by way of renourishment. It is evident therefore, that a large percentage of the sediment contained within the beaches consists of material which has been brought in artificially from a variety of sources.

Commonly-occurring beach materials, found within the section of coastline under consideration include the following:

(a) *Cobbles.* These cobbles consist of well rounded or sub-rounded flints; most of these are probably recharge material derived from land based quarries added to sea dredged aggregate in order to increase the proportion of coarse material in the replenishment (McFarland et al, 1994).

(b) *Flint Pebbles.* Both angular and rounded varieties of flint pebbles are very common in the beach deposits. The flints may be black, brown or yellow in colour and may have a partial or completely oxidised dull white coating on the surface. These flints may have been derived from the glacial deposits (head gravels) or from the ancient river deposits. Alternatively, the flints may have been derived from sea dredged aggregates used for beach replenishment.

(c) *Black Flint Pebbles.* These pebbles are very well rounded and show the same characteristics as the black flints at the base of the Oldhaven Beds.

(d) *Claystone Fragments.* These fragments are yellow-brown in colour and are derived from concretions in the Tertiary rocks. Frequently the claystone fragments are bored by marine mollusca.

(e) *Calcium Carbonate Clasts.* These include intact and broken shells, with sizes which range from sand to pebbles. Shells are particularly common in the western part of the study area.

(f) *Sand and Silt.* Large quantities of sand are found, both mixed in with the shingle in the beach ridges and spread over the foreshore. Finer sands and silt are also common on the lower foreshore.

2.4.4. Beach and Nearshore Sediment Mobility

Beach sediment is mobile under fairly moderate wave action forming shingle ridges at the high tide mark. There has been little work carried out into the mobility of the shingle beaches within the study area; the main aim of the present study is therefore to gain an understanding of the shingle beach mobility and identify patterns of longshore transport. The results of the studies into beach mobility are presented in Chapters 5 and 6.

2.4.5. The Street and Long Rock

Of particular interest along the coastline within the study area are the features known as: (a) the Street; and (b) Long Rock. Each of these features comprises a significant volume of sand and shingle within the nearshore region.

The Street (Plate 2.1(b)) is a long, narrow feature extending for about three kilometres northwards from the toe of the shingle beach. Records show that this bank has been in much the same position, and form, since at least the early 18th Century (Canterbury City Council, 1993a). The Street is strongly asymmetrical with a steep western face and a more gently sloping eastern face.

Sediment samples taken from the Street demonstrate that it comprises of a poorly sorted mixture of sand, shells and shingle. At some locations, pieces of claystone (often attached to seaweed) are found on the surface. These are derived from an outcrop of harder cemented material within the London Clay located on the east flank of the Street. The existence of the Street is believed to be related to this outcrop of harder material, rather than to any archaeological relics or littoral processes (Canterbury City Council, 1993a).

Long Rock (Plates 2.1(c,d)) comprises a shingle spit, fed primarily by longshore transport of sediment from east to west. Aerial photographs of the area, taken over a period of 30 years demonstrates that the spit has not visibly increased in size, the main feature of note being the diversion (man-made) of the mouth of the stream towards the west (Canterbury City Council, 1993a). The foreshore around the spit comprises a thin fringe of coarse material, probably beach material transported offshore during periods of high stream flows.

Within the vicinity of Long Rock, there are a series of small sediment banks comprised of a mixture of sand and shingle with a similar size and grading to the beach material. Little is known about the mobility of these banks. Over most of the area, the surface of the foreshore is covered with mussels and barnacles (indicative of a lack of mobility). Where the material has been swept into banks, the sediment appears to be mobile, although there is no evidence of mass movement based on archived aerial photographs (Canterbury City Council, 1993a).

Location / Port	Tidal Parameters and Mean Springs Tidal Range, (m AOD).							
	HAT	MHWS	MHWN	MSL	MLWN	MLWS	LAT	Range
MARGATE	2.7	2.3	1.4	0.1	-1.1	-2	-2.6	4.3
Reculver / Minnis Bay	2.91	2.43	1.53	0.13	-1.18	-2.08	-2.71	4.51
East Cliff	2.97	2.47	1.57	0.13	-1.2	-2.1	-2.73	4.57
Herne Bay	3.04	2.51	1.61	0.14	-1.23	-2.13	-2.77	4.64
Tankerton / Studd Hill	3.09	2.54	1.64	0.15	-1.25	-2.15	-2.8	4.69
Whitstable / Seasalter	3.18	2.6	1.7	0.16	-1.28	-2.18	-2.84	4.78
SHEERNESS	3.5	2.8	1.9	0.2	-1.4	-2.3	-3	5.1

Table 2.1. Tidal Parameters for Coastal Locations Within the Study Area.

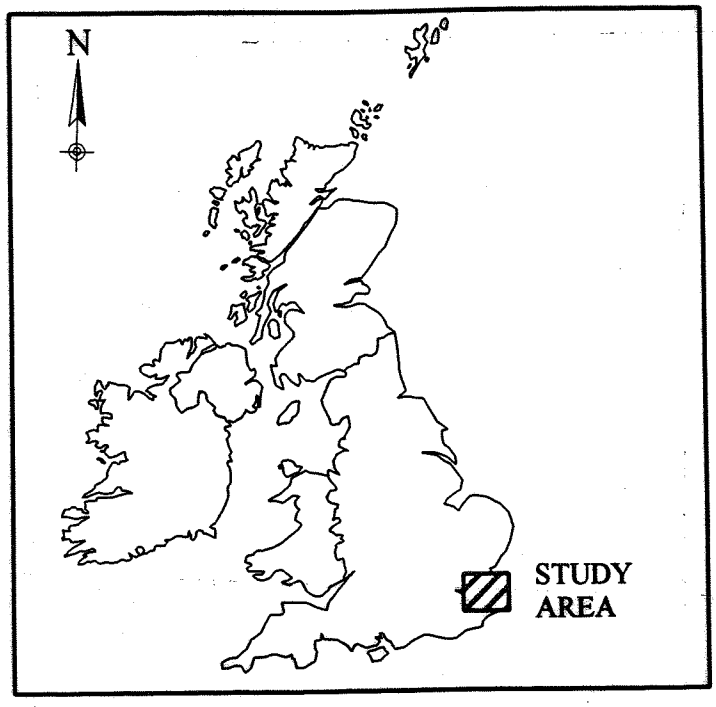

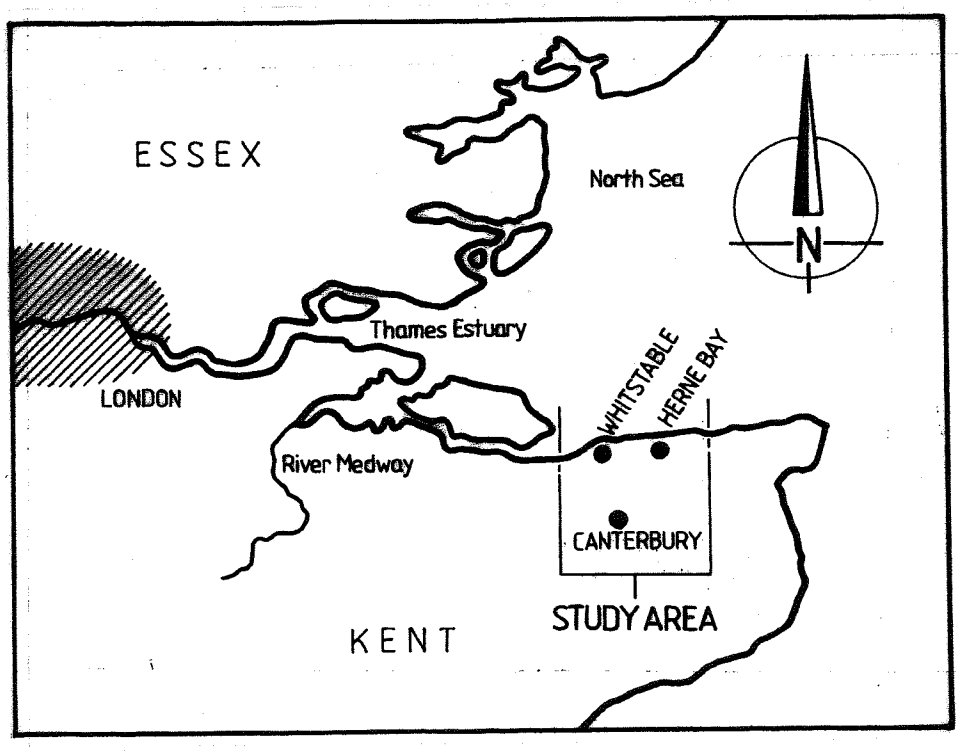

Figure 2.1. Location of the Study Area.

Figure 2.2. General layout of the study area.

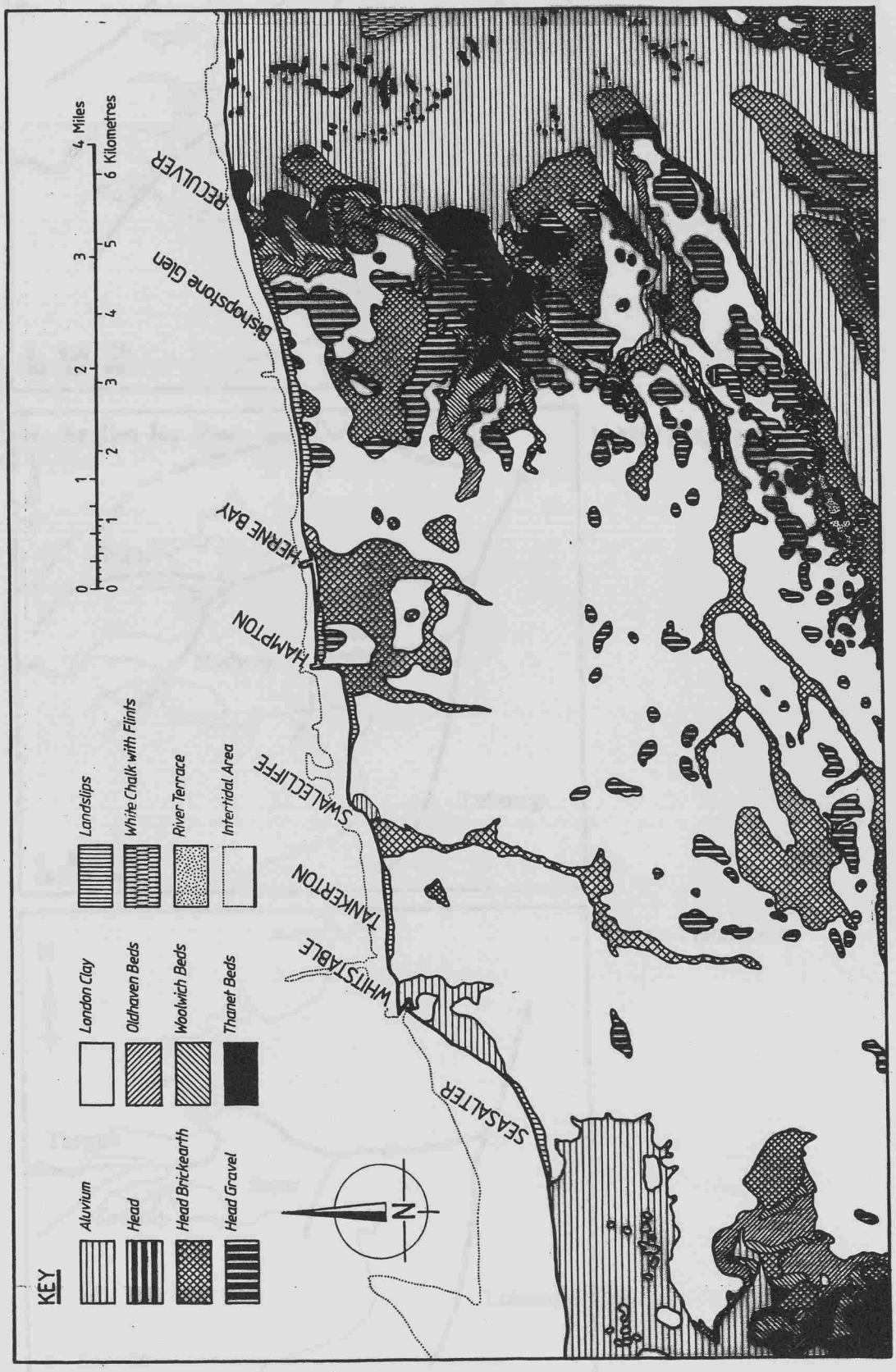

Figure 2.3. Geological Map of the Study Area, after Holmes (1981)

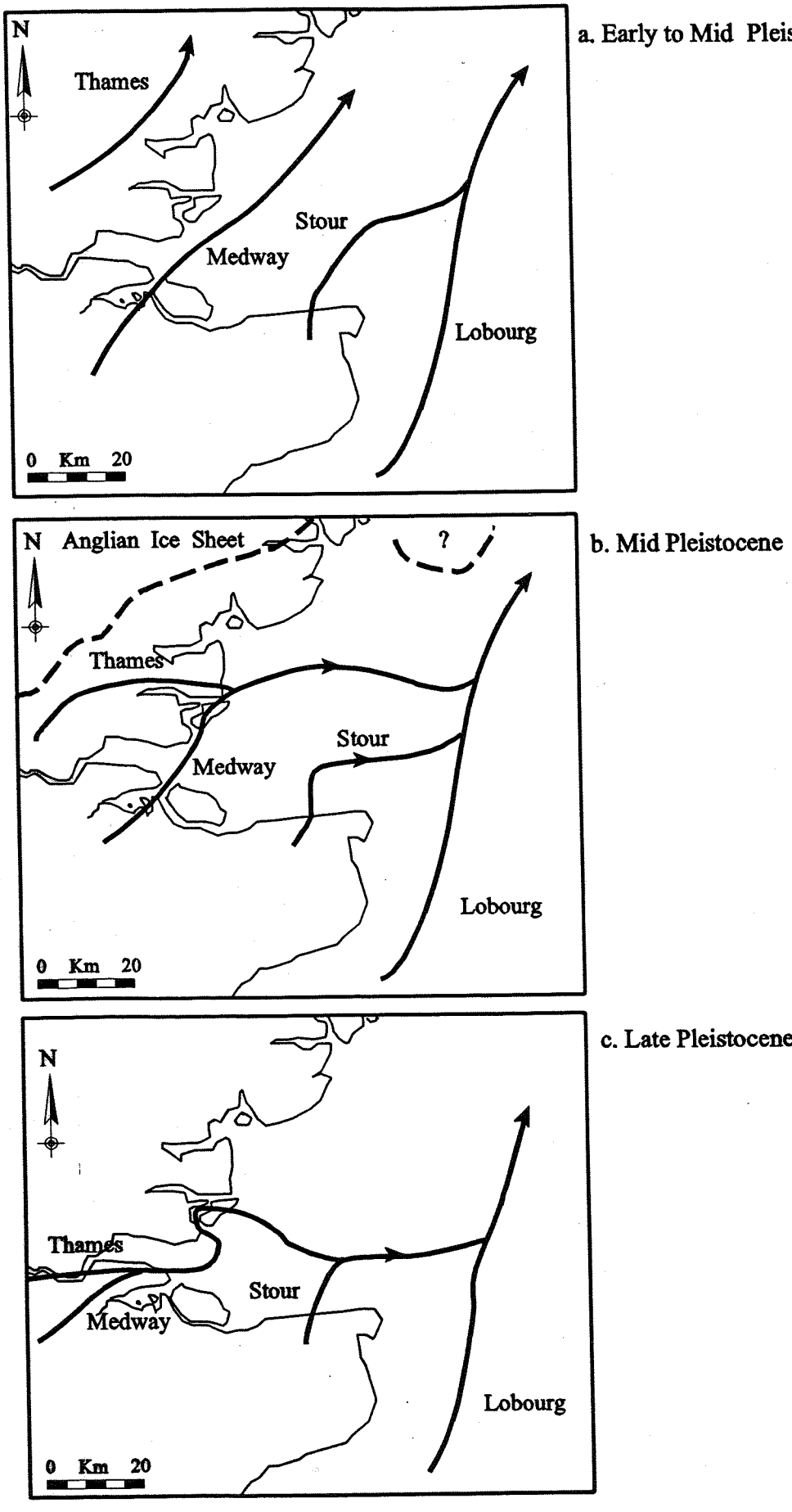

Figure 2.4. Pleistocene Development of River Systems in the Thames Estuary and southern North Sea, after BGS (1990).

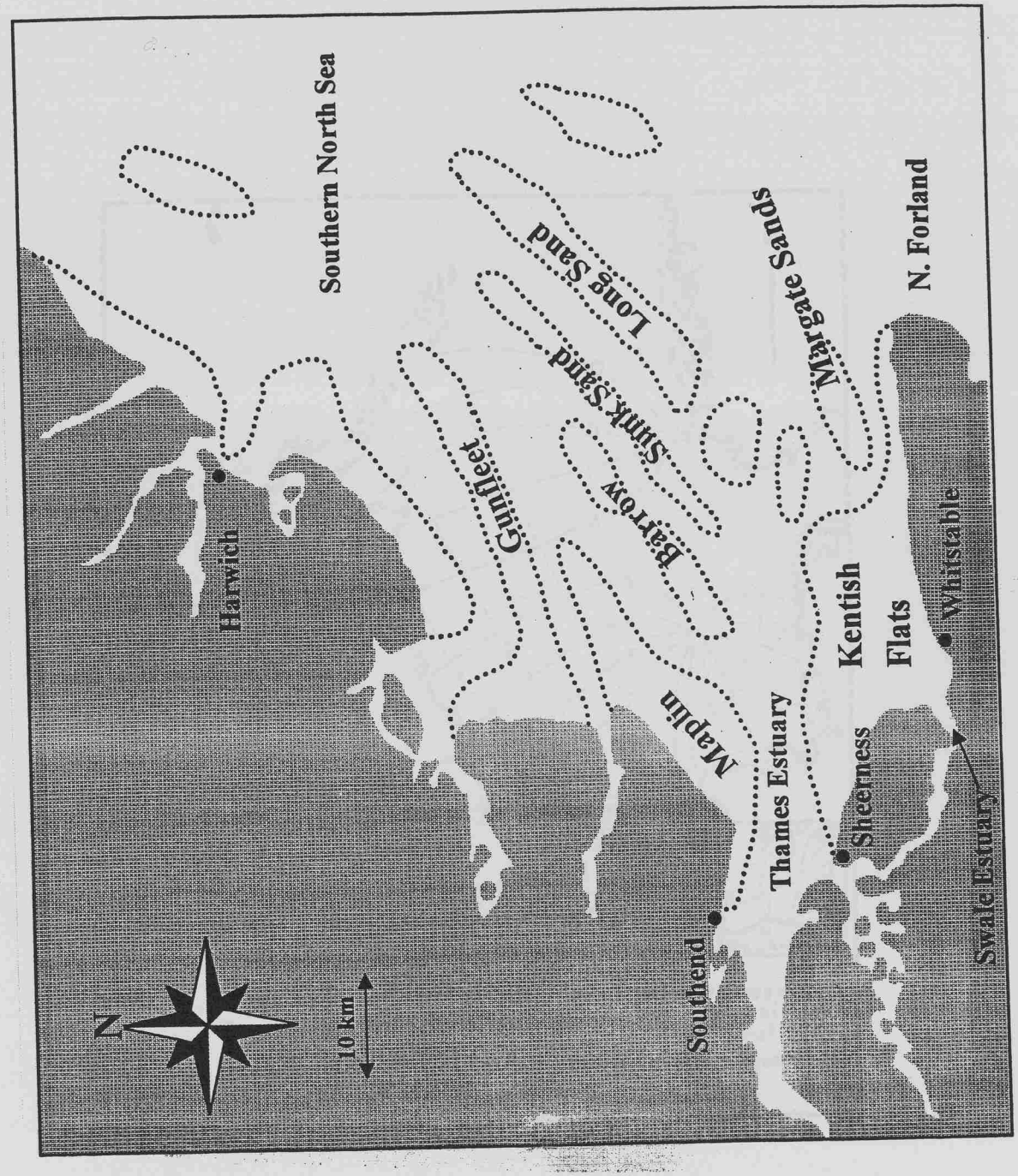

Figure 2.5. Simplified Bathymetry of the Study Area Showing Main Oceanographic Features

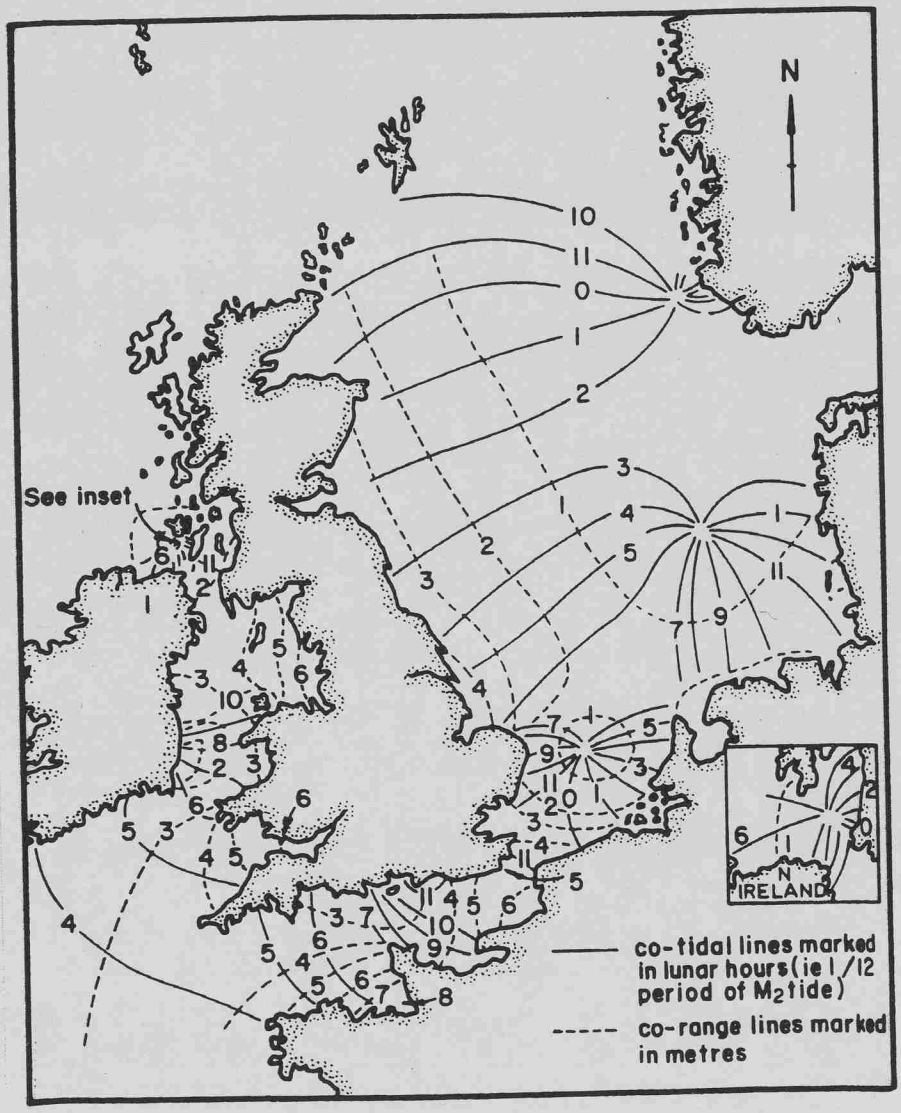

Figure 2.6. Location of Amphodromic Points and Tidal Ranges in the Study Area, after Pugh 1980

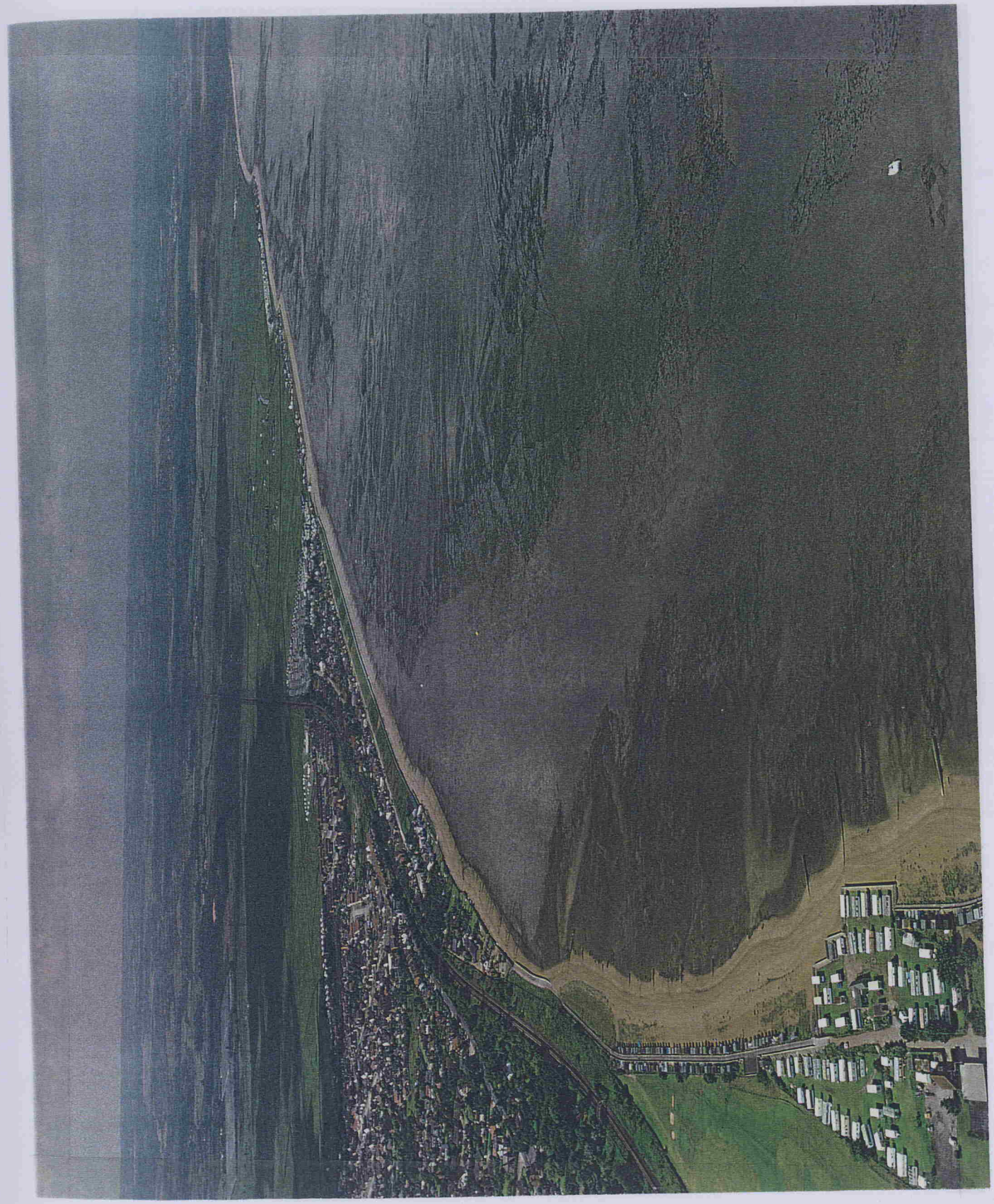

Plate 2.1(a) Aerial view of the coastline to the west of Whitstable, 1991; looking west towards Seasalter; (see Figure 2.2 for location).

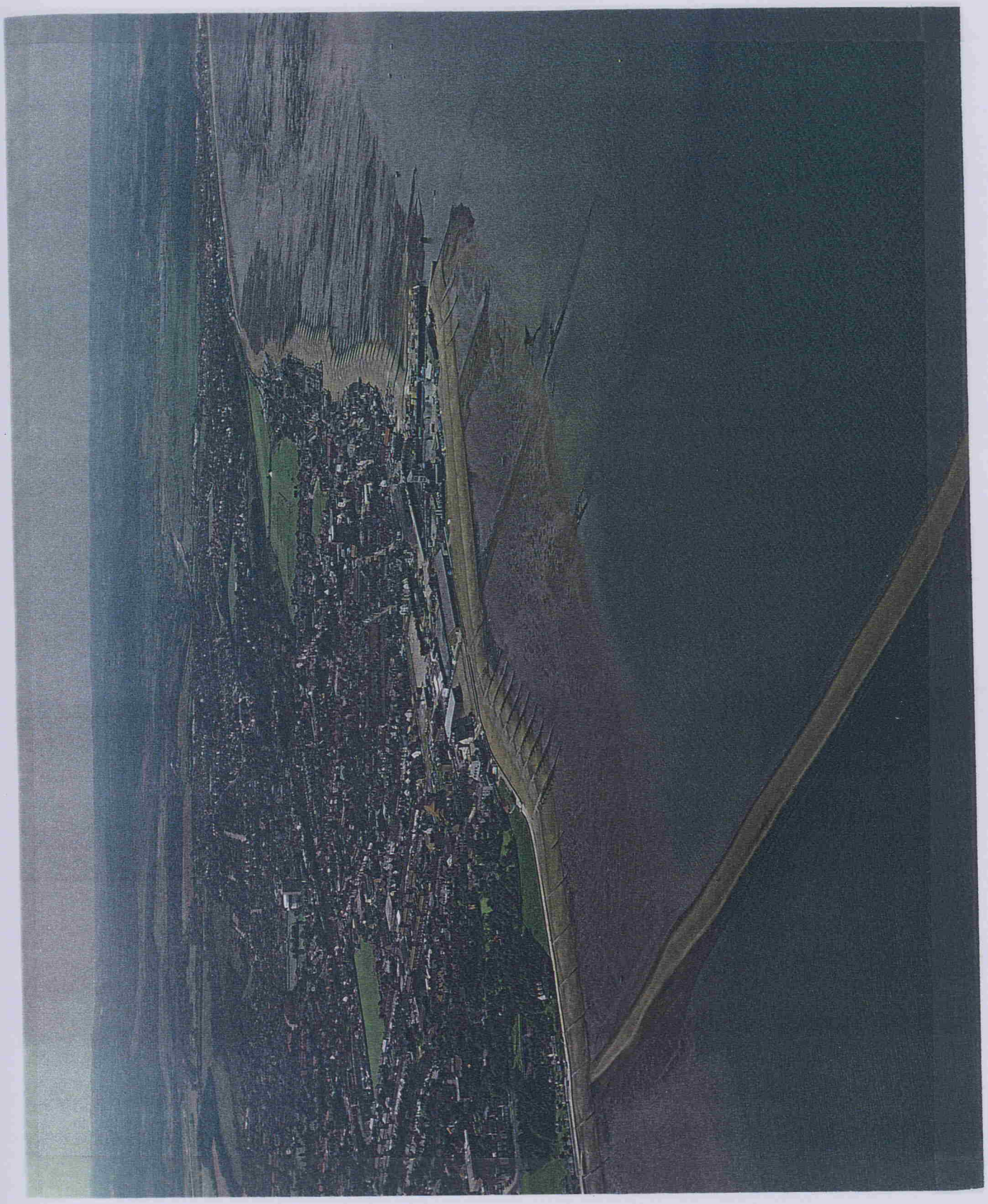

Plate 2.1(b) Aerial view of the coastline around Whitstable Harbour, 1991; showing "the Street" in the foreground, (see Figure 2.2 for location).

Plate 2.1(c) Aerial view of the coastline around Tankerton, 1991; showing "Long Rock" in the foreground, (see Figure 2.2 for location).

Plate 2.1(d) Aerial view of the coastline around Studd Hill, 1993, (see Figure 2.2 for location).

Plate 2.1(e) Aerial view of the coastline around Herne Bay, 1991; prior to the construction of the breakwater, (see section 6.3 for details of breakwater, and Figure 2.2 for location).

Plate 2.1(f) Aerial view of the coastline to the east of Herne Bay; (see Figure 2.2 for location).

Plate 2.1(g) Aerial view of the coastline around Reculver, 1991; (see Figure 2.2 for location).

Plate 2.2. Wave Overtopping of Coastal Defences at Whitstable, 1949.

Plate 2.3. Flooding to Central Whitstable, 1953.

Plate 2.4. Outcrop of "Doggers" in the Thanet Sands, Reculver.

Plate 2.5. Black pebble beds in the Herne Bay Member / Bishopstone Glen

Plate 2.6. Intermediate Head Gravels, near Bishopstone Glen.

Plate 2.7. Typical Beach in the Study Area, (seafront, Herne Bay).

CHAPTER 3: Methods and Analytical Techniques

3.1. Introduction

Sediment transport processes at any particular location on the coastline are dependant upon: tidal and meteorological conditions, the regional coastal morphology / bathymetry and on the sediment characteristics (particle size, sorting and specific gravity). The relationships between the primary controls and the hydraulic and sediment responses are shown in Figure 3.1.

This chart indicates that there is strong interaction between many of the processes. For example, sediment characteristics are a principal control on the threshold of particle movement, the longshore and on-offshore transport of sediment and thus, the evolution of the beach plan shape and profile. Each of these processes will act, in turn, to modify the sediment characteristics at a particular location over time. All the primary controls change with time and, with the exception of astronomical controls, are not easy to predict. In order to take into account this variability, long-term data sets are required. If observations are limited to short-term data, there is a possibility that these will not be fully representative (or typical) of factors which influence coastal change.

The approach adopted for the investigation has been to utilise simple mathematical models to represent: wave generation; wave propagation in shallow water; and beach sediment transport. Results obtained from the models have been compared with field measurements, at various stages in the overall modelling procedure. The use of mathematical models, combined with validation using such field data, is considered to be the optimum approach to gaining an improved understanding of coastal processes within the study area.

3.2. Long-term data sets

A number of long-term data sets exist, which are relevant to the present investigation. The general locations from which the various observations were obtained are shown in Figure 3.2. Particulars of each data set are described below.

3.2.1. Manston Airport (wind speed and direction)

The wind recorder at Manston Airport (Figure 3.2) is maintained by the Meteorological Office. The wind vane is mounted at a height of 10 m above ground level, at an exposed location. The data which are available have been compiled as hourly mean wind speeds and directions. The data are further sub-divided into wind-directional sectors, each of 30°. Data from 1979 to 1990, inclusive, have been available for the study; these are summaries providing information on the percentage occurrence of particular combinations of wind speed and direction, for individual months. A limited amount of data are also available for 1970 to 1978. However, there is some uncertainty regarding the elevation of the wind recorder vane during this earlier period.

Additional 'real time' data have been obtained from Manston, for the purpose of calibration between observations at Manston and Borstal Hill, Whitstable.

3.2.2. Borstal Hill, Whitstable (wind speed and direction)

The Borstal Hill wind recorder (Figure 3.2) is owned and maintained by the Local Coast Protection Authority i.e. Canterbury City Council. The wind vane has been sited at Borstal Hill since 1978. Wind speed and direction are recorded on a 'real time' basis and are transmitted to the Council offices in Canterbury; here, the data are logged on chart rolls. The location of the Whitstable recorder has been shown to be subject to (wind) funnelling and sheltering, due to its location (Canterbury City Council, 1993b) Hence, the data collected at Borstal Hill need to be corrected, based upon comparisons with the Manston recorder.

3.2.3. Port of Sheerness (water level data)

The Admiralty maintain a Class A tide gauge at the Port of Sheerness, on the Isle of Sheppey (Figure 3.2). Data have been collected at Sheerness since 1835; these have been used widely to obtain predictions of mean sea level rise, relative to the land, for south-east England (Suthons, 1963; Blackman and Graf, 1978; and Pugh and Faull, 1982).

The data set available for the study is for the years 1978, and 1981 to 1986. The data have

been compiled as the percentage occurrence of the predicted tides and corresponding high water surge residuals. This data set is particularly useful for: (i) analysing surge-tide interactions in the Thames Estuary; and (ii) for determining the return periods of extreme events.

3.2.4. Whitstable Harbour (water level data)

Water levels have been recorded at Whitstable Harbour (Figure 3.2) since 1979, using a vented pressure transducer. The data are collected in 'real time' and transmitted to the offices of Canterbury City Council, where it is logged on chart rolls. Data from 1979 to 1992 are available for use in the present investigation.

Additional water level data were available from the deployment of a self-recording (pressure type) tide gauge (TDR-3A), for a period of 16 days, over a spring / neap cycle in March 1990. Deployment of this recorder was part of a study undertaken by Delft Hydraulics (1990a) of coastal defences at Herne Bay. The recording site was located approximately 5 km to the north of Herne Bay (Figure 3.2), with the recorder deployed 0.5 m above the seabed at a depth of 2 m below Chart Datum (CD).

3.2.5. Whitstable Harbour (wave records)

Wave conditions have been recorded, at a site located 600 m to the north of Whitstable Harbour, since 1979 (Figure 3.2). The recorder consists of a pressure transducer, which utilises a parallel plate capacitor enclosed in a partial vacuum. As the water depth over the transducer increases, the plates are squeezed closer together. The capacitor functions as the tuning capacitor of an LC oscillator, which produces a frequency which is dependant upon the water pressure. The low frequency variations in pressure, due to the tidal component and atmospheric pressure can be filtered out; this leaves a signal which is a response to wave activity alone.

From 1979 to March 1990, data analysis was based upon the statistical method of Tucker (1963); this generates statistically-derived significant wave heights ($H_s = H_{1/3}$) and zero crossing periods (Tz). Throughout this time, the wave recorder sampled 12 minutes of data, at three-

hourly intervals. After March 1990, the data have been analysed spectrally, producing as output spectrally-derived significant wave heights ($H_s = Hm_o$) and periods (T_p). The time period and the frequency of sampling after March 1990 was increased to 20 minutes, every 1.5 hr. In addition, a trigger was incorporated into the software; this switches the recorder to a continuous mode, if a threshold wave height of 0.5 m was exceeded. This was to obtain more detailed information on wave conditions during storm conditions. Over the period 1990 to 1992, the bulk of data was not collected; this was due to a series of recorder failures, including a severed underwater cable and a damaged transducer due to a collision with a ship. In order to maintain the integrity of the data set, the small amount of spectrally-processed data collected after March 1990 has not been used in the long term data sets.

3.2.6. Beach Profile Data

Since 1974, the Coast Protection Authority has been recording beach profile changes at a number of locations within the study area. Beach profiles are recorded at quarterly intervals, by measuring levels at points along the profile (using a dumpy level and aluminium staff). The number of profiles recorded has varied at between 50 and 75, depending upon the degree of monitoring considered necessary at particular times or locations. The data are stored in a database, which also has the capability to calculate the cross-sectional area of material contained within the shingle beach profile. The database does not have any other analytical ability; hence, it is necessary to extract data for analysis elsewhere.

3.3. Numerical modelling

The numerical modelling was carried out in 4 stages, as shown in Figure 3.3.

Stage 1 involved the development of a model relating wind conditions to the generation of waves within the Thames Estuary and the southern North Sea. The output from this stage of the modelling was a description of the offshore wave conditions for the area.

Stage 2 of the modelling was to determine the propagation of waves, from offshore and in towards the coastline. Modelling of shallow water wave processes (such as wave breaking, shoaling and refraction) was carried out to obtain characteristic nearshore wave conditions for

the study area.

Stage 3 involved combining the wind climate for the area with the results of the wave modelling, to obtain a nearshore wave climate. In relation to the strong tidal influences over the study area, it was found necessary to include the effects of water levels on the nearshore wave climate at this stage.

Stage 4 of the modelling procedure was to predict the longshore transport patterns and rates of movement of the beach sediments, in response to the derived wave climate. The longshore transport model was used to obtain transport rates and directions along the whole of the length of coastline under investigation.

Long-term data sets representing wind conditions, water levels, wave conditions and beach area changes are all available for the area (see Section 3.2). These data, combined with field measurements, have permitted validation to be undertaken of the mathematical models at the following stages in the analysis:

(a) comparison of nearshore wave conditions from the model (Stage 2 output), with the wave records collected to the northwest of Whitstable Harbour; and

(b) calibration of the sediment transport formulae, using tracer pebbles and beach plan surveys (Stage 4).

Details of the numerical modelling results and calibration are given in Chapters 4 and 5, respectively.

3.4. Offshore Wave Generation Model (Stage 1)

3.4.1. Model Description

Several investigations have established relationships between wind conditions and the generation of waves (for example: Darbyshire, 1963; Sverdrup and Munk, 1947; Hasselmann et al., 1973). For the present study, the method of Sverdrup and Munk (1947), modified for

shallow water conditions by Bretschneider (the SMB method) and as outlined in the Shore Protection Manual (CERC, 1984), was used. This particular method is well suited to modelling wave generation in shallow water basins such as the study area.

The equations were derived by combining two separate relationships. In the first of these relationships, deep water wave forecasting relationships are used to calculate energy added to the sea surface by the wind stress; in the second, the relationships developed by Bretschneider and Reid (1953) are used to derive energy losses, caused by bottom friction and water percolation. The final equations are based upon a combination of these two numerical methods and are expressed in equations 3.1 - 3.3, where $Hs = Hm_o = 4\ m_o^{½}$, (m_o is the area under the wave spectral curve) and Tp is the wave period corresponding to the spectral peak;

$$\frac{gHs}{Ua^2} = 0.283 \tanh\left[0.530\left[\frac{gd}{Ua^2}\right]^{\left(\frac{3}{4}\right)}\right] \tanh \frac{\left[0.00565\left[\frac{gF}{Ua^2}\right]^{\left(\frac{1}{2}\right)}\right]}{\left[\tanh\left[0.530\left[\frac{gd}{Ua^2}\right]^{\left(\frac{3}{8}\right)}\right]\right]} \tag{3.1}$$

$$\frac{gTp}{U_a} = 7.54 \tanh\left[0.833\left[\frac{gd}{Ua^2}\right]^{\left(\frac{3}{8}\right)}\right] \tanh \frac{\left[0.0379\left[\frac{gF}{Ua^2}\right]^{\left(\frac{1}{3}\right)}\right]}{\left[\tanh\left[0.833\left[\frac{gd}{Ua^2}\right]^{\left(\frac{3}{8}\right)}\right]\right]} \tag{3.2}$$

$$\frac{gt}{U_a} = 0.0537\left(\frac{gT}{U_a}\right)^{\left(\frac{7}{3}\right)} \tag{3.3}$$

The data required as input into the offshore wave generation model, represented by the equations is described below.

(a) U_A, the wind stress factor (where $U_A = 0.71\ U_C^{1.23}$, and U_C is the recorded wind speed in m s^{-1}, corrected for location and elevation of the recording device). For Stage 1 of the model construction, a range of nominal values of U_A were used (0 - 50 at intervals of 5). This range was considered to encompass all possible values of U_A which were likely to occur within the area of study.

(b) The 'geographical fetch' is the distance that the wind blows over a body of water in the mean direction of the wind. However, since wind imparts its energy to a water body at angles of up to 45°, to either side of the wind direction, an effective fetch (F) was determined (as outlined in the Shore Protection Manual (CERC 1984)). In the case of northeasterly and easterly winds, long geographical fetches are possible. In these situations, the fetch limits are more likely to be controlled by meteorological influences such as the extent of a particular depression system. Fetches to the northeast and east were set at 120 km; this was considered to be consistent with a typical weather system occurring in the area. Under actual conditions, the fetch lengths will vary; this, however, was not accounted for in the hindcast model.

(c) Water depth (d) is controlled by the bathymetry and the tidal elevation (related to phase). Because the water depths varied in response to tidal and meteorological influences, a range of nominal water levels, from -2.74 m AOD (i.e. equal to Chart Datum) to a maximum value of +5.5 m AOD, were used (at intervals of 0.5 m). This range was considered to represented the limits of all the possible water levels which were likely to occur.

(d) Wind duration is defined as the length of time that the wind blows, at a more or less constant speed and direction. For any given wind speed, there is a maximum wave height and period which can be generated (a Fully Arisen Sea - FAS). The minimum time required (t) to reach a FAS state was calculated using equation 3.3. Because of the relatively shallow water and short fetches within the study area, the duration of time required to achieve a FAS was found to be short i.e less than 3 hours, in most cases. For this reason it was assumed that, for any combination of wind speed and direction, an FAS would have formed over the area of investigation.

Modifications to the SMB formulae outlined by Hurdle and Stive, (1989) were not applied, as they are only relevant to longer fetches and greater water depths than those which occur in the study area.

3.4.2. Directional Sectors and Coastal Units

Fetch length, together with the water depth over which the wind blew, varied with wind direction. Therefore, values for these parameters were chosen for each of seven wind directions. These sectors correspond to the wind-directional sectors into which the wind data, provided by the Meteorological Office, were compiled (Section 3.2).

Along the coastline, there are variations in: the fetch length; the bathymetry; and in the tidal elevation. In order to take account of these variations, the area was divided into six coastal units within which each of these parameters could be considered to remain constant. The subdivision of the research area, into longshore coastal units and directional sectors, is summarised in Figure 3.4. The directional sectors correspond to the wind directional sectors outlined in Section 3.2. Due to morphological changes in the nearshore area, a further subdivision was required for the wave propagation model, providing a total of ten coastal units / subunits; these subunits are included in Figure 3.4.

In order to carry out all the calculations involved in the offshore wave generation model, a spreadsheet-based computer program SHALLPRE was written. Each run of the program solved the SMB equations (Section 3.4.1.) for the pre-defined range of wind stress factors and water levels within an individual coastal unit and directional sector. The program was run to solve the equations, for each of the seven directional sectors within each of the six coastal units in turn.

3.5. Nearshore Wave Conditions (Stage 2)

Waves generated offshore are modified by interaction with the seabed, as they approach the coastline. Computer programs available to model these processes include INRAY and OUTRAY (Hydraulics Research), RCPWAVE (US Army), REFRACT and ENDEC (Delft Hydraulics). Some of the models are two-dimensional (RCPWAVE, REFRACT) in character,

whereas others are one-dimensional i.e. the wave modification calculations are carried out along a pre-determined profile (ENDEC). In general, the two-dimensional models are superior, in that they provide an overview of wave modifications within a defined area; likewise, they can be used to identify areas of wave focusing along the coastline. Two dimensional models are unreliable, however, in areas of extensive shallow water with complex bathymetry. There, energy losses due to wave breaking and frictional losses tend to be more important that wave refraction, (Delft Hydraulics, 1990b).

In an earlier study undertaken for the eastern part of the area under investigation, the program RCPWAVE was used for the investigation of coastal defences (Robert West & Partners, 1993). Useful data were obtained only for high tidal conditions, when waves were approaching the coastline at small angles. Consequently, for the present investigation no attempt was made to use RCPWAVE or another two-dimensional model. Instead, the model ENDEC (ENergy DECay) was used; this was considered to be the most suitable available, for modelling wave modifications in extensive areas of shallow water. The processes considered by ENDEC, in order of importance are:

(i) shoaling;
(ii) depth-controlled wave breaking;
(iii) bottom friction;
(iv) bottom and current wave refraction;
(v) energy gain, as a result of local wind conditions; and
(vi) water level variation, in response to radiation stresses.

The input required for the ENDEC model is as follows:

(a) "offshore" wave height (Hs_i);
(b) "offshore" wave period (Tp_i);
(c) incident wave angle (theta);
(d) local wind speed (w);
(e) bottom profile;
(f) current profile;
(g) tidal variation (eta);

(h) PSI value;

(i) wave breaking coefficient (α);

(j) wave breaking coefficient (β); and

(k) friction factor (f).

The "offshore" wave heights and periods were derived during Stage 1 of the model development for: (a) each of the coastal units and directional sectors: and (b) for a range of wind speed and tidal variations. Wave periods were assumed to remain constant throughout the wave propagation process, whereas the wave heights and wave angles were altered by shoaling, wave breaking and the effects of bottom friction.

The incident wave angle was determined, for each sector within a particular coastal unit, by examining the orientation of the seabed contours in relation to the prevailing wind direction. In the majority of cases, the seabed contours are aligned from east to west. Hence, a wave ray which is approaching from the north will have an incident wave angle of 0 (zero) degrees. Waves originating from directions to the west of north were defined as negative angles; those to the east of north, as positive.

Local wind speeds were included in the computations and modelling, so that energy increases caused by a local wind field could be considered.

The sea bottom profile is a description of the variation in water depths (bathymetric) along the wave trajectory (for this study, the profile depth was defined in relation to CD). Depths below CD were set as positive; those above CD are presented as negative values. Separate bathymetric profiles were defined for each sector, within each zone, using a combination of Admiralty Collector Charts (Fair Sheets) and other local bathymetric surveys commissioned by the Coast Protection Authority.

Water level variations (defined by eta) are controlled by tidal, meteorological and local hydrodynamic effects and these need to be accounted for in the computations. For example, a tide of 3.0 m AOD at Whitstable (where Chart Datum is -2.74m OD) would generate an eta value of 5.74 m (since the bathymetric water depths are relative to CD). Additional changes in water level, caused by wave set up / set-down, were calculated by ENDEC and added

automatically to the defined eta value.

The variation in (tidal) current speeds and directions throughout the water column (the current profile) was included, to determine how these variables would affect wave refraction patterns over the area.

The optimum values of the wave breaking coefficients (α and γ), which define the point at which waves break, were calculated by ENDEC as the computations progressed.

The friction factor (f) depends upon the roughness of the seabed and, hence, the degree of interaction with the overlying wave orbitals. A value of f=0.01, which is typical of a smooth sandy bottom, (CERC, 1984) was used in this study.

Finally, although not listed above, the horizontal 'step-size' is a program parameter which can be adjusted to allow a balance between the speed of calculation and the accuracy of the results. If the minimum step size is too large the program can return errors. However, if the step size is too short, then processing time becomes excessive with no gain in the programme accuracy. In this study, the step size was set initially at 10 m; it was then varied, as necessary, by the programme to provide optimum performance.

An analysis was carried out to determine how sensitive the final computer output (the nearshore wave conditions) was to each of the input parameters described above. The effects of each parameter was tested, over a range of tidal levels and wind stress factors. Feedback from the sensitivity analysis was used to optimise the input data, reducing the potential for large errors to occur. Further details of the wave model sensitivity analysis are given in Chapter 4.

Having defined the input parameters, the program "ENDEC" was used to model changes in wave conditions, for a range of combinations of water levels and wind conditions (for each of the coastal units and directional sectors). The results were plotted as a series of graphs, from which the nearshore wave conditions could be determined for any combination of wind stress factor and water level (see Section 4.2).

3.6. Calibration of Nearshore Wave Conditions.

Wave data obtained from the recorder sited 600 m to the north of Whitstable Harbour have been compiled as a series of scattergraphs, in which the occurrence of combinations of wave height and period are plotted. These data were plotted on an annual and monthly basis, to determine how wave conditions varied (Section 4.4).

In order to calibrate the nearshore wave conditions generated by the model, a data set of actual events was compiled (where an event is defined as having a recorded wave height of 0.5 m or more). The data required for each event are as follows:

(a) recorded wave height (above a threshold of 0.5 m);
(b) recorded wave period;
(c) recorded water level;
(d) recorded wind speed; and
(e) recorded wind direction.

Significant wave height and wave period, obtained from the wave records, are based upon statistical analysis of the wave trace; therefore, they are not directly comparable to the wave parameters generated by the wave model which are spectrally-derived. This limitation needs to be bourne in mind when correlation of the predicted and recorded waves is attempted.

Water levels were obtained from the tide gauge (vented pressure transducer), located in Whitstable Harbour. The wind (speed and direction) data used were collected from the wind vane on Borstal Hill, Whitstable.

The recorded water level, wind speed (corrected) and direction were used in conjunction with the Stage 1 and Stage 2 models, to hindcast the characteristic wave conditions for each of the individual events. The hindcast conditions were correlated then with the actual recorded wave conditions. Graphs of predicted and recorded wave heights and periods were plotted, with correlation between the two data sets examined as described in Section 4.2.

3.7. Nearshore Wave Climate (Stage 3)

The wave climate describes the wave activity which would be expected, at a particular coastal location, in a typical or average year. The wave climate contains information on the likely occurrences of combinations of wave height, wave period and wave angle; it is useful for studying factors which control beach stability over longer periods of time. Such information is particularly relevant for coastal scientific and engineering applications.

Within the area, the effects of water level on wave generation and propagation are important and have to be included in the analysis. A water level climate was determined, based upon results obtained from the 16 day deployment of the tide gauge to the north of Herne Bay (Figure 3.2). The data collected were used to produce a water level frequency distribution, or water level climate. Since these data were relevant only to Herne Bay, the data were corrected to provide the distribution of water levels within the remainder of the coastal units. Correction factors were determined, through the interpolation of the tidal parameters between the principal ports of Sheerness and Margate (Figure 3.2). The correlation factors are reproduced in Table 3.1.

Wind data, supplied by the Meteorological Office and collected over the period 1979 - 1989 (inclusive) at Manston Airport (Figure 3.2), were used to obtain the wind climate. These data had been analysed previously, as the occurrence (in hours) of particular combinations of wind speed and direction for each calender month. A wind climate was produced from the Manston data by summing up all the hourly wind speed and direction occurrences; these were divided then by the number of years of data used to obtain the occurrences for a typical year.

The water level climate was then combined with the wind climate, using a joint probability approach to produce details of the likely occurrence of a range of wind and water level conditions (a joint wind - water level climate) under which waves are generated and propagate. The results of this analysis were used, in turn, together with the nearshore wave conditions calculated by ENDEC to produce a nearshore wave climate.

All the calculations involved in obtaining a nearshore wave climate were carried out using a spreadsheet computer program (COMBINER); this was written especially to undertake the

large number of calculations involved for each of the coastal units / sub-unit.

3.8. Longshore Transport Calculations

There is a wide selection of mathematical models available for the determination of longshore sediment transport rates; most of these have were derived for sand beaches (for example, the CERC, (1984) formulae. For the present study, use was made of the "shingle" transport formula derived by van der Meer, (1990) on the basis of physical model studies. This formula was found to perform well when compared with a comprehensive data set of longshore transport rates recorded in the field, (Schoones and Theron, 1996).

The equations used are as follows:

(a) For sand / gravel beaches ($H_s / \Delta D_{n50} > 50$)

$$Q_{ls} = 0.0038 H^2_s . c_{op} . \sin 2\beta \qquad (3.4)$$

For shingle / rock beaches ($10 < H_s / \Delta D_{n50} < 50$)

$$Q_{ls} / g . D_{n50} . T_p = 0.0012 (H_s . \sqrt{} \cos \beta / D_{n50}) . ((H_s . \sqrt{} \cos \beta / D_{n50}) - 11) . \sin \beta \qquad (3.5)$$

For coarse-grained beaches under gentle wave action, ($H_s / \Delta D_{n50} < 10$) it was determined that no significant transport would occur.

Longshore transport calculations for each coastal unit were carried out by adding a transport module onto the wave climate spreadsheet (COMBINER). This procedure allowed the previously-calculated nearshore wave climate to be used, as input into the sediment transport model directly; this removed the risk of errors arising, due to transfer of the data from one model stage to the next.

The following input data to the longshore transport model were required:

(a) the wave height at the toe of the beach;
(b) the wave angle at the toe of the beach;
(c) the wave period;
(d) the median grain size of the sediment;
(e) the specific gravity of the sediment; and
(f) the orientation of the coastline / beach.

Wave height, wave period, and wave energy were obtained as output from the nearshore wave climate model (Stage 3), as described earlier (Section 3.5).

The mean grain size of the sediment was determined on the basis of sediment samples collected from the beach. In order to obtain a representative mean grain size, samples were taken at a number of sites and along a shore normal profile at beach levels corresponding to: (i) mean high water springs; (ii) mean high water neaps; (iii) mid-beach; and (iv) at the toe of the beach. Beach sample analysis, performed for an earlier coastal management study (Canterbury City Council, 1988), were used to create a larger data base of particle size distribution data.

The specific gravity of the sediment is defined by the composition of the beach material itself. As the beaches are dominated by flint particles, a specific gravity of 2.65 g cm^{-3} was used for each of the coastal units.

As the angle of orientation of the beach varies along the coastline, the sediment transport calculations were carried out for a range of coastal orientations. A deviation of $\pm 20°$, from the main coastal orientation of east - west, was used as the upper and lower limits for the calculations. The computations were undertaken at increments of 5°, in the coastal orientation.

Depending upon the value of $H_s / \Delta D_{n50}$ the appropriate transport equation (3.4) or (3.5) was selected by the computer program. Longshore sediment transport equations were solved for wave height, period and angle, corresponding to each combination of wind stress factor and water level. The resulting sediment transport is output in terms of hourly rates. Annual potential transport was obtained, by multiplying each hourly transport rate by the

corresponding occurrence of the wave conditions; then summing the totals. The model parameters were set up in such a way that transport from east to west is regarded as positive. Having derived the annual transport rates, for a range of predetermined coastal orientations, the net transport rates for the actual coastal orientations were obtained by interpolation.

3.9. Calibration of the longshore transport formulae

3.9.1. Electronic tracer pebble development

The concept of a tracer pebble, which utilises electronic tagging for the purposes of detection and recovery (developed by the Departments of Oceanography and Electronics at the University of Southampton), was recognised as a means for studying shingle movement in the area. Consequently, an undergraduate project was undertaken, to fabricate a number of sample tracers and to build a prototype detector (Prettijohn, 1992). Field trials were undertaken at Long Beach (Whitstable), to determine if the concept was feasible in practise. As a result of the comparative success of the first trials, a second undergraduate project was undertaken to upgrade the electronic tracer pebble design and provide improved performance (Workman 1993). More extensive field trials of the electronic pebbles, than were undertaken in the previous projects, were carried out at both Whitstable and at Hayling Island (southern England) (Whitcombe 1995).

Field trials at Long Beach (Whitstable) were designed as part of the present study and were carried out in collaboration with the undergraduate projects. The field trials are described in this Chapter and the results, which have been largely reanalysed, are presented in Chapter 5.

3.9.2. Sediment Dynamics Experiments (Long Beach, Whitstable)

Field investigations of longshore transport, in response to waves, were undertaken; these were in order to calibrate the predictive equation and to compare the transport rates derived using three different types of tracer pebble (painted, aluminium and transmitting) and the results of a beach plan area survey. Two experiments were carried out; the first in March 1992, the second in January 1993. The Long Beach site was selected for the experiments, as it provided a relatively long and straight beach confined at either end by major structures. Few

obstructions to transport were present along the beach itself. The experimental set-up used is shown in Figure 3.5.

Water levels during both of the experiments were abstracted from records obtained from the tide gauge in Whitstable Harbour.

Waves were measured using the Canterbury City Council wave recorder (which was operational throughout both experiments), located some 700 m to the northwest of the trial site. Because the wave recorder was located some distance away from the experimental site, an array of pressure transducers, located at the toe of the shingle beach, were used to provide additional wave data. The sensors were attached to metal posts, which were inserted into the beach so that their upper surfaces were located 20 cm above the beach sediments. An electromagnetic current meter was used to measure the horizontal component of the flow velocity, adjacent to one of the pressure sensors, at a height of 50 cm above the beach surface. The data produced by the sensors were sampled over 10 min, every half hour throughout the high tide cycle.

Measurement of the nearshore waves and their angle of approach depends upon several factors, including: (i) the sensor array dimensions; (ii) the wave speed; (iii) the actual wave angle; and (iv) the sampling frequency.

The pressure sensors were arranged in a square, with a base length of 10 m. This spacing was found to be the optimum arrangement for measuring wave parameters on shingle beaches elsewhere (eg at Shoreham (Chadwick, 1987) and at Hayling Island (Whitcombe 1995)). Wave speed is controlled by water depth at the location of the instrument. Water depths over the sensor head varied during the recording period, from 0.5 to 3.0 m; these relate to speeds of between 2.5 and 5.0 ms^{-1}, on the basis of Airy wave theory. Assuming a wave period of 3 s, the corresponding wavelengths are of the order of 6 to 15 m; consequently, a high frequency of sampling was required. The optimum sampling frequency has been investigated elsewhere by Whitcombe (1995). For water depths comparable to those found at Long Beach, it was determined that a frequency of 5 Hz was sufficient (provided that the angles of wave approach were not large).

A beach plan and level survey was carried out using a Wild (T1000) theodolite, fitted with an Electronic Distance Measurement (EDM) capability. The surveys were undertaken during daytime low tides, when the entire shingle beach was exposed. A temporary bench mark (TBM) was established, so that absolute beach levels could be recorded. The baseline for the survey lay approximately parallel to the beach orientation. Levels were determined at a number of profiles along the length of the beach, in order to determine volumetric changes over different parts of the beach.

Electronic, aluminium and painted pebbles were injected into the beach and their movement recorded. Electronic pebbles were detected using the specially-developed detector (Prettijohn, 1992; Workman, 1993). Aluminium pebbles were detected using a standard metal detector, with a discriminator. (Painted pebbles were not utilised as tracer material during the second study; this was due to the low recovery rates experienced during the first field trial and problems with interference from members of the public).

The beach was scanned, for both electronic and aluminium pebbles, in longitudinal strips. Hence, as the water level fell following high water, the search would commence, with the detector operators following the tide down the beach. This arrangement provided a search window of up to 10 hr (light permitting). Painted pebbles were located visually, at the same time that the beach was scanned with the electronic and metal detectors.

The positions of the pebbles and their depth of burial (not applicable for painted pebbles) were recorded using the EDM theodolite. In the case of the aluminium and electronic pebbles, the individual pebble number / code was also recorded.

The aluminium tracers consisted of 6 size / shape configurations; these were the same as those used by Wright (1982), in studies of beach shingle movement in the West Solent.

On the other hand, the electronic pebbles were cast in moulds obtained from pebbles found on Long Beach (Workman, 1993). Other studies on pebble populations on Start Bay (Gleason et al, 1975) have suggested that the mean pebble characteristics could be determined (within 0.2ϕ, at $p<0.01$) from a sample of 30 pebbles taken from the surface of the beach. Consequently, samples of 30 pebbles were collected from the beach along the tracer profile,

at 1 m intervals, from the beach crest to the beach toe (equating to 17 locations). For each pebble within a sample, the following parameters were determined: a, b and c axis; roundness; maximum projection sphericity (MPS); and oblate-prolate index (Dobkins and Folk, 1970). The mean and standard deviations of each of the (17) samples was determined and, in each case, the most typical pebble within the sample was selected for moulding (Workman, 1993).

The pebble parameters for each of the transmitting pebbles and for the six aluminium size / shapes are listed in Table 3.2. Although the electronic tracers are coarser in grain size than the mean composition of the beach, they may be considered as representative of the shingle portion of the distribution. The aluminium pebbles are generally larger and represented only the largest portion of the indigenous shingle material, (Figure 3.6).

Cores of painted pebbles were inserted into the beach at a number of locations, to determine the depth of the mobile layer. The location of the cores were marked using a metal post. Numbered aluminum pebbles were placed within the painted pebble core, at set levels. The pebble number, its level relative to Ordnance Datum and the levels of the top and bottom of the cores themselves were noted. These combined cores, of aluminium and painted pebbles, were used to determine the depth of disturbance of the beach sediments.

3.10 Sediment Budget.

3.10.1. Introduction.

Because of the length of the study area and the quantity of data which exists (and, therefore, requires validation), the sediment budget analysis has been carried out for selected sections of coastline; these are Whitstable - Central; Herne Bay - West and at Tankerton (see Figure 6.1). Historical beach profile data, as described in Section 3.2. were used to derive volumetric changes of the shingle beach as described below.

3.10.2. Beach management units and beach volume calculations.

For the sediment budget, each section of coastline was divided up into a number of beach management units (BMU). Beaches within each BMU have a similar coastal orientation and

groyne field pattern. Thus, since the beach at any part of the BMU is subjected to similar hydraulic stresses and physical restrictions on sediment movement, it should behave in a similar manner.

For each BMU, the volume of beach material present, over time, was calculated using the data from the beach monitoring stations. The supply of sediment to the beach, resulting from artificial replenishment, was also noted. In this way, temporal changes in beach volumes could be derived for each BMU.

Having determined the patterns of change within each individual BMU, the section of coastline was examined as a whole, in order to produce a balanced sediment budget and identify relationships between adjacent BMUs. The results are presented in Section 6.3.

Location / Port (Principal port in bold)	Tidal Conversion Coefficients(1) from			
	Sheerness		**Margate**	
	m	c	m	c
Sheerness	1	0	1.223	.103
Seasalter	.938	-0.029	1.148	0.067
Whitstable	.927	-0.034	1.134	.062
Tankerton / Studd Hill	.906	-0.046	1.109	0.047
Herne Bay	.895	-0.05	1.095	0.042
East Cliff	.878	-.055	1.075	0.036
Reculver / Minnis Bay	.865	-.063	1.059	0.026
Margate	.817	-.084	1	0

(1). Where tidal conversion coefficients are in the form $y = mx + c$

Table 3.1. Tidal Relationship Between Principal Ports and the Coastal Units within the Study Area.

Tracer Ref Number	"A" axis (cm)	"B" axis (cm)	"C" axis (cm)	Sphericity	Roundness	O-P Index
1	5.1	3.4	1.4	0.48	0.38	-1.4
2	4.8	3.8	2.1	0.62	0.15	-2.9
3	5.8	4.4	2.3	0.52	0.53	-2.5
4	6.3	4.0	2.6	0.65	0.41	+2.94
5	6.4	4.3	2.8	0.65	0.46	+1.90
6	4.1	3.0	2.1	0.71	0.64	+0.97
7	6.4	3.4	2.6	0.68	0.28	+7.12
8	5.2	4.4	3.0	0.73	0.35	-2.3
9	5.1	4.1	2.6	0.68	0.20	-1.96
10	5.2	3.6	2.9	0.77	0.33	+3.5
11	4.0	2.9	2.1	0.72	0.36	+1.5
12	4.9	3.8	2.7	0.74	0.36	+4.02
13	4.2	3.2	2.6	0.68	0.56	+2.01
14	4.3	3.0	2.2	0.72	0.33	+2.32
15	4.4	2.8	2.3	0.75	0.64	+5.01
16	4.0	3.0	2.4	0.78	0.50	+2.08
17	4.8	3.0	2.2	0.70	0.28	+4.19

(a)

Tracer Ref Number	"A" axis (cm)	"B" axis (cm)	"C" axis (cm)	Sphericity	Roundness	O-P Index
LR	5.7	4.9	4.4	0.88	0.31	+1.49
LA	7.0	6.5	3.5	0.68	0.37	-1.43
MR	6.1	3.4	3.0	0.75	0.44	7.54
MA	6.7	3.8	2.5	0.63	0.20	+5.10
SR	4.4	3.4	3.1	0.86	0.86	3.82
SA	5.8	4.5	2.4	0.60	0.17	-2.84

(b)

Table 3.2. Sedimentological Characteristics of: (a) Transmitting (after Workman, (1993)); and (b) Aluminium Tracer Pebbles (after Bray, (1990)).

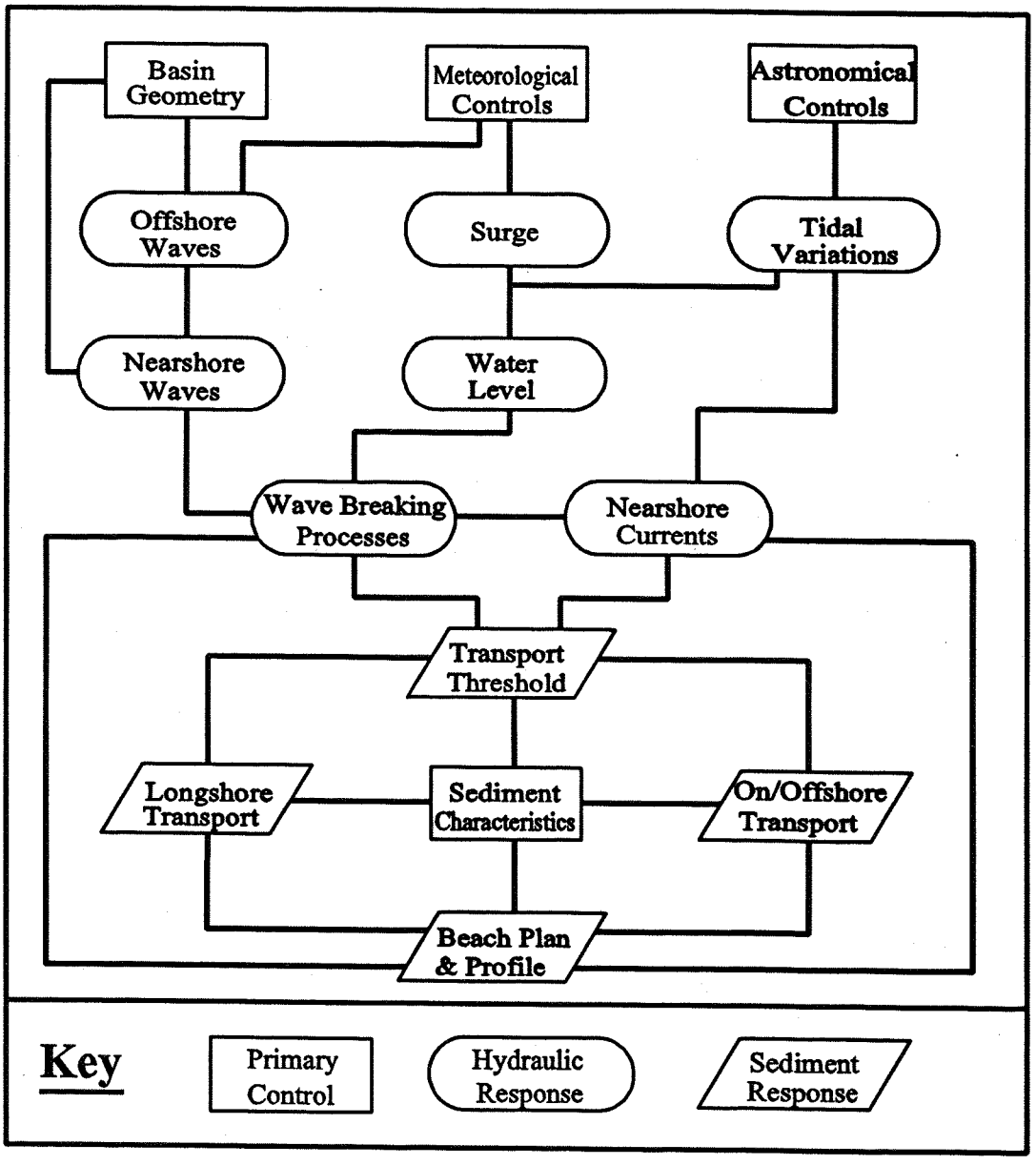

Figure 3.1. Relationship Between Primary Controls and the Hydraulic / Sediment Responses.

Figure 3.2. Location of Oceanographic Instrument Sites for the Data Sets Used in Study Area.

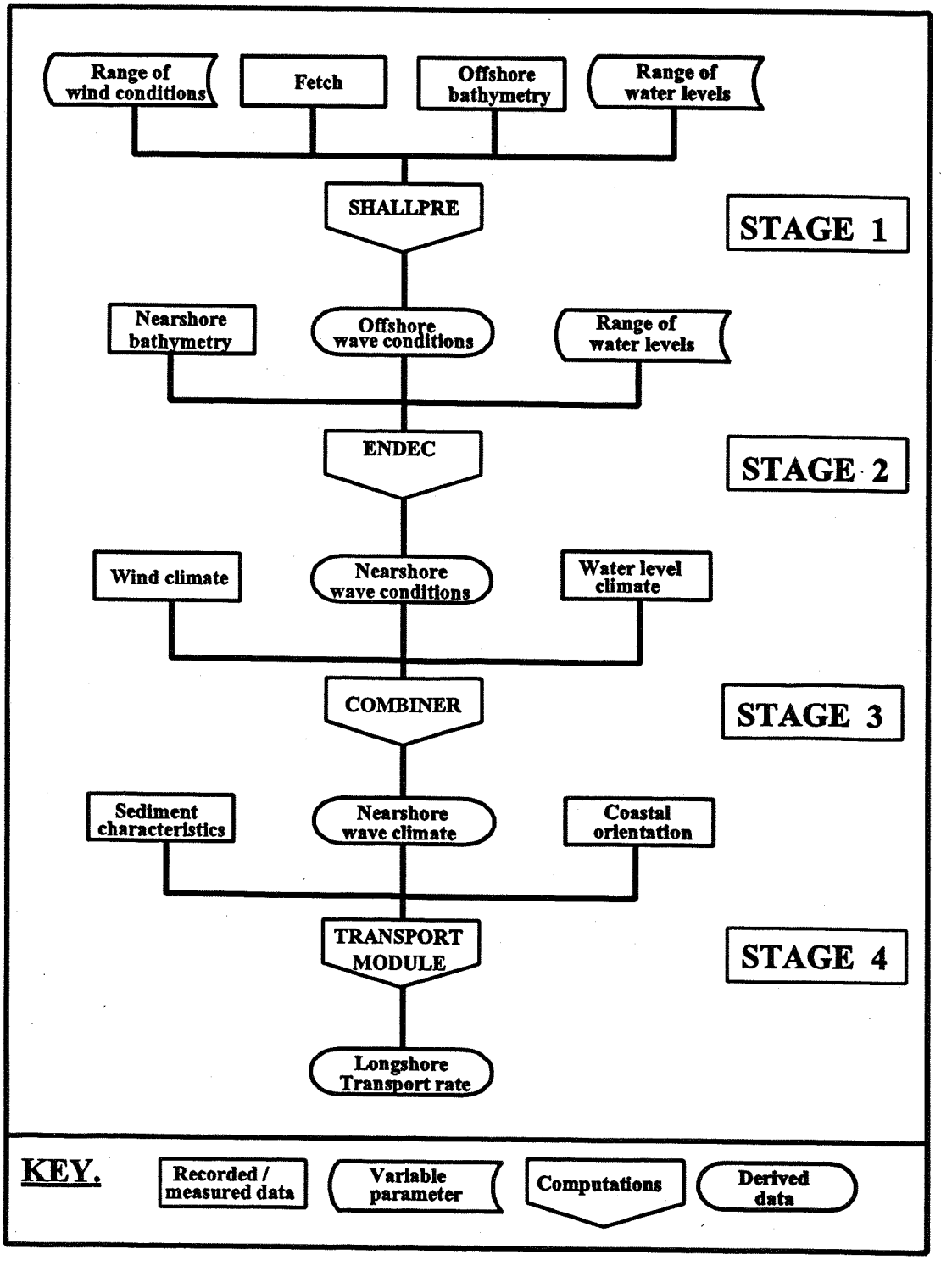

Figure 3.3. Stages Involved in the Development of a Numerical Model for the Study Area.

Figure 3.4. Subdivision of the Coastline into Coastal Units and Wind Directional Sectors, (see Section 3.4.2. for Explanation).

Figure 3.5. Experimental Setup for the Beach Process Field Study at Long Beach, Whitstable.

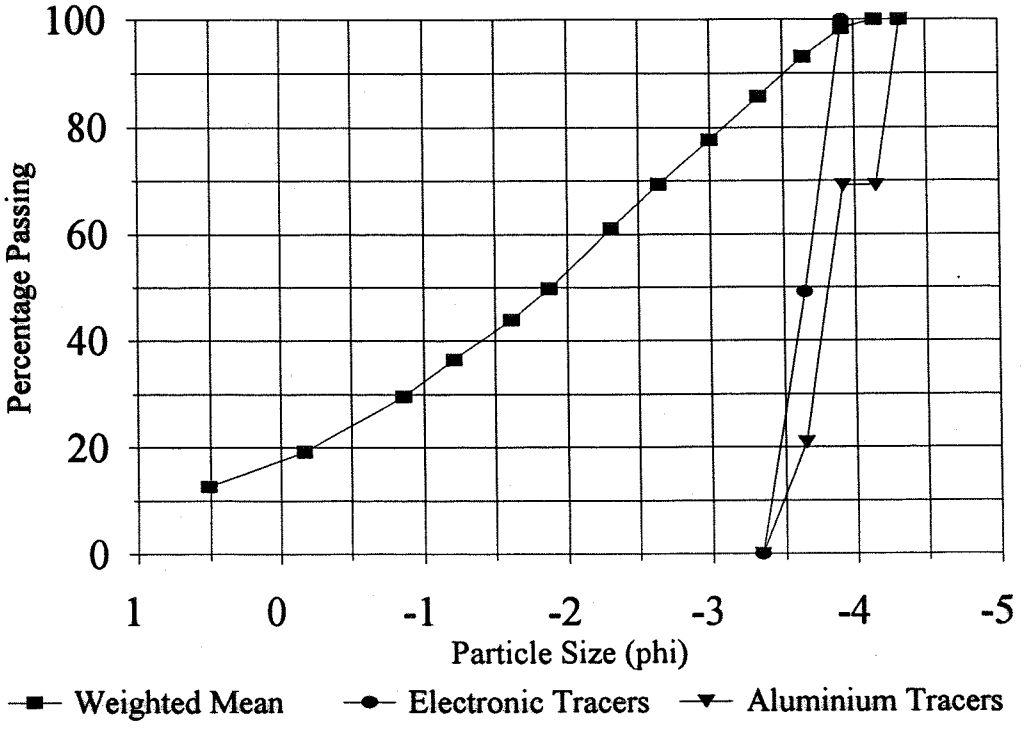

(see section 3.9 for explanation of weighted mean)

Figure 3.6. Particle Size Distribution Curve Showing Relationship Between Tracers and the Indigenous Beach Sediments.

CHAPTER 4: Results - Coastal Hydrodynamics Model

4.1. Introduction

Results of the first three stages of the coastal model (Figure 3.3) are presented in this chapter, including:

- offshore wave conditions;
- nearshore wave conditions;
- calibration of nearshore wave conditions with recorded wave data;
- derivation of a wind climate;
- derivation of a water level climate;
- derivation of offshore and nearshore wave climates;
- extent of year to year and seasonal variations in wind and, hence, wave conditions; and
- the nature of extreme (storm) events water levels and waves, in the study area.

The results described in this chapter will, in turn, be used to assist in the determination of potential longshore transport rates (Stage 4 of the coastal model), along the whole of the coastline in the study area (Chapter 5 and 6).

4.2. Offshore Wave Conditions

The program "SHALLPRE", written to solve the equations in the SMB hindcast model, has been used to produce offshore wave conditions for the 6 coastal units: (1) Seasalter & Whitstable; (2) Tankerton; (3) Studd Hill; (4) Herne Bay & Hampton; (5) East Cliff; and (6) Reculver, the Northern Sea Wall & Minnis Bay. Fetch lengths and typical water depths for each of the coastal units and directional sectors were selected, as described in section 3.2.1.; these are reproduced in Table 4.1.

An example of the output from "SHALLPRE" is shown in Table 4.2. These results are the offshore wave conditions for Unit 6 (Reculver to Minnis Bay) over a range of water levels and for wind stress factor (U_A) of 25. The maximum water depths referred to in the Tables represent the depth of water which is required so that there is no interaction between the

generated waves and the seabed (ie deep water waves). It can be seen from the results presented in Table 4.2. that the offshore waves generated have a high degree of interaction with the sea bed (ie they are shallow water waves); this justifies the use of the SMB equations, for modelling wave generation within the study area.

As expected, the offshore wave height and wave period increases with fetch length, water depth and with the wind stress factor. Fetch lengths and water depths increase from Sector 1 (westerly winds) to Sectors 5-7, (northeasterly and easterly winds) and the offshore waves show a corresponding increase in height and period, (Figure 4.1(a)). As the fetch and water depths also increase from Unit 1 (in the west) to Unit 6 (in the east) there is a similar increase in the offshore wave conditions (Figure 4.1(b)). This increase in wave activity towards the east of the study area represents a more open marine environment, compared with the west (as described in Chapter 2).

4.3. Nearshore Wave Conditions

4.3.1. Sensitivity Analysis

Having prepared the data required as input for the wave propagation model, ENDEC, a single profile was selected for the sensitivity analysis; the aim of this was to determine which of the input and processing parameters were the most important as regards their effect on the final results. The nearshore wave computer program (ENDEC) was run a number of times, using fixed offshore wave conditions. Each time the program was run, one of the program parameters was changed and the effect on the results noted. The process was then repeated, for a range of offshore wave conditions.

The results show that the nearshore wave conditions are most sensitive to: (i) water level / tidal state (eta); (ii) the bathymetric profile (Bp); and (iii) the bed friction factor, (f). The offshore wave height (Hs_o), period (Tp_o) and angle (θ) are important only when the water level is high and the wind speeds are low. Full results of the sensitivity analysis are reproduced elsewhere, (Canterbury City Council, 1993b).

Optimum breaking factors α and γ were selected by the software, based upon the particular

situation being modelled and on the results of laboratory tests of wave breaking with bed slopes of 0.01 to 0.02 (Delft Hydraulics, 1990b). However, it was noted that for more gentle slopes (0.001), wave heights after breaking may be underestimated by up to 10% when modelling non-steep waves (Delft Hydraulics, op cit). The nearshore region within the study area, is typified by shallow slopes however, modelling is generally restricted to steep waves and errors related to the selection of breaking parameters are considered to be secondary to water level, bathymetric profile and the friction factor.

4.3.2. Nearshore Wave Model Results

ENDEC was used to model the changes to waves which occur as they propagate towards the beaches in each of the ten coastal units / sub-units. For each directional sector, the program was run for a range of water levels (z = 0,1,2,3,4 and 5 m AOD.) and a range of wind stress factors (U_A = 5,10,15,20,25,30,35,40,45 and 50). The procedure was then repeated, for each of the coastal sub-units

The offshore wave height and period required as input were obtained from the results presented in the SHALLPRE Tables, by reading off the values which corresponded to the wind stress factor and water levels which were being used. Wave angles were fixed for each sector, by assuming that the offshore wave direction corresponded to the direction of the wind.

For each scenario modelled, the wave conditions at the toe of the beach were noted. In the case of the Whitstable unit (1B), wave conditions at the wave recorder position were also noted. Results were then compiled in a tabular format, (see, for example Table 4.3), for each of the coastal sub-units and directional sectors. These results are reproduced in full elsewhere; (Canterbury City Council 1993b). From each table of results, three graphs were plotted. These graphs show the variation of nearshore wave height, wave period and nearshore wave angle with the wind stress factor and water level; examples of these graphs are reproduced in Figures 4.2(a-c). Using the graphs, it is possible to hindcast the nearshore wave conditions resulting from a combination of wind stress factor, wind direction and water level, for any of the coastal sub-units.

Examination of Figure 4.2(a) demonstrates how the wave height increases with wind stress

factor for each tidal level, initially linearly; however, with increasing wind stress factor the rate of increase reduces. This reduction is due to the limiting effect that the water depth imposes upon the wave height. The water level limiting effect is more apparent in situations where there are large wave heights / periods, relative to the water depth at the beach toe.

It has been assumed that the wave period remains constant during the shoaling process; thus variation in wave period with water level and wind stress is defined in the offshore area and is unaltered as the waves propogate towards the beach . As with the wave height, wave period increases with the wind stress and water level, although the variation with the latter is small (Figure 4.2(b)).

Nearshore wave angles depend upon the water depth, wave height and the initial wave angle. In relatively deep water and with small wave heights, quite large wave angles may be maintained up to the beach toe, (Figure 4.2(c)). With larger wave heights (associated with larger wind stress factors) and relatively shallow water, the wave angles at the beach toe are reduced accordingly.

4.4. Recorded Wave Data

4.4.1. Wave record analysis (Whitstable Harbour).

The follow scattergraphs have been produced from the Whitstable wave data following the method of Draper (1967);

- yearly scattergraphs (July 1979 - June 1991);
- monthly (all years) scattergraphs;
- seasonal - summer and winter months (all years) scattergraphs; and
- summary - all data scattergraph.

Data recorded as part of a "continuous run", during a period of high wave activity, was used only if the individual wave record coincided with the normal frequency of recording (ie once every three hours). This approach avoided creating a bias in the scattergaphs, towards higher wave heights.

The summary (all data) and the seasonal scattergraphs are shown in Figure 4.3(a-c). Yearly and monthly scattergraphs are reproduced elsewhere (Canterbury City Council, 1993b).

A total of 22396 individual wave records were used to compile the "all data" scattergraph in Figure 4.3a. This scattergraph demonstrates the low wave energy nature of the study area (eg. only 0.1% of significant wave heights recorded exceed 1m). Wave periods are typically in the range of 3 to 5 seconds (Tz), rising to 5 to 7 seconds for waves with an Hs exceeding 1 m.

Waves with periods exceeding 7s rarely occur other than when associated with wave heights of less than 20cm. Such waves are likely to represent remnants of 'swell' waves, probably originating from North Sea storms (as records and visual observations show that they are dominantly northeasterly in direction) (Canterbury City Council, 1991)). As waves with longer periods interact more with the sea bed and the study area is characterised by a wide shallow nearshore region, the absence of larger waves with long periods is not unexpected.

Comparison of the wave records compiled for the winter and summer seasons (Figure 4.3(b&c)) show that there is more wave activity in the winter months (0.19% Hs exceeding 1.0 m) than in the summer months (0.02% Hs exceeding 1.0 m). The overall increase in wave heights seen in the winter season is reflected by an overall increase in wave period.

Breaking down the wave data into individual months reveals the degree of variation which occurs in wave energy throughout the year. Wave height exceedence graphs for Hs values of 0.5m, 0.75m, 1.0m and 1.25m are shown for each month, (averaged over the period 1979 to 1990), (Figure 4.4(a)). The monthly variation shows a seasonal variation, with the large waves most likely to occur in the winter months; an exception is the month of April which has the second greatest number of waves greater than 0.5 m, after February. Since the equivalent of just over seven years of data is available, (67% of data successfully collected and recorded over a period of eleven years), it would not be appropriate to draw any wide ranging conclusions from the data set, other than the existence of a summer / winter cycle.

Wave height exceedence graphs for Hs values of 0.5m, 0.75m, 1.0m and 1.25m (Figure 4.4(b)) have also been produced for each year of records, for comparative purposes. These results show that there is a degree of variation in the wave activity, from year to year, although the

effects are not as pronounced as for the monthly records (Figure 4.4(a)). There does appear to be a reduction in wave activity in the yearly graphs although, as in the case of the monthly charts, the data set is too short and incomplete to draw any conclusions as to the nature of the inter-annual trends in wave height exceedence.

4.4.2. Calibration of Wave Conditions with Recorded Wave Data.

From the wave data collected over the period February 1979 to December 1994, 1016 events were noted when the recorded wave height exceeded 0.50 m. For each of these events, the recorded wave height and wave period was noted. The wind speed and direction and the water level for each of these events was extracted from analogue chart rolls, which contain the raw data from the Local Authority tide and wind recorder at Whitstable (for locations see Figure 3.2). Having allowed for gaps in the wind and water level data sets, a total of 840 events were logged; in these all of the data required to carry out comparison between the recorded wave conditions and wave conditions predicted by the model were available. This represents an unusually good wave data set both in terms of the number of observations and the long period over which the data were collected.

The data outlined above were divided into seven sets, depending upon the wind direction. The sets corresponded to the wind directional sectors used in the study. Thus, for each sector, there is then available a set of actual recorded wave heights and periods, accompanied by wind speed and water levels at the time of the wave recording. As the data are not distributed evenly throughout the seven sets, the correlation will have a greater confidence in some of the wind directions than in others.

Tables of the available data for each sector are reproduced elsewhere (Canterbury City Council, 1993b). The following information has been included, for each event:

- a unique event reference number;
- wind direction recorded at Whitstable;
- wind speed recorded at Whitstable;
- wind direction recorded at Manston;
- wind speed recorded at Manston;

- corrections to Whitstable wind records;
- the calculated wind stress factor;
- recorded tide height;
- predicted wave heights;
- predicted wave periods;
- recorded wave height; and
- recorded wave period.

The data were sorted into ascending order on the basis of the recorded tidal level for each sector. Depending upon the number of events, the data for each set were split into sub-sets; each sub-set was made up of events with similar tidal levels. A regression analysis was then carried out, for both the predicted and the recorded wave heights and periods for each data sub-set to obtain a calibration coefficient. The results of this analysis are reproduced in Table 4.4. Where practical, the regression analysis has been carried out on sub-data sets defined by tidal level (see above), to determine how the correlation varies with water depth.

Wave heights and periods derived from the hindcast procedure are determined from spectral parameters. Hence the significant wave height ($Hs = Hm_o$) and wave period (Tp), used in the analysis will not correspond exactly to the significant wave height ($Hs = H_{1/3}$) and wave period (Tz) obtained from the wave records (as these are obtained statistically from the wave traces themselves).

In the case of significant wave height, the differences between Hs and Hm_o are small. A commonly-quoted relationship is $Hm_o = 1.05\ H_{1/3}$, on average (WMO, 1988). In shallow water and with steep waves, however, Hm_o becomes smaller than $H_{1/3}$; this is due to deformation of the wave form (CERC, 1984). The extent of the difference was estimated for the study area, based upon the theoretical relationship derived by Dean (1974), and field studies carried out by Thompson and Seelig (1984), and Hotta and Mizuguchi (1980). Once again, the estimated differences are small (ie. $Hm_o \simeq 0.97\ H_{1/3}$), with the exception of very shallow water conditions when the waves are at the point of breaking (when $Hm_o \simeq 0.85\ H_{1/3}$).

Comparisons between the peak spectral wave period (Tp) and the zero crossing wave period (Tz) are, likewise, problematical; an average correlation of $Tp \simeq 1.2Tz$ has been quoted by

WMO (1988). Muir Wood and Fleming (1981), state a correlation of Tp ≈ 1.4Tz, whilst Chadwick and Morfett (1993), simple state that the peak frequency Tp does not have a direct equivalent in the time domain.

The results of the regression analysis demonstrate that the correlation is dependent upon both the directional sector and the water depth. Generally, the predicted wave heights are lower than the recorded wave heights for the westerly directions and higher for the north and northeasterly directions. Comparison of the wave periods shows that the predictions are lower than the recorded values for westerly and northwesterly directions but are, on average, about equal for the remaining directions.

If events with a water level of less than 1.0m AOD (that is less than 2m of water above the recorder head) are ignored, then the calibration coefficients (for both wave height and period) fall within a much smaller range. Calibration coefficients for wave height are greater in shallow water than in deep water for directional Sector 1 - 6; there is insufficient data to identify the same pattern for Sector 7.

The most distinctive example of water level affecting the calibration coefficient is for Sector 1. Figure 4.5(a) shows plots of the predicted and recorded wave heights for Sector 1, sub-divided into four water level classes. Correlation between wave heights, for water levels in excess of 2.0m AOD, show a good visual correlation; a calibration coefficient of 1.01 obtained by the regression analysis supports this. With reducing water levels, the predicted wave heights become progressively lower than the corresponding recorded values. In the case of wave period, a plot of predicted v recorded wave periods (Figure 4.5(b)) identifies a similar water level influence albeit less, distinct than was noted for wave height, (Figure 4.5(a)).

The entire data set is presented elsewhere (Canterbury City Council, 1993b), as a series of line graphs showing the predicted and recorded wave heights / periods of the individual events. The corresponding water levels and wind stress factors are also included, to illustrate how they affect the correlation.

Whilst the correlation between predicted and recorded wave heights and periods is generally quite reasonable, the fact that spectrally derived parameters are being compared with

statistically derived parameters in shallow water means that the correlation factors themselves need to be treated with some caution. This limitation is discussed further in Section 4.4.3.

4.4.3. The Correlation between Predicted and Recorded Nearshore Wave Conditions

The available wave records have offered an opportunity to correlate the nearshore wave heights and periods, obtained using the coastal model, with recorded data. This is an unusual situation in coastal engineering since correlation (calibration) is often carried out at the final stages of modelling; this tends to be based upon features such as long term sediment accumulation against a prominent structure eg a jetty (Frihy et al, 1991).

Before selecting and applying general calibration coefficients to the coastal model it is worth considering the attributes of the output of the wave model and of the recorded data set. Errors and uncertainties which are likely to occur can be sub-divided into three categories: (i) errors in the wave records; (ii) errors associated with the correlation data set; and (iii) coastal model errors.

(a) Wave Record Errors

Wave records available for the study area were analysed, on behalf of the local Coast Protection Authority by an external consultant using C90 cassette recordings of the frequency modulation of the transducer. The analysed data is in the form of a list of tables of tide level, wave height (Hs) and wave period (Tz). The raw data on the tapes were not stored after analysis; consequently it has not been possible to reinspect or reanalyse the original data. The accuracy of the recordings is quoted in the operation manual as ±10%; however it is not clear as to how this error range should be interpreted.

Wave data from pressure transducers are very sensitive to the correction of the wave trace, for depth attenuation. Simplistically, the data collected by the pressure transducer has to be corrected, by multiplying the wave height by a factor which depends upon the water depth and wave period. This sensitivity is greatest when dealing with short period waves in shallow water (Figure 4.6). For example, for a water depth of 4m and a wave period of 3s, (typical of the study area), an error in the initial wave period calculation of only 0.2s would result in an error

in the attenuation correction factor of around ±15%.

Before March 1990, the data analysis was based upon the zero-crossing method: the significant wave heights were corrected for attenuation, based upon a single value of Tz. After March 1990, the data were analysed spectrally. In the case of the spectral method, it was possible to correct separately each frequency component for pressure depth attenuation. The effect of this procedure is to provide better estimates of the higher frequency components, than was possible with the zero-crossing method (Driver, 1992). Data analysed prior to March 1990 is likely to have longer periods and lower wave heights compared with the same data could it be reanalysed spectrally (Driver, 1992).

The bulk of the analysed wave data probably underestimated the significant wave height and overestimated the wave period, as a result of depth attenuation corrections. The extent of these errors cannot be ascertained, without obtaining the original raw data. Since the extent of the analysis errors varies with wave period, the difference in calibration coefficients between westerly (shorter wave periods) and northeasterly sectors (see above) could, at least in part, be a consequence of the data analysis technique.

The problem of correlating the statistically-based parameters from the wave records with the spectral wave parameters from the model has already been noted in Section 4.4.2.

The frequent breaking of waves, either on or in the near vicinity of the instrument head during a recording period, would adversely affect the results of the wave recording. This phenomena is more likely to occur at low water levels. Having examined the data sets it was considered prudent to exclude data for the correlation analysis where the still water level was below a nominal 1.0m AOD.

(b) Correlation Data Set Errors / Bias.

In selecting to use only data for which the recorded wave heights were greater than 0.5m, other events during which wind and water levels conditions would have led to predicted waves greater than 0.5m (but were recorded as being below the threshold level) are neglected. This approach would have had the effect of providing higher calibration coefficients, than would

be the case if all the recorded data were used. Ideally, the correlation should be carried out using the entire wave data set. However, due to the method of data logging, digitisation of the entire data set was not feasible.

(c). Wave Model Errors.

It was noted, for Sectors 5 and 6 in particular, that the same values of wind stress and water level were associated with a range of values of recorded wave heights and periods. The variation was considerably less in Sectors 1, 2 and 3. This difference may be attributed to the difficulty encountered in defining a representative fetch length, for the sectors which are "open" to the North Sea. The effective fetch will be controlled by the prevailing weather systems and, as such, could be either longer or shorter than the representative fetch which has been selected. The assumption that, for all of the events, the sea will be in a fully arisen state is less likely to be valid for the northern and eastern sectors.

According to the sensitivity analysis described in Section 4.3.1, errors in the sea bed friction factor and the wave breaking factors (used in the nearshore wave model) could result in errors of up to ±15% and ±5% respectively in the wave heights; however they would have little effect on the wave period. These errors are the main ones for which the calibration procedure was intended to compensate. Whilst errors in these parameters would affect wave heights in all the directional sectors, the effects may vary from sector to sector; this is related to the changes in the bathymetric profile and/or water depth.

The results of the correlation exercise describe above, demonstrate that the model predictions for wave height and period fall within the error ranges, normally associated with mathematical modelling (Soulsby, 1997). In terms of consistency, the model presented in the present study, performs well in comparison to many other studies, eg Henderson and Webber (1978) considering many of these studies were rather selective in the data sets chosen for evaluation. Model performance is considered further in the Discussion, (Chapter 7).

(d). Selection of Calibration Factors

Due to the changes in the wave field, for example brought about by refraction and diffraction, nearshore wave conditions will vary over short distances. Waves recorded at a particular point will not necessarily be the same as those contemporaneously recorded in similar water depths a short distance along the coast. Hence, the calibration coefficients obtained by the method outline previously (section 4.4.2) must be treated with some care, as there may be site-specific influences at the point of the recording.

The long length of the wave record data set, and the ability to carry out a directional comparison between hindcast wave conditions and recorded data, close to the shoreline, provides a high level of model validation. There are however, limitations upon both, the model itself, and the recorded wave data (as described in (a) to (c) above). It was decided not to correct the predicted waves to their exact recorded equivalents. Instead; calibration coefficients were selected which reflected the general trends in correlation with wind direction (Table 4.5).

In the short-term the calibration coefficients may be checked by collecting data on sea and weather conditions, over a period of a few days. During such a period the data collected from existing recording devices can be controlled and where possible, supplemented with additional recording methods. An example of an approach of this type is included in Chapter 5, as part of the Long Beach Study.

In the longer-term it would be desirable to up-date the existing instrumentation and analysis techniques, to provide better quality data sets for correlation purposes; this is discussed further in Chapters 7 and 8. Ideally, wave conditions at several sites in the study area would be recorded over a period of a number of years, to allow more effective calibration of the model; however, this is likely to prove prohibitively expensive.

4.5. Derivation of the Wave Climate

The derivation of the wave climate has been achieved by combining the calibrated nearshore wave conditions, with the wind and water level climates for each coastal unit (as described in

Chapter 3). The results from each stage of the procedure are presented and discussed in this Section.

4.5.1. Wind Climate

The hourly- averaged wind data obtained from Manston Airport, over the period January 1979 to December 1989, has been compiled and analysed to provide the likely occurrence of each combination of wind speed (Beaufort Scale) and wind direction in an average year. These results are presented in Figure 4.7(a). The likely occurrences of the stronger winds are low, and hence, wind speeds have been plotted on a logarithmic scale. Winds blowing from directions other than those defined by the directional sectors, accounting for 54.2% of occurrences, are not included.

The results presented in Figure 4.7(a) show that winds from the west (Sector 1), northwest (Sector 2 and 3) and northeast (Sector 5) are more frequent and tend to reach higher speeds on more occasions. Winds from the north (Sector 4) and from the east (Sector 6 and 7) are less common. This pattern gives a distinct asymmetry to the wind climate for the area, with the implication that locally-generated waves will be experienced more frequently as a result of westerly and northwesterly winds than with easterly and northeasterly winds.

The variation in the occurrence of the wind speed and direction, between summer and winter months, is demonstrated in Figure 4.7(b and c). The majority of the more extreme winds (Ws >force 7 (ie. >14.1ms^{-1})), occur in the winter period, (Figure 4.7(b)). The winter period also shows a dominance of westerly and northwesterly winds (Sectors 1 to 3). The main feature of the summer data set is that northeasterly winds (Sector 5) are the most common (Figure 4.7c). From the ten years of data available there would appear therefore to be a seasonal effect; in this, the onshore winds in winter are dominated by westerly winds, whilst those in summer are more likely to be northeasterly.

4.5.2. Water Level Climate

The results of the water level recordings carried out near Herne Bay, over two tidal cycles in March 1990, have been analysed to produce a water level distribution (or climate), (Table 4.6).

These data show the likelihood of exceeding each of the water level classes, for each of the coastal units. For units other than Herne Bay, the distribution was obtained by correcting the recorded water levels, based on the interpolation of tidal parameters between the principal ports of Sheerness and Margate (as described in Table 3.1).

4.5.3. Offshore Wave Climate.

Wave conditions for each combination of wind speed, wind direction and water level have been extracted from the tables produced by "SHALLPRE"; their likely occurrence is taken from the wind climate data. By summing all the occurrences of wave height and direction classes, an offshore wave climate can be produced for each of the coastal units. The results are shown in Figure 4.8 (a) and (b) for Unit 1 (Seasalter / Whitstable) and Unit 6 (Reculver to Minnis Bay).

Maximum offshore wave heights are generally quite small (not exceeding 3.0m) compared with similar studies (eg Whitcombe 1995), who found offshore wave heights of up to 10m (hindcast) off Hayling Island, Southern England. This suggest, that in contrast to sites along the south coast of England, coastal processes will be subjected to a wave climate containing considerably less energy; consequently sediment transport rates and their frequency of occurrence will be lower. The offshore wave climate results compare well with Delft Hydraulics studies undertaken for Herne Bay (Delft Hydraulics, 1990(a)), except that slightly higher wave heights were found in the northeasterly and easterly sectors; this is due to the longer fetches and deeper average water depths being used by Delft, for the offshore wave generation calculations. As shown in the sensitivity analysis, such differences in the offshore waves heights are unlikely to be reflected in the nearshore wave conditions. Hence, the differences between the studies is not considered to be significant in terms of the eventually wave conditions which are experienced on the shoreline and the subsequent transport of beach material.

The inequality between wave heights in the west and north, compared with the northeast is apparent in all of the offshore wave climates. Since the wave period tends to be larger associated with northeasterly and easterly winds, the inequality in terms of wave energy would be even more pronounced. Wave heights, in general, increase from Unit 1 (in the west) to Unit 6 (in the east); this reflects the increasingly open marine environment, with longer fetches and

deeper water. The increase in wave heights with respect to unit is most strongly marked with westerly and northwesterly winds. This relationship gives the impression that there is a reduction in the inequality of wave energy due to westerly / northwest and easterly / northeasterly winds, from Unit 1 (Seasalter) (Figure 4.8(a)), towards Unit 6 (Reculver to Minnis Bay), (Figure 4.8(b)).

4.5.4. Nearshore Wave Climate

The nearshore climates can be obtained using the wind speed, wind direction and water level occurrences, in combination with the results of the wave model results (section 4.3). For each combination of wind and water level conditions, the wave height, wave period and wave angle can be obtained from the graphs (as described in section 4.3.2). A nearshore wave climate can then be built-up in a similar fashion to the offshore wave climate. The nearshore wave (height) climate for Whitstable (Unit 1B) and Reculver (Unit 6A) are shown in Figure 4.9(a) and (b).

The nearshore wave climate shows that the directional inequality, in terms of wave height, has been reduced significantly - although waves from the north - northeast remain dominant. As in the case of the offshore wave climate, wave period has not been considered. Since northerly and easterly wind generated waves have the longest period, these directions are likely to remain dominant in terms of wave energy.

The maximum significant wave heights shown in Figure 4.9 are between 1.25 m and 1.5 m, (Hs), as would be anticipated from examination of the "all data" wave record scattergraph (Figure 4.3(a)). However it is important to remember that the results presented in Figure 4.9 are based upon what may be considered as "typical" water level conditions only. During storms the actual water levels are observed frequently to be elevated above 3.0m AOD.

Based upon the results of the nearshore wave modelling (for example, Figure 4.2), the main effect of these higher water levels would be to allow larger waves and / or waves with larger wave angles to reach the beach. Although such events are, by definition, infrequent, there is the potential to move large volumes of sediment in a short time period. Extreme events are considered in more detail, therefore, in the next section.

4.6. Extreme Events

During an extreme event, strong winds generate large waves which are incident upon the coastline. Storms within the area of study are associated frequently with an elevation of the still water level, above its normal tidal height. The effect of this water level elevation is two-fold, as far as shingle beach dynamics is concerned: (a), a larger area of beach is exposed to wave activity over the tidal cycle; and (b), larger nearshore wave heights and angles are possible, due to the increased water depth (see wave model results (section 4.3.2)). Thus, extreme events provide the potential to transport relatively large volumes of material over short periods of time compared, with the net annual drift (Seymore et al, 1990; Brampton 1993).

A full understanding of the nature of extreme events in the area is outside the scope of this study, but it important that the potential effect of such events on beach processes is considered and, if possible, quantified in some way. Indeed it may be that extreme events are an important, perhaps even controlling factor in the sediment dynamics of the region.

Six extreme events are to be considered and have been defined by their return periods; they are described as the 1 in 1, 1 in 5, 1 in 10, 1 in 20, 1 in 50 and 1 in 100 year events. Each event can be characterised by a series of nearshore wave heights, periods, angles and still water levels, throughout a tidal cycle.

4.6.1. Extreme Wind Conditions

Ten years of available wind data (mean hourly wind speed and direction), obtained from the Meteorological Office recorder at Manston Airport, have been fitted to a probability distribution. These results have been extrapolated to extreme return periods; the results, which are presented in Table 4.7, have been corrected for the inland location of the monitoring station following the procedures outlined in the Shore Protection Manual (CERC, 1984)

4.6.2. Extreme Water Levels

The water level z(t), observed at any location and time, can be described by the following equation:

$$z(t) = zo(t) + x(t) + y(t) + xy(t) \quad (4.1)$$

where zo(t) is the mean sea level, x(t) is the astronomical tidal component, y(t) is the meteorologically-induced surge component and xy(t) represents the surge - tide interaction. The term 'surge' is used to describe any deviation from the normal astronomical tide, which has resulted from weather conditions. Such deviations include barometric effects, external surges generated in the North Atlantic, internal surges generated in the North Sea (in response to either northerly or easterly winds, and wind-wave setup (Canterbury City Council, 1993b).

The southern North Sea and Thames Estuary are particularly prone to large surges (Pugh, 1987). Such large surges result from an increase in tidal energy, over dissipative losses, as the surge wave propagates down the eastern coastline of Britain, encountering increasingly shallow water depths.

The degree of interaction between the astronomical tide and the surge component (xy(t)) varies from site to site. In deep water areas, surge - tide interactions have not been observed (Pugh, 1987). In the study area, there is evidence of a strong interaction, which acts to reduce the size of the surge residual over the period of predicted high water. Examination of the distribution of larger surges (> 0.6 metres) at Southend (Figure 4.10). shows that they tend to "avoid" high water with most occurring a few hours before predicted high water. Pugh (1987) has also noted that the extent of the surge-tide interaction increases with the total water level.

In order to determine extreme water levels, the joint probability method of Pugh and Vassie (1979) was used. This approach is based on separating the water level into the tidal component x(t) and the surge component y(t). Separate probability distributions are fitted to each component; these are extrapolated to extreme values and recombined. Early joint probability studies carried out for ports in the southern North Sea and Thames Estuary were considered as suspect, due to the presence of the surge - tide interaction (Pugh, 1987). In order to reduce the effects of the surge - tide interaction, the analysis used in this study was based upon data recorded at the time of high water, ie the predicted high tide and the high water surge residual (Hydraulics Research 1981; 1985).

No suitable water level records existed within the study area, which could be used for the joint probability analysis. Therefore, data collected at the port of Sheerness, during 1978 and 1981 - 1986, were used. The distribution of high tides and the high water surge residual for Sheerness are shown in Table 4.8. Having extrapolated the distribution of the high water surge residual, the two data sets were recombined using a spreadsheet program "JOINTPRO", to provide the distribution of the maximum water levels at Sheerness. Using the conversion factors derived in Table 3.1, the high tide level distributions at coastal sites within the study area were obtained from the Sheerness data set. The results are presented in Figure 4.11.

Extreme water levels for Whitstable, obtained using the joint probability technique, were compared against actual data recorded at Whitstable Harbour. These results are presented in Table 4.9.

4.6.3. Extreme Wave Conditions.

The use of short term data sets to obtain extreme (storm) conditions has been applied to a number of studies. The most common technique which has been used involves fitting existing data into an established statistical distribution, which is then extrapolated to obtain the characteristics of more rare occurrences.

Le Mehaute and Wang (1984), have identified three types of errors which could lead to large uncertainties in predicting extreme wave conditions: (i) errors in measurement (instrumentation), (ii) errors resulting from a lack of knowledge on the functional relationship characterising the "true" long-term underlying distribution, particularly at low probability levels; and (iii) errors due to climatological variations or cycles related to the extrapolation of a small sample, to extreme events of low probability.

Whilst account could not be taken easily of the climatological / cyclic errors, Le Mehaute and Wang (op cit) derived formulae to quantify the errors related to instrumentation and the long-term distribution. Table 4.10, derived from the formulae of Le Mehaute and Wang (op cit), was constructed to relate the standard deviation of the recording method, the return period (T) and the standard deviation of T obtained for the number of years of data available. Assuming a standard deviation of 0.05 in the recording method and analysis, the data which are available

are sufficient to predict the 20 year wave with a standard deviation of 0.15; similarly the 50 year wave with a standard deviation of 0.20. The standard deviation of the 100 year wave would be in excess of 0.20.

The available significant wave height data and its likely probability of being exceeded were plotted as a number of distributions including the Weibul, Gumbel and Log normal relationships. The 'best-fit' was found by plotting the wave height on a linear scale against the probability of exceedence on Napier log scale (Figure 4.12). From the graph an equation was derived from which the significant wave height, Hs, with a probability of being exceeded once in a given period (T) could be found.

$$Hs = 15.1422 \cdot \ln(p) - 7.3784 \qquad (4.2)$$

Values of Hs with return periods of 1, 5, 10, 20, 50 and 100 years were derived from equation 4.2; these are reproduced in Table 4.11. The corresponding wave periods were estimated by examination of the pattern of larger waves in the "all data" scattergraph (Figure 4.3(a)).

4.6.4. Interdependence of Water Level - Wind / Wave Conditions.

A number of studies (Ackers, 1972; Hydraulics Research 1985; and Canterbury City Council, 1994a), have identified a relationship between the height of surges and the wind speed and direction in the Thames Estuary.

If surge heights were independent of the wind speed, then the joint probability ($P_{(Ws,z)}$) of extreme winds occurring at the same time as an extreme water level is equal to the sum of their individual probabilities,

$$P_{(Ws,z)} = P_{(Ws)} \cdot P_{(z)} \qquad (4.3)$$

Alternatively, if the still water level and wave heights are fully dependant, then the joint probability will be equal to the probability of either of the two single probabilities,

$$P_{(Ws,z)} = P_{(Ws)} = P_{(z)} \qquad (4.4)$$

Insufficient data are available to carry out a full examination of the degree of dependency between wind speed, wind direction and water levels in the study area. However, data from a number of sources have been used to carry out a qualitative assessment of the levels of dependency. The sources used are as follows:

(i) wind data from Shoeburyness and surge data from Southend, (1929 - 1968) (Ackers, 1972);

(ii) wind data from Shoeburyness and surge data from Sheerness (1963 - 1979) (Hydraulics Research, 1985),

(iii) recorded wind and water level data at Whitstable (1979 - 1993) (Canterbury City Council, 1994).

Ackers (1972), correlated wind direction with surge residuals at Southend. The results are reproduced in Table 4.12(a); these show clearly a strong relationship between wind direction and surge height. Large surges are most likely to occur associated with westerly or northwesterly winds, than with northerly or northeasterly winds.

The relationship between wind speed and surge height was also examined by Ackers (op cit); these results are summarised in Table 4.12(b). This analysis shows that strong winds are more likely to be associated with larger surges. Wind speeds equal to or greater than force 7 occur for less than 7%of the time; this is associated with over 14% of surges of between 0.6 and 0.9m and over 22% of surges greater than 0.9m at Southend.

Hydraulics Research (1985) carried out a study into the dependency of wind conditions and water levels for Whitstable. Examination of the frequency distribution of wind speeds for various surge residuals gave similar results to those of Ackers (op cit), in that large surges were more commonly associated with stronger winds.

With regard to wind direction and the surge residual, the Hydraulics Research (op cit) surge data was divided into four sets, depending on the wind direction (north west, north, north east and "other" winds). For each wind direction set, a high water surge height exceeded - return

period graph was plotted. The data were corrected using the factors obtained in Table 3.1, to provide the equivalent water levels at Whitstable. Finally, regression analysis was carried out on these data sets so that they could be extrapolated to greater return periods. The results are presented in Figure 4.13.

The results illustrate the dependancy of high water surge residuals on wind direction. From the graph, the high water surge residuals of various return periods for each wind direction can be obtained.

The final approach to the examination of the dependency between wind, water levels and waves is to examine actual storm events over the study area. However, as the Whitstable wind and tide data is not in a digital format, only specific storm events can be considered.

Examination of flood warning records for Whitstable, obtained between 1978 and 1993, lead to the identification of a number of events where the high water surge residual was in excess of 0.5m. For each event, subject to availability, the following were determined:

- recorded maximum water level;
- recorded surge residual;
- recorded wind speed;
- recorded wind direction;
- recorded wave height;
- recorded wave period;
- predicted wave period; and
- predicted wave height.

The results are reproduced in Table 4.13. All the events have recorded surge residuals greater than 0.5m and all (except for the 19/09/90 event), are accompanied by westerly or northwesterly winds. With the exception of the 11/01/93 event, the surges were accompanied by moderate to strong wave activity.

Examination of the individual return periods for the still water level, wind conditions and wave heights during the February 1953 event (which has also been included in Table 4.13),

demonstrates that all three parameters have low probabilities of occurrence, which may be interpreted as evidence of dependancy.

Due to the infrequent nature of extreme events, insufficient recorded data is available to quantify the interdependence of wind speed and direction on surges, maximum still water levels and wave conditions. Nevertheless, the evidence which is available suggests that interdependency does exist and should be taken into account when determining the frequency of storms, at any location within the study area.

As the purpose of the investigations into extreme events was aimed at examining the resulting longshore transport rates, a series of data sets of water level and nearshore wave conditions at the wave recorder has been compiled, for each of the storm return periods (Table 4.14). Because the water level - wave dependency data are based upon only three wind directional sectors (north-westerly, northerly and northeasterly), the same three wind direction sectors have been used.

The main observation which can be derived from the results presented in Table 4.14 is that the still water levels are significantly higher for northwesterly events; likewise, that this allows larger waves to reach the coastline, (see section 4.3).

	Unit $1_{(2)}$		Unit 2		Unit 3		Unit 4		Unit 5		Unit 6	
Sector $_{(2)}$	$F_{(1)}$	$D_{(1)}$	F	D	F	D	F	D	F	D	F	D
1	8	0	10	1	11.5	1	18	2	25	2	25	2
2	10	1	22	2	25	3	29	4	33	6	33	6
3	26	4	27	4	31	5	33	5	42	6	42	6
4	45	6	55	6	60	7	65	7	65	7	65	7
5	100	8	100	9	100	9	100	10	100	10	120	10
6	100	8	100	9	100	9	100	10	100	10	120	10
7	100	8	100	9	100	9	100	10	100	10	120	10

Where (1) F is the fetch length in kilometres and D is depth of water in metres (below Chart Datum);
(2) Refer to Figure 3.4 for location of sectors and units.

Table 4.1. Summary of Fetch Water Depths Used in the Offshore Wave Model.

Reculver to Minnis Bay (Unit 6). Wind Direction 345-015 (Sector 4).						
Fetch (metres) 65000 Water Depth (metres BCD) 7 Wind Stress Factor (Ua) 25						
Tide Height (mAOD)	Depth of Water (m)	Wave Height (m)	Wave Period (s)	Minimum Duration (hrs)	Max Water Depth (m)	Wave Type (Shallow or Deep)
-2.7	7.0	1.72	5.35	2.1	36.7	Shallow
-2.0	7.7	1.82	5.44	2.2	37.9	Shallow
-1.5	8.2	1.88	5.50	2.3	38.7	Shallow
-1.0	8.7	1.94	5.55	2.3	39.4	Shallow
-0.5	9.2	2.00	5.59	2.4	40.1	Shallow
0.0	9.7	2.05	5.64	2.4	40.8	Shallow
0.5	10.2	2.10	5.68	2.5	41.4	Shallow
1.0	10.7	2.15	5.72	2.5	41.9	Shallow
1.5	11.2	2.20	5.75	2.5	41.9	Shallow
2.0	11.7	2.24	5.79	2.5	42.5	Shallow
2.5	12.2	2.28	5.82	2.6	43.0	Shallow
3.0	12.7	2.31	5.85	2.6	43.4	Shallow
3.5	13.2	2.35	5.88	2.6	43.9	Shallow
4.0	13.7	2.38	5.90	2.7	44.3	Shallow
4.5	14.2	2.41	5.93	2.7	44.7	Shallow
5.0	14.7	2.44	5.95	2.8	45.1	Shallow
5.5	15.2	2.47	5.98	2.8	45.7	Shallow

Offshore Wave Hindcast Spreadsheet (Shallpre ver 1.3)

where; Unit 6 (Reculver to Minnis Bay) and Sector 4 (Northerly Wind direction) are shown in Figure 3.4.

Table 4.2. Example of SHALLPRE Output: Unit 6; Sector 4.

Wind Stress (Ua)	Tide Height (m. AOD).	Offshore Wave Height (Hs, m)	Offshore Wave Period (Tp, s)	Wave Height at Recorder (Hs, m)	Wave Angle at Recorder (α)	Beach Toe Wave Height (Hs, m)	Beach Toe Wave Angle (α)
5	-1	.55	3.05	.28	23	.23	14
10	-1	1.14	4.35	.29	17	.24	11
20	-1	1.92	5.66	.30	14	.25	10
30	-1	2.48	6.48	.31	13	.25	9
40	-1	2.93	7.10	.32	13	.25	9
50	-1	3.31	7.61	.32	13	.26	9
5	0	.56	3.07	.50	25	.40	20
10	0	1.18	4.40	.54	20	.45	16
20	0	2.02	5.75	.55	17	.47	14
30	0	2.62	6.59	.56	16	.48	13
40	0	3.12	7.23	.57	16	.48	13
50	0	3.54	7.74	.57	16	.48	13
5	1	.56	3.09	.55	26	.49	22
10	1	1.21	4.45	.69	22	.62	19
20	1	2.10	5.83	.79	19	.68	17
30	1	2.76	6.69	.82	18	.72	16
40	1	3.29	7.34	.83	18	.73	15
50	1	3.75	7.87	.83	18	.73	15
5	2	.57	3.11	.56	27	.50	24
10	2	1.23	4.49	.85	24	.76	21
20	2	2.18	5.90	1.04	21	.94	19
30	2	2.88	6.77	1.08	20	.97	18
40	2	3.45	7.43	1.10	19	.98	17
50	2	3.94	7.97	1.11	19	.99	17
5	3	.57	3.13	.57	28	.50	27
10	3	1.26	4.53	1.00	25	.89	24
20	3	2.24	5.96	1.28	22	1.17	21
30	3	2.99	6.85	1.36	21	1.24	19
40	3	3.61	7.52	1.38	20	1.26	18
50	3	4.13	8.07	1.39	20	1.27	18
5	4	.57	3.14	.57	29	.50	29
10	4	1.28	4.57	1.04	26	.93	26
20	4	2.31	6.02	1.45	23	1.36	23
30	4	3.10	6.92	1.61	22	1.48	21
40	4	3.75	7.60	1.67	21	1.53	20
50	4	4.31	8.16	1.71	21	1.56	19
5	5	.57	3.16	.57	30	.50	30
10	5	1.29	4.60	1.09	27	1.05	27
20	5	2.36	6.07	1.62	24	1.50	24
30	5	3.19	6.99	1.86	23	1.74	22
40	5	3.88	7.68	1.94	22	1.81	21
50	5	4.47	8.24	1.97	22	1.83	20

where; Unit 1B (Whitstable) and Sector 5 (Northeasterly Wind direction) are shown in Figure 3.4.

Table 4.3. Example of Endec Results for Unit 1B; Sector 5.

Directional Sector (1)	Water Level Class, (m AOD)	Calibration Coefficients (2)		Number of Observations
		Wave Height Coefficient (cHs)	Wave Period Coefficient (cTp)	
1	<1.1 1.0 - 2.0 > 1.9	1.55 (.09)(3) 1.13 (.03) 1.01 (.02)	1.12 (.03)(3) 1.13 (.02) 1.16 (.02)	27 27 34
2	<1.0 >1.0	1.24 (.06) 1.10 (.07)	1.14 (.04) 1.26 (.04)	12 15
3	<1.1 1.0 - 2.0 >1.9	1.03 (.04) .86 (.02) .85 (.02)	1.03 (.01) 1.10 (.01) 1.15 (.01)	32 59 63
4	<1.1 1.0 -2.0 2.0 - 2.5 >2.5	.87 (.02) .80 (.01) .79 (.02) .76 (.02)	.91 (.02) 1.02 (.01) 1.09 (.02) 1.11 (.02)	32 61 49 38
5	<1.1 1.0 -2.0 2.0 - 2.5 >2.5	.87 (.02) .76 (.01) .76 (.02) .77 (.01)	.88 (.01) .96 (.01) 1.06 (.02) 1.02 (.01)	65 109 90 49
6	<1.5 1.0 -2.0 >1.9	.89 (.03) .83 (.02) .80 (.02)	.92 (.03) .98 (.03) 1.09 (.03)	36 35 44
7	all	1.14 (.03)	.98 (.03)	22

where (1) Directional Sector is defined in Figure 3.4;
(2) Calibration coefficients are calculated by regression analysis;
(3) Numbers in brackets are the standard errors for the calibration coefficients; and
(4) Recorded Hs or Tp = predicted Hs or Tp multiplied by cHs or cTp

Table 4.4. Correlation Statistics of Predicted / Recorded Wave Heights and Periods.

Directional Sector (1)	Calibration Coefficient (2)	
	Wave Height Coefficient	Wave Period Coefficient
1	1.15	1.15
2	1.15	1.15
3	.95	1.05
4	.85	1.05
5	.80	1.0
6	..85	1.0
7	1.15	1.0

where (1) Directional Sector is defined in Figure 3.4;
(2) Calibration coefficients are calculated by regression analysis;
(3) Recorded wave height / period = predicted wave height / period times calibration coefficient

Table 4.5. Calibration Coefficients to be used with the Nearshore Wave Model.

Still Water Level Range (z, m AOD).	Percentage Exceedence of Still Water Level Range.			
	Seasalter / Whitstable (Unit 1).	Tankerton / Studd Hill (Units 2&3).	Herne Bay / East Cliff (Units 4&5)	Reculver - Minnis Bay (Unit 6)
> 3.0	0	0	0	0
2.5 to 3.0	4	3	2.1	1.5
2.0 to 2.5	12	10.3	8.5	7.0
1.5 to 2.0	23	21.9	20.6	19
1.0 to 1.5	34	33.1	32.1	31
0.5 to 1.0	44	43.3	42.6	42
0.0 to 0.5	52.5	52	51.5	51
-0.5 to 0.0	65.5	64.9	64.4	63.5
-1.0 to -0.5	77	77.4	77.7	78
-1.5 to -1.0	86	86.8	87.4	88.5
-2.0 to -1.5	95	95.5	96.2	97
-2.5 to -2.0	98.5	98.8	99.1	99.5
-3.0 to -2.5	100	100	100	100

Table 4.6. Still Water Level Frequency Distribution for the Study Area.

Return Period (yrs) of Extreme Wind Speeds (ms^{-1})	Wind Directional Sector						
	1	2	3	4	5	6	7
1	23	22.1	21.9	18.4	20.1	19.2	18.6
5	25	23.4	23.8	20.7	21.9	21.6	20.4
10	26.3	24.1	25	21.3	23	22.2	21.6
20	27	24.7	25.6	22.4	23.6	22.8	22.2
50	27.7	25.4	26.9	23	24.2	23.4	23.4
100	29.0	26.7	28.1	23.6	24.7	24.6	24

where; wind speeds are statistically extrapolated from 10 years of recorded wind data at Manston Airport and are location corrected based on the SPM (CERC, 1984); see section 4.6.1 for details.

Table 4.7. Occurrence of Extreme Wind Conditions at the Coastline in the Study Area.

Predicted High Water Level		Percentage Occurrence of Predicted High Water	Recorded High Water Surge Residual		Percentage Occurrence of Surge Residual
Lower limit of Range (m AOD)	Upper limit of Range (m AOD)		Lower limit of Range (m)	Upper limit of Range (m)	
1.0	1.25	0.03	-1.5	-1.25	0.063
1.25	1.5	1.22	-1.25	-1.0	0.081
1.5	1.75	5.95	-1.0	-0.75	0.252
1.75	2.0	10.9	-0.75	-0.5	1.24
2.0	2.25	15.9	-0.5	-0.25	8.91
2.25	2.5	19.0	-0.25	0.0	41.37
2.5	2.75	21.8	0.0	0.25	40.92
2.75	3.0	16.8	0.25	0.50	5.96
3.0	3.25	7.87	0.50	0.75	0.99
3.25	3.5	0.53	0.75	1.0	0.117
3.5	3.75	0	1.0	1.25	0.099

Where; the Predicted High Water Levels and Recorded High Water Surge Residuals at Sheerness are after Hydraulics Research, 1984).

Table 4.8. Frequency Distribution of Predicted High Water Levels and High Water Surge Residuals At Sheerness, (1978, 1981-1985).

Date of Recorded Event	Still Water Level (1) (m AOD)	Return Period (3) (yrs)
01/11/86	3.544	2.3
24/12/88	3.388	0.8
26/02/90	3.285	0.4
27/02/90	3.385	0.6
28/02/90	3.485	1.7
19/09/90	3.485	1.7
21/09/90	3.285	0.4
07/10/90	3.585	2.9
12/12/90	3.285	0.4
25/12/92	3.273	0.4
11/01/93	3.467	1.3
25/01/93	3.667	5.9
21/02/93	3.767	8.3
31/12/78	4.206	33.7
01/02/53	4.764(2)	136.3

Where (1) water levels are corrected to 1982 equivalent values for isostatic sea level rise.
(2) 1953 water level is visually observed
(3) Return periods of extreme water levels are based on figure 4.11.

Table 4.9. Extreme Water Levels Recorded At Whitstable Harbour.

Return Period (years)	Standard Deviation of Estimate	Standard Deviation of Recording Method		
		0.05	0.10	0.15
		Number of years of records required		
100	0.20	18	23	40
100	0.15	40	-	-
50	0.20	9	12	22
50	0.15	-	21	35
20	0.20	4	7	12
20	0.15	8	11	17
20	0.10	25	-	-

after the method of Le Mehaute and Wang (1984).

Table 4.10. Theoretical Accuracy of Extreme Wave Predictions.

Return Period (yrs)	Significant Wave Height (1) (Hs)	Wave Period (2) (Tz)
1	1.13 (±0.6)	5.5
5	1.38 (±0.6)	6
10	1.48 (±0.7)	6
20	1.58 (±0.7)	6.5
50	1.72 (±0.7)	6.5
100	1.83 (±0.7)	7.0

Where, (1) extreme wave heights are derived from a statistical fit for data recorded at Whitstable Harbour (1978 to 1990) (figure 4.12); and
(2) associated wave periods are obtained from the wave height / period scattergraphs, Figure 4.3(a)

Table 4.11. Extreme Wave Conditions at Whitstable based on Statistically Extrapolated Recorded Data.

	Wind Direction Sector (1)							
	1	2	3	4	5	6	7	Other
All Tidal States (2)	7.268	8.315	6.435	6.056	8.004	6.117	4.818	52.969
With High Water Surge Residual (2) 0.6 - 0.9m	16.1	14.6	10.9	6.9	4.5	5.8	3.6	37.6
With High Water Surge Residual (2) > 0.9m	18.2	23.7	20.7	5.6	1.5	1.5	0.5	28.3

Where (1) Wind Direction Sector is shown in Figure 3.4 and is recorded at Shoesburyness; and
(2) Water Levels / Surges are recorded at Southend.

Table 4.12(a). Percentage Occurrence of High Water Surge Residuals (Southend) by Wind Direction (after Ackers, 1972).

	Wind Speed, Beaufort Scale (1)									
	1	2	3	4	5	6	7	8	9	10
High Water Surge Residual (2) < 0.6m	93.2						4.48	1.89	0.35	0.03
High Water Surge Residual (2) 0.6 - 0.9m	0	0.52	5.57	27.2	31.2	21.3	9.98	3.47	.63	0.11
High Water Surge Residual (2) > 0.9m	0	.76	2.53	20.2	28.3	26.0	15.2	4.80	1.77	0.51

Where (1) Wind Direction Sector is shown in Figure 3.4 and is recorded at Shoesburyness; and
(2) Water Levels / Surges are recorded at Southend.

Table 4.12(b). Percentage Occurrence of High Water Surge Residuals (Southend) by Wind Speed (after Ackers, 1972).

Table 4.13. Recorded Maximum Still Water Levels and Wind / Wave Conditions for Storm Events at Whitstable.

Date of Recorded Event	Still Water Level Whitstable Harbour (1)		Wind Conditions Whitstable (2)			Recorded Wave Conditions Whitstable Harbour			Predicted Wave Conditions Whitstable Harbour		
	Still Water Level mAOD.	Estimated Return Period (3) (yrs)	Recorded Wind Speed (ms^{-1})	Recorded Wind Direction (Sector)	Estimated Return Period (4) (yrs)	Wave Height (Hs)	Wave Period (Tz)	Estimated Return Period (5) (yrs)	Wave Height (Hs)	Wave Period (Tz)	Estimated Return Period (5) (yrs)
01/11/86	3.54	2.3	11	3	<1	-	-	-	0.97	4.4	0.3
24/12/88	3.39	0.8	7	1	<1	-	-	-	0.45	2.4	-
26/02/90	3.29	0.4	17	1	1.0	0.84	4.29	0.2	0.86	3.1	0.2
27/02/90	3.39	0.6	12	1	<1	0.85	4.38	0.2	0.74	2.8	-
28/02/90	3.49	1.7	17	1	1.0	-	-	-	1.26	4.7	2.5
19/09/90	3.49	1.7	8	3	<1	-	-	-	1.02	4.55	0.5
21/09/90	3.29	0.4	13	5	<1	-	-	-	0.65	2.5	-
07/10/90	3.59	2.9	10	1	<1	-	-	-	0.85	3.8	0.2
12/12/90	3.29	0.4	19	1	7	-	-	-	1.38	5.0	5.0
25/12/92	3.27	0.4	12	3	<1	1.26	4.00	2.5	1.04	4.3	0.5
11/01/93	3.47	1.3	13	-	<1	0.30	3.30	-	-	-	-
25/01/93	3.67	5.9	8	4	<1	0.66	3.96	-	0.69	3.5	-
21/02/93	3.77	8.3	16	3	(0.5)	1.40	4.40	5.8	1.38	5.4	5.0
01/02/53	*4.76 (6)*	*136.3*	*21*	*3/4*	*30*	*1.8*	*6.5*	*80*	*1.71*	*6.1*	*45*

Where; (1) Still water levels are recorded at Whitstable Harbour and have been corrected to 1982 equivalent values for isostatic sea level rise;
(2) Wind conditions are recorded at Borstal Hill, Whitstable; (3) Still water level return periods are based upon results presented in Figure 4.11.;
(4) Wind speed return periods are based upon results presented in Table 4.7;
(5) Significant wave height return periods based on results presented in equation 4.2 / Figure 4.12; and
(6) Water levels, and Wave conditions for the 1st February 1953 are based on visual observations.

Wind Direction	Event Return Period, (yrs).	Maximum Still Water Level (1), (mAOD).	Wind Speed (2) (ms^{-1})	Predicted Wave Height (3) (Hs, m)	Predicted Wave Period,(3) (Tp, s)	Predicted Wave Angle (3), (α°).
Northwesterly	1	3.41	21.9	1.43	5.0	-23
	5	3.66	23.8	1.50	5.2	-23
	10	3.86	25.0	1.57	5.3	-23
	20	4.05	25.6	1.65	5.4	-24
	50	4.31	26.9	1.73	5.5	-24
	100	4.59	28.1	1.82	5.6	-24
Northerly	1	3.09	18.4	1.32	5.4	0
	5	3.21	20.7	1.39	5.5	0
	10	3.38	21.3	1.45	5.6	0
	20	3.52	22.4	1.51	5.8	0
	50	3.72	23.0	1.56	5.9	0
	100	3.98	23.6	1.62	6.0	0
Northeasterly	1	3.09	20.1	1.40	6.7	22
	5	3.21	21.9	1.45	6.9	22
	10	3.38	23.0	1.50	7.0	22
	20	3.52	23.6	1.53	7.2	22
	50	3.72	24.2	1.59	7.3	23
	100	3.98	24.7	1.65	7.4	23

Where; (1) Maximum still water levels are obtained from the results presented in Figure 4.14;
(2) Wind speeds are based on results presented in Table 4.7; and
(3) Predicted wave conditions are based on the coastal model output described in section 4.3.

Table 4.14. Extreme Event Criteria derived for the Whitstable Wave Recorder Site for Northwesterly, Northerly and Northeasterly Winds.

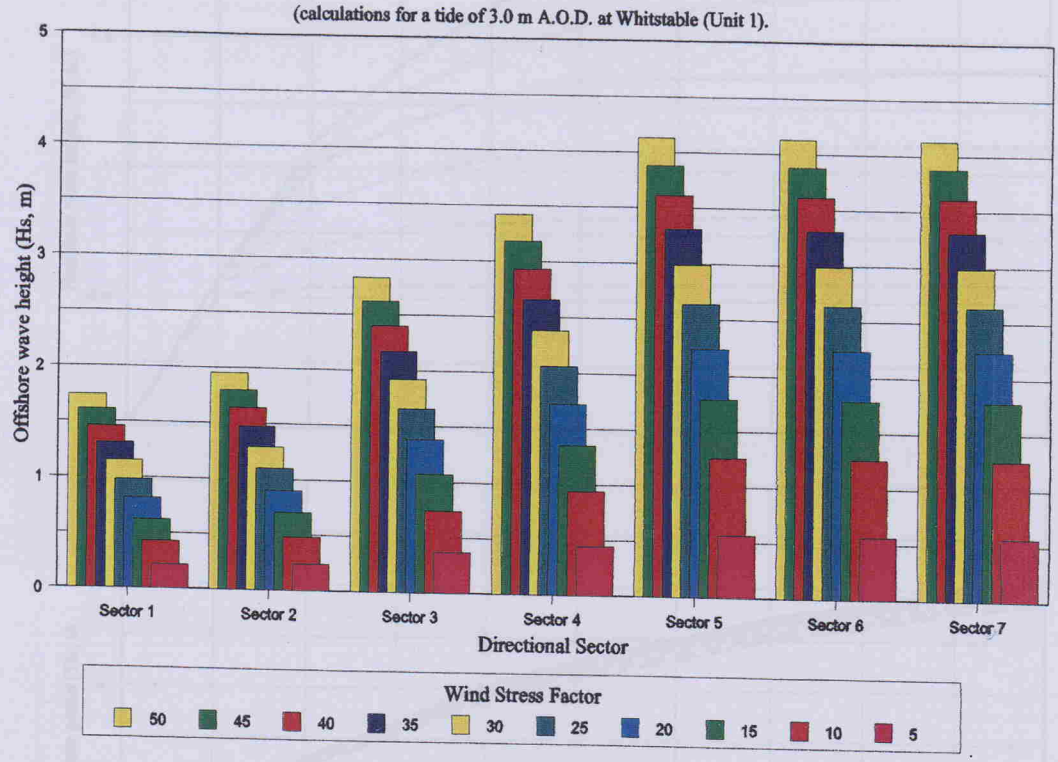

Figure 4.1(a). Comparison of Offshore Wave Heights for the Various Directional Sectors

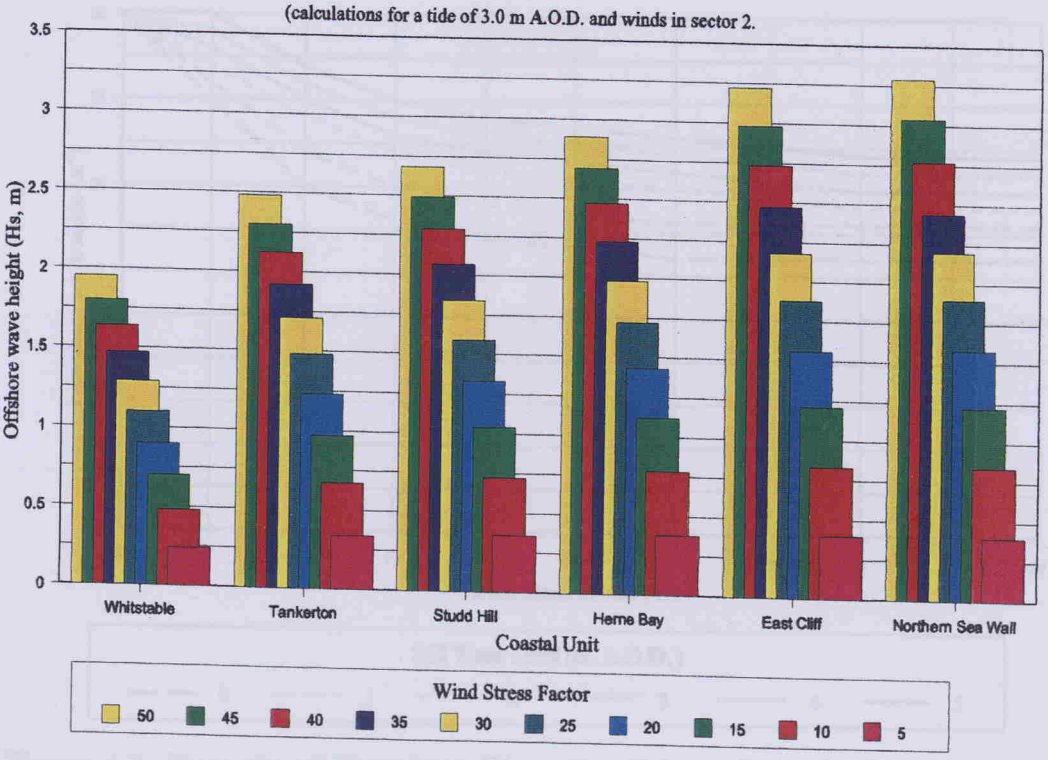

Figure 4.1(b). Comparison of Offshore Wave Heights for the Various Coastal Units.

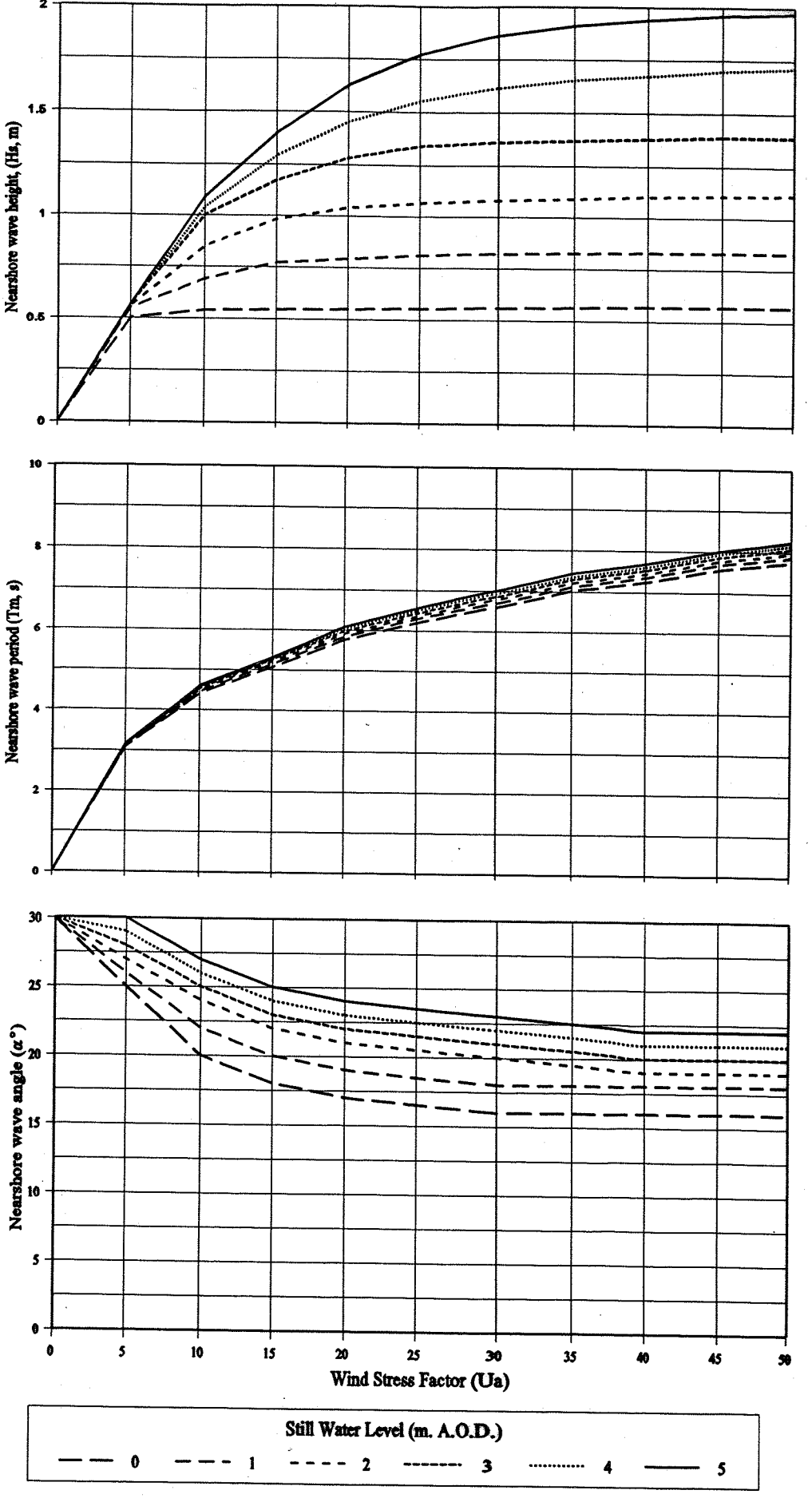

Figure 4.2. Example of Nearshore Wave Conditions from the Wave Model Showing Variation in (a) Wave Height (Hs, m); (b) Wave Period (Tz, s); and (c) Wave Angle (∝, °).

Figure 4.3(a). Wave Height / Period Scattergraph based on Records from Whitstable Harbour (1978 - 1990).

Figure 4.3(b). Wave Height / Period Scattergraph based on Records from Whitstable Harbour (1978 - 1990, Winter Months).

Figure 4.3(c). Wave Height / Period Scattergraph based on Records from Whitstable Harbour (1978 - 1990, Summer Months)

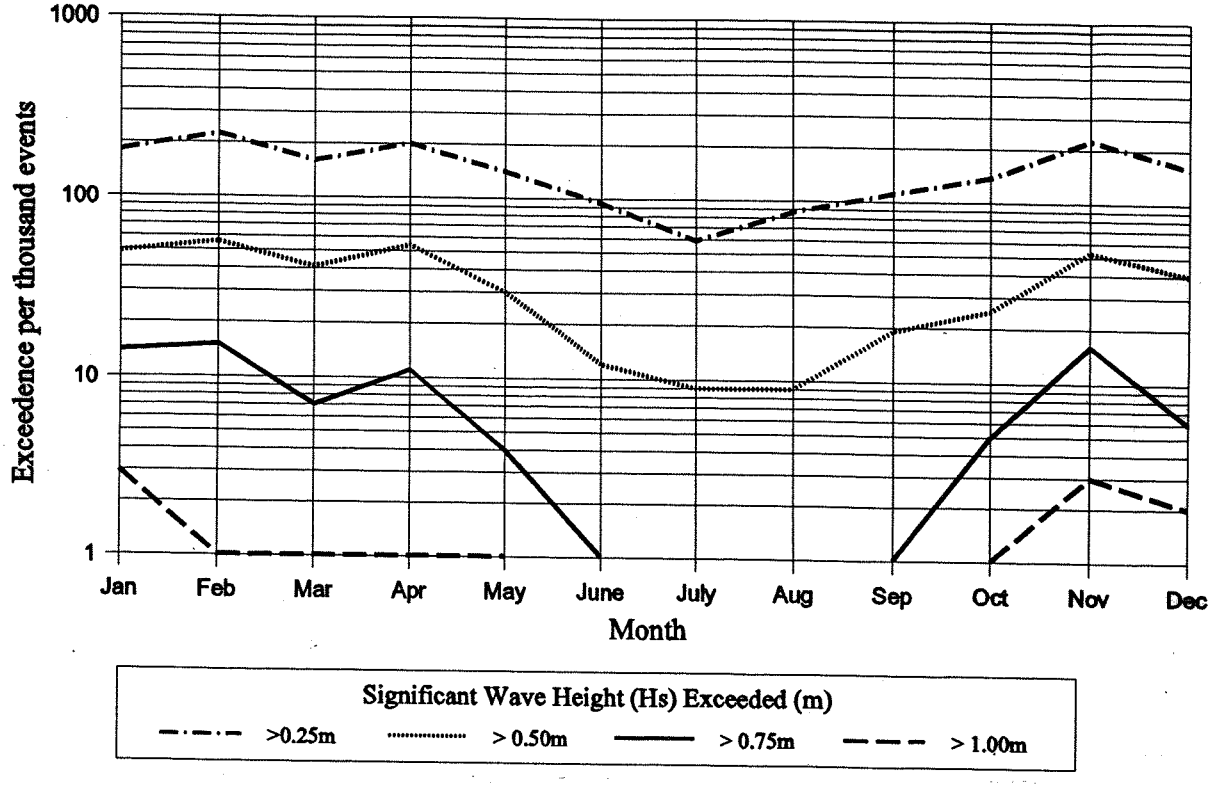

Figure 4.4(a). Monthly Variation in the Exceedence of Recorded Wave Heights at Whitstable Harbour, (1978 - 1990).

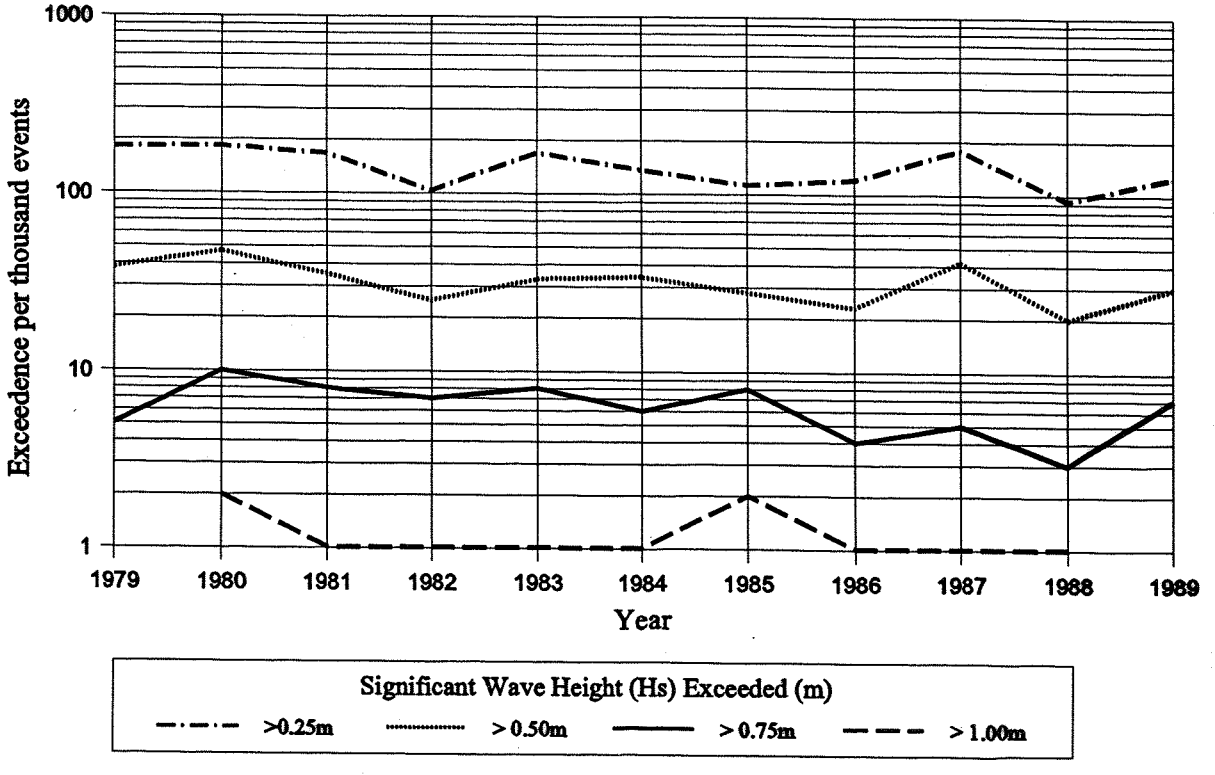

Figure 4.4(b). Yearly Variation in the Exceedence of Recorded Wave Heights at Whitstable Harbour, (1978 - 1990).

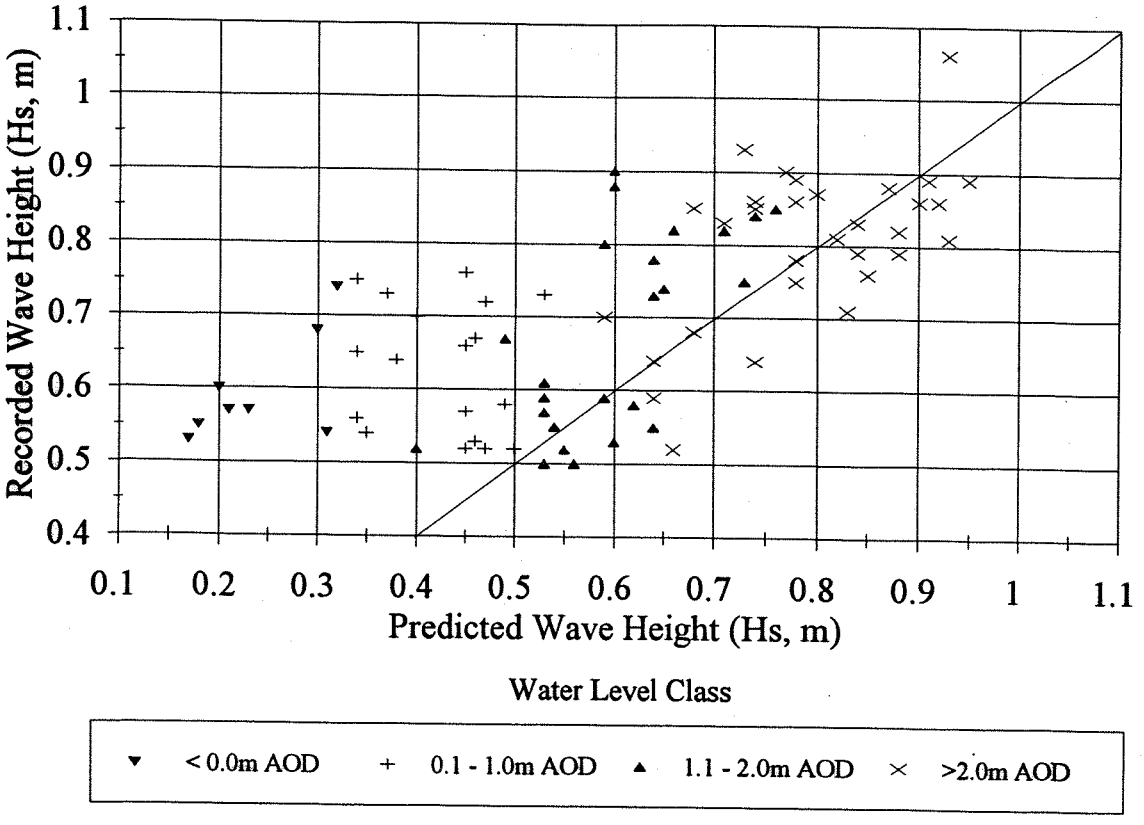

Figure 4.5(a). Predicted Wave Height (Hs, m), versus Recorded Wave Height (Hs, m), at the Whitstable Harbour Recorder (for Sector 1), Showing the Effects of Water Level.

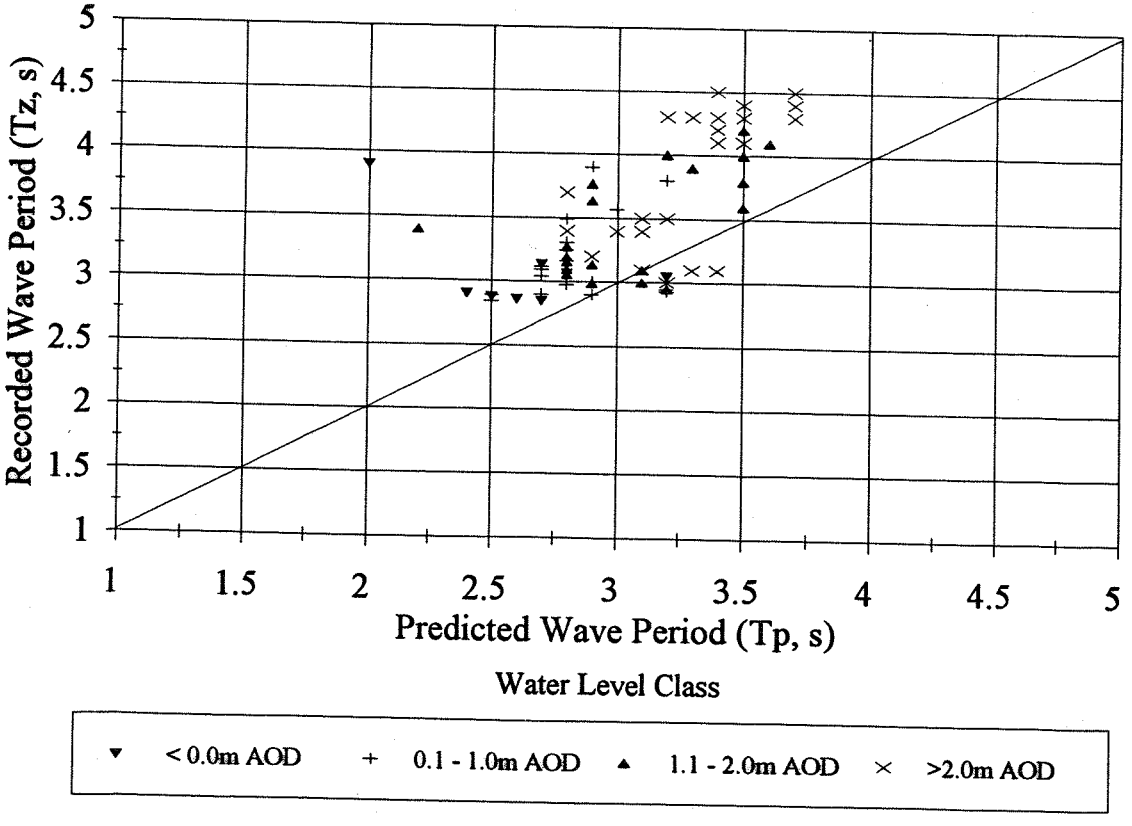

Figure 4.5(b). Predicted Wave Period (Tz, s), versus Recorded Wave Period (Tp, s), at the Whitstable Harbour Recorder (for Sector 1), Showing the Effects of Water Level.

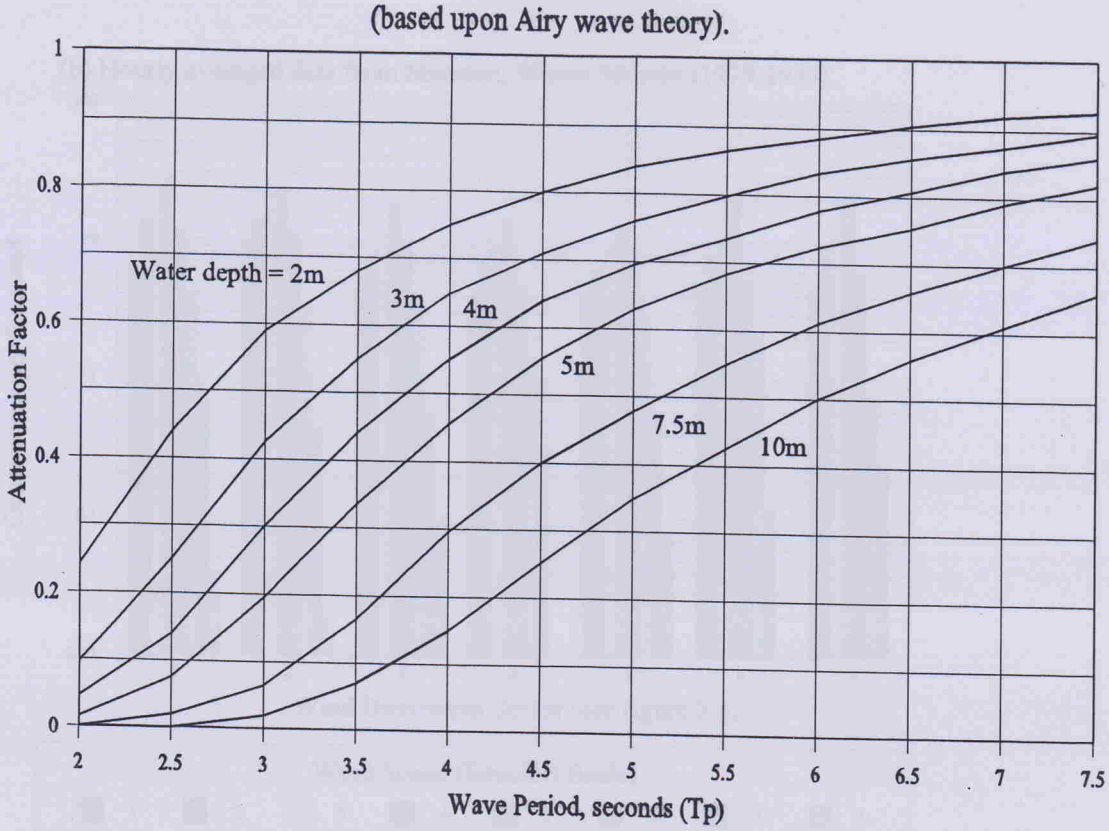

Figure 4.6. Depth Attenuation of Surface Waves with Wave Period and Water Depth.

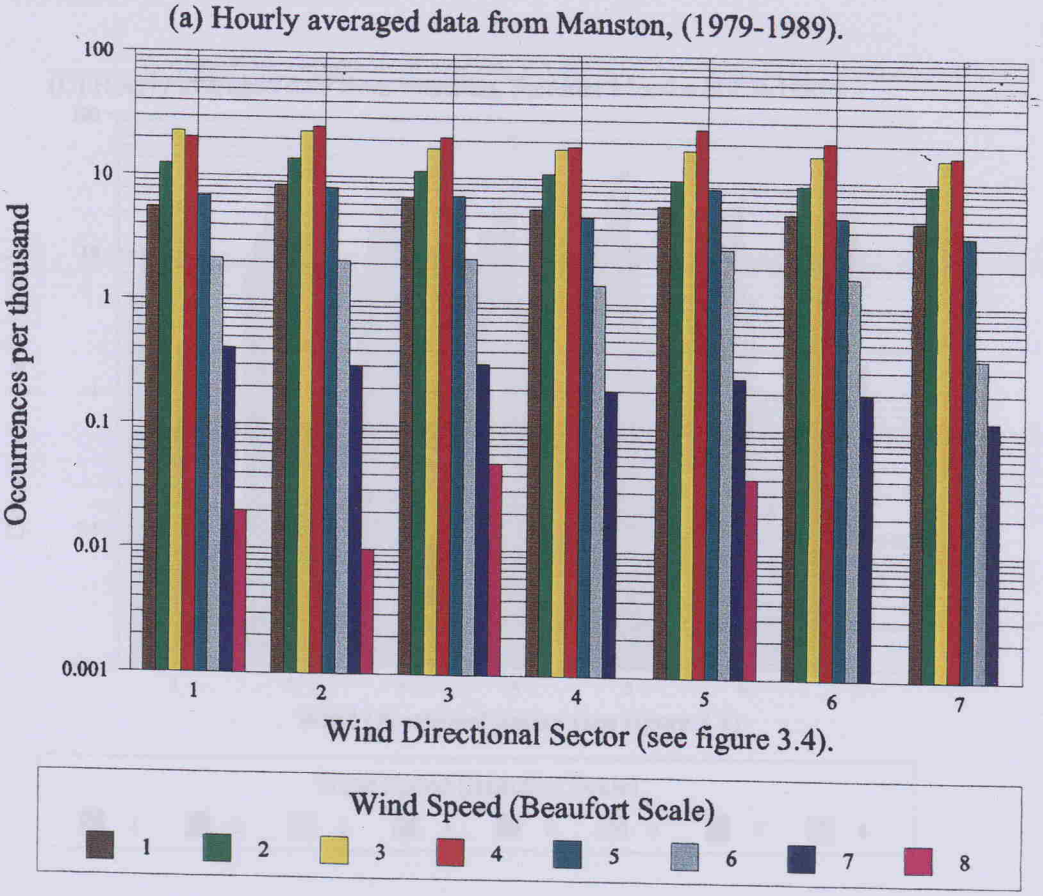

Figure 4.7(a). Annual Wind Climate At Manston Airport (1979 to 1989).

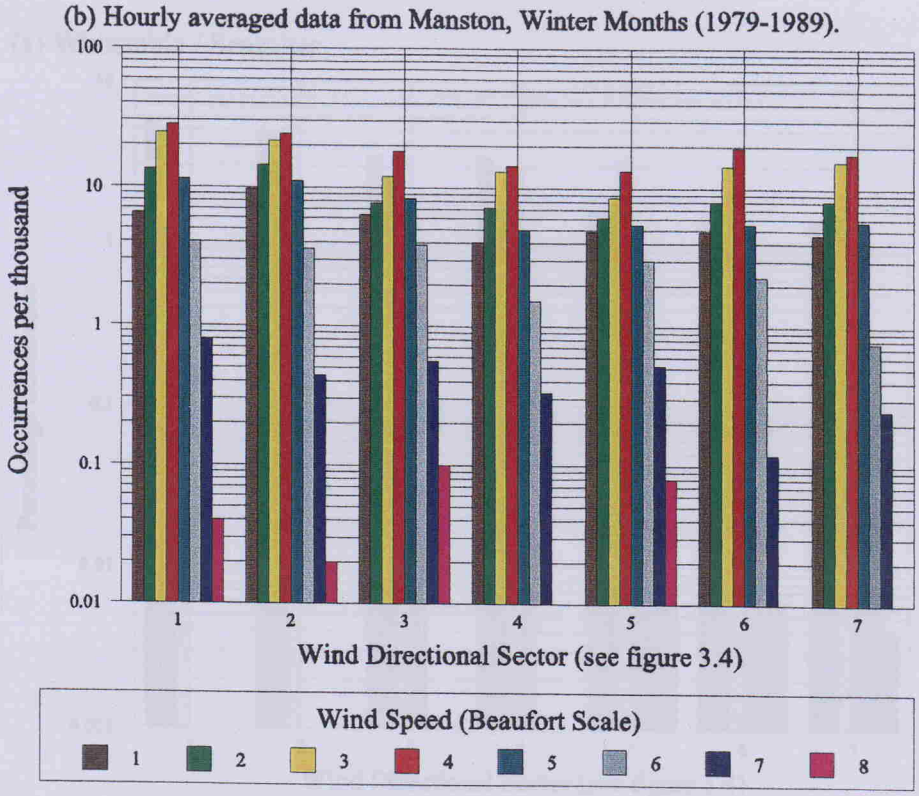

Figure 4.7(b). Winter Wind Climate At Manston Airport (1979 to 1989).

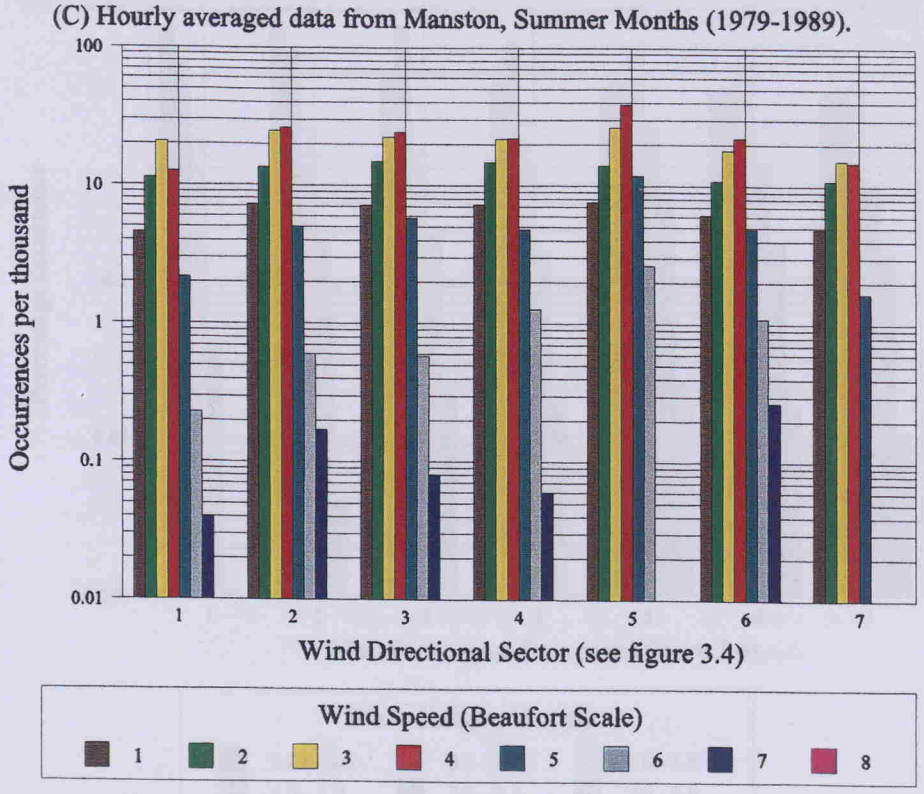

Figure 4.7(c). Summer Wind Climate At Manston Airport (1979 to 1989).

(a) Whitstable / Seasalter

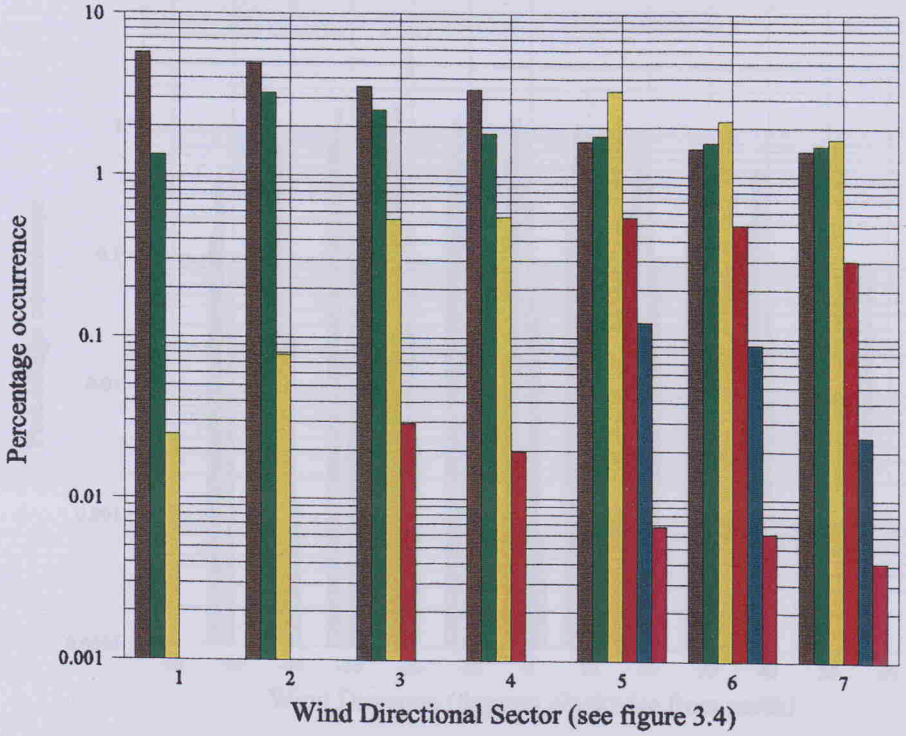

Figure 4.8(a). Offshore Wave Climate for Seasalter / Whitstable (Unit 1), (1979 to 1989).

(b) Reculver to Minnis Bay

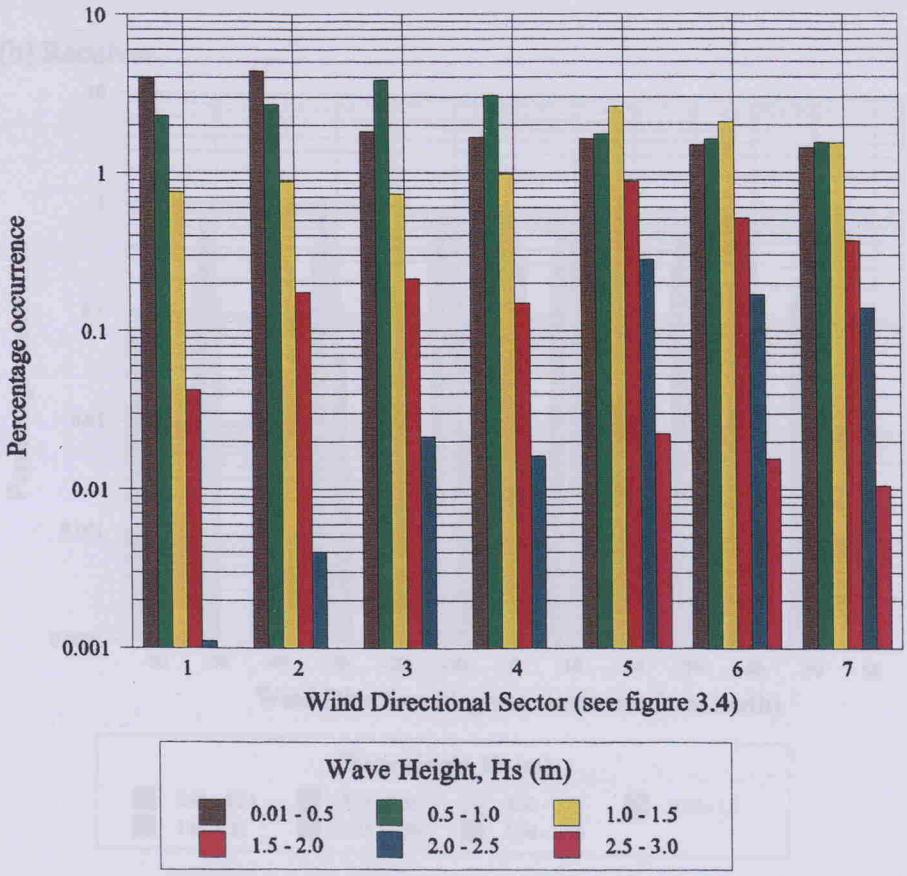

Figure 4.8(b). Offshore Wave Climate for Reculver / Minnis Bay (Unit 6), (1979 to 1989).

(a) Whitstable

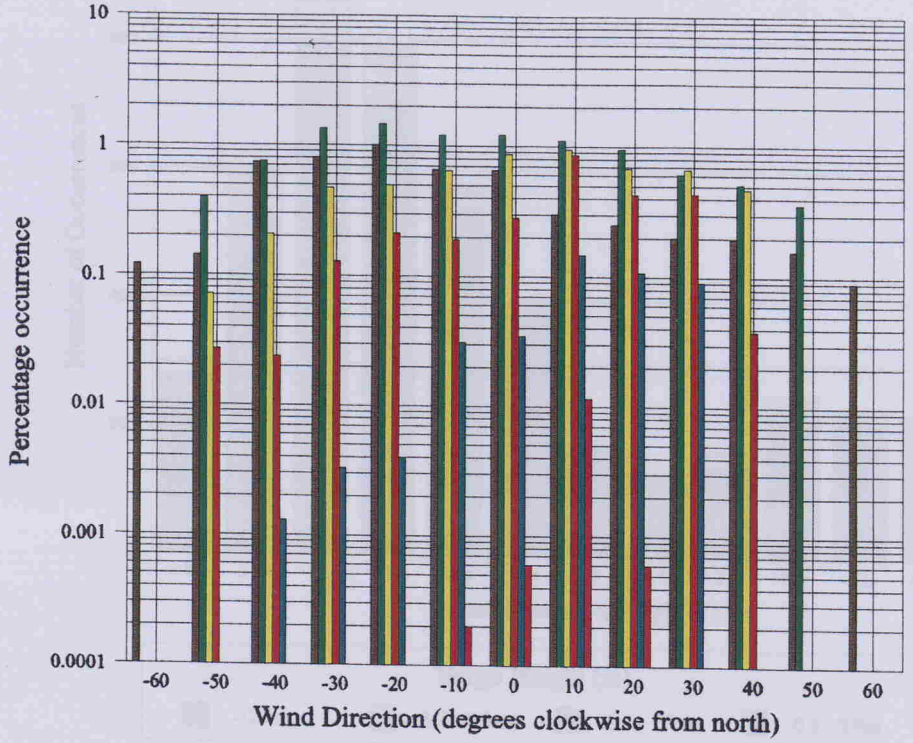

Figure 4.9(a). Nearshore Wave Climate for Whitstable (Unit 1A), (1979 to 1989).

(b) Reculver

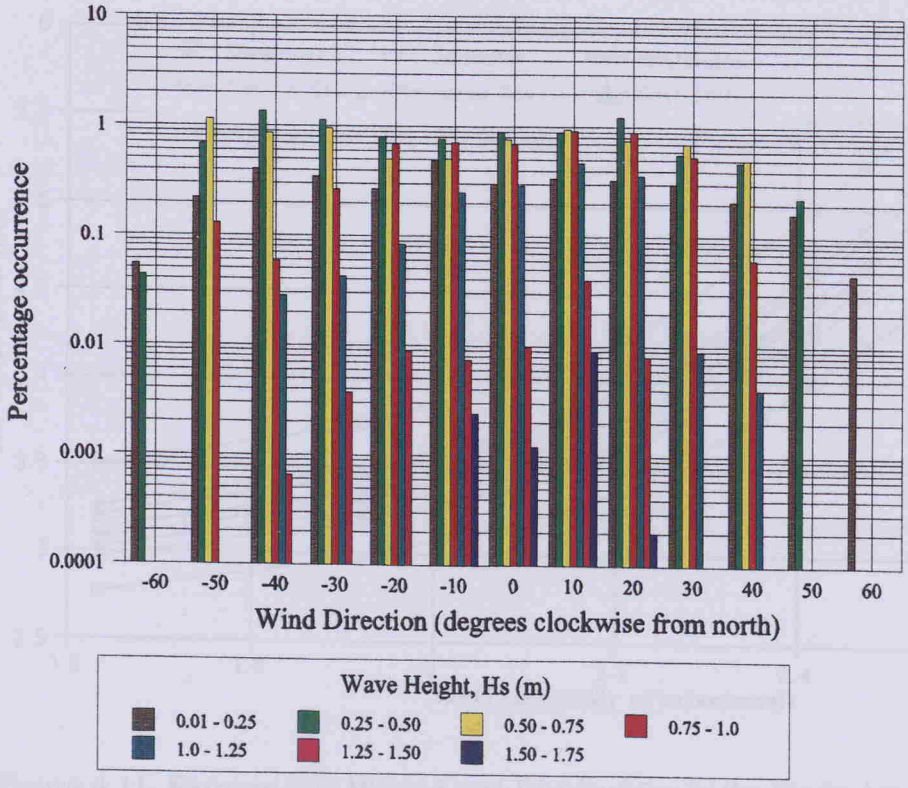

Figure 4.9(b). Nearshore Wave Climate for Reculver (Unit 6A), (1979 to 1989).

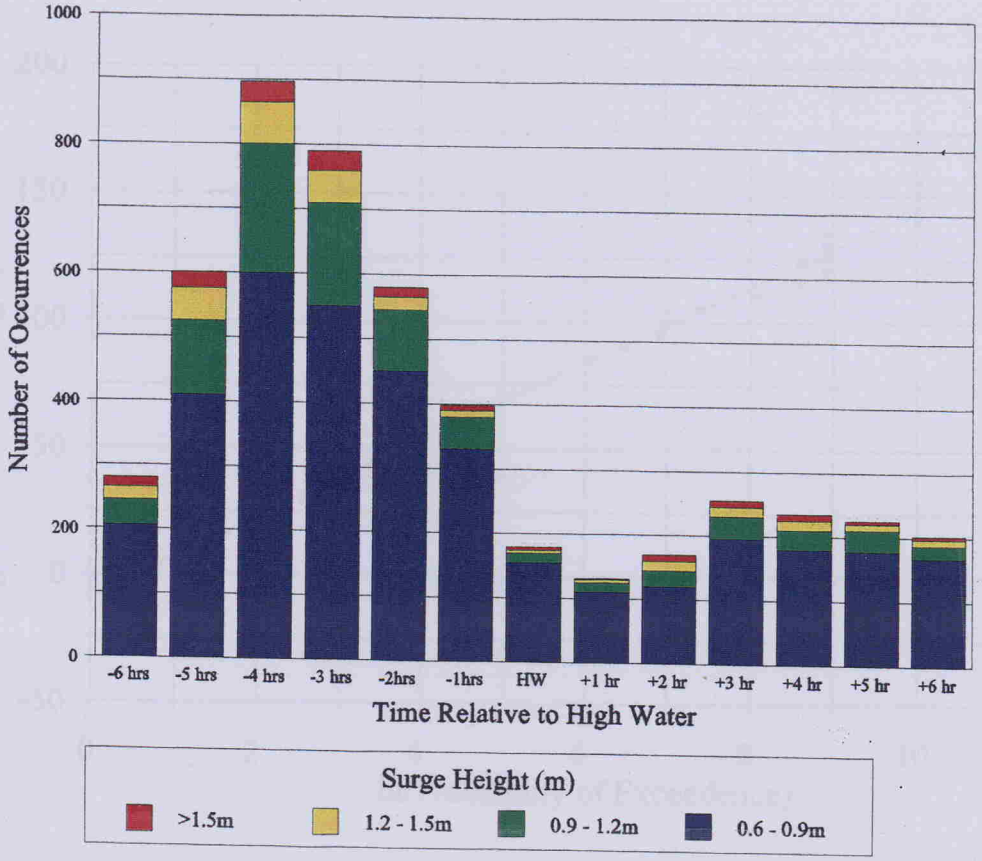

Figure 4.10. Distribution of Large Positive Surges (>0.6m) at Southend, Relative to the Time of Predicted High Water, (after Pugh 1987).

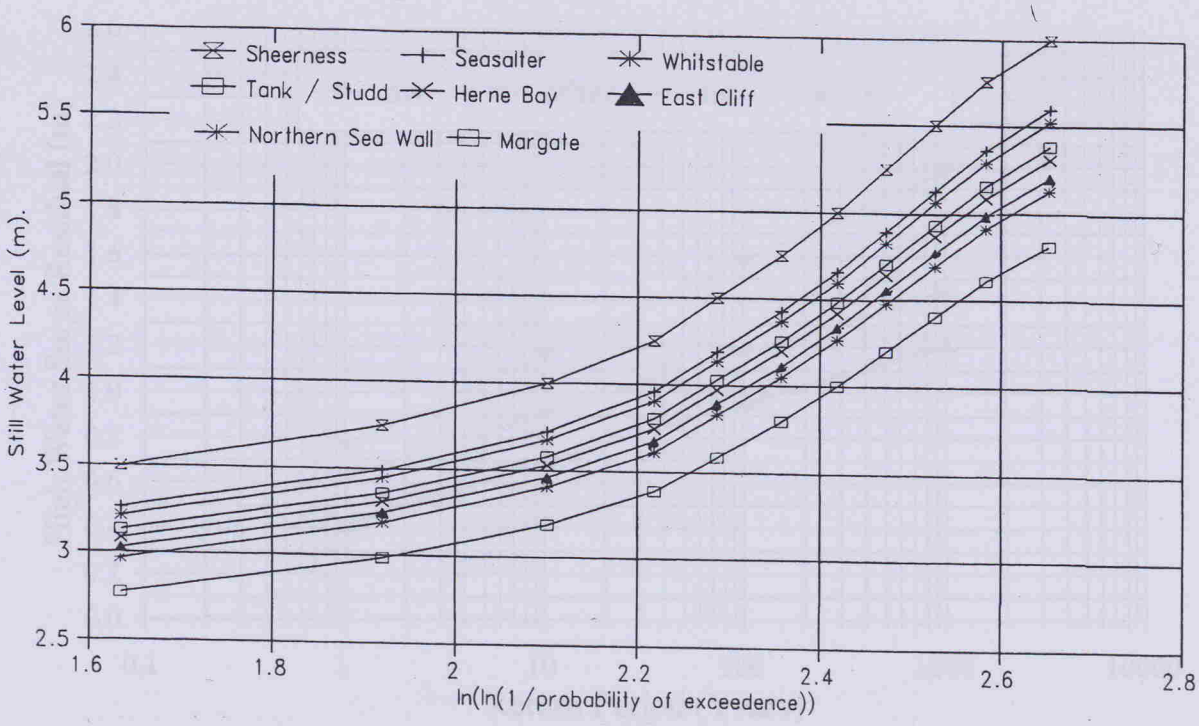

Figure 4.11. Extreme Still Water Level Distributions in the Study Area (Based on Data From Hydraulics Research (1981, 1985)).

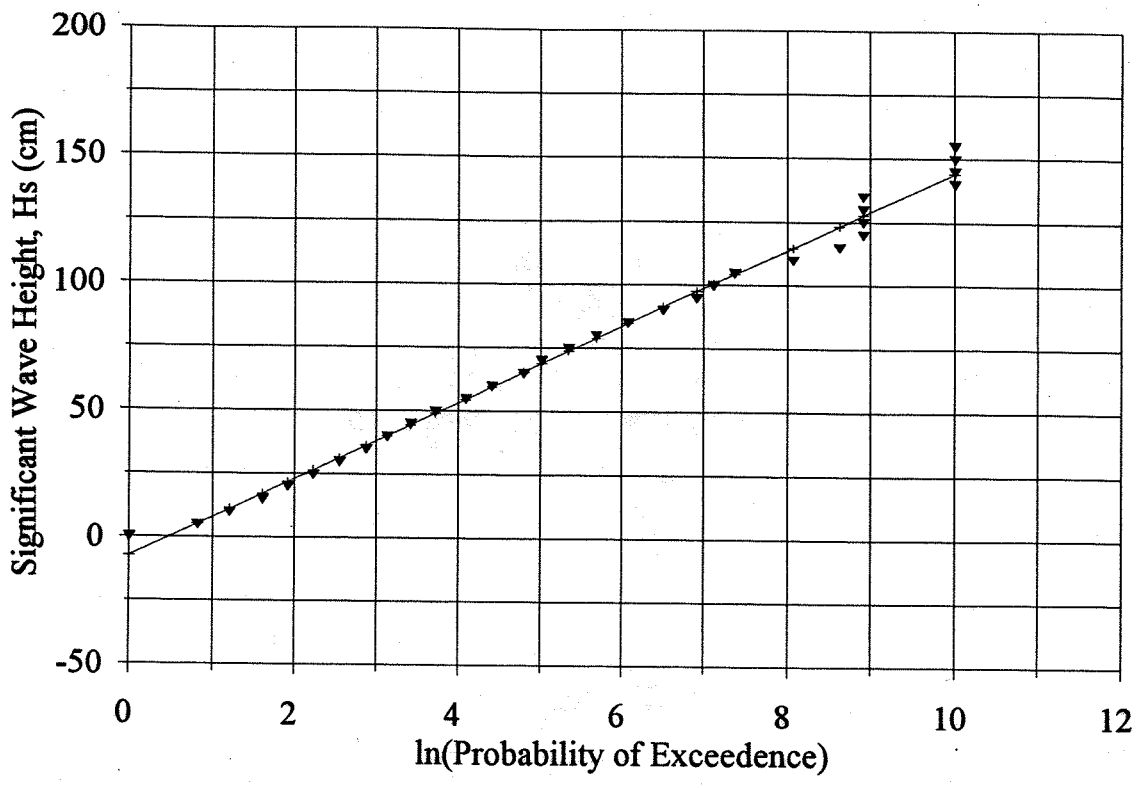

Figure 4.12. Probability of Exceedence of Wave Height at Whitstable, (Based Upon Recorded Data from Whitstable Harbour (1978 to 1990)).

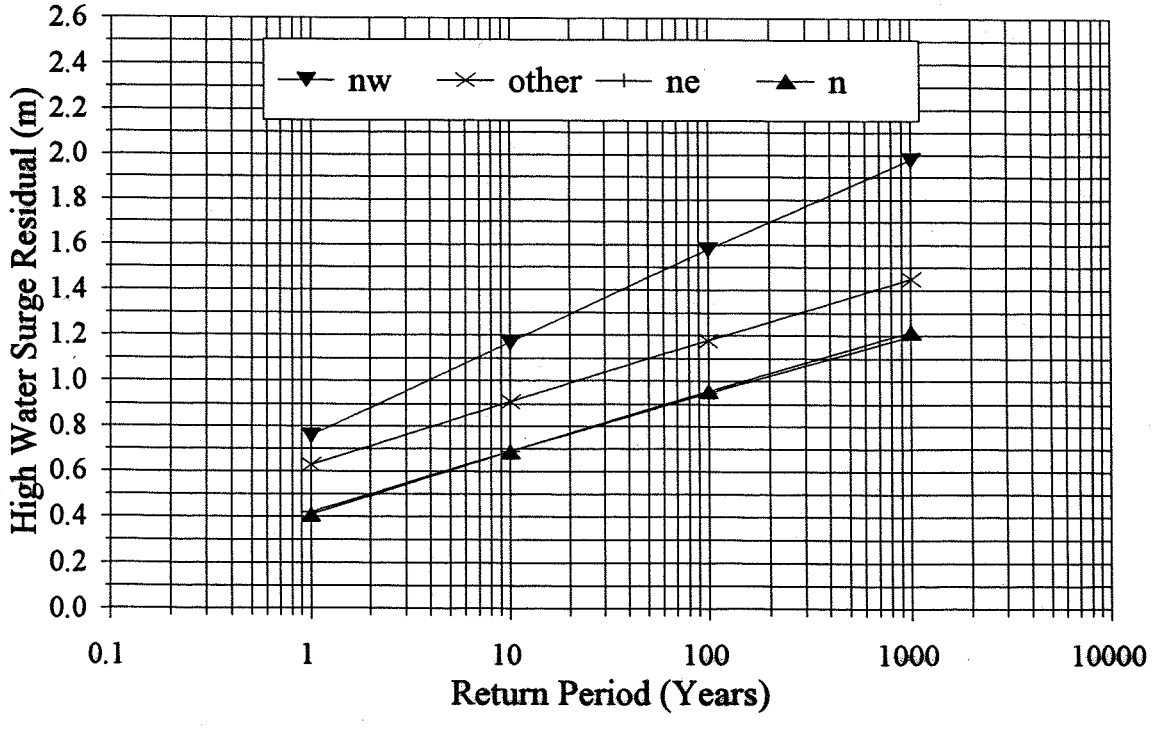

Figure 4.13. Dependency Between the Return Period of Extreme Still Water Levels on Wind Direction (Based on Data From Hydraulics Research (1981, 1985)).

Chapter 5: Results - Sediment Transport Studies

5.1. Introduction

In this Chapter, the nearshore wave climate, derived for each of the ten coastal units / sub-units (as described in Chapter 4), has been used to determine the averaged annual potential longshore transport rates on beaches within the study area. As described in the Literature Review (Chapter 1), existing longshore transport formulae may be unreliable (Greer and Madison, 1978). This is due to a lack of the detailed understanding of processes occurring on shingle beaches, particularly beaches of a mixed sand and shingle type (Kirk, 1980), which are characteristic of the study area.

For this reason an attempt has been made to determine actual shingle transport rates in the field, over a short time period (2-3 days). The site chosen for the field trial was at Long Beach, Whitstable (Figure 5.1), the nature of which is described in Section 5.2. Transport rates of beach material have been determined at the trial site, using tracer techniques and beach profile surveys. Calculated transport rates based on the prevailing sea conditions (which were recorded using pressure sensors and current meters), were compared then with the measured transport rates in order to assess the performance of the equations for longshore sediment transport.

Averaged annual potential longshore transport calculations have then been compared also against estimated long-term accumulation rates of the beach against large coastal structures to investigate the longer-term performances of the model (Chapter 6). Finally, the longshore transport model has been used to examine the effects of both the seasonal variations in the wave climate and storms, on shingle transport patterns.

5.2. A Description of the Long Beach Study Site

The field study beach is 440m in length with a predominant orientation of 3° clockwise of east - west. The beach is retained at the western end by the East Quay of Whitstable Harbour; at its eastern end by the first in a series of large timber groynes, constructed in 1989 as part of the Whitstable Sea Defence project, (Plate 5.1). Apart from a small quantity of shingle which

bypasses the quay at the west end, coarse material is retained generally between the two end structures. There are three small intermediate groynes at each of the east and west ends of the beach leaving a central section (260m in length), where there are no structures to interrupt longshore transport. There is also a boat launching ramp, adjacent to one of the groynes at the east end.

The beach consists of a mixture of sand and shingle sediment, typically with a series of shingle beach ridges located around high water mark and a mixed sand and shingle beach face. Towards the eastern end of the beach the upper storm ridge intersects the seawall; this demonstrates that, during storms, wave action reaches the seawall. The width of the non-active beach behind the upper storm ridge, increases westward.

At the time of the second field trial, two prominent beach ridges were present. The landward ridge consists exclusively of pebbles having shapes comparable with the imbricated discs described by Bluck (1967). The surface layer of the seaward ridge contained pebbles of a similar shape to the upper ridge; however, the individual pebbles were on average smaller. Beneath the surface layers, sand was present in the interstices between the pebbles. Sediment in the beach ridge can be described as well sorted.

Seaward of the beach ridges the beach face is planar, typically with a slope of 1 in 9 to the toe of the shingle beach. Surface layers of the beach face range from patches which are exclusively pebbles, to patches which are exclusively sand; sub-surface layers always consist of a mixture of both sand and shingle. Apart from a general trend where the surface of the beach lying immediately to seaward of the ridges is more likely to be sandy (the sand run), the proportion of sand and shingle in the surface layers varies in both a longshore as well as in a more obvious onshore / offshore direction.

The toe of the shingle beach consists of spherical and rod-shaped cobbles and pebbles, infilled with sand and some coarser material. Here, the beach was more compact and digging, to recover tracers or take beach samples for example, was difficult. Further, during searches for tracer pebbles it was noted that the sediment retained a significant amount of water, even after the falling tide had exposed the toe two or three hours earlier. This part of the beach corresponds broadly to the large cobble frame and infill of Bluck (1967).

Beyond the shingle toe, there is a sharp transition to a gently sloping (≈1 in 500) lower foreshore; this consists of a thin layer of sand and silt over weathered London Clay bedrock. There are also isolated patches of pebbles, cobbles and shells.

A particle size distribution curve for locations down a shore-normal profile at Long Beach is reproduced in Figure 5.2. Profile locations, shown on Figure 5.2 are described as: ((i)) upper ridge; (ii) lower ridge; (iii) sand run; (iv) mid-beach; and (v) toe. The particle size distribution graphs demonstrate the extent of the variation up the profile, together with the problem of selecting a nominal mean grain size for transport calculations. A sixth particle size distribution curve (the weighted average) has been included in Figure 5.2. This curve has been derived by 'mixing' the other five distributions together, in proportion to the approximate amount of time that the breaking / surf zone is active within each area of the beach.

A further feature of interest is that along the length of the beach there are angular kelp-rafted "clay stones" of local origin. The most likely source of these stones is an outcrop on "the Street" (see section 2.4), located about 600 m to the east, Figure 5.1. Kelp rafting is not thought to contribute a major input into the beach, as the clay stones are quite soft and are soon eroded as a result of abrasion with the flint particles (Canterbury City Council, 1993a).

The experimental set-up for the Long Beach experiment is shown in Figure 5.3; it should be noted that the beach has been sub-divided into 5 cells. These cells, which vary in width from 27.5m to 50.5m, are defined on the basis of the presence of existing structures located on the beach and the orientation of the beach itself. This sub-division was created following completion of the field studies, for the purpose of interpretation of the field study results.

The pressure sensors were arranged in an array, with one sensor inserted at each corner of a ten metre square located just beyond the toe of the shingle beach. Two electromagnetic current meters were deployed, to measure longshore and on-offshore currents (Plate 5.2). One of the current meters was placed adjacent to the inshore pressure sensor; the second was placed adjacent to the pressure sensor furthest from the beach toe. Because the sensors were deployed seaward of the shingle beach, problems of sensors burial which had occurred during similar experiments at Hayling Island (Whitcombe, 1995) were not experienced.

5.3. Initial Field Study At Long Beach (16th to 18th March, 1992)

An initial field study was carried out between the 16th and 18th March 1992, to determine the effects of waves and currents on the mode and transport rate of shingle size material. The weather forecast on the 14th March 1992 had predicted moderate to strong winds, from the north-east during the course of the field trial; however, these did not occur. As a result, during the period when the instrumentation was on site (16/3/92 - 18/3/92), only light wave activity was recorded.

During the three days of the field trial, wave and current data were recorded successfully; however, the wave activity was not sufficient to cause notable transport of tracers. Consequently, no effort was made to check the transport formulae which was being used in the present study. Wave conditions peaked, with a Significant Wave Height (Hs) = 0.18m and Zero Crossing Period (Tz) =2.4s on the morning of 18th March 1992. Longshore and onshore currents measured at the beach toe reached maximum values of 0.06 ms^{-1} and 0.04 ms^{-1} on the same morning, (Prettijohn 1992).

Between 18/3/92 and 31/3/92 the wind backed to the west and increased in speed; it reached a maximum of force 8 (Beaufort) scale, on the 27/3/92. This change resulted in wave action which caused significant beach movement, from the west to the east, over that period. Based upon a limited number of beach profiles measured between the 16th and 31st March, it was estimated that between 2000 and 3000 m^3 of beach material was transported into the eastern 100 m length of the study beach. Beach levels rose by an average of 1.1 m, against the terminal groyne. Unfortunately, the pressure transducers and current meters had been deployed elsewhere; hence, no wave or current data were collected during this period. Wave data collected by the Whitstable Harbour recorder over the period 15/3/92 to 31/3/92 are reproduced in Figure 5.4(a) (Hs) and Figure 5.4(b) (Tz).

Sixty numbered aluminium and 140 painted tracers were deployed, to allow the volume of shingle transport to be calculated. Three prototype electronic pebbles were also deployed, to determine their performance in the field relative to conventional tracing techniques.

Tracers were deployed at low tide, on the afternoon of 16/3/92. The painted pebbles were introduced on the beach surface, along a profile normal to the beach crest at intervals of 0.15m between the high water mark and the beach toe. The aluminium tracer pebbles were introduced along two profiles parallel to, and 1m to either side of, the profile containing the painted pebbles. The spacing between the aluminium tracer pebbles along the profile was 1m. Most of the aluminium tracer pebbles were buried to a depth of 0.05 m. However, at two points along the profile which corresponded to MHWN and MSL, tracers were introduced at various depths up to 0.4 m, to form a "column" of pebbles. The column of pebbles was designed to assist in the calculation of the mobile layer thickness (Nicholls, 1985).

Tracers were located on the afternoons of the 17/3/92 and 18/3/92: no significant movement was noted on 17/3/92. Some movement had occurred by the 18/3/92; however, most tracers remained stationary or moved by a few metres only. Movement of the aluminium tracers, occurring between the 16/3/92 and 18/3/92, are shown in Table 5.1. The maximum displacement of a painted pebble during this period was 2.5 m, with the mean (longshore) displacement being 1.1m. For the aluminium pebbles, the maximum and mean displacements were 3.12m and 0.17m, respectively. The greater average displacement of the painted pebbles is considered to be due to the fact that they were introduced on the beach surface; they were, therefore, immediately available for transport.

On 31/3/92, a final search for tracers resulted in the recovery of 8 aluminium pebbles and 3 painted pebbles; this corresponded to recovery rates of 13% and 2.5%, for aluminium tracers and painted pebbles, respectively. The low rates of recovery were attributed to "deep" burial resulting from a progressive build-up of sediment against the terminal groyne at the eastern end of the study area.

The electronic pebbles were deployed during the period 16/3/92 to 18/3/92 only. All three pebbles were recovered with ease; however, these had not been displaced more than 1m by the wave activity.

Only after the instruments were removed did conditions persist which transported significant volumes of shingle and tracer. Prettijohn (1992) attempted to quantify the longshore transport rates between 16th and 31st March 1992; however, it was concluded that insufficient data

were available to provide any meaningful results.

Despite the failure of the initial field study, to provide any useful data for calibrating the longshore transport formulae, a number of observations were made which were used to refine the experimental set-up prior to use in the main field experiment. These observations are summarised below.

- Thresholds for the movement of tracers were lower than expected, with tracer movement occurring in response to wave heights less than 0.2m (Hs).
- Tracer movement was greater when the pebbles were placed on the beach surface.
- Tracers located initially on sandy patches on the beach face were more likely to move (Plate 5.3).
- Currents are low, with recorded current velocities not exceeding 6cms^{-1} over the 3 day survey period.
- Painted pebble recovery rates declined markedly, as mixing commenced with only 2.5% of pebbles located on the 31st March.
- The aluminium tracer recoveries also declined markedly (13%, on 31st March), as they became progressively more deeply buried under the shingle accumulating at the terminal groyne.
- Metallic debris on the beach severely hindered the rate of progress, when searching for the aluminium pebbles.
- The electronic pebbles could be found much more rapidly than their aluminium counterparts.
- Beach profile survey data could provide a valuable data source, for studying the overall transport behaviour of the beach on a daily basis.

5.3. Main Field Study At Long Beach (23rd to 26th January, 1993).

The experimental set-up for the second field trial was identical to that used in the previous experiment, apart from the number of tracer pebbles deployed. For this second study, 17 transmitting pebbles were deployed, together with 80 aluminium pebbles. Painted pebbles were used as beach cores, only in an attempt to record the depth of disturbance. As described in Chapter 3, the transmitting pebbles casings were cast in moulds made from pebbles taken from the experimental beach.

5.3.1. Weather Conditions, 23rd to 26th January, 1993

Wind speed and direction were recorded throughout the experiment at Borstal Hill, Whitstable. The wind speed and direction data extracted from the recorder chart rolls for the period of the field study, are reproduced in Figure 5.5(a) (wind speed) and Figure 5.5(b) (wind direction). Wind speed has been corrected for the location of the recorder.

In the two days prior to the study commencing, winds were recorded as westerly to southwesterly, with wind speeds peaking at 14.4 ms^{-1} on the evening of the 21st January. By the morning of the 23rd January, when the instrumentation arrived on site, the wind speed had dropped to around 4ms^{-1} from the south-west. During the afternoon of 23rd January, wind speeds increased sharply, to a peak of 17.2ms^{-1} at midnight and the wind veered to the west.

Over the course of the field trials, the wind direction became progressively more northerly, until the morning of the 26th January; at this time, the wind backed to the west - southwest. The wind speed dropped off gradually, until the morning of the 26th January, when the experiment was terminated.

5.3.2. Water Levels, 23rd to 26th January, 1993

The still water levels recorded using the pressure sensor at Whitstable Harbour are shown in Figure 5.6. Also shown on the Figure is the predicted tide for the same period and the calculated surge residuals. Of particular interest in these water level records is the frequent deviation from predicted tides, due to a series of large meteorological surge residuals. The most prominent of these surges is the large positive surge occurring on the afternoon of the 25/1/93; this resulted in a high water of +3.7m AOD at Whitstable Harbour (return period of 5.9 years (Table 4.9)). The peaks of the surge residuals tend to not coincide with high water, as demonstrated by Pugh (1987) for Southend (see also section 4.6.2).

5.3.3. Wave Conditions derived from the Whitstable Harbour Wave Recorder

Wave conditions were recorded using the Local Coast Protection Authority wave recorder, situated approximately 1 km to the north-west of the Long Beach (Figure 5.1). Waves were

recorded for 20 minutes, at intervals of 1½ hours. Wave heights (Hs) and periods (Tz) derived from the Whitstable Harbour wave recorder, over the period 21/1/93 to 26/1/93, are shown in Figure 5.7.

Recorded wave heights remained generally below 0.5m (Hs), until the morning high tide on the 24/01/93. During this high tide and for the following two high tides, the maximum significant wave heights recorded were Hs = 1.1m. This pattern is consistent with the period of strong westerly to north-westerly winds. Wave heights decreased from the afternoon of the 25/01/93 to the morning of the 26/01/03; once again, this is consistent with the more moderate wind conditions.

Wave periods varied between 2.5 and 4.5s, (some longer wave periods were present; however, these tend to coincide with small wave heights during low water), with a slight increase in average wave periods from the morning of 22/01/93 to the evening of 25/01/93.

5.3.4. Visual Observations of Wave Conditions at Long Beach, Whitstable

Throughout the duration of the field study, hourly visual observations of waves were made. Wave heights were determined over a period of 2 minutes at the eastern limit of Long Beach, where they could be calculated based on the number of groyne planks exposed. A correction was then applied, to obtain the equivalent heights along the length of beach in the immediate vicinity of the instrumentation site. Generally, it was found that wave conditions did not vary noticeably along the 250m of frontage examined. Waves were also observed for 2 minutes to determine the average wave crest orientation at the point of breaking. The wave angles were then recorded, using a compass to determine the angle between the wave crests and geographical North. The results of the visual wave observations, for the 23/1/93 (pm) to 25/1/93 (am), are shown in Table 5.2.

Generally, the wave angles were difficult to determine, as breaking occurred over a range of wave angles. On the mornings of the 23/01/93 and 25/01/93, it was possible to estimate two wave angle components in the wave field; these are described in Table 5.2 as wind and swell components. Whilst it was also possible to estimate heights associated with the two components on 23/01/93, wave conditions were too confused on the 25/01/93 to establish the

separate wave heights. No wave height data were recorded at night, due to a lack of light. Wave angle data could only be obtained with the assistance of a flashlamp; consequently, the uncertainty associated with readings taken at night is higher. All the measurements taken refer to the height and angle of the waves, at the point of breaking.

5.3.5. Data obtained from the Long Beach Array

Once the instrumentation had been installed a number of problems arose with the equipment. Two of the pressure sensors were found to be not functioning and a third failed after only a few hours of use. Only one pressure sensor was available therefore, for the duration of the study period. In addition, both of the EM current meters failed within a few hours of commencing the field experiment.

Although one pressure sensor is sufficient to provide useful data on the wave heights and periods (for example), it is not possible to calculate the wave angle. Twenty six records of the wave conditions were made during the period, with each record consisting of a 20 min sampling period, at a frequency of 5 Hz. The wave conditions were recorded at intervals of 1 hr.

Before analysis, the absolute pressure variations from the pressure sensor were converted to equivalent water level variations. Each data set was then plotted as a time-series and any 'spikes' in the data removed. These anomalies were replaced by interpolating between the adjacent values. Since the pressure sensor data were recorded during either a period of a rising or falling tide, it was necessary to remove this low-frequency background variation. This modification was accomplished by obtaining the average water level, during the first and last 3 min of the records; then calculating the rate of change in tidal height, with time, to obtain a tidal gradient. Upon removal of the tidal contribution, only variations in the wave amplitude then remained.

Time Domain Analysis of Wave Records, 23-25th January 1993

Representative 5 min samples of the variation in wave amplitude and velocity, for each of the data sets, are shown on Figure 5.8 (a) to (e).

Data for the morning of 23/1/93 (Figure 5.8(a)) shows a gradual increase in wave activity, in response to strengthening wind conditions. The traces are dominated generally by low (<10cm), short period (≈1s) wave activity. In the traces for 1115, 1315 and 1415, however, there is evidence for a low, longer period (8 - 10s) variation representing a gentle swell.

For the evening of 23/1/93 (Figure 5.8(b)), the data show further development of wave conditions with increasing wave heights, longer periods and the organising of the waves into groups (with a group period of around 30s).

Data recorded during late morning and early afternoon on 24/1/93 (Figure 5.8(c)), show a similar pattern to the previous evening; however, there is a general decrease in wave heights and a less regular pattern to the wave groups.

From the wave traces obtained, the largest waves were recorded during the evening of 24/1/93 and the early morning of 25/1/93 (Figure 5.8(d)). Unfortunately, problems with the instrumentation resulted in the loss of 3 data sets for the falling tide. The traces show longer wave periods (≈ 3.5s), than were previously recorded, together with the presence of wave groups with a (group) period of approximately 35s.

Data recorded on the late morning and early afternoon on the 25/1/93 (Figure 5.8(e)), show a definite increase in wave periods and an increase in irregularity of the wave traces; this is possibly due to the interference of two or more discrete frequencies. The trace recorded at 1415, for example, seems to be dominated by a wave component with a period up to 10s. Although this component appears to be present in some of the other traces (1515, 1215 and, perhaps, 1615) the wave traces are dominated by a higher frequency component (≈ $0.2s^{-1}$).

Significant wave heights (Hs) and zero crossing periods (Tz) were calculated using the Tucker method (1963). The wave heights were corrected for the number of waves in the record (WMO, 1988) and for depth attenuation (Draper 1967). The results of this analysis are shown in Table 5.3.

Frequency Domain Analysis of Wave Records, 23-25th January 1993

The wave traces were analysed in the frequency domain, using a Fast Fourier Transform technique (Teukolsky et al, 1992), to produce a series of spectral energy density curves (Figure 5.9 (a) to (z)) for each of the recording periods.

On the morning of 23/01/93, the wave energy is very low; the most prominent feature is the appearance of a spectral peak, with a frequency of 0.13 Hz (Tp ≈ 8secs), which later becomes dominated by a higher frequency component (also of low energy). The low frequency peak is most likely to be the remains of a swell component; the higher frequency component probably corresponds with the onset of westerly winds.

By the evening of 23/01/93, a prominent spectral peak is present; this represents waves with a dominant period of around 3.5s. The energy in this band reaches a peak around high tide; thereafter, the spectral form becomes broader with a shift to spectral peaks of higher frequency.

The same pattern is continued into the next tide (the morning of 24/01/93), with a spectral peak at a frequency of 0.3Hz up to high tide; this becomes broader on the falling tide. By the evening tide on the 24/01/93, the spectral peak which develops to high water is of lower frequency (≈0.25Hz) and of greater magnitude ($0.36m^2\ Hz^{-1}$). No data related to the falling tide were available.

During the last tide for which data were recorded at Long Beach (am on 25/01/93), the wind veered around to the north, coinciding with the appearance of the large positive tidal surge. The wave energy spectra for this tide commences in a similar manner to the previous tides, with a near symmetrical spectral form of peak frequency (equal to 3.5Hz). As high water is approached, two separate spectral peaks arise, with frequencies of ≈0.15Hz and ≈0.3Hz. The higher frequency component is dominant in terms of wave energy; except for the high tide record, where the low frequency component dominates.

The bimodal spectral peaks exhibited on the 25/01/93 may be the result of either: (a) two wave fields being present which are arriving from different directions; or (b) some form of resonance

resulting from wave energy being reflected from the beach or nearby structures.

A description of the wave spectra in the form of wave parameters (H_{rms}, H_{mo} and Tp) can be obtained by following the procedures in WMO (1988). H_{rms}, is the height of a single sinusoidal wave having the same energy as the spectrum. H_{mo} is the equivalent to the time domain significant wave height ($H_{1/3}$) and is equal to $\sqrt{2}.H_{rms}$ and $4(mo)^{0.5}$, where m_o is the 'area' under the spectral curve.

In theory, the relationship $H_{mo} = H_{1/3}$ applies only in deep water with a narrow spectrum; however, the differences are small. A commonly quoted relationship is $Hm_o = 1.05\ H_{1/3}$, on average (WMO, 1988). In shallow water and with steep waves, however, Hm_o becomes smaller than $H_{1/3}$ due to deformation of the wave form (CERC, 1984). The extent of the difference was estimated for the study area, based upon the theoretical relationship derived by Dean (1974) and field studies carried out by Thompson and Seelig (1984) and Hotta and Mizuguchi, (1980). Once again, the estimated differences are small ($Hm_o \simeq 0.97\ H_{1/3}$), with the exception of very shallow water conditions (when $Hm_o \simeq 0.85\ H_{1/3}$).

Derivation of wave periods is more difficult, due to the variety of spectral shapes which occur; these include multiple peaks, as illustrated in the data for 25/1/93. The period of the peak wave energy Tp (equivalent to Fp^{-1}, where Fp is the wave frequency corresponding to the peak frequency) was obtained. The results of the frequency domain analysis are presented in Table 5.3.

Comparison of the wave heights derived by time domain analysis, with those derived in the frequency domain, shows a higher than expected level of variation; this can be attributed to the generally shallow water and short wave periods. Overall, it was found that $H_{mo} = 0.92H_{1/3}$ which is considered fairly typical of shallow water.

Wave periods derived by time domain analysis are shorter than those derived in frequency domain, although this is exaggerated where there are bimodal spectra. Ignoring data from the morning of 23/01/93, when the total energy was very low, the relationship Tp = 1.07Tz was established. Including data from the morning of 23/01/93 leads to Tp = 1.25Tz.

5.3.6. Wave Conditions from Model and Comparison with Wave Records

In Chapter 4, the development of a wave model for the north Kent coast was described; this enabled the wind and water level data, collected at Whitstable, to be used to produce wave conditions at any location along the coastline. The model was calibrated using data from the (Whitstable Harbour) wave recorder. Using the same approach, the wind and water level data collected during the Long Beach field trial were used to obtain the wave conditions at both the Local Authority wave recorder site and at the toe of the shingle beach (ie where the pressure sensors were deployed). The results of the hindcasting are shown, together with the recorded data, in Figure 5.10 (a to e).

Significant wave heights hindcast for the wave recorder site over the duration of the field trial are shown in Figure 5.10(a). During the two tides on the 23/01/93, winds were blowing from the west and southwest such that sometimes the wind direction was classified as directional Sector 1; at other times, as an offshore wind, since the mean wind direction was marginally to the south of Sector 1. Offshore winds, by definition, will not generate wave activity which impacts on beach processes.

In reality, the wind direction is such that it is within a few degrees of Sector 1 and wave conditions for these winds have been determined as if they were all relating to Sector 1. This assumption, it was considered, would lead to predicted wave heights and periods which were larger that those recorded on some occasions. There is some indication that this may be the case on the morning of 23/01/93; however, by the evening, the reverse was true with the recorded waves greatly in excess of the predictions.

During the morning tides on 24/01/93 and 25/01/93, the predictions are similar to, or marginally higher than, the recordings; however, there are only a few points where there is a large variation. This variation could be attributed to differences in timings for the data sets. For example, the wind speed and directions used in the hindcasting, represent conditions over 5 to 10 minutes either side the hour (1150 to 1210, for example), whereas the wave records are averaged over a 20 min period commencing on the hour.

The data set for the evening of the 24/01/93 shows recorded wave conditions in excess of

predictions, although to a lesser extent than the previous evening.

A common correction applied to the wind speed, when hindcasting waves, is the "Stability Correction Factor, R_T" (Resio and Vincent, 1977); this allows for the difference in temperature between the air and sea. The factor is a measure of the effectiveness by which wind energy is transferred to waves.

If the air temperature is low relative to that of the sea ($R_T > 1.0$), the air / sea interface is less stable; it has a lower difference in viscosity and more energy is transferred to the sea in the form of waves; the opposite is true if the air is warmer than the sea. The field trial was carried out in late January, when air temperatures at night are likely to be well below sea temperature. For example, if the air temperature were 10°C lower than the sea temperature, the value of R_T would be 1.18 (based upon the Shore Protection Manual, CERC (1984)). For a wind speed of $10ms^{-1}$, the increase in U_A is 22%; this leads to increases in wave height and period of up to 20%, depending upon the water level. Much of the discrepancy between the recorded and predicted wave heights, in the night-time records, could be attributed to the temperature differential. During the day time recording period, air and sea temperatures are likely to be close and $R_T = 1.0$.

In the case of the data sets for the 23/01/93, another factor may be introduced. If winds are blowing from the boundary between Sector 1 and a south-westerly (offshore), direction towards the wave recorder site, the presence of the Swale Estuary (ignored in the calculations of fetch length and water depth, in Chapter 4) effectively increases the fetch lengths over which waves are generated. With the exception of a short stretch of beach to the west of the harbour, waves generated in the Swale Estuary are unlikely to be important in the study as they are propagating largely parallel to the coastline. Due to its location, the wave recorder is ideally placed to measure these waves. Together with the temperature / stability effects, described earlier, this could help explain why the recorded waves are much higher than those which were hindcast from wind conditions during the two evening high tides.

Comparison between hindcast waves and records obtained at Long Beach itself (Figure 5.10(b)), shows a very similar pattern to the wave recorder site, although the significant wave heights are lower as would be expected in the shallower water. The discrepancy between

predicted and recorded wave heights on the evening tides is still present. Notably, the differences on the evening of 23/01/93 are less than they were, for the same time, at the wave recorder. Less energy from waves generated in the Swale Estuary would be expected at Long Beach, than at the recorder; this is due to the effects of wave refraction and sheltering. Figure 5.10(c) shows the revised, hindcast wave conditions obtained at Long Beach, allowing for a the temperature stability correction (R_T = 1.18), (based upon the Shore Protection Manual, CERC 1984).

Hindcast wave periods are shown in Figure 5.10(d) together with recorded data from both Whitstable Harbour and the Long Beach sensor. With the exception of the morning of 23/01/93, when the wave energy levels were low, wave periods from the three data sets are very similar. The relatively low spectral peak period, identified in the wave records at Long Beach on the morning of 25/01/93, does not appear in the records at the recorder site. This absence lends support to the idea that the phenomena may be related to local wave reflections at Long Beach itself. However, without spectral energy density graphs for the Harbour site it is impossible to be certain of this relationship.

Hindcast wave angles are shown in Figure 5.10(e). As expected, the wave angles relative to the beach orientation decrease from the Whitstable Harbour recorder site, towards Long Beach. A reduction in wave angles, on the evening of the 24/01/93 and morning of 25/01/93, is also apparent; this represents the change in wind direction. Unfortunately, there are no instrumentally recorded wave angles for comparison.

5.3.7. Transport Rate Calculations from Wave Conditions.

(a). Available wave data sets

Several data sets on wave conditions are available, including three sets at the experimental site: these are ((i)) the visually observed wave heights and angles; (ii) the recorded wave heights and periods; and (iii) the model hindcast wave heights, periods and angles.

Visually-recorded wave data incorporates a high degree of uncertainty, due to dependance on the observers judgement on wave conditions. The problem is particularly acute at night, when

waves can only be measured with the aid of a flashlamp.

The recorded data lacks any indication of the wave angle which is required for the longshore transport calculations. On some occasions, the data set is incomplete due to technical problems with the equipment; for example, only three (hourly) wave data sets out of a possible eight were recorded on the evening of the 24/01/93.

The hindcast wave data consists of wave heights, wave periods and wave angles, for each tidal cycle throughout the duration of the field study; as such they represent the most complete data set. In Section 5.3.6, a comparison between the hindcast waves and the recorded data was discussed. This comparison showed that the hindcast data provided a good match with the recorded data for all the tidal cycles; an exception was the evening of 23/01/93, when hindcast wave heights were, on average, 20% less than those recorded.

For the purposes of calculating longshore transport rates associated with the field studies, the hindcast data set has been used. Wave heights for the evening of 23/01/93 have been divided by 0.8, to produce wave heights equivalent to the recorded wave conditions.

(b). Beach data sets

To complete the data required for calculating longshore transport rates, the orientation of the beach and the nominal mean grain size (Dn_{50}) are required. However, both of these vary, depending upon location within the field study area. To the east of the instrumentation array, the orientation of the beach itself changes gradually towards the terminal groyne, from its typical east - west orientation to an east-northeast / west-southwesterly orientation (Figure 5.3). The angle which the waves are incident upon the beach alter accordingly. Because of this change in orientation of the beach, and, hence the incident wave angles within the field study area, calculations of longshore transport rates were repeated for a series of incident wave angles.

Examination of the particle size distribution graphs for the field study area (Figure 5.2) shows the variation in nominal mean grain size of the surface layer of particles, up the face of the beach. As the water level rises and falls during a tidal cycle, different sediment distributions

are available for transport. However, in the present study, no attempt has been made to use different particle sizes for the transport calculations in different vertical zones in the beach face. Instead, the Dn_{50} of the weighted mean grain size, (≈6.5 mm) has been used (Section 5.2).

Transport rates calculated for each tidal cycle, for each day and for the duration of the experiment are given in Table 5.4. These results shows that negligible transport occurred during the morning of the 23/01/93 and the evening of the 25/01/93 whilst transport rates over a tidal cycle reached a peak during the evening of 24/01/93. Transport rates calculations vary between cells (see Figure 5.3); this is due to the change in the orientation of the beach and, hence, the angle of breaking waves.

It has been assumed in the calculations that there are no barriers to longshore transport in any of the cells, which would affect the transport processes. The presence of groynes within Cells A, B and at the eastern side of C would result in the reduction of transport rates, from those calculated. Further, close to the large terminal groyne at the eastern side of Cell A, there is the likelihood of waves being reflected off the structure, before they break on the beach; thus the transport calculations could be not only incorrect in quantity, but also in direction.

Due to the presence of the groynes in Cells A to C, it is considered that only the transport rates calculated for Cells D / E are likely to fulfill the criteria of no interference from coastal structures. Therefore, net longshore transport rates for the 3 day duration of the field experiment are calculated to be in the order of 450 to 500 m^3 in an easterly direction based upon the calculations at Cells D / E.

5.4. Transport Rate Calculations based on Tracer Pebbles.

Both the electronic and the aluminium tracer pebble aspects of this study have been described in detail by Workman (1993) (electronic pebbles) and Bland (1993) (aluminium pebbles). Therefore, the following is a summary of the tracer deployment, search techniques and the resulting displacement of tracers. The majority of the data which were collected has been reanalysed however, to improve its applicability for the estimation of longshore transport rates over the duration of the experiment.

5.4.1. Tracer pebble deployment.

A review of tracer pebble experiments reveals that tracers have been deployed at various locations on the beach profile, depending upon the aim of a particular experiment. For example, Caldwell (1983), introduced tracer material (painted cobbles) at a single point on the beach ridge, close to the main storm ridge. No movement of the tracer pebbles occurred for 9 days until spring tides were approached. Wright et al (1978) introduced aluminium tracer pebbles at 'the foot of the shingle scarp face of the backshore zone'; the site was chosen as the indigenous material most closely resembled the size and shape of the injected tracer. When aluminium pebbles were used on Hurst Spit (Nicholls and Webber 1987), the tracers were introduced in three identical sets: one on the upper foreshore; the second on the middle foreshore; and the final set on the lower foreshore. The injection point was found to influence the subsequent recovery rates and positions for about the next four tides Nicholls and Webber (op cit).

Regarding the depths of tracer injection, most studies have placed the tracers on the surface; this was because visual identification of most types of tracer is required for recovery. In the case of the aluminium tracers, the standard practice adopted has been to bury the pebbles to a depth of about 5 to 10 cm (Wright et al, 1978; Nicholls and Webber, 1987).

For the Long Beach study, the electronic pebbles were placed in a line normal to the beach ridge line, at an equal spacing down the beach face, as far as the toe. Pebbles were placed in numerical order, such that individual pebbles were placed at a position in the profile corresponding to the location where the pebble used for the tracer mould was collected. All the pebbles were buried to a depth of 5 cm below the surface. Placement of the pebbles occurred as the tide was rising up the beach, on the morning of 23/01/93. The intention of the experimental procedure adopted was to provide coverage of the transport rates occurring over the entire beach profile.

Aluminium pebbles were scattered on the surface of the beach at a point immediately seaward of the beach ridge, corresponding to the previous high tide in a similar position to that used by Wright et al (1978). A total of 80 pebbles were deployed; 60 of these were deployed on the morning of 23/01/93 (at the same time as the transmitting pebbles), the remaining 20 were

deployed prior to the evening high tide on the 24/01/93. A negative surge coincided with the first high water following deployment of the initial batch of tracers; these were then mostly mobilised on the following high tide.

5.4.2. Tracer Search and Recovery

Search techniques used for tracer experiments depend upon the number of personnel (or detectors) available, the dispersion of the tracers and the time available. For aluminium pebbles Wright (1982), identified that one person with a single metal detector could carry out a thorough search of approximately 1250m^2 of beach in 3 hours. Where searches over larger areas are required, the services of local treasures seekers clubs have been required (Nicholls, 1985). Where this is not possible, Nicholls and Webber (1987) have suggested that a search could be carried out over a period of several tidal cycles, provided that wave conditions were less than that which is required to remobilise the tracers further. Nicholls and Webber (op cit) suggest a wave height threshold of 0.5m for movement to occur. However, the studies at Long Beach in Whitstable (Prettijohn (1992); Workman (1993)) demonstrate that movement of tracers will occur for wave heights in excess of only 0.2m.

As the tide receded, the search for electronic pebbles at Long Beach commenced. The detector operator proceeded to scan the beach, in longitudinal strips, effectively following the contours of the beach. The first area to be uncovered by the falling tide was the beach ridge; hence this was the first area to be searched. Searches then continued in parallel lines down the beach following the falling tide.

On the first two tides after injection of the tracers, the area searched was approximately 1500m^2; a thorough search of this taking about 4hrs. Later in the experiment, the search area was increased to 3000m^2 as the dispersion of the electronic pebbles reached its peak. By dividing the search area into two parts (east and west) and searching one part on the falling tide and the second area on the next rising tide (searching from toe to ridge, as the water level rose), the entire area was covered easily by a single operator in the time available. Searches undertaken during the night were carried out with a second searcher carrying a torch.

Recovery rates for the electronic tracers are shown in Table 5.5. Tracers which were not

mobilised, as a result of being located to landward of the high tide mark, were not included in the calculation of recovery rates; these would have biased the results towards higher recovery rates. The results show recovery rates in excess of 80%, for all the tides except for the evening of the 25/01/93 when a combination of darkness and difficult operating conditions (high winds and rain) reduced the recovery rate to just 63%.

Importantly, pebbles not found in a particular search were normally found on the subsequent search; this indicates that they had remained within the area surveyed and their non-detection was due to shortcomings in the search procedures; this is apparent from examination of the cumulative recovery rates (Table 5.5). The rates of recovery are considered to be very satisfactory; only Bray's (1990) results obtained from beaches in South Dorset and where recovery rates of 22% to 86% were obtained, are comparable.

The search for aluminium pebbles was carried out at the same time and in the same manner as for the transmitting pebbles, except that the special detector was replaced with a standard "treasure seekers" device.

Searches for the aluminium pebbles were hampered severely by the presence of a large amount of aluminium debris (mainly drinks can ring pulls); these had to be located and disposed of, since the signal these items produced was identical to that given by the aluminium pebbles. Over the course of the experiment, approximately one contact in three proved to be "trash". Due to the presence of this 'trash' it was found to be impossible to search the beach properly, at the rate of over $400m^3\ hr^{-1}$ suggested by Wright (1978). Search and recovery of aluminium pebbles during night-time low waters was particularly difficult, even when an assistant was available (this was due to the difficulty in identifying whether a contact was a tracer pebble or a small item of 'trash').

The rates of recovery for the aluminium tracers (also shown in Table 5.5) are much lower than for the electronic pebbles, ranging from 26% to 49%. The lower recovery rates, compared with the electronic tracers, can be attributed to: (a) the inability to thoroughly search the whole area over which tracers were dispersed, in the time available; and (b) apparent limitation on depth of detection, when using the metal detector (20cm for the deepest buried aluminium tracer, compared with 35cm for deepest buried transmitting pebble). The maximum depths of

recovery for the aluminium pebbles, at 20cm, is significantly less than that achieved by Wright et al (1978) - 0.4m, Nicholls and Webber (1987) - 0.33m; and Bray (1990) - 0.45m.

Recovery rates for the aluminium tracers used in this experiment are lower than those achieved by Bray (1990) (16 - 99%), but compare favourably with the results of Wright et al (1978), (27 - 63%), Nicholls and Webber (1987), (1 - 25%) and Bland's (1993) results from a similar study at Hayling Island, (8 - 22%). Recovery rates would have improved if an additional detector and operator were available, for the duration of the experiment.

5.4.3. Tracer Displacement

a. General Comments

A good mixing condition is required, if the movement of tracers is to accurately reflect the behaviour of the beach material. Poor mixing occurs if the tracers are unrepresentative of the indigenous particles in terms of size, shape and specific gravity; the electronic pebbles were moulded from actual Long Beach pebbles, to improve the chances of a good mixing condition occurring. Powell (1990) has noted a rapid dynamic response of shingle beaches in response to wave action (such that changes in profile would occur with a relatively small number of waves). On a tidal beach such as Long Beach, the whole profile will be reshaped as the tide rises and falls again. Hence providing the tracers are compatible with the indigenous material, they will become mixed within the beach rapidly, probably within a single tide.

Unrepresentative pebbles tend to be rejected from the body of the mobile beach (Moss, 1963) and become concentrated on the beach surface. Such concentration leads to large displacements, as the tracers are retained at a location where the transport is at a maximum. In the case of the Long Beach experiment, the aluminium pebbles represent only the most coarse part of the indigenous sediment and therefore, are most likely to be rejected.

There are many different measures of tracer movement, with the type used being often dependant upon the aspect of longshore transport intended for a particular study. Where the aim is to estimate transport rates, these can be determined using all the tracers recovered or particular sub-populations (sub-groups) of tracer. For example, Wright (1982) and Nicholls

(1985) calculated tracer centroids relating to every search. Neither researcher distinguished between sub-populations of, for example, mobile and non-mobile tracers; this leads to the concept of tracer availability (Bray, 1990). If a tracer is buried too deeply to become part of the mobile layer, or it is located too far landward to be affected by wave action, consideration should be given as to whether or not its location should then be used in the calculation of the tracer displacement over that particular period of time.

Bray's (1990) concept of tracer availability has to the identification of five separate sub-groups of tracer:

(a) the entire recovered sub-group (all);
(b) the moving tracer sub-group which has spent at least some time in the mobile layer since the previous search (move);
(c) a second moving tracer sub-group, where the tracers have been recovered also in the previous search so that displacement over one tide cycle can be made (prmove);
(d) stationary tracers above the high tide mark, not available for transport; and
(e) stationary tracers which are buried below the mobile layer and are not available for transport.

The "prmove" sub-group was considered by Workman (1993) to be the best for use in determining tracer displacement; this is because all tracers not available for transport, or whose position at the beginning of the tidal cycle is not known, are ignored in the displacement calculations.

For the present study, three further sub-groups have been defined:

(f) that part of the prmove sub-group which have moved for the first time (prfmove);
(g) that part of the prmove sub-group which have moved on at least one previous location following injection (prpmove); and finally
(h) that part of the prmove sub-group for which the individual tracers have not been directly affected by the presence of groynes, ie are located on an "open" section of the beach (promove).

Sub-groups (f) and (g) were defined so that the effectiveness of mixing of tracers, with indigenous beach material after a single tide, could be assessed. The latter sub-group (h) was defined so that the transport rates of beach material, unaffected by groynes or other structures, could be defined; this is important for assessing the transport formulae used in the coastal model.

b. Electronic Pebbles

Electronic tracer pebble displacements, throughout the experiment are shown in Figures 5.11 (a to f). Because the beach orientation varies within the experimental study area, the beach crest and toe are not parallel to the survey base-line. The consequence of this arrangement is that as tracers move to the east, the distance from the survey base-line will decrease even if the pebbles maintain an equivalent position on the beach profile. The opposite occurs (apparent increases in distance from the baseline), if the tracers move towards the west. The survey co-ordinates need to be corrected, therefore, such that both offshore and alongshore pebble positions are known relative to the beach ridge. Having corrected the pebble positions in this manner, it is then possible to assess the onshore - offshore and alongshore displacement of tracers. The results are presented in Table 5.6.

Onshore movement of the electronic tracers (30m over the period of 3 day experiment) was described by Workman (1993), based upon the same data reported in this study. Workman (op cit) neglected, however, to correct the survey data for the changing orientation of the beach. Having corrected the data, a different pattern emerges. For the first two tides after significant movement first occurred, the mean position of the tracers remains within a band less that 1m to either side of the mean offshore / onshore position at the time of injection.

Only after the bulk of the tracers have reached the groyned area of the experimental beach (on the morning of the 25/01/93) does a small offshore movement of the mean position occur. The mean offshore displacement of the mobile tracers (prmove) during the last 3 tides of the experiment, varies from 2.6m to 4.6m per tide. A cumulative mean offshore displacement of 7.2m, for the mobile tracers, occurs over the duration of the experiment. All of this movement occurred in the area where the beach movement was affected by the presence of artificial structures, such as groynes. Hence, it is not possible to draw any conclusions about the

onshore - offshore movement of tracers, relative to the natural beach material.

Workman's (1993) failure to correct the pebble positions for changing beach orientation, as described above, is less significant in the case of longshore displacement; this is because longshore displacements are large, compared with the correction which needs to be applied.

Longshore displacement of the electronic tracer pebbles, following the high tides on the evening of 23/01/93 and the morning and evening tides of 24/01/93, demonstrate comparable mean longshore displacements of the mobile tracer pebbles (prmove) of between 20 and 35m towards the east. Thereafter, tracer movement is negligible as a consequence of the combined effects of the change in beach orientation (which results in smaller wave angles, at breaking) and the trapping effect of the groynes.

An interesting observation is the comparison of the mean displacements of the prpmove (tracers which have moved on the previous tide, together with (at least) one other occasion) sub-group and the prfmove (tracers which have moved for the first time on the previous tide) sub-group for the evening search on the 24/01/93. The prfmove subgroup has a mean longshore displacement which is 50% greater than the prpmove sub-group. As the prfmove sub-group, in this case, is located higher up the beach than the prpmove sub-group, the greater displacement may be due to: (a) the greater wave energy which occurs at this point on the profile, as a result of deeper water in the nearshore area; or (b) the fact that the prfmove pebbles were located on the sand run, where transport rates would be expected to be larger (Bluck, 1967). The fact that the difference between the two sub-groups is not larger suggests that mixing between the tracers and the indigenous sediments occurs very rapidly, under the wave conditions encountered at Long Beach during the experiment.

In order to allow time for mixing of the tracers and indigenous beach material to occur, Workman (1993) rejected data collected during the first two searches after the initial injection. Only data derived from the 3rd to 6th searches (evening of 24/01/93 to morning of 26/01/93) were used in the calculation of longshore transport rates. The results presented in Table 5.6 suggest that it would also be reasonable to utilise data from the 2nd search after injection (morning of 23/01/93), as mixing appears to have occurred very rapidly.

(c) Aluminium tracers

Because of the lower recovery rates associated with the aluminium pebbles and the absence of any data for the evening of 25/01/93, it was not possible to divide the recovered pebbles into sub-groups for analysis. The results for the aluminium pebble displacements (Table 5.6) are presented, therefore as the mean onshore - offshore and alongshore positions of all the tracer pebbles which were recovered which had moved since injection; they are comparable, therefore, to the "all" sub-group of the electronic pebbles.

The onshore - offshore displacements of the aluminium pebbles represents that which occurred with the electronic tracers. Initially, there was no apparent onshore - offshore movement of the tracers recovered. However, upon reaching the groynes at the eastern end of the site, a net offshore displacement of 6.4m (from injection) occurred.

The mean longshore displacement of the aluminium pebbles differs from that displayed by the electronic tracers, in that the initial displacement of the aluminium tracers on the evening of 23/01/93 was almost 70% greater than for the electronic pebbles. Because of this high initial rate of transport, the tracers tended to reach the boat ramp and groynes before the transmitting pebbles (the retarding effect on the tracer displacement, at these structures, has been noted previously).

5.4.4. Mobile Layer Calculations

(a). General Observations

In order to convert the displacement of the tracer pebbles into transport rates, it is necessary to define the extent of the material which is mobile (the mobile layer), in terms of both its width and its depth. The two main methods utilised have been: (a) insertion of beach cores (Nicholls, 1985); and (b) the analysis of the depths of burial of tracer pebbles themselves Bray, 1990).

For shingle beaches, the width of the mobile layer is quite narrow at any one time; it is restricted to a band a few metres wide, between the breaker and swash zones. However, as

tracer displacement can only be averaged over a tidal cycle, it is practical to consider the width of the mobile layer in a similar manner ie over a tidal cycle.

Using the same data as utilised in this study, Workman (1993) defined the width of the mobile layer on the basis of the tracer; which was located farthest up the beach, and which was known not to have not moved during the previous tide. As the maximum number of tracers available was only 17, the likelihood of the uppermost tracer representing the full extent of the mobile layer could be questioned. Therefore, in the present study, the mobile layer width is defined as the distance from the beach crest formed by wave run-up to a point 2 m from the shingle toe of the beach (the lower 2m of the beach is effectively immobile, due to depth limitations on wave heights). Mobile layer widths for the duration of the study are given in Table 5.7.

Definition of the depth of the mobile layer is more complex. Generally, it has been assumed that the depth of the mobile layer is equal to the depth that sand mixes vertically within the beach Kraus (1985). King (1961) used dyed sand, in cores, to show that the depth of disturbance increased with wave height at the rate of 1cm disturbance depth to 30 cm increase in wave height. Virtually all investigations undertaken into depths of disturbance have been related to sand beaches, where wave breaking and resulting sediment response processes are likely to be different.

For shingle beaches, all the information available on the depth of disturbance is based upon the analysis of the depths of burial of mobile and, in the case of Bray (1990), non-mobile tracer pebbles. The most recent and comprehensive treatment of determining mobile layer depths, from burial depths of tracers, is based upon studies undertaken of beaches in South Dorset (Bray, op cit). This investigation found that, whilst breaking wave heights did indeed control the thickness of the mobile layer, the actual depths of disturbance were approximately 3 times greater than those for sand beaches.

Previous investigators, Wright (1982) for example, have estimated the mobile layer thickness on the basis of the depth of the deepest buried tracers. However, use of this method tends to overestimate the actual depths, as the deepest buried tracers may have been stranded by infrequent (but large) waves (Whitcombe, 1995); or simply by being buried below the mobile layer by natural sediment accretion.

Bray (1990) attempted to solve this particular problem, by defining the depth of the mobile layer as "the average of the mean depth of the deepest buried 50% of mobile tracers and the mean depth of the upper 50% of non-mobile tracers".

Nicholls and Wright (1991) reported mixing layer depths of between 9 and 19cm based upon an aluminium tracer experiment carried out at Hurst Castle Spit; breaking wave heights during this experiment peaked at around 1.3m, but were typically in the order of 0.3 to 0.7m ie similar to the present study. Wave periods were in the order of 4 to 8s, which is longer than those of the present study. A depth of disturbance of 17cm was typically found on beaches in South Dorset (Bray, 1993), for wave heights of around 1m.

Burial of a tracer due to natural sediment accumulation can lead to overestimates of the depth of the mobile layer. Such a situation is most likely to arise where sediment is moving in the vicinity of groynes, or other features which interrupt longshore drift. An aluminium tracer experiment was carried out within the study area at Tankerton, in 1991, to track the dispersal of shingle-sized material within a groyne field following a beach replenishment scheme (Canterbury City Council, 1991). It was noted that aluminium tracers becoming trapped against groynes would be buried by up to 1m of shingle in a single tide, even thought, the mobile layer was estimated to be between 10 and 20cm.

Whitcombe (1995), in a similar study (to the present Long Beach study) carried out at Hayling Island, chose to calculate the mobile layer thickness from cores of aluminium pebbles inserted into the beach; this was rather than determine the depth from tracer burial depths. Tracer recovery rates at Hayling Island were low, due to limited exposure of the beach; this probably contributed to the decision.

Depths of the mobile layer, calculated from the electronic pebble data set, are reproduced in Table 5.7. These results have been calculated on the basis of Bray's (1990) formulae (average of upper 50% non-mobile and lower 50% mobile tracer formula (as described earlier)). The exception is the mobile layer depth for 24/01/93 am search, when no pebbles were stranded below the mobile layer. The majority of the pebbles were located in the upper 5 to 10 cm of the beach; however, a single tracer was located at a depth of 30cm. The estimated mobile layer depth (n = 15cm) for this occasion was selected on the basis of comparison of the mobile layer

depths for other searches and the wave heights on the tide previous to the search (as the depth of disturbance depends upon wave height, Section 5.4.4)). Wave heights recorded at Long Beach on the evening of the 23/01/93 were only slightly lower than on the next evening (when n = 16cm); they were noticeably higher than on the high tide on the morning of 24/01/93 (when n = 12cm). The mobile layer depth on the evening of 25/01/93 was only 10cm, despite following a tide during which the largest waves of the experimental period were recorded. However, by this stage, the majority of the tracers were located within the groyned section of beach. Here, localised accretion and erosion would further confuse the interpretation of the relationship between depths of burial of the tracers and the calculation of the extent of the mobile layer.

Burial depths for the aluminium tracers was less than those obtained for the electronic pebbles, as noted in Section 5.4.2. This difference may be due to either: (a) a higher level of rejection of the coarser aluminium pebbles (Moss, 1963); or (b) a reflection on the limitations on the depth of tracer pebble recovery, achieved by the metal detector / aluminium pebble system. Bland (1993) assumed that the reduced depths of burial were attributed to the second factor, utilising instead the mobile layer depths calculated for the transmitting pebbles (Workman, 1993). However, if the reduced burial depths of the aluminium pebbles is related to greater rejection, than for the electronic pebbles, the resulting estimates of longshore transport will be too high.

Results of the deployment of 3 cores of pebbles in the beach, on the morning of 24/01/93 were inconclusive. Depths of disturbance of 1, 4 and 6cm were obtained from the cores, (Bland, 1993); nonetheless several electronic pebbles were buried to depths of greater than 10cm, in the close vicinity of the cores. The small depths of disturbance recorded by the cores is attributed to the cores becoming buried, with mobile material moving landward as the tide rises. Due to a lack of confidence in the first set of results from the cores, together with the lack of time to undertake core studies (in addition to tracer searches, beach plan surveys and instrument maintenance) the cores were not replaced after the first attempt.

As noted by Greer and Madsen (1978), there does not appear to be a satisfactory method of determining the depth of the mobile layer and its variability both throughout the tidal cycle and across the beach profile. Further, the limited number of tracers available for use means that

there is likely to be poor statistical significance associated with the mobile layer calculations. Nevertheless, the mobile layer thickness calculated from the recovered electronic tracer pebbles, utilising Bray's formula, are consistent with the observations of other similar studies. In addition, the increase in the wave height on the beach during the previous high tide is generally reflected in an increased depth of the mobile material. The mobile layer depths presented in Table 5.7 are used, therefore, in the transport rate calculations (Section 5.4.5.); they are considered to be the best available estimates.

5.4.5. Transport rates based upon tracer movement

Calculation of the longshore transport rates depends upon the tracing technique which is applied. For the present study the quantity of material transported alongshore, during each tidal cycle (Qt), has been calculated using:

$$Qt = U(sg).m.n \qquad (5.1)$$

where U(sg) is the mean longshore displacement of a particular tracer sub-group over the tidal cycle; m is the mobile layer width; and n is the depth of the mobile layer.

Longshore transport estimates, based upon the electronic pebble sub-groups, are available for 5 tidal cycles; the results are presented in Table 5.8. Estimates of longshore transport, using a combination of the mean longshore displacement of all the recovered aluminium pebbles and the mobile layer depths calculated for the electronic pebbles, have been included for comparison.

As expected, the largest estimates are obtained using the promove sub-group; this excludes both non-mobile tracers and those tracers where displacement has been retarded by the boat ramp / groynes at the eastern end of the system. Longshore transport rates, for this sub-group range from 80 to 130m^3 per tidal cycle. The lowest transport rates are obtained using the "all" sub-group, which includes both mobile and non-mobile tracers. For the first three tidal cycles, the estimated transport rates range between 50 and 80m^3 per tidal cycle. For the two remaining tidal cycles, negligible transport rates are obtained as the tracers are all located between the boat ramp and terminal groyne at the eastern end.

Interpretation of the results for the aluminium pebbles is difficult because: (a) not all the tracers were mobilised by the morning of 24/01/93, as the previous high tide did not extend far enough up the beach; and (b) the second injection of 20 tracers, following the evening search on the 24/01/93, meant that there were two distinct populations of aluminium tracers on the beach. By combining these two populations of aluminium tracers, when calculating the mean tracer displacement, an anomaly will occur in the search carried out immediately after the second injection. This explains why, on the morning of 25/01/93, the estimated longshore transport rate using aluminium pebbles is only 13.6m^3; this compares with 77m^3, when the electronic pebbles (all sub-group) is used.

5.5. Beach survey and analysis

Beach surveys were undertaken using an EDM theodolite, on each of four daylight low tides on the 23 - 26/1/93. The beach is fully exposed at low tide, so that surveys could be carried out along the full extent of the beach from the crest to the toe. The beach area surveyed was closed to shingle transport towards the east, by a large timber groyne.

The major problem associated with determining the rate of longshore transport, from a series of profiles or beach plans, is often that of closing the system. Whitcombe (1995) reported this problem in a parallel study carried out on Hayling Island. However at Hayling Island it was not possible to survey the toe of the shingle beach, which was located well below low tide level. Also, there were no cross-shore structures which could act as a barrier to longshore transport. The difficulties experienced in closing the shingle system at Hayling Island do not occur on Long Beach.

In some similar studies (for example, Workman 1993), the beach level data has been analysed using the "Surfer" package. However, the method of analysis used by the package is not suited to data sets collected on steep "shingle" beaches. Instead, the data was converted into 8 cross-shore profiles; these are also shown on Figure 5.3. The changes in each of the 8 profiles, over the 4 day period, are illustrated in Figure 5.12 (a to h).

Moving from east to west there is a decrease in the level at the toe; this drops from approximately 0.0m AOD at Profile 1, to -0.7m AOD at Profile 8. The profile also becomes

longer, partially due to a decrease in toe level and partial due to an increase in the width of the beach berm. The gradient of the beach face varies between 1 in 7 and 1 in 9. The beach face in Profiles 1-3 slope at approximately 1 in 8, compared with Profiles 6-8 which are steeper at approximately 1 in 7.5. All the profiles show a general steepening of the beach face from 23 - 26/1/93, increasing in slope from about 1 in 8.3 to 1 in 8.0, at the western end, and from 1 in 7.7 to 1 in 7.5, at the eastern end. A notable feature of all the profiles are the effects of the storm surge occurring on the afternoon of 25/1/93. Within each of the 8 profiles, the surge resulted in the accretion of a pronounced storm crest, with the movement of a significant amount of shingle above the +4.0m AOD contour.

For each profile, the cross-sectional area was determined; these, in turn, were used to calculate the total volume of beach material within the 5 cells for each morning. Daily volumetric changes for the cells were then calculated over the four day period (Table 5.9). All five cells increased in volume, from the 23/01/93 to 24/01/93. However, only Cells D & E continued to accrete for the duration of the study. Net losses occurred in Cell A between 24/01/93 and the 25/01/93 and in Cells A, B and C on the following day.

Because the system is closed to shingle transport at its eastern end, it should be possible to determine not only the volume of material which is added to, or removed from, each cell but also where sediment originates or where it is transported to . Assuming that the large terminal groyne at the eastern end of Cell A effectively closes the system, any net build-up of material in Cell A must have been transported alongshore from Cell B. Likewise, a loss of material in Cell A would have to be balanced with longshore transport, into Cell B. Progressing westwards, this sediment budget balancing approach can be applied to the remaining cells, to determine longshore transport at the boundaries between each cell (Table 5.9).

Longshore transport rates, determined from the volumetric analysis (Figure 5.12), show that neither the calculated rates of transport nor the direction of net transport are consistent between individual cells. Between the 23/01/93 and the 24/01/93, there is a steady decrease in the longshore transport rates, from the east to the west. This pattern is consistent with the change in orientation and increasing depth of water, towards the west. A very similar pattern is seen between the 24/01/93 and 25/01/93, although the estimated transport rates are lower and show a reversal in direction at the western end.

Net sediment movement into the study area as a whole is much reduced between 25/01/93 and 26/01/93 ($62m^3$, compared with 265 & $307m^3$ on previous days); likewise the variation in transport rates between cells is more irregular.

There are two factors which could lead to errors in the above analysis, as outlined below.

(i) The small groynes and boat ramp, whilst buried for much of their length, were noted to have "trapped" some of the aluminium and transmitting pebbles; this indicates that some retardation of longshore transport was likely, in the vicinity of these structures.

(ii) The foreshore beyond the shingle toe, at the eastern end, was noted to become sandier as the experiment progressed; this indicates that the system may "leak" sand-sized material at this location. There was no evidence of shingle moving in the same direction.

Best estimates of the longshore transport rates are likely to be those determined for the western part of the study area, where there were no structures to impede longshore transport, and there was a plentiful supply of shingle up-drift. If sand-sized material moves offshore at the eastern end of the study area, then the calculated transport rates will be underestimated.

Finally, the transport rates calculated on the basis of volumetric analysis represent total sediment transport rates, of both sand and shingle. This interpretation is in contrast to the tracer method, where the transport rates of the coarse shingle fraction is being measured.

5.6. Comparison of Transport Rate Calculations

5.6.1. Summary of Data Collected

The main data sets collected for the Long Beach Study are summarised in Table 5.11 and include:

(a) wind data recorded at Borstal Hill, Whitstable (showing maximum average wind speeds and direction, over a tidal cycle);
(b) water level data at Whitstable Harbour (showing still water level at high water and time of

high water);

(c) wave records from the Whitstable Harbour wave recorder (showing maximum recorded significant wave height (Hs) and wave period (Tz), over a tidal cycle);

(d) wave records from a pressure transducer at Long Beach (showing maximum recorded significant wave height (Hs) and wave period (Tp), over a tidal cycle);

(e) visual wave records at Long Beach (showing maximum significant breaking wave height (Hsb) and breaking wave angle ($\propto$b), over a tidal cycle);

(f) maximum significant wave height (Hs) and wave period (Tp), over a tidal cycle at Long Beach, based upon the output from the wave model;

(g) percentage recovery of electronic and aluminium pebbles; and

(h) the day-time low waters, during which time the beach plan surveys were undertaken.

Table 5.11 provides limited details of the data collected; full details of the data sets are reproduced in the relevant Sections of this Chapter.

Recordings of the forcing parameters (wave conditions) are made around high water, whilst recordings of the resulting transport of material relate to the following low water. In order to avoid confusion in the subsequent discussions, successive data sets recorded during each tidal cycle are labelled "as number of high waters since tracer injection". For example, (i) + 1, represents the high water immediately after tracer injection and also the following low water; during this time, beach changes or tracer displacements are recorded.

5.6.2. Summary of Results

The results of the various longshore transport estimations are summarised in Table 5.12. All the quantities presented refer to net longshore transport rates over a tidal cycle and are given in cubic metres; negative quantities represent transport from west to east. Where the estimate of transport rates have been determined for different sections of the beach (Cells A to E (see Figure 5.3)); this is shown in Table 5.12.

A pattern common to each of the three sets of results is the reduction of westerly to easterly transport, which occurs as the terminal groyne at the eastern end is approached. In the case of the estimates based upon the coastal model (modelled wave conditions and longshore

transport rates, using the "Delft" equation). This reduction is due to the change in beach orientation and, hence, breaking wave angle along the experimental beach. However, in the case of the estimates based upon the displacement of tracers and the beach volumetric changes (determined from the beach plan surveys), the retarding effects of the groynes and boat ramp also influence the system. This effect is in addition to any modifications of wave conditions which may occur, due to the presence of these structures and the terminal groyne itself.

Because the model results ignore the effects of the boat ramp and groynes at the eastern end, the only results which are directly comparable for all three methods of estimating longshore transport are those which are calculated for Cells D and E. These two cells are located on a section of beach, which is located sufficiently far away from the effects of cross-shore structures.

In order to compare the results based upon both the coastal model and upon tracer displacement, with the transport rates obtained from volumetric changes, it is necessary to sum the results for the two tidal cycles for each day. This approach is because beach plan surveys were only undertaken on one low water each day; this is due to the requirement for light, to be able to use the EDM. Daily transport rates are shown in Table 5.13. These transport rates are for Cells D and E; in the case of longshore transport estimates from volumetric changes, the average of the rates calculated for cells D and E has been used. Cumulative daily longshore transport rates are listed also in Table 5.13.

5.6.3. Comparison of Longshore Transport Rates: 23rd to 26th January 1993

Comparison of transport rates is described below on: (a) a daily basis; and (b) over the duration of the whole experiment. In each case, the promove tracer subgroup has been used for the calculation of transport rates from tracer displacement; this neglects results from tracers which have been influenced by the groynes.

(a) 23rd January 1993 to 24th January 1993 (((i) + 1), ((i) + 2))

Wave conditions were such that no significant transport occurred during the ((i) + 1) period and the bulk of the transport for this period can be attributed to the waves during the evening

high water ((i) + 2). Transport rates derived from the model and from the displacement of tracers are very similar, at between -100 and -110 cubic metres towards the east. However the longshore transport rate based upon volumetric changes is greater, by a factor of greater than 2.

(b) 24th January 1993 to 25th January 1993 (((i) + 3), ((i) + 4))

On the second day of the experiment, significant wave activity occurs over both tides, with the result that net longshore transport rates calculated from both the tracers and from the coastal model are double those of the previous day, at -210 and -270 m^3 (from west to east), respectively. The transport rate derived from the volumetric changes are also in the order of -210 m^3 ie towards the east; this demonstrates a high degree of similarity between the different methods of estimation.

(c) 25th January 1993 to 26th January 1993 (((i) + 1), ((i) + 2))

Because all of the tracers were trapped amongst the groynes, no results for the open part of the beach were available. Results were obtained from both the model and the volumetric analysis techniques. Longshore transport estimates of -103 and -33 m^3 (west to east) were obtained, from the model and the volumetric changes, respectively. On the basis of records of weather and wave conditions, it can be concluded that the bulk of this movement occurred during the morning high tide. Although the morning high water coincided with a large tidal surge (resulting in a high tide level, with a return period of around 5 years, (see Figure 5.6)), transport rates appear to have been similar to those which were associated with the previous 4 high tides.

(d) 23rd January 1993 to 26th January 1993(((i) + 1) to ((i) + 6))

Longshore transport over the three day period is estimated to be between -450 and -550 m^3, based upon both the results of the coastal model and the volumetric changes derived from the beach plan surveys (Table 5.14). No longshore transport rates (for the open beach) were available from the tracer displacements on the final day of the experiment; hence, a cumulative 3 day transport rate cannot be determined. However, after the end of the second day, a

cumulative longshore transport rate of -310 m^3 was obtained (compared with -370 and -480 m^3 for the wave model and volumetric analysis, respectively (Table 5.13).

Longshore transport rates obtained from the coastal model compare very well with the two methods used to directly measure transport quantities, over the three day experimental period. Whilst the performance of the model over this period is satisfactory, the short duration of the experiment provides no guarantee that it will perform equally well over the longer term. During the three days, only waves from the west and northwest were encountered.

On the evenings of both the 23/01/93 and 24/01/93, the predicted wave heights were lower than those which were recorded and had to be corrected (probably for air / sea temperature differences). When compiling longer-term transport rates (annual, for example); it is not possible to record wave conditions at the beach toe along the whole length of coastline; in this way the model could be checked and corrected, if necessary. Therefore, whilst the Long Beach experiment suggests that no calibration factors need to be applied to the transport module of the coastal model, the performance of the model needs also to be checked over the longer term.

5.7. Calculation of Potential Annual Net Longshore Transport Rates

The approach for determining net annual potential longshore transport rates, from the nearshore wave climate, has been described in Section 3.8. Calculations are based upon the annual wind climate (derived from data collected at Manston Airport, between 1979 and 1990 (Figure 4.7 (a to c)), together with the frequency distribution of still water levels recorded at Herne Bay in March 1990 (Table 4.6)).

Potential net longshore transport rates have been determined, for a range of coastal orientations, in 9 of the 10 coastal sub-units in the study area (Table 5.14); these are Seasalter, Whitstable, Tankerton, Studd Hill, Herne Bay, East Cliff, Reculver, Northern Sea Wall and Minnis Bay (for locations see Figure 3.4). These results do not allow for the presence of structures, such as groynes, which would disrupt longshore transport. (No results have been included for Hampton Pier Avenue (sub-unit 4A), because there is no beach present over this particular section of coastline. The foreshore along the whole length of the sub-unit is, instead,

protected by rock armour). An example of the results is shown in graphical form; Figure 5.15.

For each of the graphs presented in Figure 5.15, it can be seen that there is a particular angle of the coastal orientation at which the longshore transport is zero; this represents the stable or equilibrium orientation, where gross transport rates in opposite directions are equal. There is, therefore, no net annual longshore transport. This angle represents the orientation at which natural processes will work to establish as the 'normal', on an ungroyned beach. The angles of coastal orientation, at which transport equilibrium is achieved for each coastal section, are given in Table 5.15. Deviations of the actual coastal orientation angle, from these equilibrium values, will result in a net annual longshore transport; the extent and direction of this transport can be obtained from Table 5.14, or from graphs, such as Figure 5.15, for example.

Examination of the equilibrium angles shows that, between Whitstable and Reculver, there is a general change in the equilibrium angle along the coastline. At Whitstable, equilibrium is achieved with an orientation of -10° (that is 10° clockwise, from east to west), compared with 0° (east to west orientation) at Reculver. In Section 4.5.5, it was noted that there was a reduction in the directional asymmetry in the nearshore wave climate between Whitstable and Reculver. The change in equilibrium angle described above is a representation of the changes in the wave climate. At Reculver and East Cliff, the effect is enhanced, probably due to the presence of sediment banks to the north and east of Reculver; these will reduce wave energy from northeasterly directions.

Equilibrium angles at Seasalter, the Northern Sea Wall and at Minnis Bay do not follow the general trend (see below).

At both the Northern Sea Wall and Minnis Bay, the offshore sand-banks provide some degree of sheltering from wave action from all directions; this is in comparison to Reculver and East Cliff, where there is a clear directional sheltering effect

Seasalter is a very sheltered site, located on the south "bank" of the Swale Estuary. Typically, the beach toe is at or above +1.0 m AOD. Wave action can only reach these beaches for two or three hours around high tide; likewise, wave energy which reaches the beaches will be much reduced. The model output reflects the strong sheltering from wave action which occurs at

Seasalter however, it does not take account of the small (but significant) amount of wave energy generated within the Swale Estuary itself.

An assessment of the model predictions is described in Chapter 6, in terms of: (a) the equilibrium angles; and (b) the potential net annual transport rates

5.8 Seasonal Variations in Potential Net Longshore Transport Rates

It is possible to determine the seasonal (winter / summer) variation in longshore transport potentials, using the coastal model. This calculation has been carried out by replacing the input data from the average annual wind climate data (Figure 4.7(a)), with data averaged over the winter (Figure 4.7(b)) and summer (Figure 4.7(c)) periods.

A seasonal variation in wind conditions (recorded at Manston Airport (1979 to 1989)), has already been described in Chapter 4 (Section 4.5.1). The winter period is more likely to be dominated by westerly and northwesterly winds; during summer, wind speeds are generally lower and winds from the northeast are more common.

Potential net longshore transport rates determined for Long Beach, Whitstable, over the summer and winter seasons are reproduced in Figure 5.16; the annual averaged transport rate is shown also, for comparison. It should be noted that the time-scale for the annual transport rate is 12 months, compared with just 6 months for each of the two seasonal transport rates.

Using the central section of Long Beach as an example (where the coastal orientation is +3°), net potential longshore transport quantities of +320, -1200, and +1520 m^3 are derived for the annual, winter and summer periods, respectively (where transport from west to east is -ve).

Net annual transport rates at Long Beach have been estimated at +250m^3, on the basis of the quantity of material which by-passes the east quay of the harbour and is removed by dredging (Canterbury City Council, 1988).

Averaging data over several years to produce a "typical" year, disguises much of the variation which occurs over the shorter term. For example, reference to Section 5.6 demonstrates that

over a period of effectively four tidal cycles (the evening of 23/01/93 to the morning of 25/01/93), an estimated 500 m^3 of beach material was transported from west to east during a "fairly modest" storm. This value represent a transport quantity which is double the modelled annual averaged quantity.

Examination of the modelled transport rates for the summer and winter seasons demonstrates that the annual transport rate at Long Beach is made up of a summer component (1520 m^3 transported east to west), and a winter component (1200 m^3 transported in the opposite direction, west to east). Both are in excess of the modelled annual net transport quantities.

Further dissection of wind condition into smaller clusters of time will inevitably produce a situation where significant volumes of material are seen to be transported in opposite directions at Long Beach over periods of days or weeks. Over a period of one "average" year all the transport quantities will tend to balance out to produce a small net transport rate predicted by the model.

5.9. Impact of Climatic Anomalies on Potential Net Longshore Transport Rates.

Clearly transport rates determined from "averaged" data (whether annual or seasonal as used in the previous section) will disguise much of the variation in longshore transport which occurs over shorter time periods. For example, the effects of storms (extreme events) may last for only a few hours, but during that period, significant volumes of transport may occur.

At the other end of the scale, changes to weather patterns (and hence patterns of longshore transport), caused by climate change, occur over a timescale of years. Since the minimum timescales considered in the design and management of the coastline is now 50 years (MAFF, 1997), the impact of climate change does therefore need to be taken into account.

For the Long Beach site, the effects of a number of climatic anomalies have been assessed. The assessment has been divided into three sections, depending on whether the timescale is considered to be short term (hours / days); medium term (weeks / months) or long term (years).

(a) Extreme events, (short-term effects)

Extreme events describe relatively short periods of time, during which wave energy on the beach is well in excess of "normal" levels. From the discussion presented at the end of Chapter 4, these events are associated commonly with still water levels which are also raised above normal levels. The raised water levels, in turn, allow larger waves to reach the beaches. Although extreme events are rare, by definition, they have the capacity to transport large volumes of sediment over relatively short periods of time.

The most valuable information which can be obtained on transport rates during extreme events can be derived by modelling real events. Three storm events were selected for the study of resulting longshore transport rates: (a) 12th December 1990; (b) 20th February, 1996; and (c) 1st February, 1953.

Wind conditions, water levels and the resulting (modelled) wave conditions for the three events (at Long Beach, Whitstable) are listed in Table 5.16. Also shown are the longshore transport quantities for the open section of Long Beach, based upon the modelled wave data and the "Delft" longshore transport equation. In each case, only a single tidal cycle has been modelled. However it should be noted that high levels of wave energy may be experienced for a number of tides, either preceding or succeeding the modelled period.

The storm which occurred in the early morning of 1st February 1953 caused devastating flooding across the east coast of the UK and northern Europe. As can be seen from Table 5.16, such a storm, has the capacity to transport an estimated 1000 m^3 (at a maximum hourly rate of 172m^3) of beach material in a longshore direction at Long Beach, over the passage of a single tidal cycle. The transport rates (and directions) at other locations along the coast will vary, depending primarily upon the coastal orientation.

A storm of lesser intensity, in terms of still water level and significant wave height, occurred on 20th December 1990. This event resulted in minor flooding to coastal roads, but little damage throughout the study area. During the storm, winds were blowing from the west (Sector 1). The estimated transport rate over a tidal cycle, for this event, is around 640 m^3 at Long Beach; with a maximum hourly rate of 109 m^3.

Since 1978, only the storm which occurred on the morning of the 20th February 1996, has resulted in flooding to coastal properties in the study area. The still water level reached an upper level of 3.7m AOD, giving a high water surge residual of 0.8m. The wind direction was north-northeasterly. The return period of a surge of this level is approximately 1 in 30 years, when associated with northeasterly winds (Figure 4.13). High water surge residuals of this level are more common with north-westerly winds where the return period would have been just 1 in 1 year.

Total longshore transport at Long Beach, during the morning of 20th February 1996, is estimated to be around 280 m^3; this is less than half the quantity which occurred in the case of the previously described lesser storm. The reason for this difference is that waves break at a smaller angle on the beach and consequently, there is less energy expended in a longshore direction. The extent of transport which occurs during a storm depends not only on the still water level, the wave height and the wave period, but also upon the wave angle; this is, in fact, evident from the transport equations.

Breaking wave angles at Long Beach, during this latter storm, were in the order of 6 to 8° allowing for the - 3° orientation of the coastline itself. At other locations within the study area, where the coastal orientation would have resulted in larger breaking wave angles, there would have been larger quantities of material transported alongshore. For example, had the orientation at Long Beach been +5°, then the resulting transport rates for the three events would have been: -490 m^3 (1st February 1953); -580 m^3 (12th December 1990); and +570 m^3 (20th February 1996).

(b) Atypical weather conditions (medium-term weather pattern changes)

Significant volumes of material may be transported in one particular direction, as a result of weather conditions; these produce winds blowing from a more or less constant direction, over a long period of time. Such an event occurred during the winter of 1995 / 1996, when the normal pattern of domination of westerly and northwesterly winds, over easterly and northeasterly winds, was reversed, Figure 5.17.

The occurrence of wind speed and directions (monthly-averaged), for the period September

1995 to April 1996, is shown in Table 5.17(a to h). Examination of these data show a high level of variation between the individual months. For example, during October 1995, wind speeds are low (maximum hourly-averaged wind speed of Force 4 (Beaufort Scale)); similarly there is no strong asymmetry in wind direction. This pattern is in contrast to that observed in January 1996, for example, when there was a strong bias towards the northeasterly and easterly wind directions; hourly-averaged wind speeds for the northeasterly directions are also higher. The strongest winds occurred in February 1996, when hourly-averaged wind speeds of Force 8 were recorded; however during the month of February as a whole, there is a more even distribution of wind direction occurrences, than in many of the other monthly periods shown.

Net potential longshore transport rates have been calculated for each month, between September 1995 and April 1996; the results are reproduced in Table 5.18.

The highest estimated monthly net longshore transport rate (+2160 m^3) occurred during December 1995, when the net transport was in a westerly direction. The following month, a further 1690 m^3 of material moved in the same direction. A reversal in this pattern (1100 m^3 towards the east) occurred during February 1996; this was a month which was noted for a series of minor storms. A major storm (described in Section 5.9 (a) above), also occurred on the 20th February 1996. Interestingly, transport during this storm event was in the opposite direction to the monthly average, emphasising the variability which occurs over short time-scales. During March and April 1996, there was a return to westerly transport, with a net +1290 m^3 transported in March and +1030 m^3 in April.

Over the winter of 1995 / 1996, the normal dominance of westerly over easterly winds was reversed. This change results in a net averaged winter months transport of +3170 m^3; this compares with the 1979 to 1989 averaged "winter months" transport quantity, of -1200 m^3.

Some consequences of this reversal are described in the Discussion (Chapter 7).

(c) Climate change (long-term shifts in weather patterns)

There are two main reasons why long-term shifts in weather patterns need to be taken into

account:

(a): if, for example, the long-term shifts occur in cycles with periods of several decades or more, then the approach adopted in this study (of producing an average year from ten years of wind data) will in fact only be representative of part of the climate cycle; and

(b): a shift in climate pattern, which leads to a long-term or permanent change in the equilibrium angle of the coastline, could lead to sea defences, which are designed based upon beach and groynes systems being misaligned for the changed (wave) climate regime. This is also an important observation in coastal process scientific studies.

Insufficient data are available from this study, to attempt to assess whether long-term changes in wind conditions are likely to occur. This particular topic is addressed in the Discussion Chapter 7.

Date	16TH MARCH 1992			18TH MARCH 1992			30TH MARCH 1992		
Position	Y (m)	X (m)	d (cm)	Y (m)	X (m)	d (cm)	Y (m)	X (m)	d (cm)
C0	45.01	1.00	5	45.01	1.40	3			
C1	32.10	-1.00	20	32.10	-1.00	20			
C2	31.11	1.00	5	31.21	1.35	5	36.80	-58.08	25
C3	45.01	-1.00	25	44.91	-0.80	20			
C4	49.97	1.00	5	50.07	1.40	3			
C5	29.12	-1.00	5	29.12	-1.10	1	28.05	-67.41	5
C6	38.06	-1.00	5	38.06	1.50	2			
C7	40.04	1.00	5	40.04	1.40	2			
C8	42.03	1.00	5	42.03	-0.80	0			
C9	45.01	-1.00	5						
D0	48.98	1.00	5	49.68	-1.90	0			
D1	32.10	-1.00	40	32.10	-1.00	40			
D2	44.02	1.00	5	44.02	1.40	4			
D3	53.95	1.00	5	54.14	0.90	0			
D4	46.00	1.00	5	46.10	1.20	2			
D5	46.00	-1.00	5	46.20	-1.00	0			
D6	33.09	-1.00	5	35.58	-0.60	0			
D7	46.99	1.00	5	46.99	1.30	3			
D8	47.99	1.00	5	48.09	1.40	2			
D9	48.98	-1.00	5	49.18	-0.90	0			
E0	34.09	-1.00	5	34.78	-1.75	0			
E1	32.10	-1.00	10	32.10	-1.00	10			
E2	32.10	-1.00	5	33.69	-2.00	1			
E3	41.04	1.00	5	41.04	1.35	10			
E4	38.06	-1.00	5	38.06	-0.80	1			
E5	35.08	1.00	5	34.98	1.60	2			
E6	44.02	-1.00	5	44.02	-1.30	0			
E7	30.11	-1.00	5	30.11	-1.10	5			
E8	37.07	-1.00	5	37.07	-0.90	3			
E9	43.02	1.00	5	43.22	1.20	4	43.79	-68.29	15
F0	52.95	-1.00	5	52.95	-0.90	3			
F1	35.08	-1.00	5	35.38	-1.00	5			
F2	30.11	1.00	5	30.21	1.10	4			
F3	39.05	1.00	5	39.15	-1.50	2	38.83	-65.16	20
F4	51.96	-1.00	5	51.76	-0.90	1			
F5	33.09	1.00	5	32.99	1.20	4	29.02	-90.80	0
F6	50.97	1.00	5	50.87	1.30	0			
F7	37.07	1.00	5	37.07	1.60	5			
F8	50.97	-1.00	5	51.07	-1.90	0			
F9	32.10	-1.00	30	32.10	-1.00	30			
G0	31.11	-1.00	5	31.11	-1.00	3	23.60	-66.87	5
G1	32.10	1.00	5	32.00	1.20	6			
G2	46.99	-1.00	5	47.09	-0.70	3			
G3	29.12	1.00	5	35.58	1.70	2			
G4	43.02	-1.00	5	43.02	-0.90	0			
G5	53.95	-1.00	5	53.65	-0.90	0			
G6	45.01	-1.00	15	44.91	-0.80	10			
G7	51.96	1.00	5	51.76	0.40	1			
G8	39.05	-1.00	5	39.05	-0.90	1			
G9	34.09	1.00	5	34.78	1.30	3			
H0	42.03	1.00	5	42.03	1.20	0			
H1	49.97	-1.00	5	51.07	-4.10	2			
H2	47.99	-1.00	5	47.99	-1.00	3	45.16	-75.23	5
H3	36.07	1.00	5	35.87	1.50	1			
H4	36.07	-1.00	5	36.07	-0.90	2			
H5	40.04	-1.00	10	40.14	-0.80	20			
H6	45.01	-1.00	5	44.91	-0.80	0			
H7	52.95	1.00	5	52.95	1.10	2			
H8	45.01	-1.00	20	44.91	-0.80	15			
H9	41.04	-1.00	5	41.14	-0.80	0			

where: y is the offshore displacement; x is the longshore displacement; and d is the depth of burial.

Table 5.1. Aluminium Tracer Displacements at Long Beach, Whitstable, 16/03/92 to 31/03/92.

Date	Time (GMT)	Hb (m)	Angle ∝ (°)	Wave Type [a]
23/01/93, (am)	1015	0.05	-35 to -45	wind
	1115	0.15 0.05	0 to -10 -35 to -45	swell wind
	1215	0.15 0.05	0 to -10 -35 to -45	swell wind
	1315	0.1	-35 to -45	wind
	1415	0.15	-35 to -45	wind
	1515	0.15	-35 to -45	wind
23/01/93, (pm)	2215	-	-25 to -35	wind
	2315	-	-25 to -35	wind
	0015	-	-25 to -35	wind
	0115	-	-25 to -35	wind
	0215	-	-25 to -35	wind
24/01/93, (am)	1115	0.3	-25 to -35	wind
	1215	0.4	-25 to -35	wind
	1315	0.6	-25 to -35	wind
	1415	0.6	-25 to -35	wind
	1515	0.5	-25 to -35	wind
	1615	0.3	-25 to -35	wind
24/01/93, (pm)	2215	-	-20 to -30	wind
	2315	-	-20 to -30	wind
	0015	-	-20 to -30	wind
25/01/93, (am)	1015	0.6	-15 to -25	wind
	1115	0.6	-10 to -20	wind
	1215	0.7	-10 to -20	wind
	1315	0.8 [b] 0.8 [b]	-10 to -20 0 to -10	wind swell
	1415	0.8 [b] 0.8 [b]	-10 to -20 0 to -10	wind swell
	1515	0.6 [b] 0.6 [b]	-10 to -20 5 to -10	wind swell
	1615	0.5 [b] 0.5 [b]	-10 to -20 5 to -5	wind swell

(a) wind waves are steep, T = 3 to 4 sec; swell waves have T > 8 sec: (b) not possible to defined separate wave heights for "wind" and "swell" waves on 25/01/93.

Table 5.2. Visual Observations of Wave Conditions at Long Beach, Whitstable: 23/01/93 to 25/01/93.

Date Recording Starts	Time (GMT)	Water Depth m AOD	Time Domain		Frequency Domain		
			$H_s = H_{1/3}$ (m)	Tz (sec)	H_{RMS} (m)	$H_s = H_{mo}$ (m)	Tp (s)
23/01/93, morning	1015	1.62	0.16	2.33	0.05	0.08	7.31
	1115	2.60	0.13	3.85	0.05	0.08	8.53
	1215	3.25	0.16	6.07	0.10	0.14	8.53
	1315	3.10	0.20	2.92	0.10	0.14	8.53
	1415	2.20	0.19	2.09	0.09	0.13	2.05
	1515	0.25	0.31	1.94	0.15	0.21	1.46
23/01/93, evening	2215	0.65	0.29	2.83	0.26	0.37	3.10
	2315	1.65	0.56	3.38	0.37	0.52	3.79
	0015	2.35	0.58	3.52	0.43	0.61	3.66
	0115	2.25	0.59	3.36	0.39	0.55	3.41
	0215	1.65	0.55	3.10	0.40	0.57	3.30
24/01/93, morning	1115	1.70	0.46	3.25	0.37	0.52	3.53
	1215	2.95	0.49	3.62	0.38	0.54	3.66
	1315	3.55	0.68	3.37	0.33	0.47	3.20
	1415	3.05	0.59	3.18	0.33	0.46	3.01
	1515	2.25	0.52	2.91	0.26	0.37	2.63
	1615	1.30	0.40	2.67	0.26	0.37	2.84
24/01/93, evening	2215	1.95	0.44	3.15	0.30	0.42	3.10
	2315	2.70	0.66	3.82	0.54	0.76	4.27
	0015	3.35	0.75	3.76	0.50	0.70	4.10
25/01/93, morning	1015	1.55	0.43	2.99	0.33	0.46	3.41
	1115	2.65	0.50	3.26	0.32	0.46	3.41
	1215	3.75	0.58	3.64	0.34	0.49	3.30
	1415	4.35	0.70	4.99	0.48	0.68	8.53
	1515	3.70	0.67	4.90	0.49	0.69	4.10
	1615	2.55	0.46	3.62	0.33	0.47	4.10

See text for terminology and details of methods of analysis

Table 5.3. Analysis of wave data, (time and frequency domain), Long Beach, Whitstable: 23/01/93 to 26/01/93

Dates of Transport	Cell D / E	Cell C	Cell B	Cell A
	Transport Rate (m^3)	Transport Rate (m^3)	Transport Rate (m^3)	Transport Rate (m^3)
Transport Rates per Tidal Cycle				
23/01/93 (am)	-6	-5.7	-5.1	-4.2
23/01/93 (pm)	-101.2	-88.9	-72.8	-52
24/01/93 (am)	-71.3	-67	-59.8	-49.1
24/01/93 (pm)	-193.8	-164.3	-130.2	-89
25/01/93 (am)	-97.8	-61.8	-23.1	16.4
25/01/93 (pm)	-5.4	-5.1	-4.4	-3.4
Summed Daily Transport Rates				
23/01/93	-107	-95	-78	-56
24/01/93	-265	-231	-190	-138
25/01/93	-103	-67	-28	+13
Total Transport During Experiment				
23 - 25/01/93	-476	-393	-295	-181

where, (a) -ve rates indicate transport from west to east; (b) location of cells is shown in Figure 5.3.

Table 5.4. Longshore Transport Rates calculated using the "Delft" formula and wave model output.

Date / Time of Searching	Aluminium Pebbles Recovery (%)	Electronic Pebbles Recovery (%)	Cum. Recovery (%) (Electronic pebbles)
24/01/93 (am)	43	90	90
24/01/93 (pm)	26	80	100
25/01/93 (pm)	49	86	88
25/01/93 (am)	no search	69	94
26/01/93 (pm)	42	88	100

Table 5.5. Recovery Rates of Tracers, Long Beach, Whitstable: 23/01/93 to 26/01/93.

Tracer Sub-group	24/01/93 (am)		24/01/93 (pm)		25/01/93 (am)		25/01/93 (pm)		26/01/93 (am)	
	X[c]	Y[c]	X	Y	X	Y	X	Y	X	Y
All [a]	-19.15	-0.57	-18.75	0.74	-19.42	2.47	0.26	0.88	-1.18	1.03
All (cum)	-19.15	-0.57	-37.90	0.17	-57.32	2.64	-57.06	3.52	-58.24	4.56
Prmove [a]	-34.05	-0.57	-22.15	0.72	-27.85	3.58	0.17	1.88	-2.40	1.58
Prmove (cum)	-34.05	-0.57	-56.20	0.16	-84.05	3.74	-83.88	5.62	-86.28	7.20
Prpmove [a]	0.00	0.00	-18.38	-0.13	-27.85	3.58	0.17	1.88	-2.40	1.58
Prfmove [a]	-34.05	-0.57	-26.68	1.74	na	na	na	na	na	na
Promove [a]	-34.05	-0.57	-28.58	1.36	-32.48	3.79	na	na	na	na
Aluminium	-10.54	0.87	-22.82	3.22	-3.51	0.05	*	*	-12.5[b]	2.15[b]

where, (a) tracer sub-groups are defined in the section 5.4.3; (b) displacement over two tides; (c) x and y are the longshore and on-offshore displacements of the tracers (see Figure 5.3), and; -ve rates represent transport from west to east.

Table 5.6. Displacement of tracer pebbles, Long Beach, Whitstable: 23/01/93 to 26/01/93.

	24/01/93	24/01/93	25/01/93	25/01/93	26/01/93
Mobile Layer Depth (n)	0.15 [a]	0.12	0.16	0.10	0.09
Mobile Layer Width (m)	20.0	24.0	24.8	29.4	21.6
Volume Mobile Layer	3.00	2.88	3.97	2.94	1.94

where, (a) estimated mobile layer based on wave height (see section 5.4.4).

Table 5.7. Estimation of extent of mobile layer, Long Beach, Whitstable: 23/01/93 to 26/01/93.

	24/01/93	24/01/93	25/01/93	25/01/93	26/01/93
Qt (All)	-57.5	-54.0	-77.1	0.8	-2.3
Qt (Prmove)	-102.2	-63.8	-110.6	0.5	-4.7
Qt (Prpmove)	na	-52.9	na	na	na
Qt (Prfmove)	-102.2	-76.8	na	na	na
Qt (Promove)	-102.2	-82.3	-129.0	na	na
Qt (Aluminium)	-31.6	-65.7	-13.9	-30.5 [a]	

where, (a) transport rate over two tides, and; -ve rates represent transport from west to east.

Table 5.8. Longshore transport rates based on displacement of tracer pebbles, Long Beach, Whitstable: 23/01/93 to 26/01/93.

Profile / Cell Reference No.		Date of Surveying, (all morning low water surveys)			
		23/01/93	24/01/93	25/01/93	26/01/93
Profile [a]		Profile Cross Sectional Area (m^2)			
Profile 1		95.83	95.81	92.04	91.67
Profile 2		86.49	91.38	91.92	91.03
Profile 3		85.26	89.23	87.28	86.75
Profile 4		112.34	110.28	114.75	114.50
Profile 5		122.16	122.86	123.73	120.51
Profile 6		165.47	167.87	169.67	171.12
Profile 7		218.89	219.53	221.82	224.34
Profile 8		280.48	283.16	286.62	287.03
Cell [a]	Width, m	Volume of Beach Material (m^3), change from previous survey in brackets			
Cell A	27.5	2507	2574 (67)	2529 (-44)	2512 (-17)
Cell B	35.5	3507	3541 (34)	3586 (45)	3572 (-14)
Cell C	50.5	7262	7341 (79)	7708 (67)	7364 (-45)
Cell D	40	7687	7748 (61)	7830 (82)	7909 (79)
Cell E	40	9987	10054 (66)	10169 (115)	10227 (59)

where, (a) profile and cell locations are shown on Figure 5.3.

Table 5.9. Beach Profile Cross Section Areas and Volumetric Changes, Long Beach, Whitstable: 23/01/93 to 26/01/93.

Dates of Surveying	Cell E		Cell D		Cell C		Cell B		Cell A	
	Drift (m^3)	δVol (m^3)	Drift (m^3)	δVol (m^3)	Drift (m^3)	δVol (m^3)	Drift (m^3)	δVol (m^3)	Drift (m^3)	δVol (m^3)
23-24/01/93	307(E)	+66	241(E)	+61	180(E)	+79	101(E)	+34	67(E)[a]	+67
24-25/01/93	265(E)	+115	150(E)	+82	68(E)	+67	1(E)	+45	44(W)	-44
25-26/01/93	62(E)	+59	3(E)	+79	76(W)	-45	31(W)	-14	(17W)	-17

where, (a) (E) represents transport rate towards the east, and (W) vice versa, and; profile and cell locations are shown on Figure 5.3.

Table 5.10. Longshore Transport rates based on beach volumetric changes, Long Beach, Whitstable: 23/01/93 to 26/01/93.

	23/01/93 (am)		23/01/93 (pm)		24/01/93 (am)		24/01/93 (pm)		25/01/93 (am)		25/01/93 (pm)		26/1/93
	LW	HW	LW	HW	LW	HW	LW	HW	LW	HW	LW	HW	LW
Tides from Injection	I	I+1		I+2		I+3		I+4		I+5		I+6	
Wind Direction / Speed, Borstal Hill	SSW, 5ms^{-1}		SSW, 5ms^{-1}		SSW, 12ms^{-1}		W to NW, 10ms^{-1}		NW to N, 7ms^{-1}		SW to W, 4ms^{-1}		SW, 5ms^{-1}
High Water Level (m AOD) / Time, Whitstable Harbour		+2.4 1330		+1.6 0120 [a]		+2.7 1410		+2.8 0120 [a]		+3.6 1420		+2.4 0220 [a]	
Wave Conditions, Whitstable Harbour,		Hs, 0.2m Tz, 4.5s		Hs, 1.1m Tz, 3.3s		Hs, 1.0m Tz, 3.4s		Hs, 1.1m Tz, 3.5s		Hs, 0.7m Tz, 4.0s		Hs, 0.3m Tz, 2.8s	
Wave Conditions, Long Beach, (Pressure Sensor)		Hs, 0.14 Tp, 8.5s		Hs, 0.6m Tp, 3.7s		Hs, 0.5m Tp, 3.7s		Hs, 0.8m Tp, 4.2s		Hs, 0.7m Tp, 4.1s		na	
Visually Observed Wave Conditions, Long Beach		Hb, 0.2m ∝, varies		Hb, na ∝, -30°		Hb, 0.6m ∝, -30°		Hb, na ∝, -20°		Hb, 0.8 ∝, varies		na	
Wave Model Results, Long Beach		Hs, 0.2m Tp, 2.4s		Hs, 0.5m Tp, 3.1s		Hs, 0.6m Tp, 3.4s		Hs, 0.6m Tp, 3.3s		Hs, 0.8m Tp, 3.9s		Hs, 0.2m Tp, 2.2s	
Electronic Tracers[b]	inject 17		no move		90%		80%		86%		63%		88%
Aluminium Tracers[b]	inject 60		no move		43%		26% inject 20		49%		no search		42%
Painted Pebble Cores			install		recover, abandon								
Beach Plan Survey	1				2				3				4

where, (a) Time of High Water is on the day after recording commenced; (b) % recovery of tracers for each search is shown.

Table 5.11. Summary of Data collected during field experiment at Long Beach, Whitstable: 23/01/93 to 26/01/93

Date of Recording / Technique Used	Part of Experimental Beach (See Figure 5.3)				
	Cell E	Cell D	Cell C	Cell B	Cell A
Delft Formula and Wave Conditions[a]	Based Upon Wave Model Output Calibrated by Wave Records				
23/01/93 am (I +1)[b]	-6[c]		-5.7	-5.1	-4.2
23/01/93 pm (I + 2)	-101.2		-88.9	-72.8	-52
24/01/93 am (I + 3)	-71.3		-67	-59.8	-49.1
24/01/93 pm (I + 4)	-193.8		-164.3	-130.2	-89
25/01/93 am (I + 5)	-97.8		-61.8	-23.1	16.4
25/01/93 pm (I + 6)	-5.4		-5.1	-4.4	-3.4
Electronic Tracer Displacement	Based upon Prmove[d] (and Promove in brackets) Sub-groups of Tracers				
23/01/93 pm (I + 1)	negligible tracer displacement / mobile layer depth				
24/01/93 am (I + 2)	-102.2 (-102.2)			na	
24/01/93 pm (I + 3)	-63.8 (-82.3)			na	
25/01/93 am (I + 4)	-110.6 (-129.0)			na	
25/01/93 pm (I + 5)	na			+0.5	
26/01/93 am (I+ 6)	na			-4.7	
Beach Profile Analysis	Based on Volumetric Changes from Beach Plan Surveys				
23 to 24/01/93 (I + 1 & I + 2)	-307	-241	-180	-101	-67
24 to 25/01/93 (I + 3 & I + 4)	-265	-150	-68	-1	+44
25 to 26/01/93 (I + 5 & I + 6)	-62	-3	+76	+31	+17

where, (a)wave conditions are from coastal model; (b) (I + n) refers to the number of the High Waters or Low Waters following tracer Injection, see Table 5.11; (c) (-ve) rates represent transport from west to east; (d) for sub-group definitions see Section 5.4.3, and; all transport rates are in m^3.

Table 5.12. Comparison of longshore transport rates determined for Long Beach, Whitstable: 23/01/93 to 26/01/93.

Date of Recordings	Method of Estimation Used / Transport Volume (m^3)		
Daily Transport Rates	Model Results	Electronic Tracers	Volumetric Changes
23 to 24/01/93 (I + 1 & I + 2)	-107	-102	-274
24 to 25/01/93 (I + 3 & I + 4)	-265	-211	-208
25 to 26/01/93 (I + 5 & I + 6)	-103	na	-33
Cumulative Transport Rates	Model Results	Electronic Tracers	Volumetric Changes
23 to 24/01/93 (I + 1 & I + 2)	-107	-102	-274
23 to 25/01/93 (I + 1 to I + 4)	-372	-313	-482
23 to 26/01/93 (I + 1 to I + 6)	-475	na	-515

where, (-ve) rates represent transport from west to east.

Table 5.13. Summary of longshore transport rates determined for Long Beach, Whitstable: 23/01/93 to 26/01/93.

Unit / Subunit	Coastal Orientation (° turned clockwise from east - west - see Section 5.7 for details)								
	-20	-15	-10	-5	0	5	10	15	20
1A Seasalter	-2050	-1450	-800	-50	650	1250	1900	2500	3000
1B Whitstable	-4300	-2200	-50	2100	4100	5900	7800	9000	10000
2 Tankerton	-9900	-6150	-2300	1500	5300	9050	12650	15550	18000
3 Studd Hill	-7450	-5050	-2550	-50	2500	5000	7550	9800	12000
4B Herne Bay	-10050	-6850	-3550	-50	3350	6700	10000	12750	15050
5 East Cliff	-9000	-7550	-5000	-2450	0	2450	4950	7500	8500
6A Reculver	-6750	-5050	-3300	-1650	50	1750	3550	5300	7050
6B Northern Sea Wall	-6050	-4450	-2650	-850	950	2700	4450	6050	7600
6C Minnis Bay	-5850	-4200	-2500	-750	1000	2750	4400	6050	7600

where, (a) -ve values represent transport to the east; (b) transport rates are in $m^3 yr^{-1}$, based on wave climate modelled at the beach toe.

Table 5.14. Average annual potential net longshore transport rates for the Study Area.

Unit / Sub-unit (see Figure 3.4)	Location (see Figure 3.4)	Equilibrium Orientation [a]
1A	Seasalter	-4
1B	Whitstable	-10
2	Tankerton	-7
3	Studd Hill	-5
4B	Herne Bay	-5
5	East Cliff	0
6A	Reculver	0
6B	Northern Sea Wall	-2
6C	Minnis Bay	-3

where, (a) equilibrium orientations are angles in degrees (see section 5.7 for details)

Table 5.15. Transport Equilibrium Orientations for beaches in the Study Area.

Time to / from High Water (hrs)	Still Water Level (m, AOD)	Wind Speed (ms^{-1})	Wind Directional Sector[a]	Significant Wave Height (Hs, m)	Wave Period (Tp, s)	Wave Angle ∝ (° relative to E - W)	Transport Quantity ($m^3\ hr^{-1}$)
(a) 1st February 1953							
-4	1.1	21	3/4	.8	5.6	-10	-34
-3	2.5	21	3/4	1.17	5.8	-11	-80
-2	3.6	21	3/4	1.39	5.9	-12	-122
-1	4.4	21	3/4	1.52	6.0	-13	-157
0	4.7	21	3/4	1.58	6.1	-13	-172
1	4.5	21	3/4	1.56	6.0	-13	-165
2	3.7	21	3/4	1.41	5.9	-12	-125
3	3.0	21	3/4	1.29	5.9	-11	-98
4	1.7	21	3/4	.98	5.7	-10	-51
TOTAL							**-1004 m^3 $tide^{-1}$**
(b) 12th December 1990							
-4	1.1	19	1	0.71	4.0	-32	-40
-3	2.0	19	1	0.82	4.2	-34	-58
-2	2.5	19	1	0.98	4.3	-36	-86
-1	2.9	19	1	1.04	4.3	-38	-98
0	3.2	19	1	1.08	4.4	-38	-109
1	3.0	19	1	1.06	4.4	-38	-105
2	2.6	19	1	1.00	4.3	-37	-90
3	1.3	19	1	0.78	4.1	-33	-51
TOTAL							**-637 m^3 $tide^{-1}$**
(c) 20th February 1996							
-3	1.5	18	4/5	.81	6.1	+9	18
-2	2.6	18	4/5	1.06	6.1	+10	35
-1	3.3	18	4/5	1.25	6.2	+10	50
0	3.7	18	4/5	1.34	6.2	+11	66
1	3.4	18	4/5	1.28	6.2	+10	52
2	2.7	18	4/5	1.09	6.1	+10	37
3	1.6	18	4/5	.83	6.1	+9	19
TOTAL							**+277 m^3 $tide^{-1}$**

where, (a) for details of wind directional sector, see Figure 3.4, and; -ve rates represent transport from west to east.

Table 5.16. Longshore transport rates for extreme events at Long Beach, Whitstable: (a) 1st February 1953; (b) 12th December 1990, and (c) 20th February 1996.

September 1995

Beaufort Force	Wind Directional Sector (see Figure 3.4)						
	1	2	3	4	5	6	7
calm	0.00	0.00	0.00	0.00	0.00	0.00	0.00
1-3	0.69	0.83	0.56	0.56	0.14	0.97	0.14
4-6	1.81	1.67	1.25	0.69	0.56	0.83	0.42
7-10	4.58	2.36	4.31	1.81	1.94	1.81	1.67
11-16	2.50	2.36	1.67	1.11	0.56	0.28	1.25
17-21	1.11	1.94	0.14	2.08	0.56	0.00	0.14
22-27	0.00	0.00	0.00	1.11	0.00	0.00	0.00
28-33	0.00	0.00	0.00	0.00	0.00	0.00	0.00
34-40	0.00	0.00	0.00	0.00	0.00	0.00	0.00
41-47	0.00	0.00	0.00	0.00	0.00	0.00	0.00
Totals	10.69	9.17	7.92	7.36	3.75	3.89	3.61

October 1995

Beaufort Force	Wind Directional Sector (see Figure 3.4)						
	1	2	3	4	5	6	7
calm	0.00	0.00	0.00	0.00	0.00	0.00	0.00
1-3	0.67	0.81	0.13	0.40	1.75	2.28	0.27
4-6	0.94	0.54	0.94	0.54	1.21	1.75	1.21
7-10	0.40	0.40	0.27	0.27	0.54	0.13	1.34
11-16	0.13	0.00	0.00	0.00	0.40	0.00	0.00
17-21	0.00	0.00	0.00	0.00	0.00	0.00	0.00
22-27	0.00	0.00	0.00	0.00	0.00	0.00	0.00
28-33	0.00	0.00	0.00	0.00	0.00	0.00	0.00
34-40	0.00	0.00	0.00	0.00	0.00	0.00	0.00
41-47	0.00	0.00	0.00	0.00	0.00	0.00	0.00
Totals	2.15	1.75	1.34	1.21	3.90	4.17	2.82

November 1995

Beaufort Force	Wind Directional Sector (see Figure 3.4)						
	1	2	3	4	5	6	7
calm	0.00	0.00	0.00	0.00	0.00	0.00	0.00
1-3	1.25	0.56	0.14	0.00	0.14	0.14	0.14
4-6	5.00	0.28	0.00	0.00	0.00	0.28	0.42
7-10	2.36	1.53	0.28	0.00	0.28	0.28	0.69
11-16	1.67	4.72	5.69	1.53	0.14	0.00	0.97
17-21	0.00	1.11	0.69	0.28	0.00	0.00	0.14
22-27	0.00	0.14	0.28	0.00	0.00	0.00	0.00
28-33	0.00	0.00	0.00	0.00	0.00	0.00	0.00
34-40	0.00	0.00	0.00	0.00	0.00	0.00	0.00
41-47	0.00	0.00	0.00	0.00	0.00	0.00	0.00
Totals	10.28	8.33	7.08	1.81	0.56	0.69	2.36

Table 5.17. Wind Speed and Direction Occurrences at Manston Airport: (a) September 1995; (b) October 1995, and; (c) November 1995.

December 1995

Beaufort Force	Wind Directional Sector (see Figure 3.4)						
	1	2	3	4	5	6	7
calm	0.00	0.00	0.00	0.00	0.00	0.00	0.00
1-3	1.48	1.88	0.94	0.27	0.81	1.75	0.81
4-6	2.28	0.40	0.00	0.40	1.34	4.57	4.17
7-10	1.21	0.81	0.54	1.88	4.17	3.09	6.85
11-16	0.54	2.82	0.54	1.34	1.88	6.05	8.20
17-21	0.00	0.00	0.00	0.00	0.27	2.42	0.81
22-27	0.00	0.00	0.00	0.00	0.67	1.75	0.00
28-33	0.00	0.00	0.00	0.00	0.00	0.00	0.00
34-40	0.00	0.00	0.00	0.00	0.00	0.00	0.00
41-47	0.00	0.00	0.00	0.00	0.00	0.00	0.00
Totals	5.51	5.91	2.02	3.90	9.14	19.62	20.83

January 1996

Beaufort Force	Wind Directional Sector (see Figure 3.4)						
	1	2	3	4	5	6	7
calm	0.00	0.00	0.00	0.00	0.00	0.00	0.00
1-3	0.54	1.21	0.81	0.67	1.08	0.94	0.40
4-6	0.00	0.00	0.13	0.81	1.48	3.23	1.08
7-10	0.00	0.00	0.00	0.00	2.02	3.63	2.42
11-16	0.00	0.00	0.00	0.00	1.48	12.50	8.60
17-21	0.00	0.00	0.00	0.00	1.61	3.23	0.40
22-27	0.00	0.00	0.00	0.00	0.00	0.00	0.00
28-33	0.00	0.00	0.00	0.00	0.00	0.00	0.00
34-40	0.00	0.00	0.00	0.00	0.00	0.00	0.00
41-47	0.00	0.00	0.00	0.00	0.00	0.00	0.00
Totals	0.54	1.21	0.94	1.48	7.66	23.52	12.90

February 1996

Beaufort Force	Wind Directional Sector (see Figure 3.4)						
	1	2	3	4	5	6	7
calm	0.00	0.00	0.00	0.00	0.00	0.00	0.00
1-3	0.72	2.01	1.01	0.43	0.57	0.57	1.58
4-6	0.72	1.58	1.58	1.15	1.44	1.15	0.72
7-10	1.15	1.01	3.02	1.15	1.72	0.14	1.01
11-16	2.16	1.15	2.01	2.30	3.59	0.00	0.29
17-21	1.87	0.86	0.57	3.02	0.29	0.00	0.29
22-27	0.00	0.29	2.01	2.01	0.72	0.00	0.00
28-33	0.00	0.00	1.44	2.16	0.86	0.00	0.00
34-40	0.00	0.00	0.00	0.29	0.29	0.00	0.00
41-47	0.00	0.00	0.00	0.00	0.00	0.00	0.00
Totals	6.61	6.90	11.64	12.50	9.48	1.87	3.88

Table 5.17(cont). Wind Speed and Direction Occurrences at Manston Airport: (d) December 1995; (e) January 1996, and; (f) February 1996.

March 1996

Beaufort Force	Wind Directional Sector (see Figure 3.4)						
	1	2	3	4	5	6	7
calm	0.00	0.00	0.00	0.00	0.00	0.00	0.00
1-3	0.27	1.34	1.61	0.67	2.28	2.28	0.94
4-6	1.21	1.61	2.15	2.42	3.49	2.82	1.75
7-10	0.67	0.94	4.97	3.36	4.44	5.65	3.76
11-16	1.08	0.27	2.82	1.75	2.15	2.55	5.65
17-21	0.00	0.00	0.00	0.13	2.28	0.54	0.94
22-27	0.00	0.00	0.00	0.00	0.40	0.54	0.00
28-33	0.00	0.00	0.00	0.00	0.00	0.00	0.00
34-40	0.00	0.00	0.00	0.00	0.00	0.00	0.00
41-47	0.00	0.00	0.00	0.00	0.00	0.00	0.00
Totals	3.23	4.17	11.56	8.33	15.05	14.38	13.04

April 1996

Beaufort Force	Wind Directional Sector (see Figure 3.4)						
	1	2	3	4	5	6	7
calm	0.00	0.00	0.00	0.00	0.00	0.00	0.00
1-3	0.69	2.08	1.11	0.97	0.69	0.42	0.69
4-6	0.97	2.50	1.11	2.08	3.75	1.11	1.67
7-10	0.42	0.42	0.14	3.33	4.58	2.64	0.56
11-16	0.42	0.00	0.42	1.39	5.83	4.17	2.22
17-21	0.00	0.00	0.00	0.00	0.83	0.00	0.00
22-27	0.00	0.00	0.00	0.00	0.00	0.00	0.00
28-33	0.00	0.00	0.00	0.00	0.00	0.00	0.00
34-40	0.00	0.00	0.00	0.00	0.00	0.00	0.00
41-47	0.00	0.00	0.00	0.00	0.00	0.00	0.00
Totals	2.50	5.00	2.78	7.78	15.69	8.33	5.14

Winter Months, (1995 - 1996)

Beaufort Force	Wind Directional Sector (see Figure 3.4)						
	1	2	3	4	5	6	7
calm	0.00	0.00	0.00	0.00	0.00	0.00	0.00
1-3	0.82	1.50	0.93	0.50	0.93	1.02	0.75
4-6	1.68	1.05	0.82	1.14	1.91	2.21	1.64
7-10	0.96	0.77	1.48	1.62	2.87	2.60	2.57
11-16	0.96	1.48	1.89	1.37	2.48	4.26	4.37
17-21	0.30	0.32	0.20	0.55	0.89	1.05	0.43
22-27	0.00	0.07	0.36	0.32	0.30	0.39	0.00
28-33	0.00	0.00	0.23	0.34	0.14	0.00	0.00
34-40	0.00	0.00	0.00	0.05	0.05	0.00	0.00
41-47	0.00	0.00	0.00	0.00	0.00	0.00	0.00
Totals	4.71	5.19	5.92	5.87	9.56	11.52	9.77

Table 5.17(cont). Wind Speed and Direction Occurrences (%) at Manston Airport: (g) March 1996; (h)April 1996, and; (i) summation of winter months (October 1995 - March 1996).

Month / Year	Monthly Transport [a] (m^3)	Cumulative Transport [a] (m^3)
September 1995	-290	-290
October 1995	+63	-227
November 1995	-932	-1158
December 1995	+2157	+999
January 1996	+1691	+2690
February 1996	-1100	+1590
March 1996	+1293	+2883
April 1996	1031	+3914
Net Transport	+3914	+3914

where (a). transport rates based on coastal model and wind data from Manston

Table 5.18. Monthly Variation in Longshore Transport Rates, September 1995 to April 1996 at Long Beach Whitstable.

Figure 5.1. Location of Long Beach Whitstable, site of the shingle transport field studies: 23/01/93 to 26/01/93.

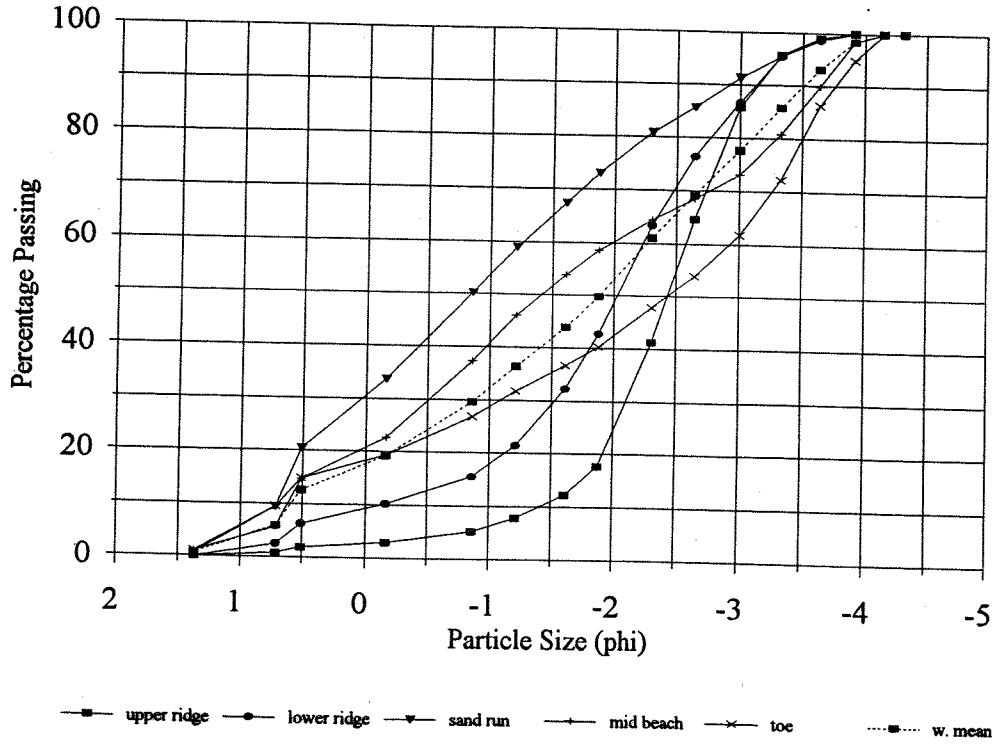

Figure 5.2. Particle size distribution variation along a "Typical" beach profile, Long Beach, Whitstable, 23/01/93.

Figure 5.3. Details of Experimental Set-up, Long Beach, Whitstable: 2301/93 to 26/01/93.

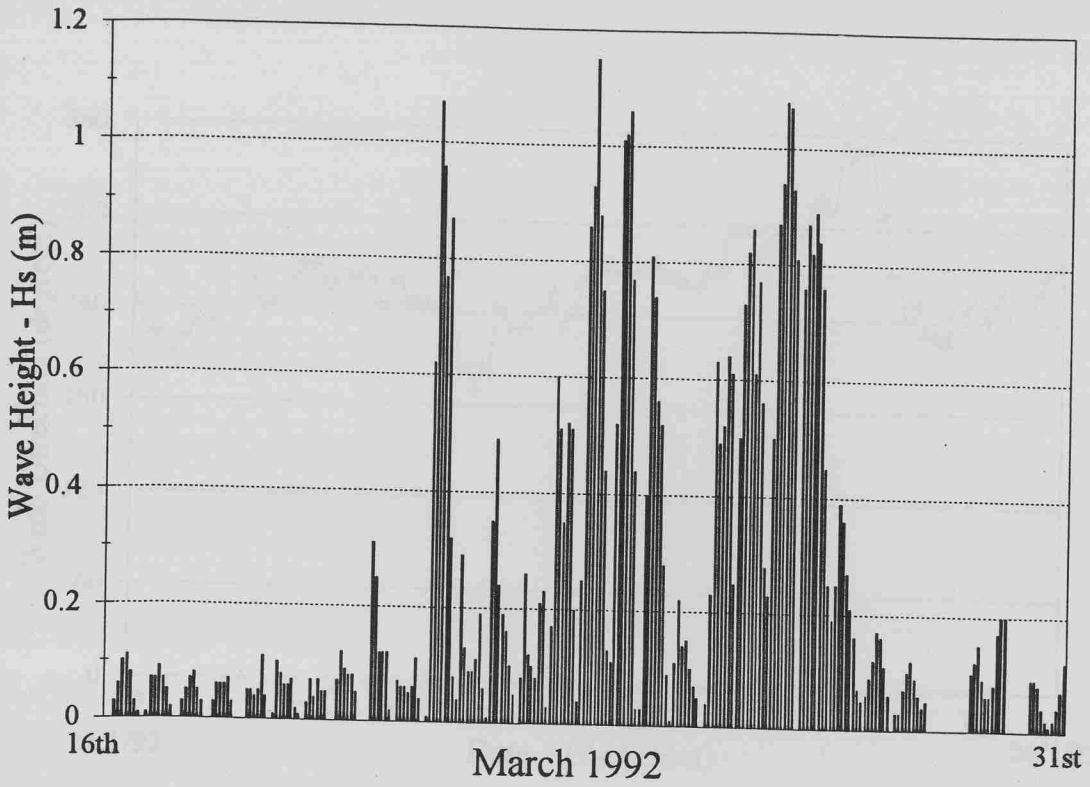

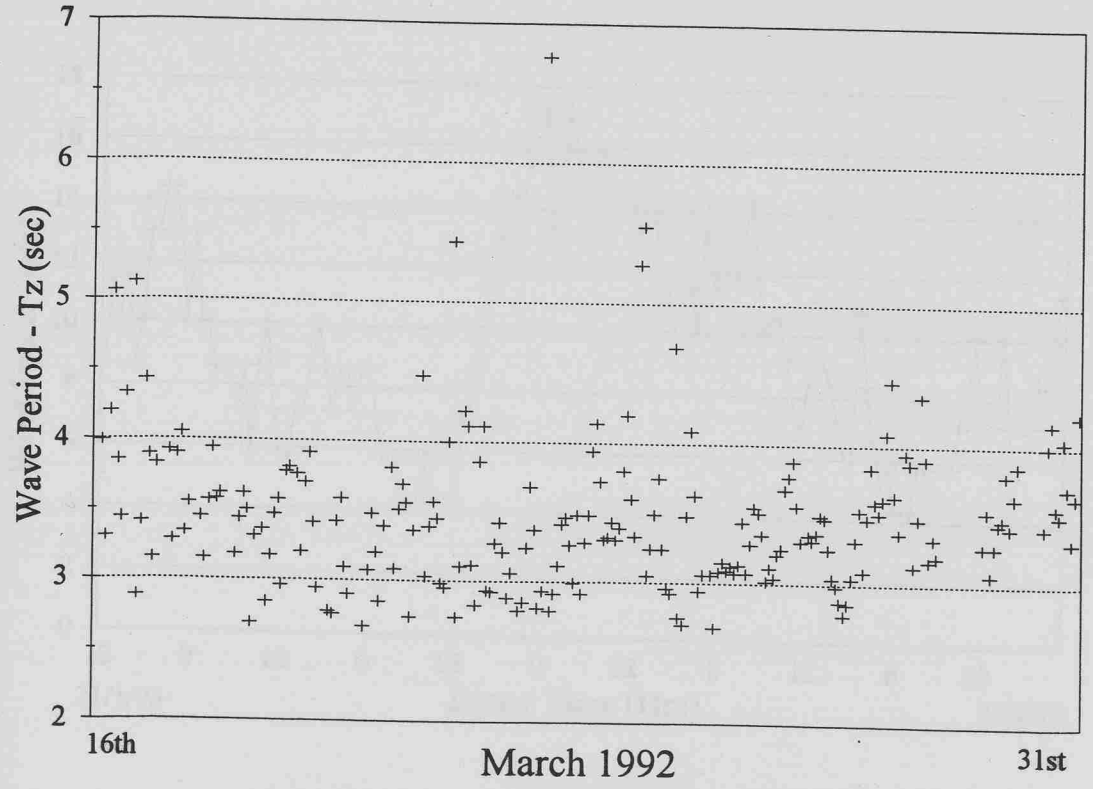

Figure 5.4 (a) Wave Height (Hs) and (b) Wave Period (Tp) data from the Whitstable Harbour wave recorder (see Figure 3.2 for location): 16/03/92 to 31/03/92

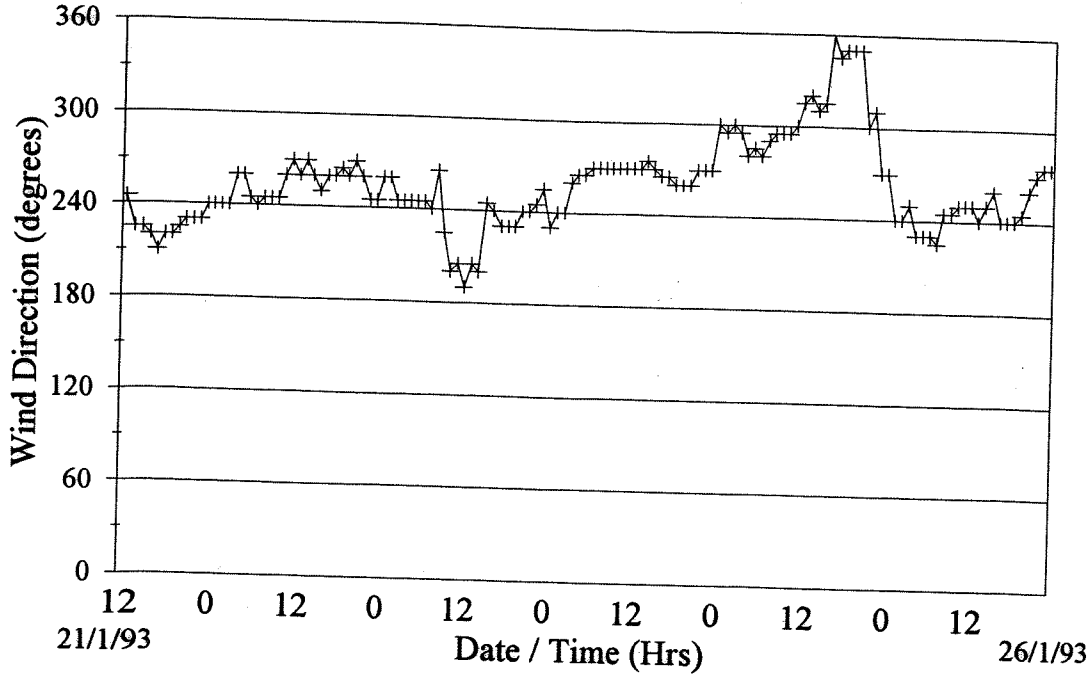

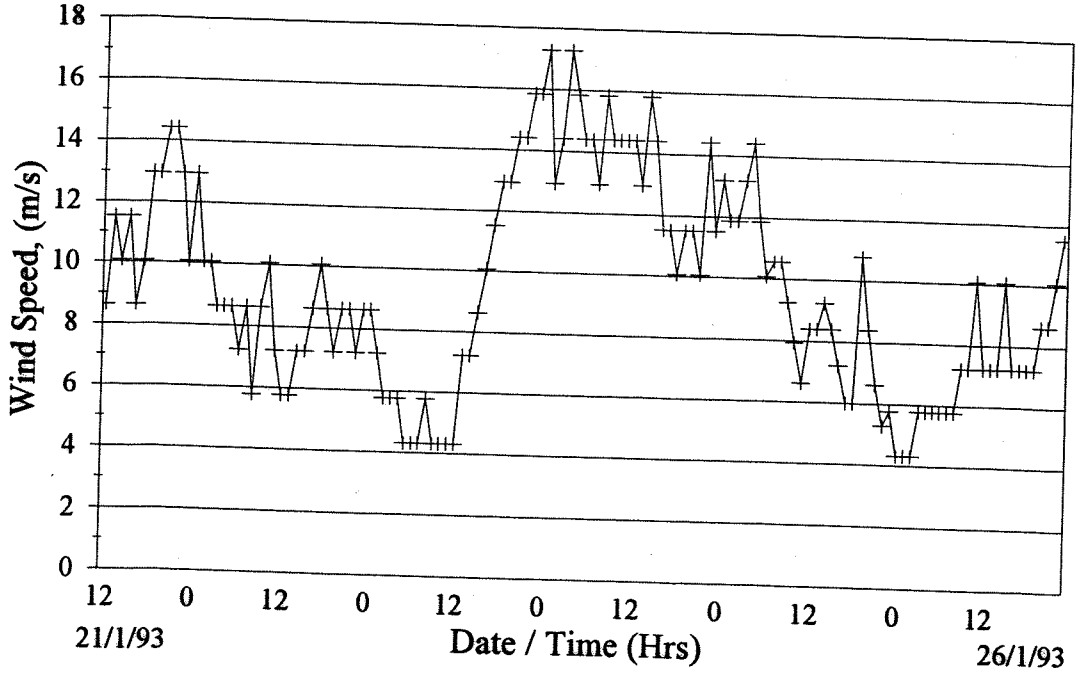

Figure 5.5 Recorded (a) Wind Direction and (b) Wind Speed data collected from Borstal Hill, Whitstable: 22/01/93 to 26/01/93.

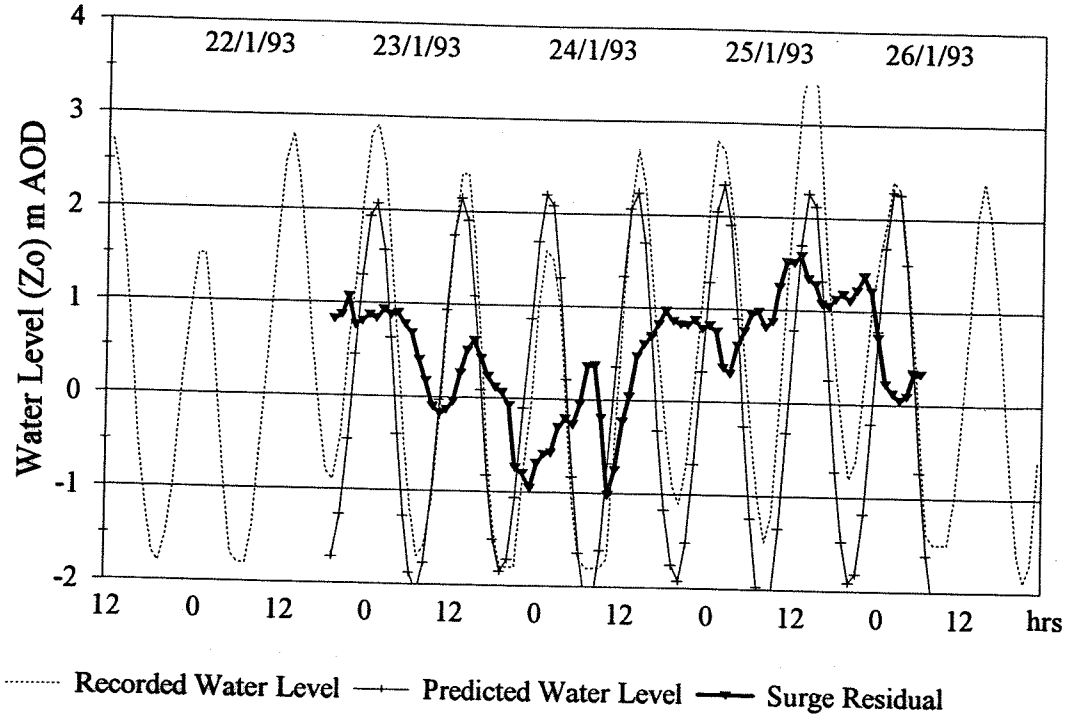

Figure 5.6. Recorded water levels, predicted water levels and the surge residual at Whitstable Harbour: 22/01/93 to 26/01/93.

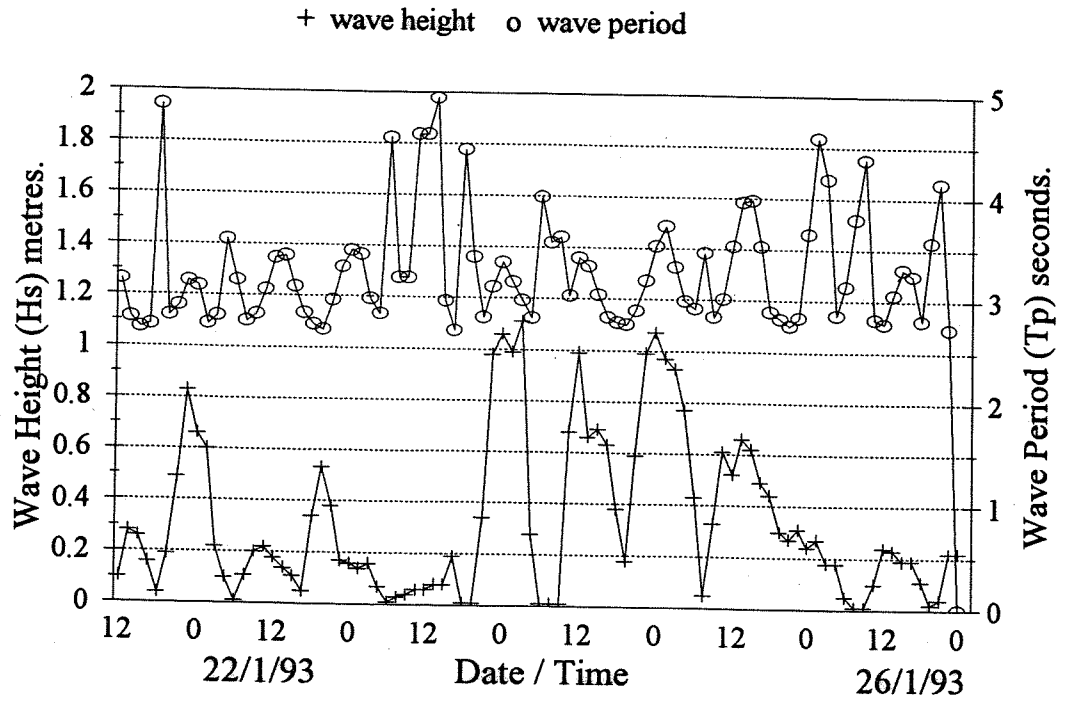

Figure 5.7. Wave Height (Hs) and Wave Period (Tp) data from Whitstable Harbour recorder (see Figure 3.2 for location): 22/01/93 to 26/01/93.

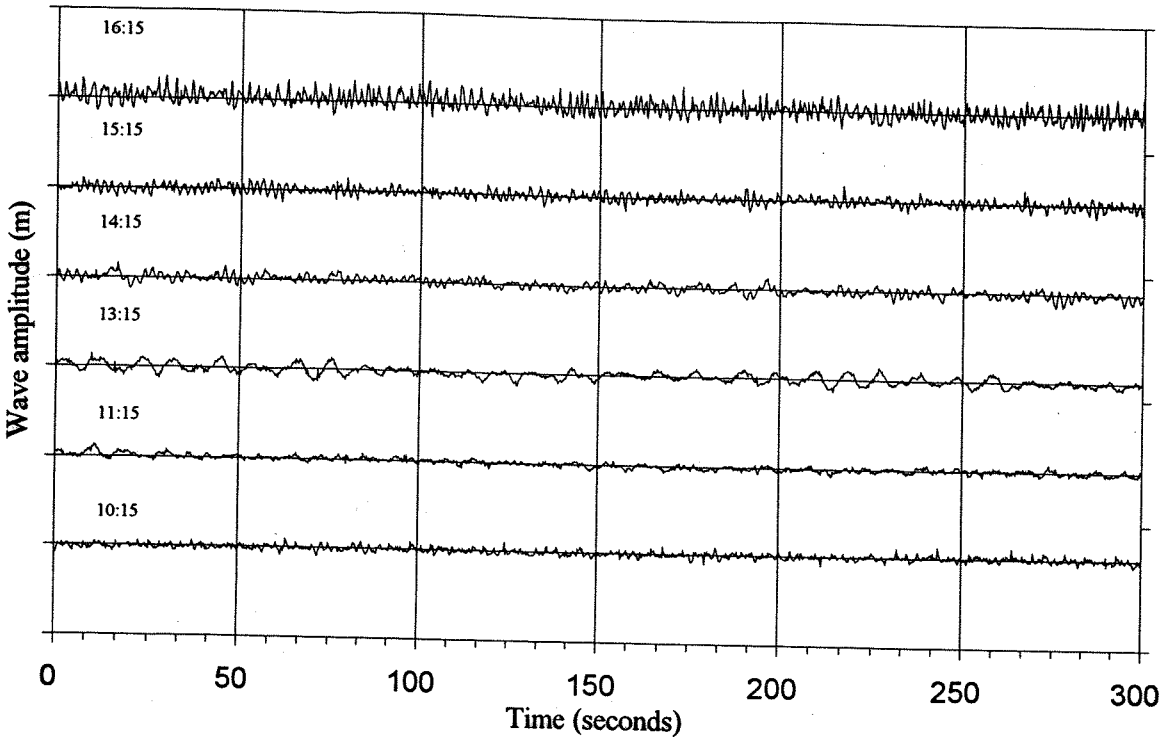

Figure 5.8(a) Time series wave conditions recorded at Long Beach Whitstable: 23/01/93 (am)

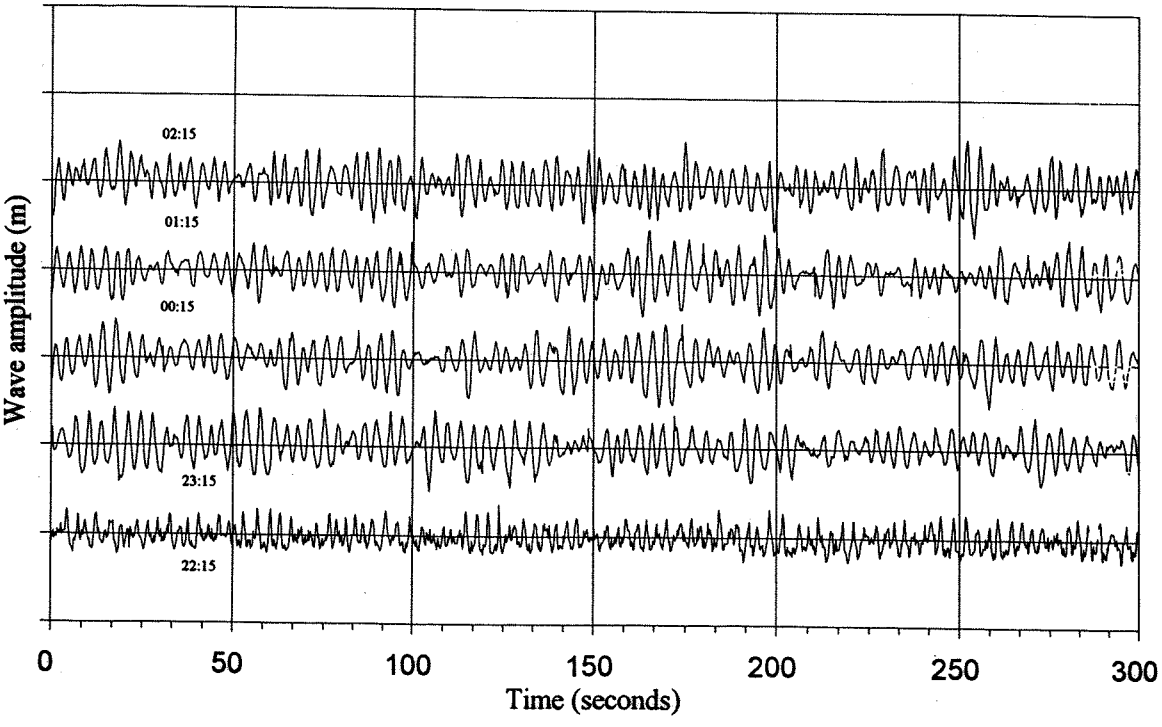

Figure 5.8(b) Time series wave conditions recorded at Long Beach Whitstable: 23/01/93 (pm)

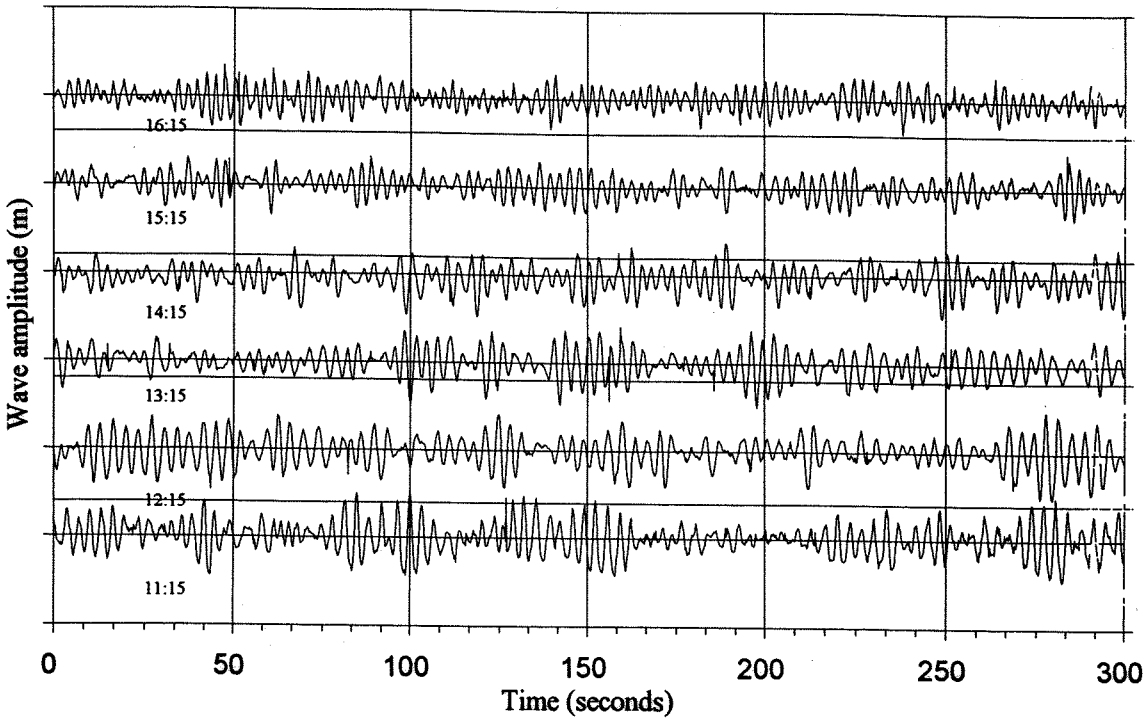

Figure 5.8(c) Time series wave conditions recorded at Long Beach Whitstable: 24/01/93 (am)

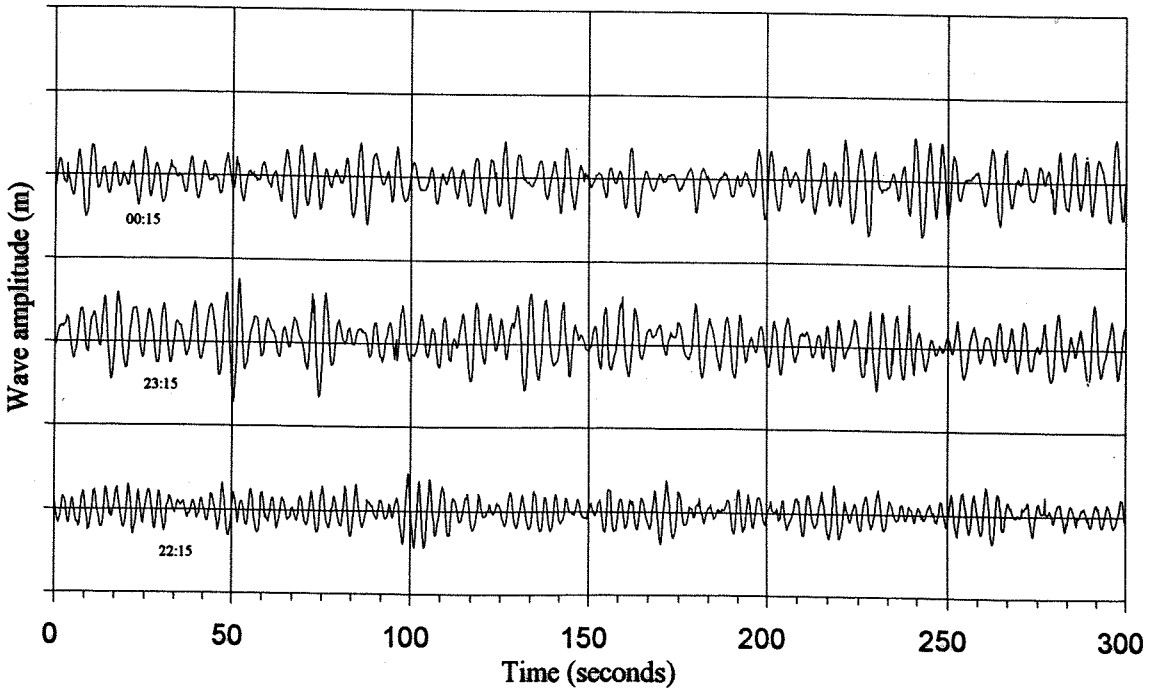

Figure 5.8(d) Time series wave conditions recorded at Long Beach Whitstable: 24/01/93 (pm)

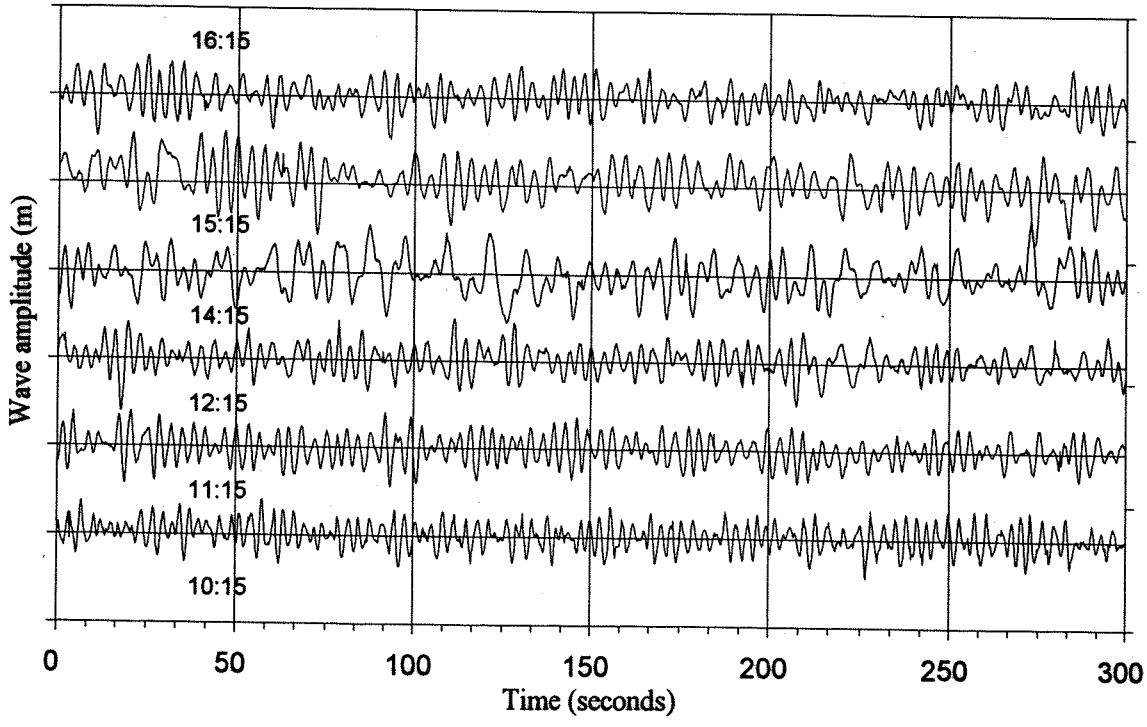

Figure 5.8(e) Time series wave conditions recorded at Long Beach Whitstable: 25/01/93 (am)

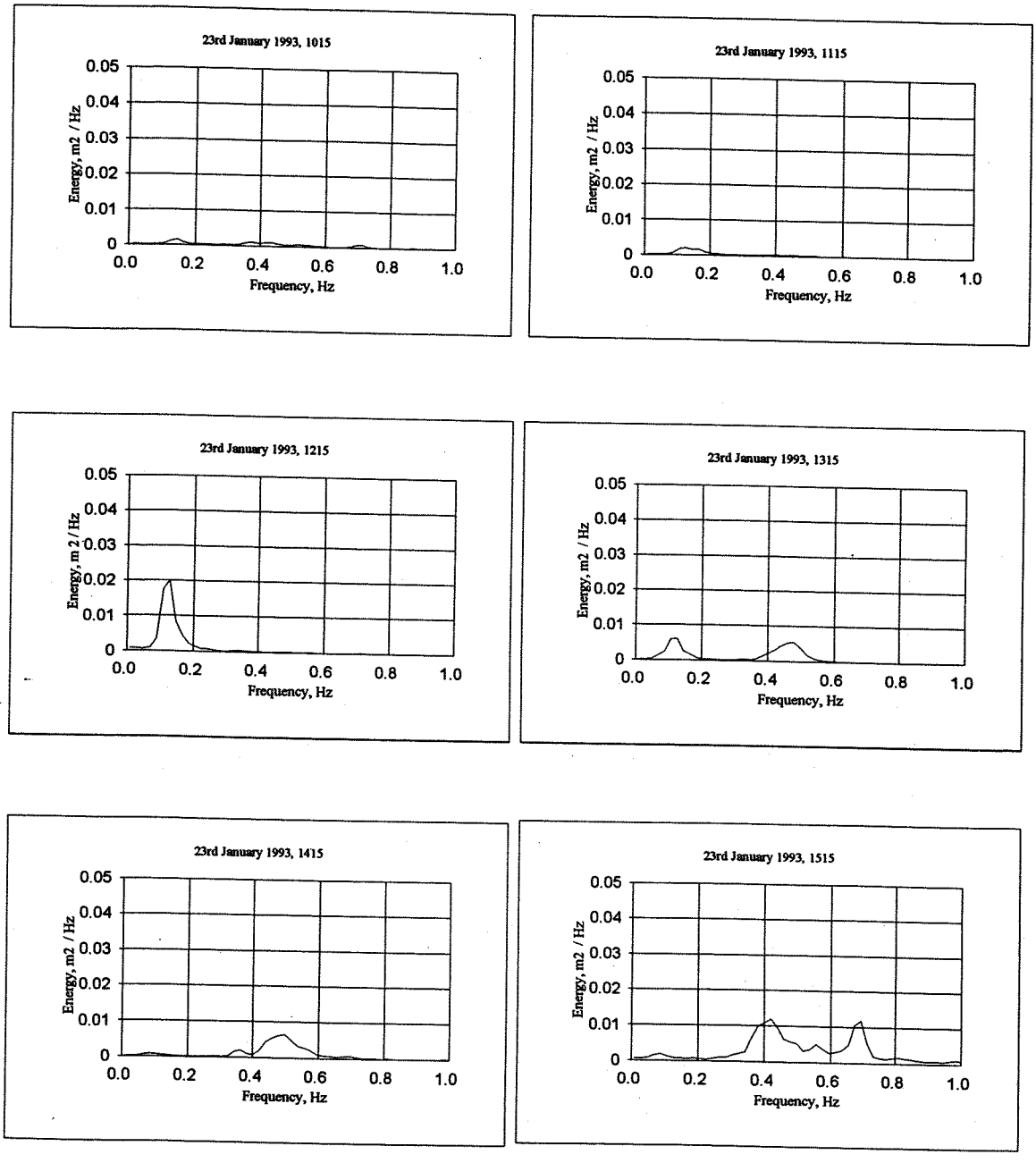

Figure 5.9(a-f). Spectral energy density for wave conditions recorded at Long Beach Whitstable: 23/01/93 (am) (vertical scale exaggerated compared to succeeding graphs)

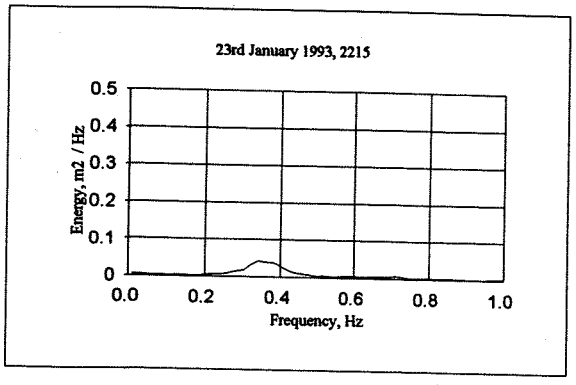

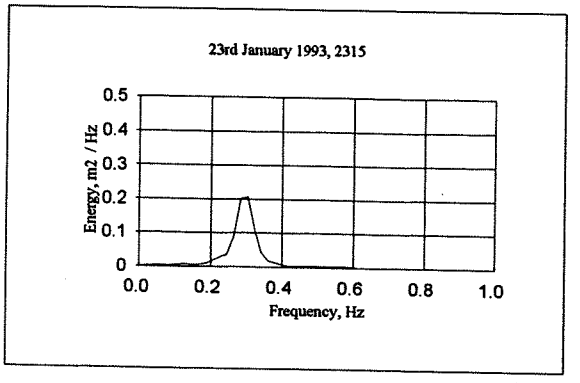

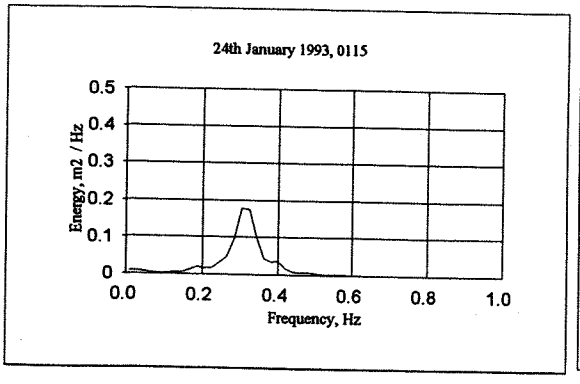

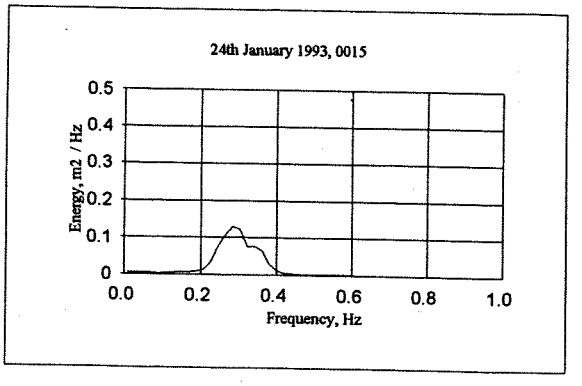

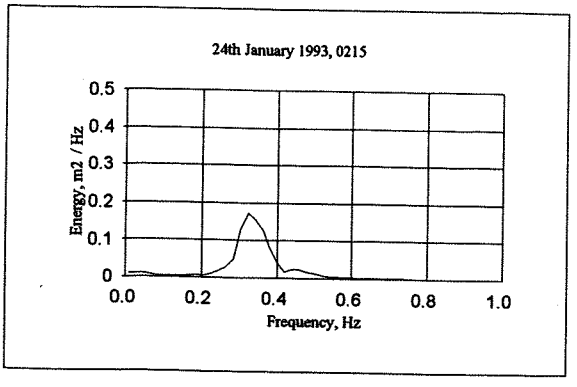

Figure 5.9(g-k). Spectral energy density for wave conditions recorded at Long Beach Whitstable: 23/01/93 (pm)

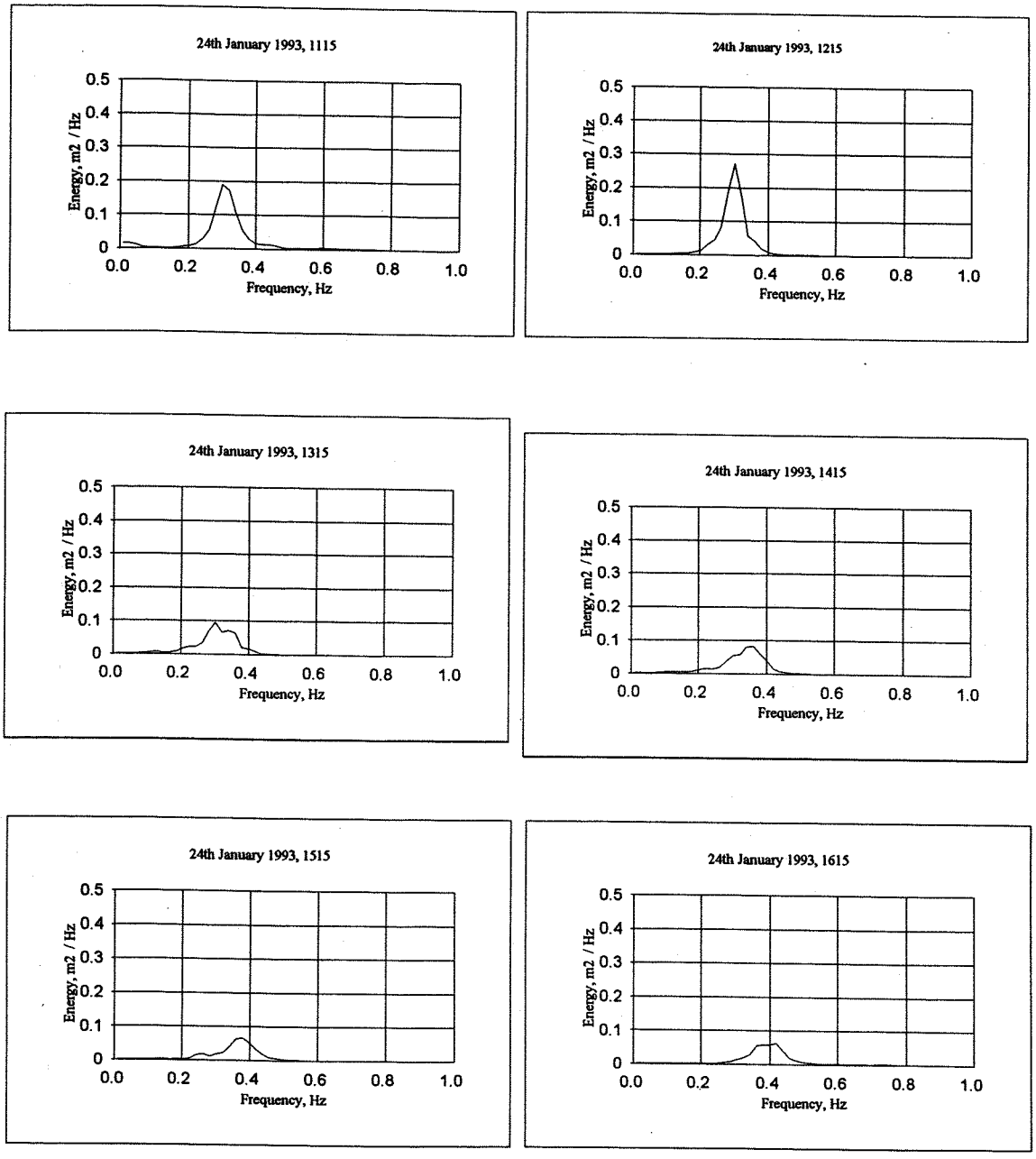

Figure 5.9(l-q). Spectral energy density for wave conditions recorded at Long Beach Whitstable: 24/01/93 (am)

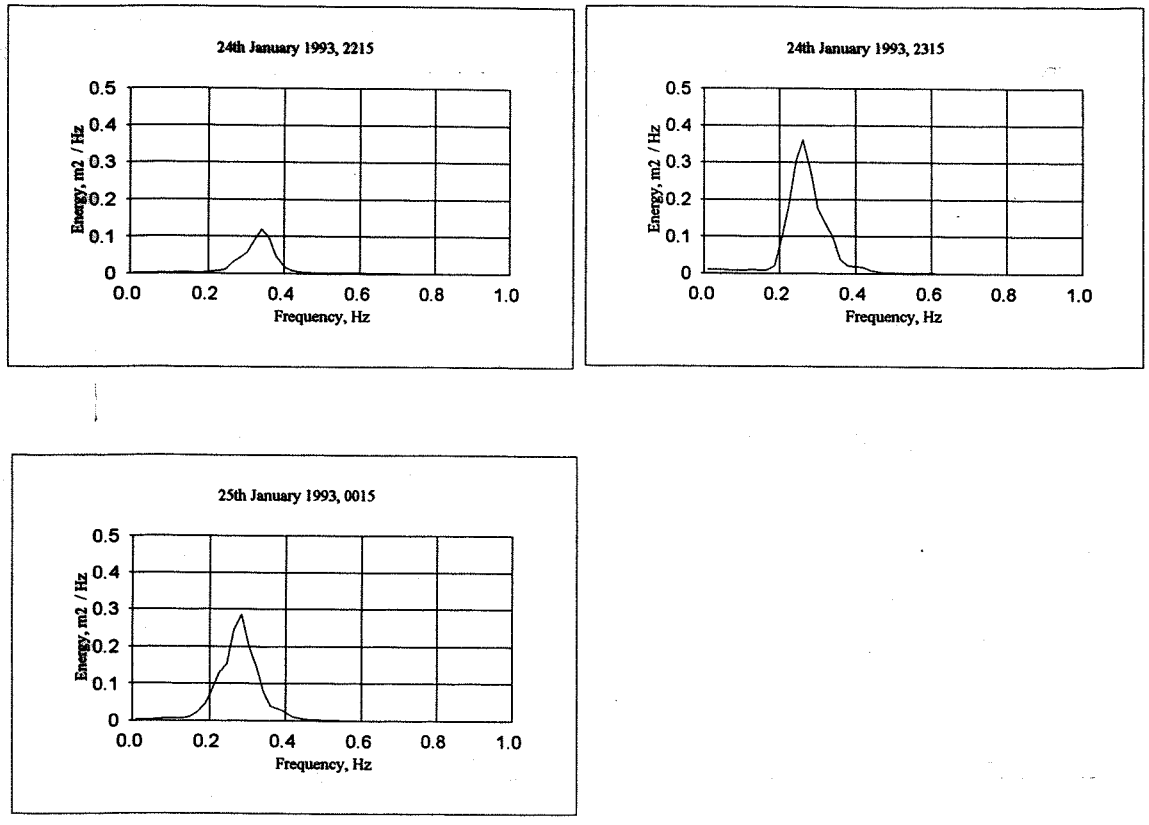

Figure 5.9(r-t). Spectral energy density for wave conditions recorded at Long Beach Whitstable: 24/01/93 (pm)

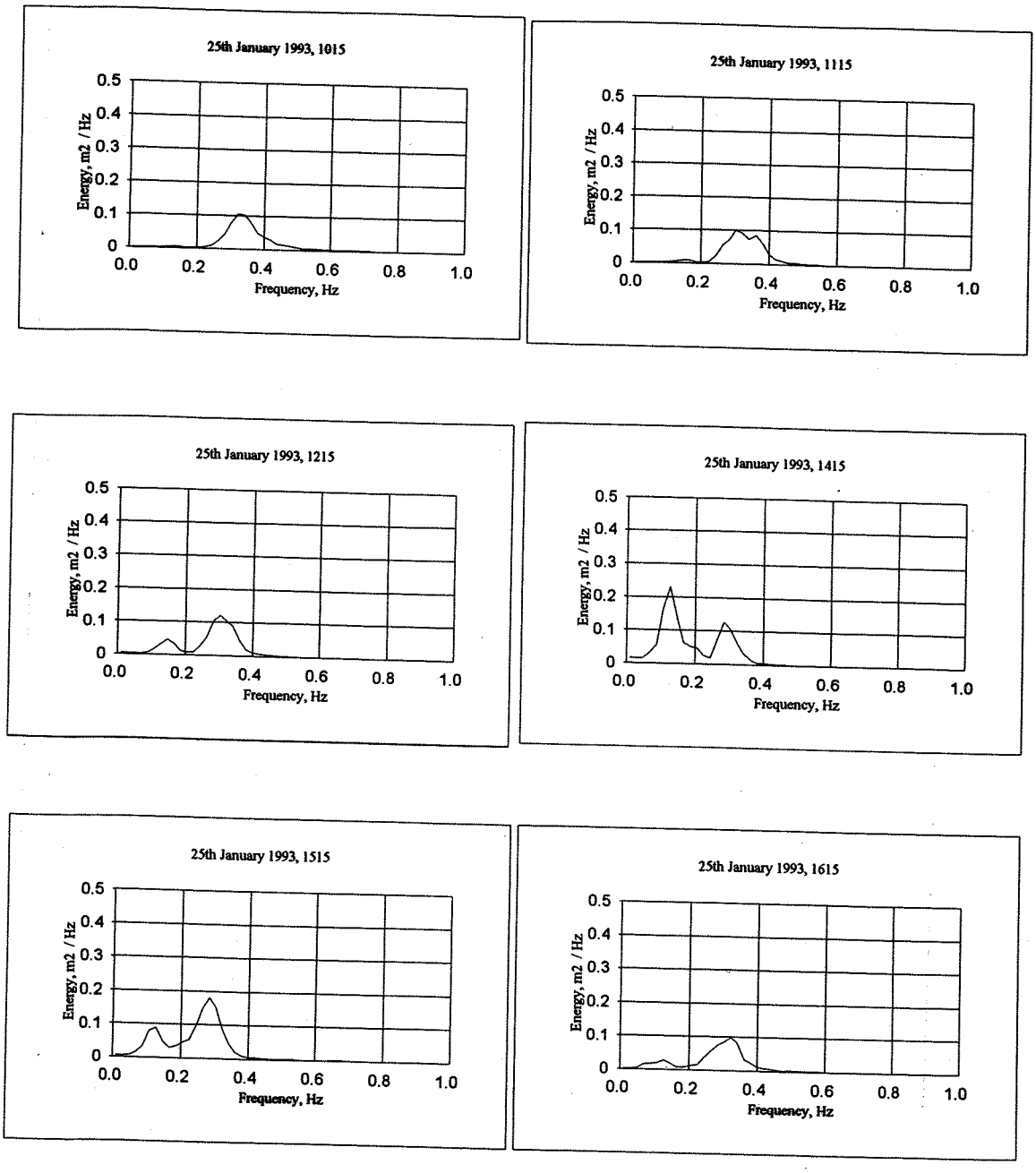

Figure 5.9(u-z). Spectral energy density for wave conditions recorded at Long Beach Whitstable: 25/01/93 (am)

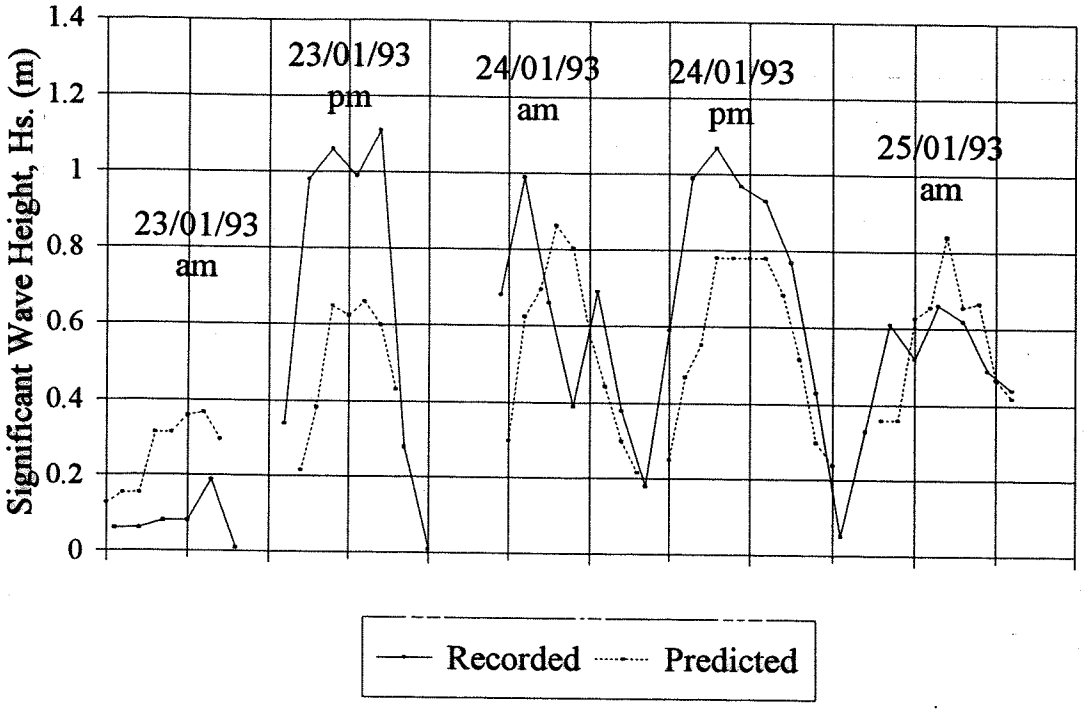

Figure 5.10(a) Comparison of recorded and hindcast significant wave height (Hs, m) at Whitstable Harbour: 23/01/93 to 26/01/93

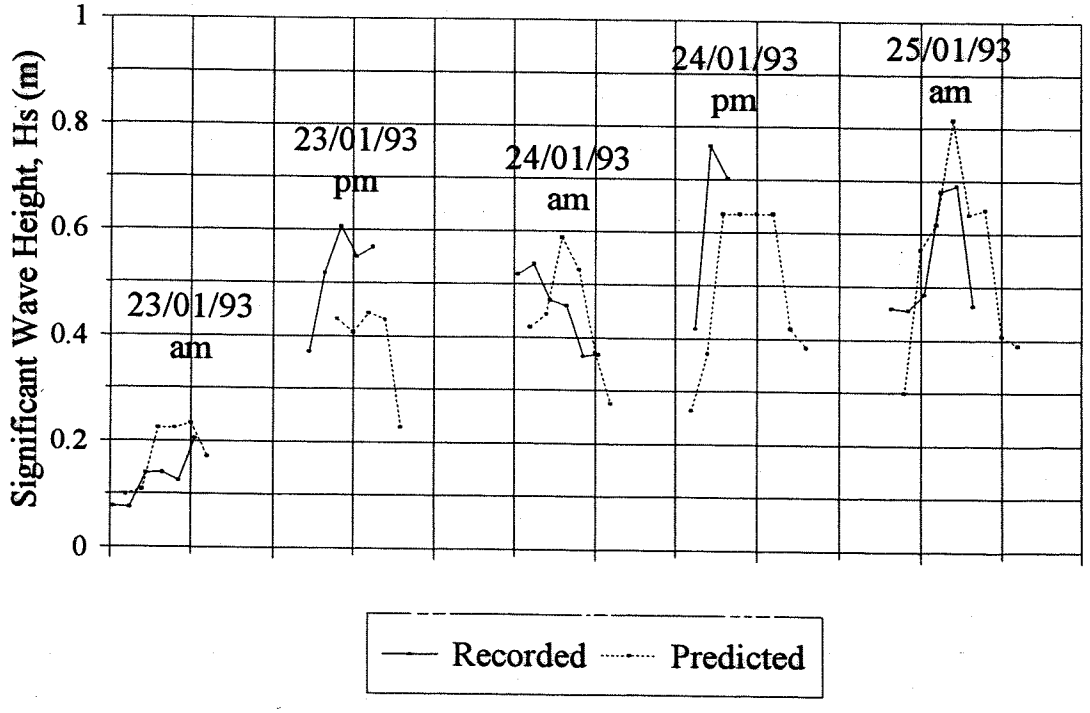

Figure 5.10(b) Comparison of recorded and hindcast significant wave height (Hs, m) at Long Beach, Whitstable: 23/01/93 to 26/01/93

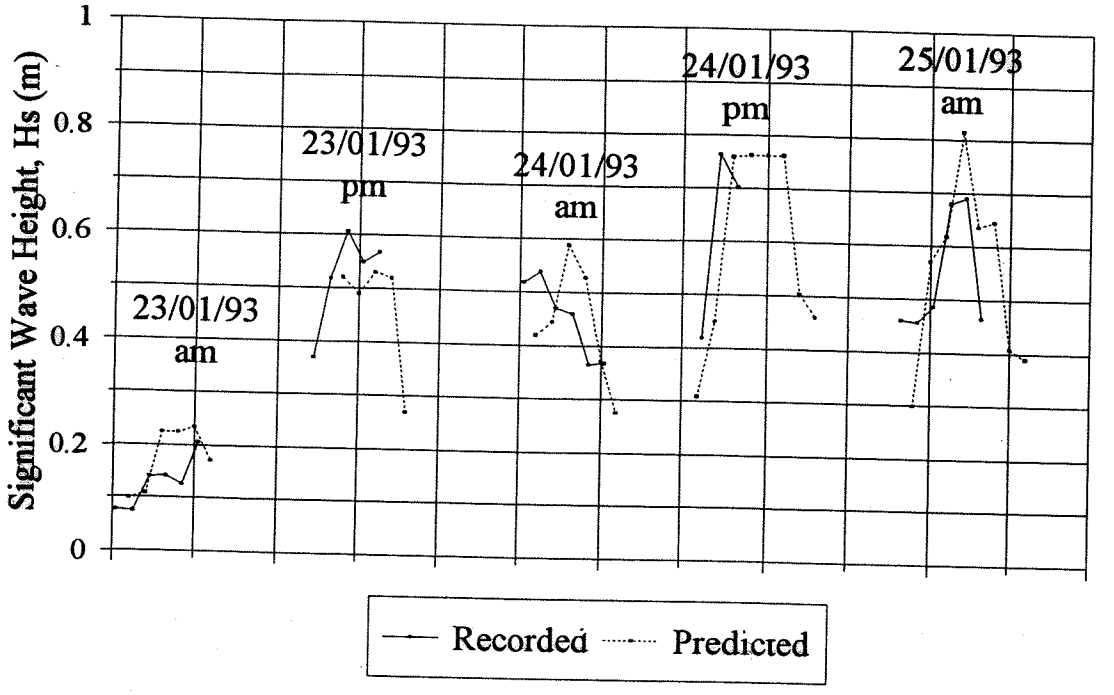

Figure 5.10(c) Comparison of recorded and hindcast significant wave height (Hs, m) at Long Beach, Whitstable: 23/01/93 to 26/01/93 (pm recordings temperature corrected)

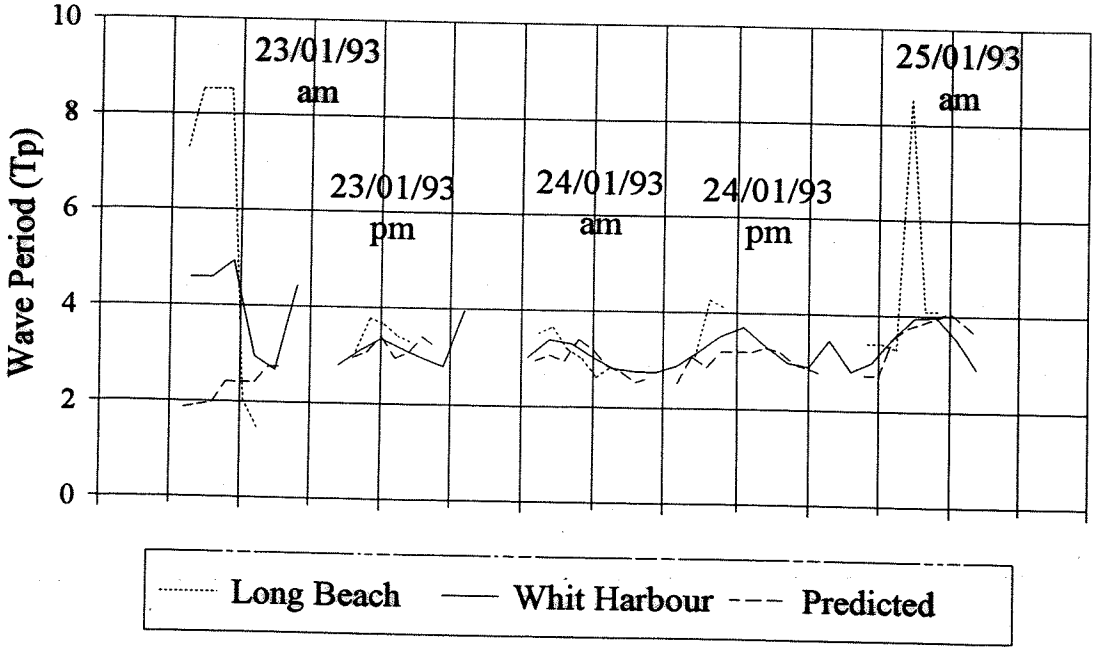

Figure 5.10(d) Comparison of recorded and hindcast wave period (T, s) at Long Beach, Whitstable: 23/01/93 to 26/01/93

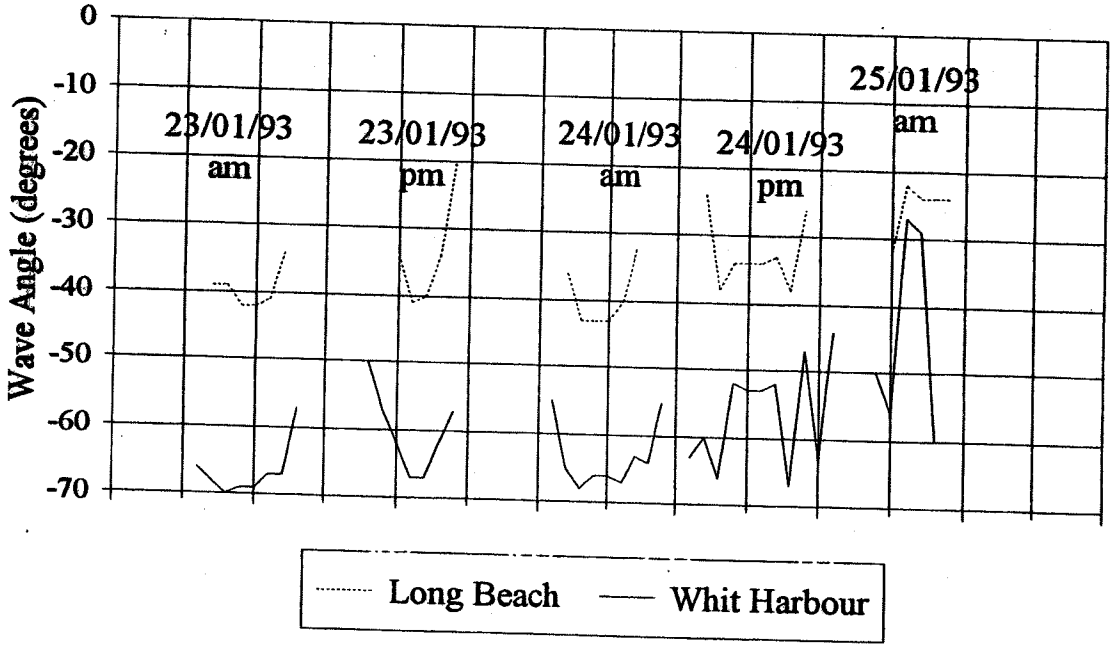

Figure 5.10(e) Comparison of hindcast wave angle (∝, °) at Long Beach, Whitstable and at the wave recorder site, Whitstable Harbour: 23/01/93 to 26/01/93

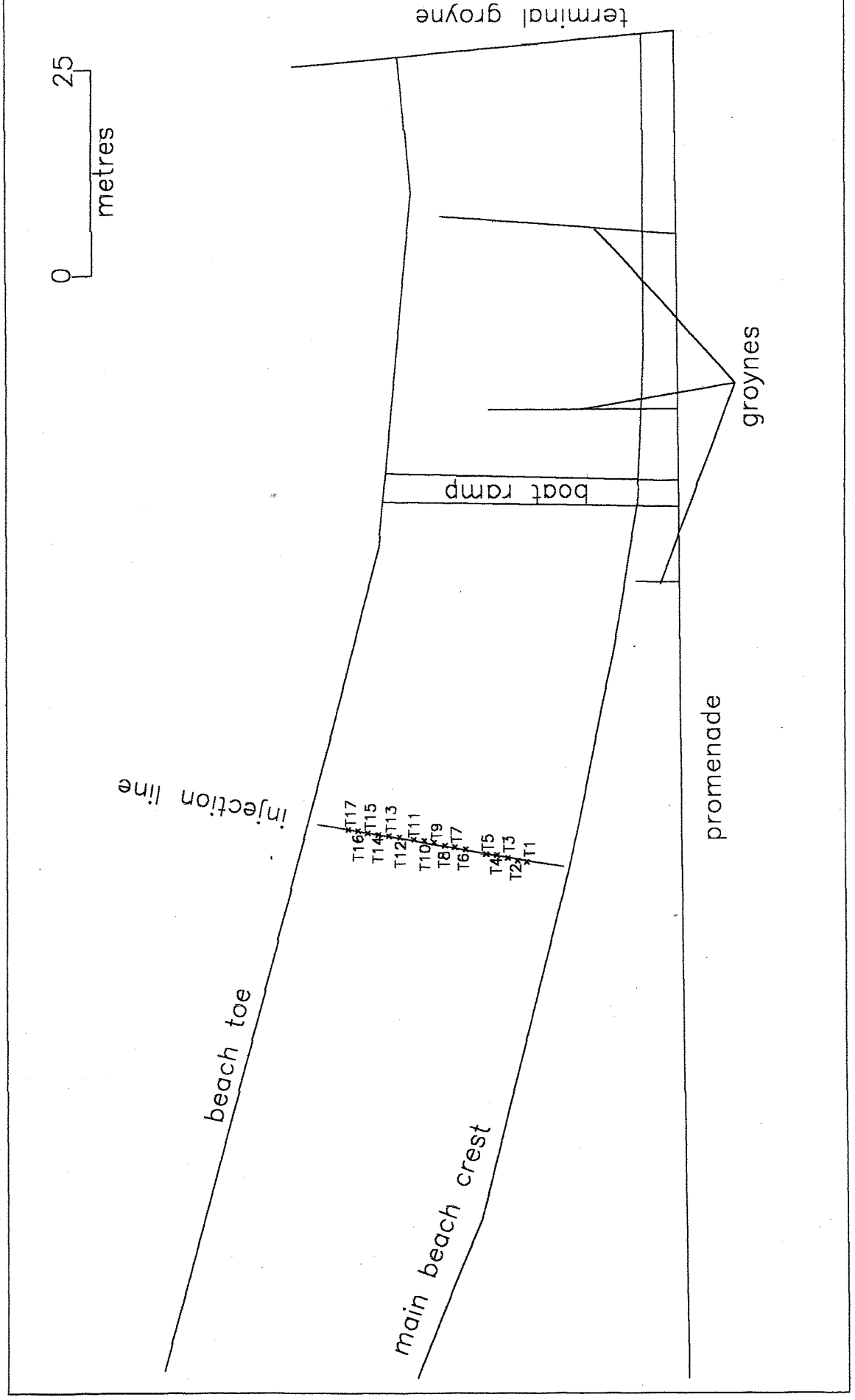

Figure 5.11(a) Location of electronic tracer pebbles at Long Beach, Whitstable: 23/01/93 (am)

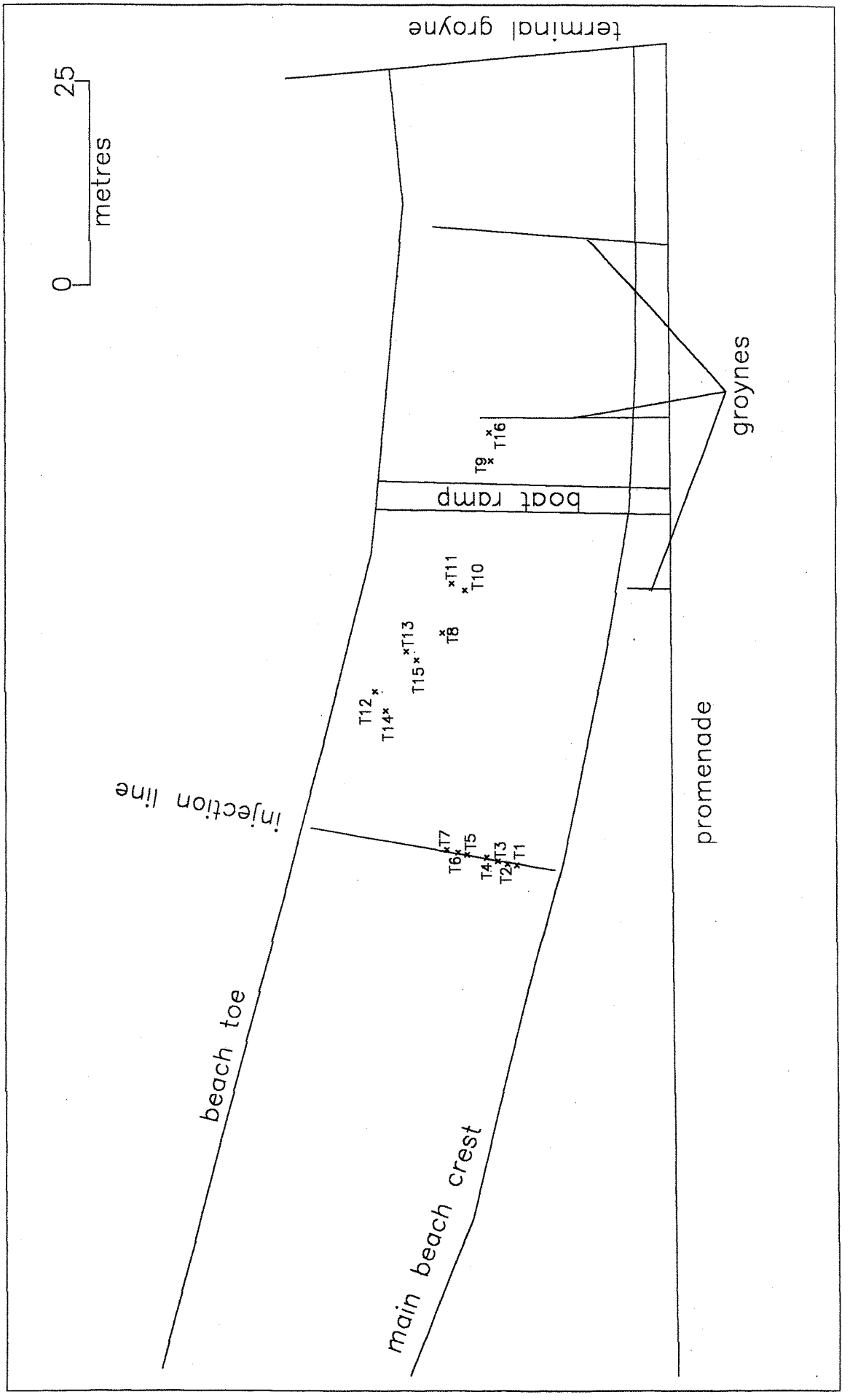

Figure 5.11(b) Location of electronic tracer pebbles at Long Beach, Whitstable: 24/01/93 (am)

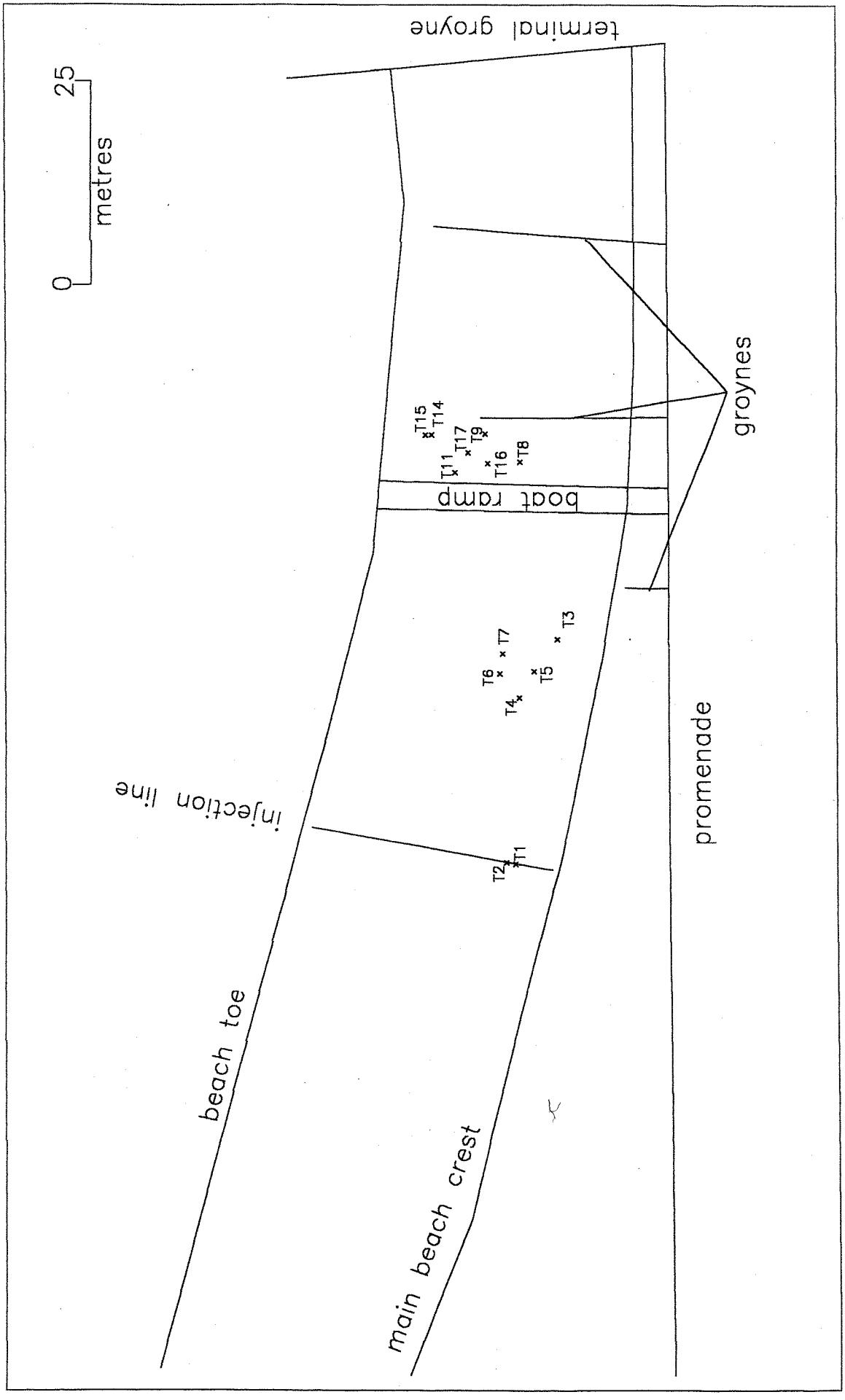

Figure 5.11(c) Location of electronic tracer pebbles at Long Beach, Whitstable: 24/01/93 (pm)

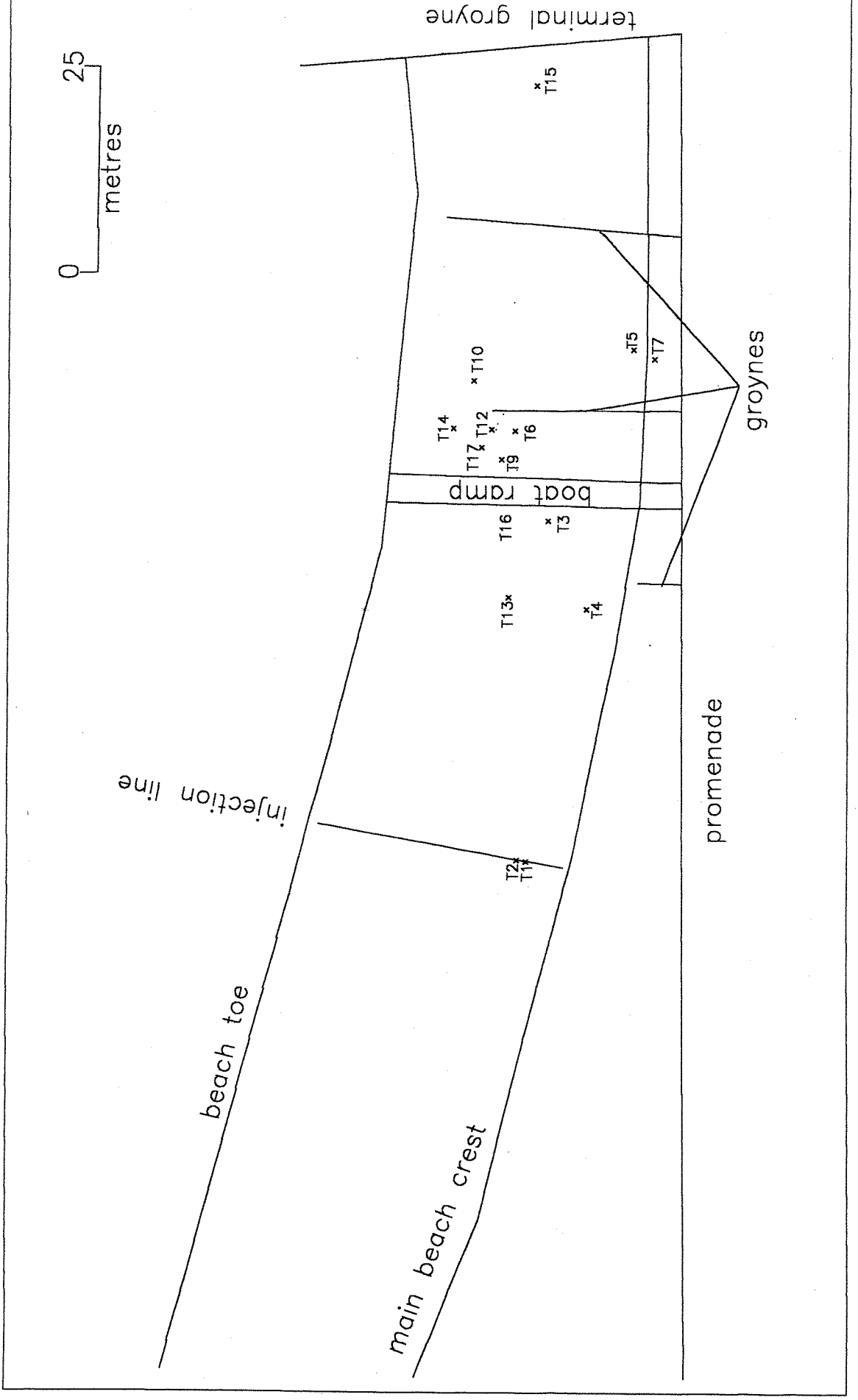

Figure 5.11(d) Location of electronic tracer pebbles at Long Beach, Whitstable: 25/01/93 (am)

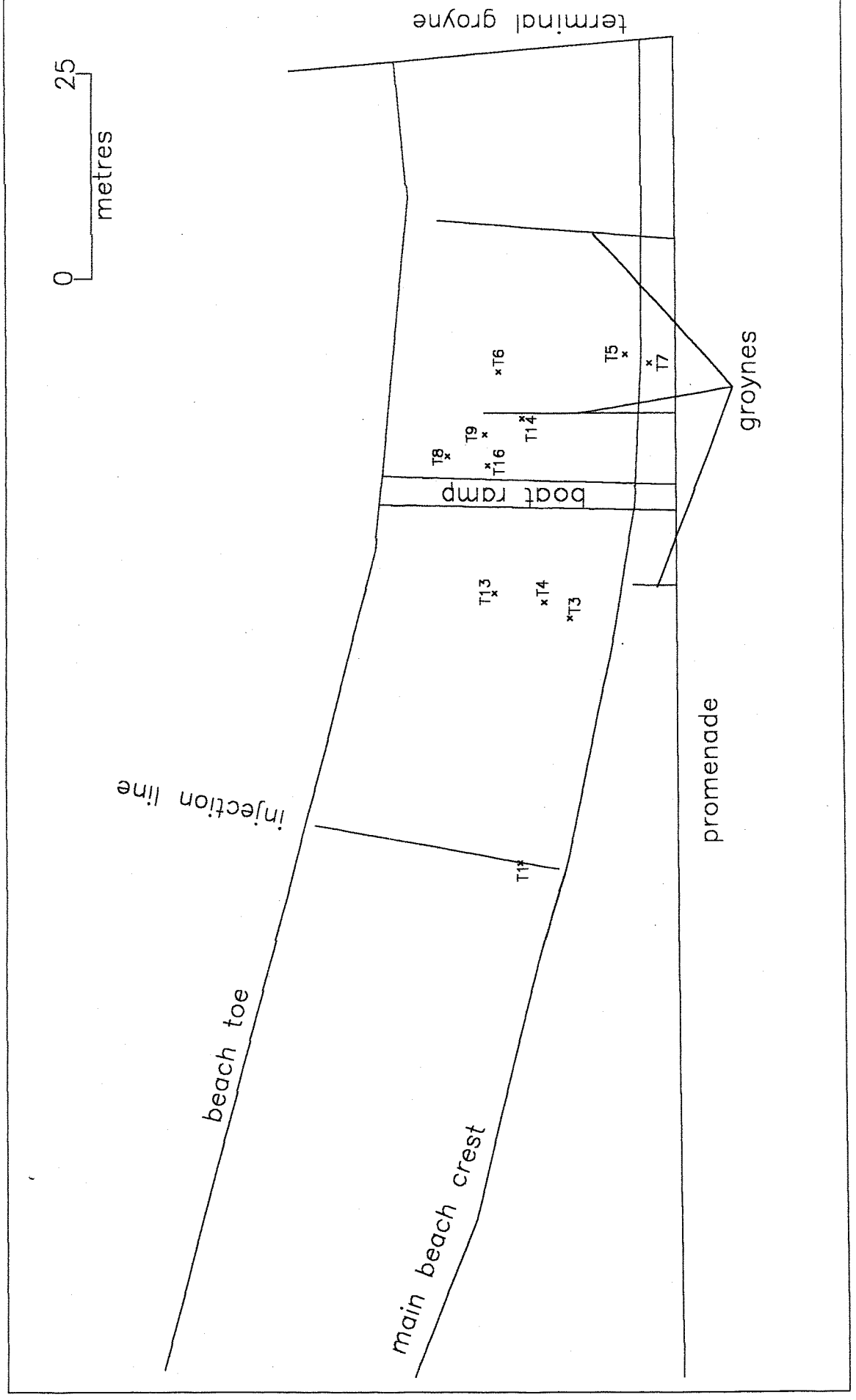

Figure 5.11(e) Location of electronic tracer pebbles at Long Beach, Whitstable: 25/01/93 (pm)

Figure 5.11(f) Location of electronic tracer pebbles at Long Beach, Whitstable: 26/01/93 (am)

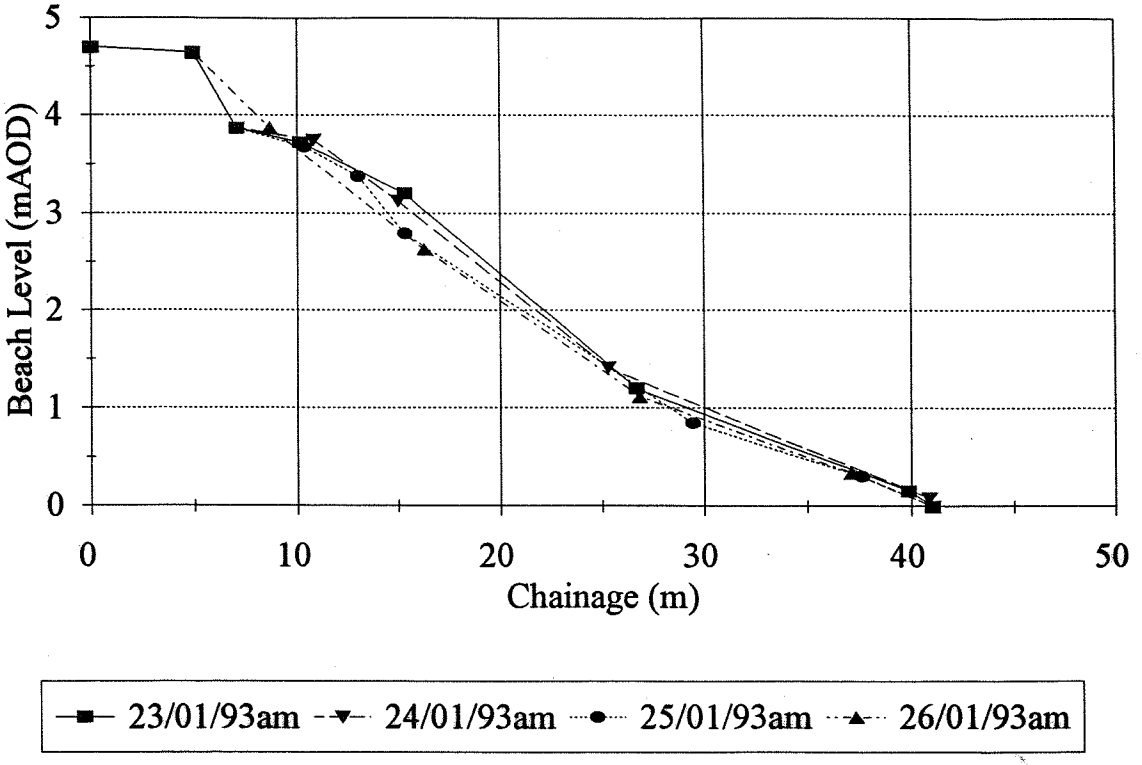

Figure 5.12(a) Beach changes at Profile 1: Long Beach, Whitstable: 23/01/93 to 26/01/93.

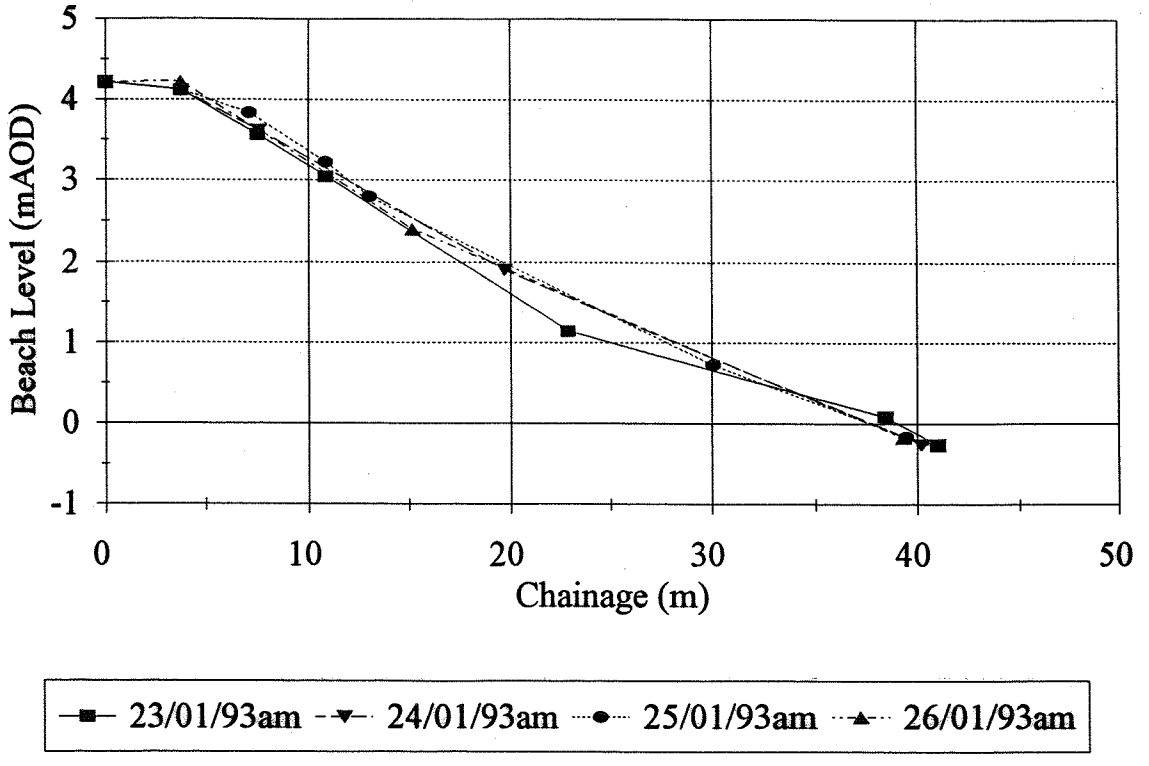

Figure 5.12(b) Beach changes at Profile 2: Long Beach, Whitstable: 23/01/93 to 26/01/93.

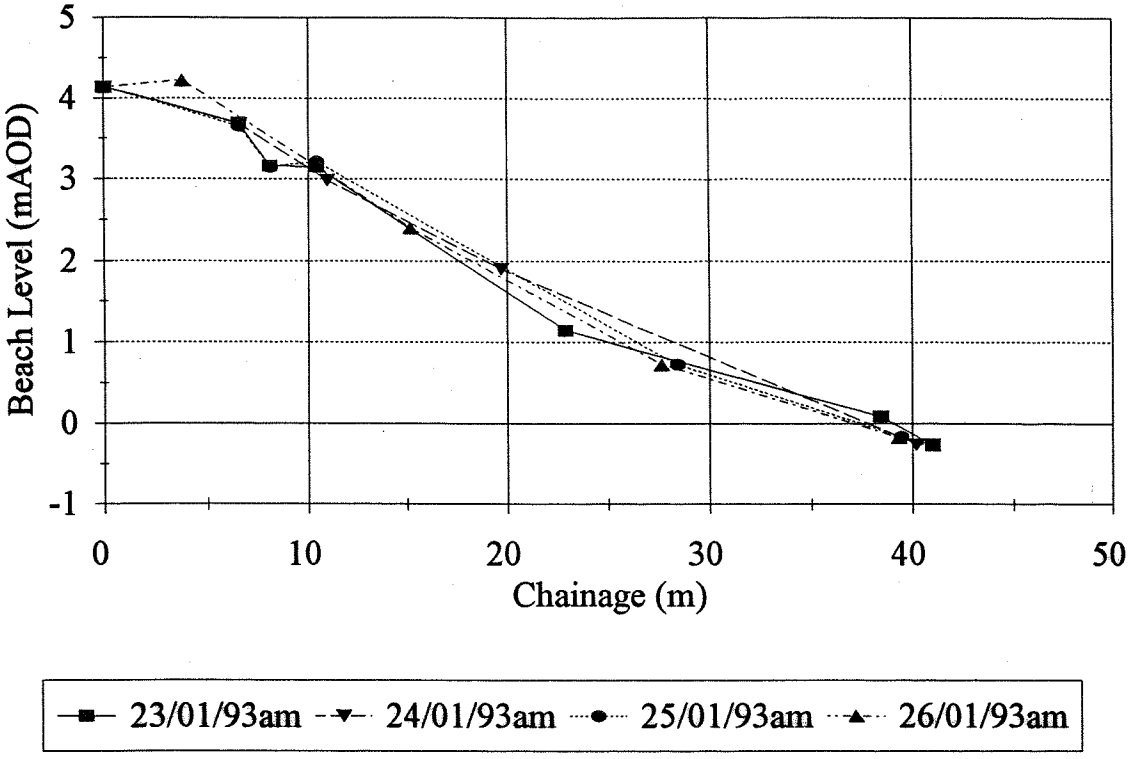

Figure 5.12(c) Beach changes at Profile 3: Long Beach, Whitstable: 23/01/93 to 26/01/93.

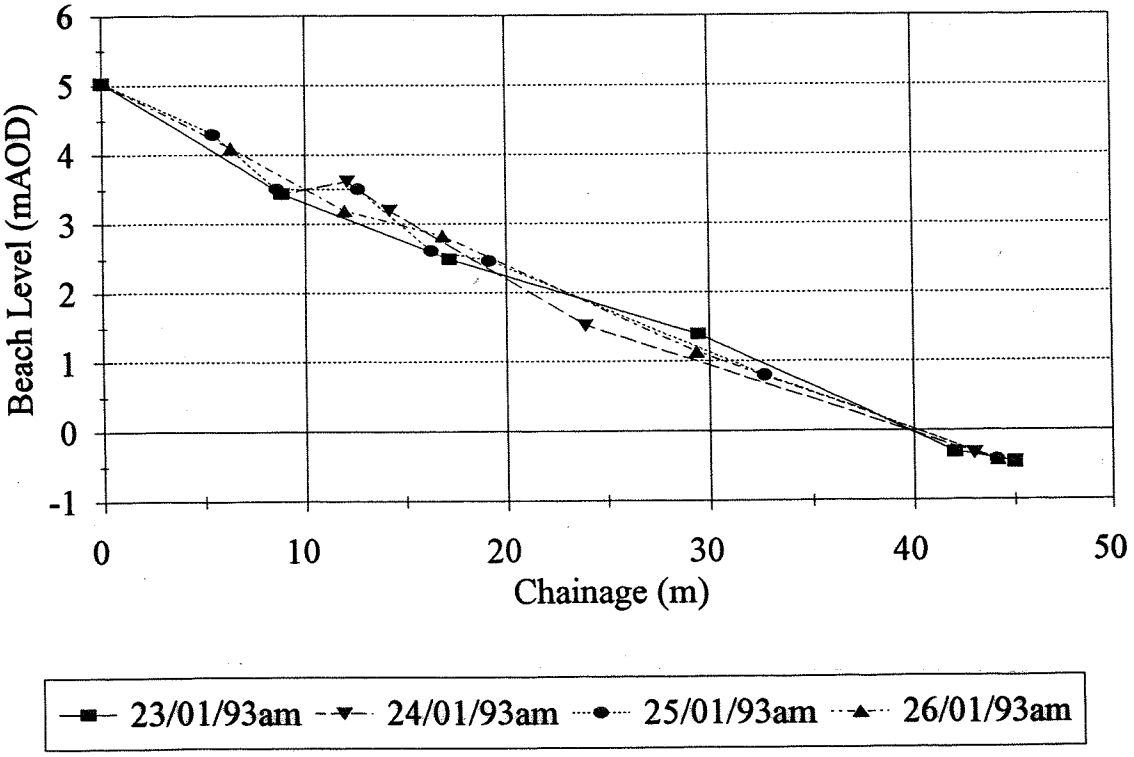

Figure 5.12(d) Beach changes at Profile 4: Long Beach, Whitstable: 23/01/93 to 26/01/93.

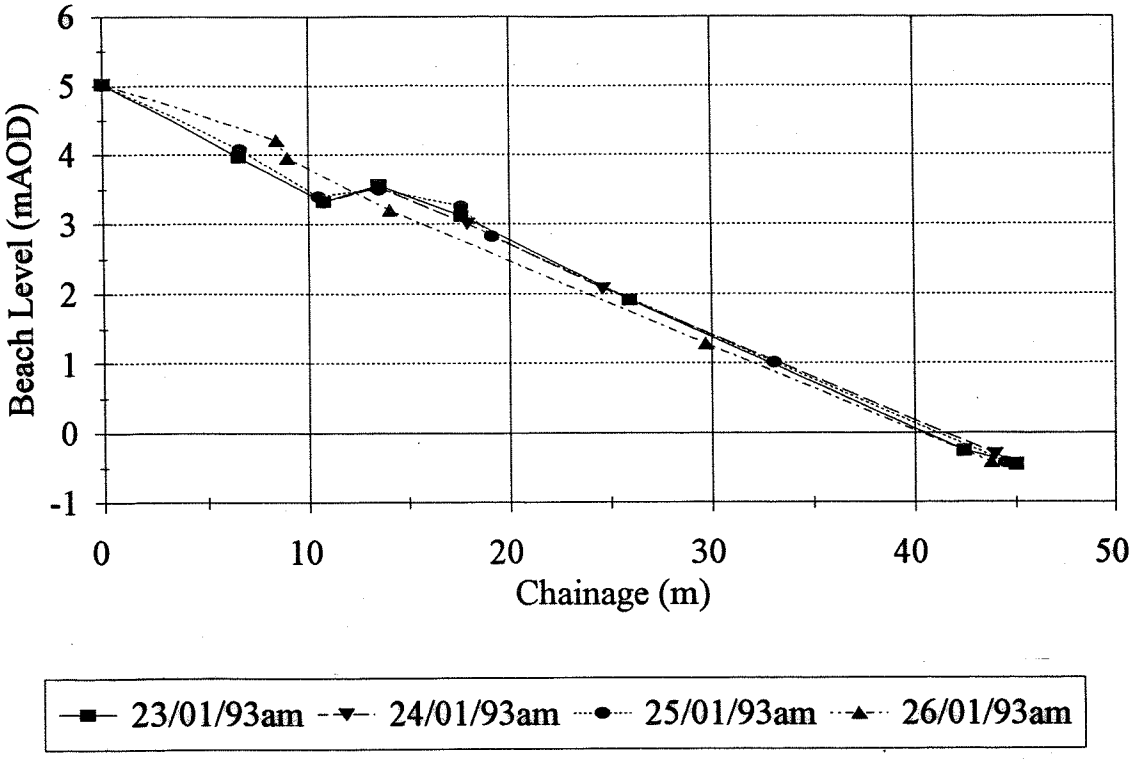

Figure 5.12(e) Beach changes at Profile 5: Long Beach, Whitstable: 23/01/93 to 26/01/93.

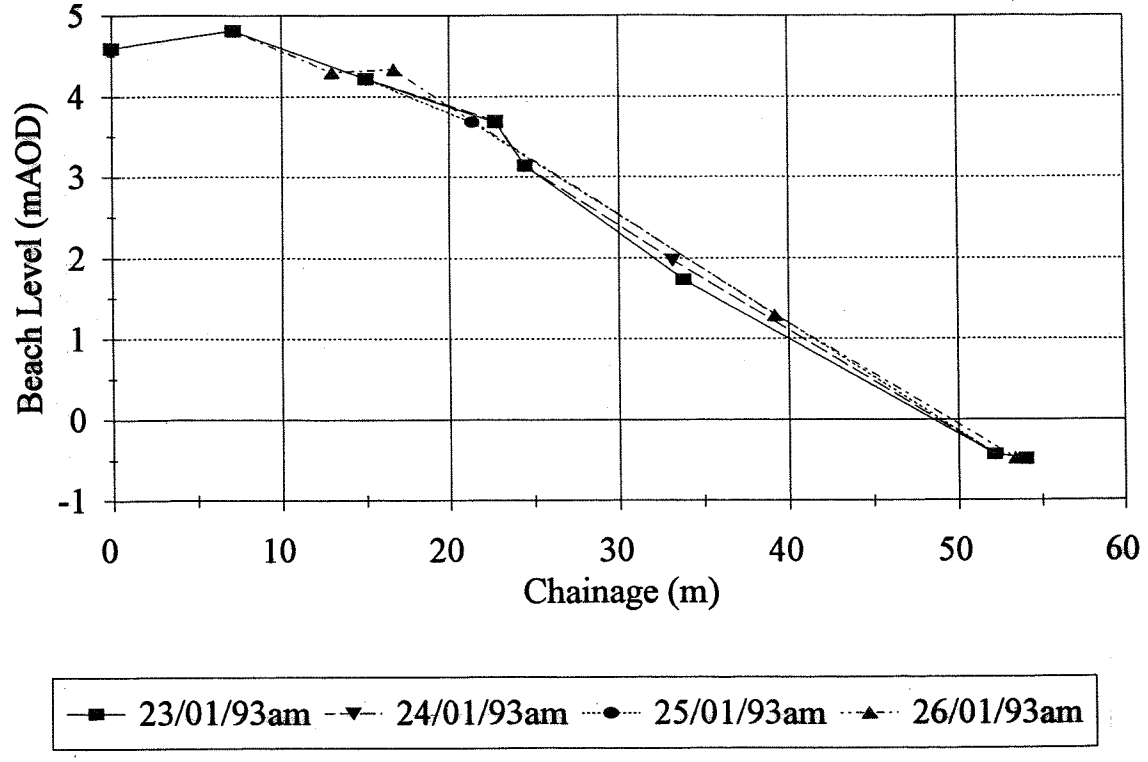

Figure 5.12(f) Beach changes at Profile 6: Long Beach, Whitstable: 23/01/93 to 26/01/93.

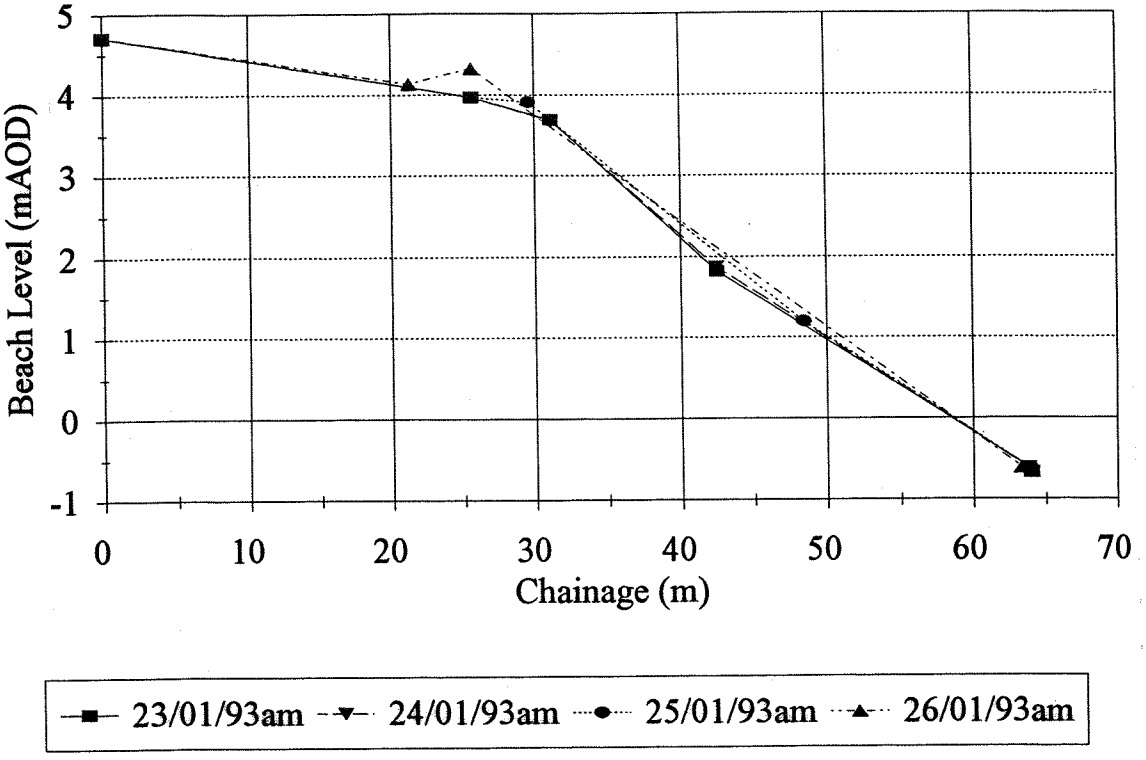

Figure 5.12(g) Beach changes at Profile 7: Long Beach, Whitstable: 23/01/93 to 26/01/93.

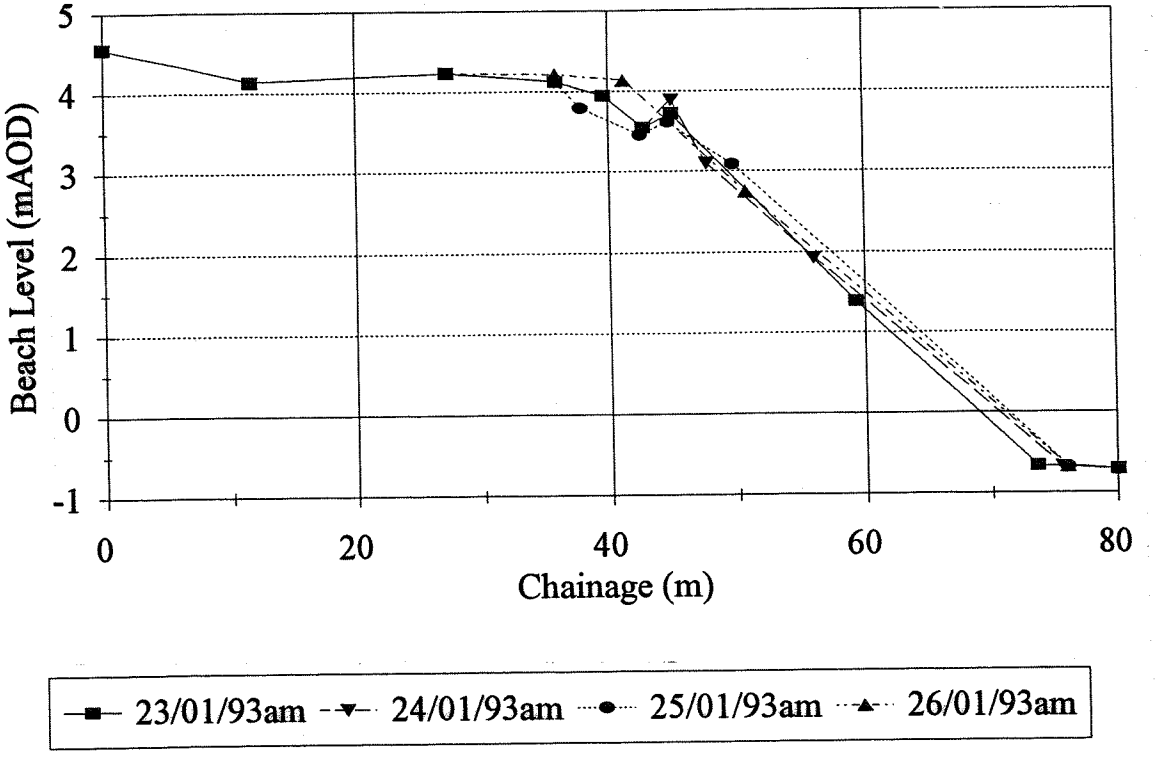

Figure 5.12(h) Beach changes at Profile 8: Long Beach, Whitstable: 23/01/93 to 26/01/93.

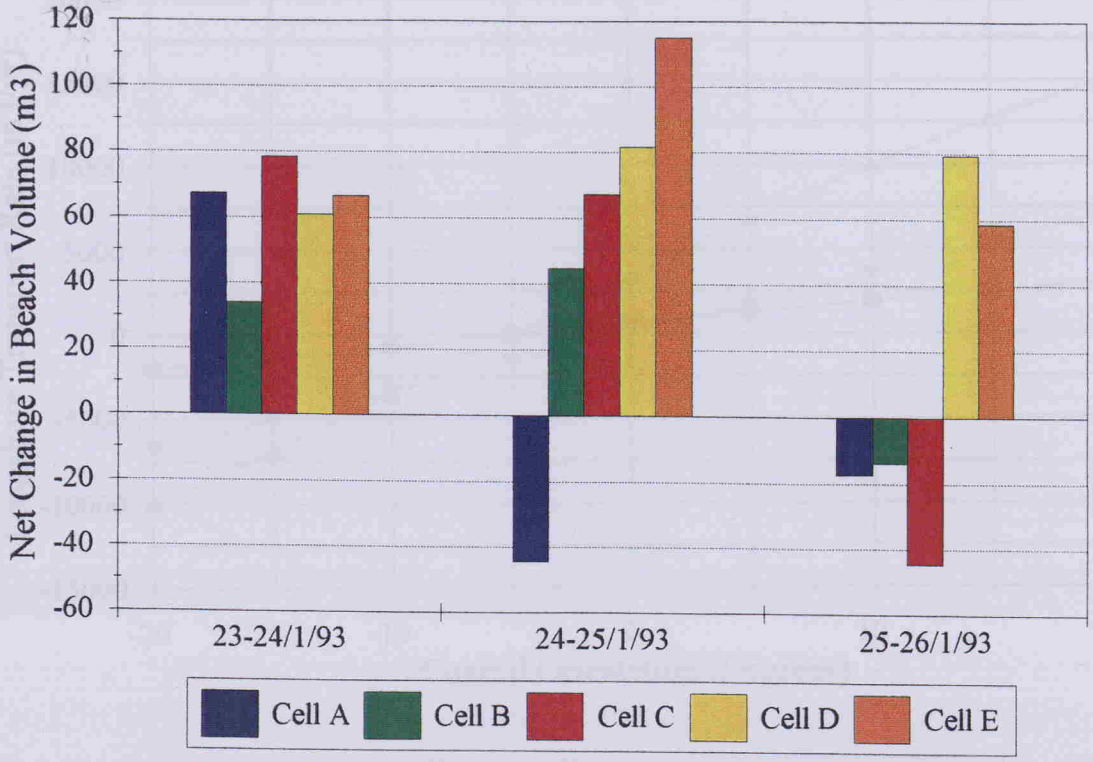

Figure 5.13 Volumetric changes for Long Beach, Whitstable: 23/01/93 to 26/01/93 (see Section 5.5 for details)

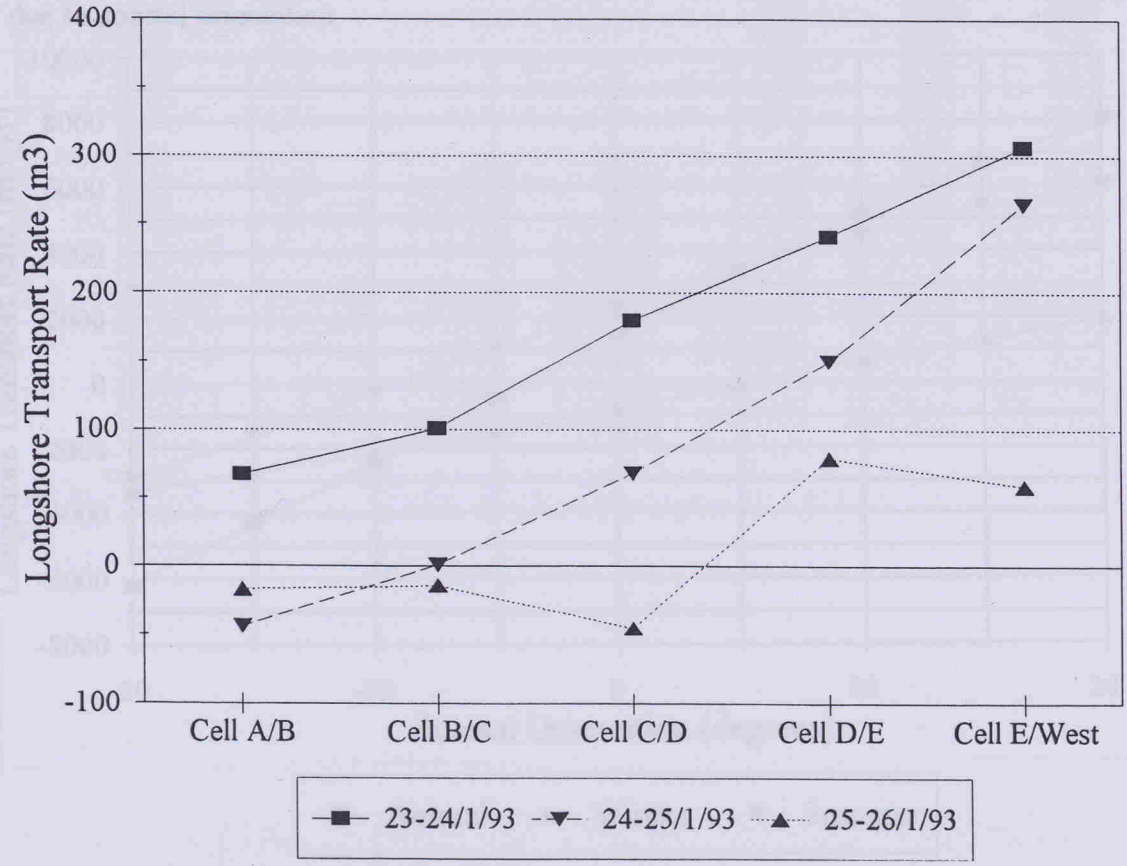

Figure 5.14 Longshore transport rates calculated from beach volumetric changes, Long Beach, Whitstable: 23/01/93 to 26/01/93 (see Section 5.5 for details)

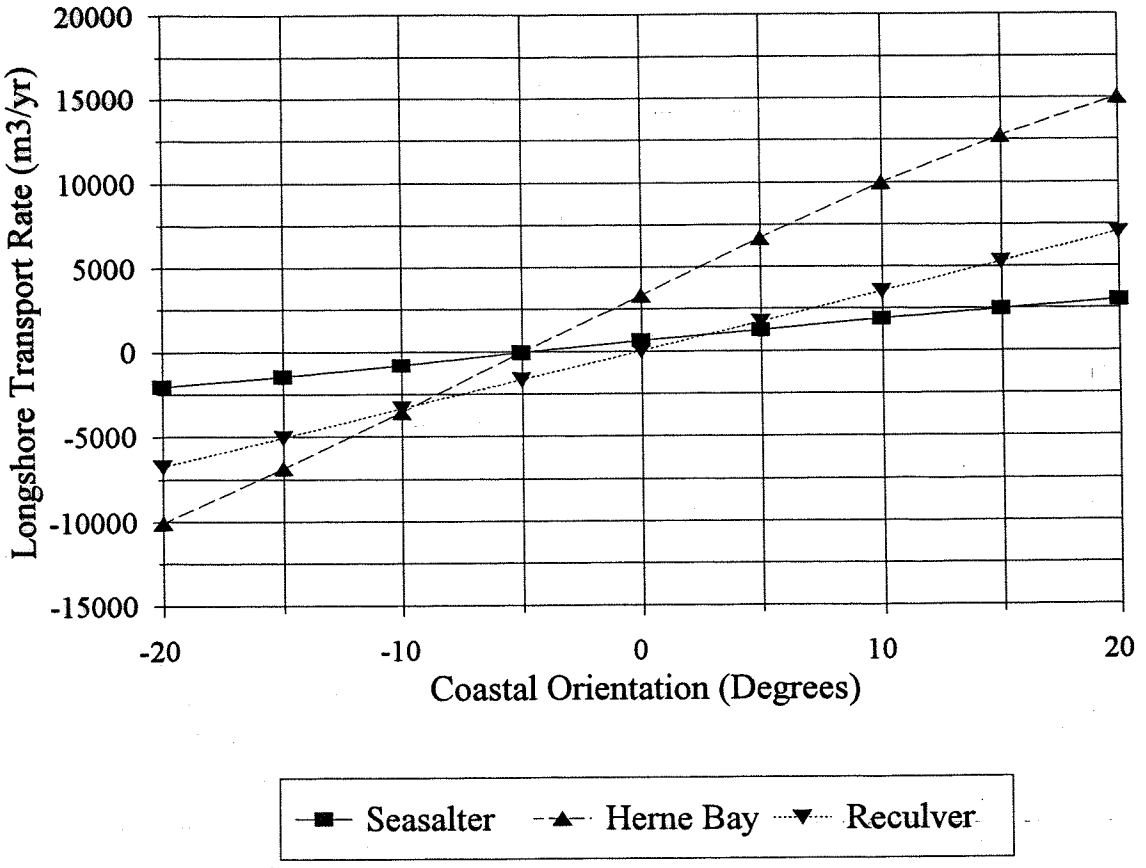

Figure 5.15. Examples of variation in average annual potential net longshore transport rates due to coastal orientation

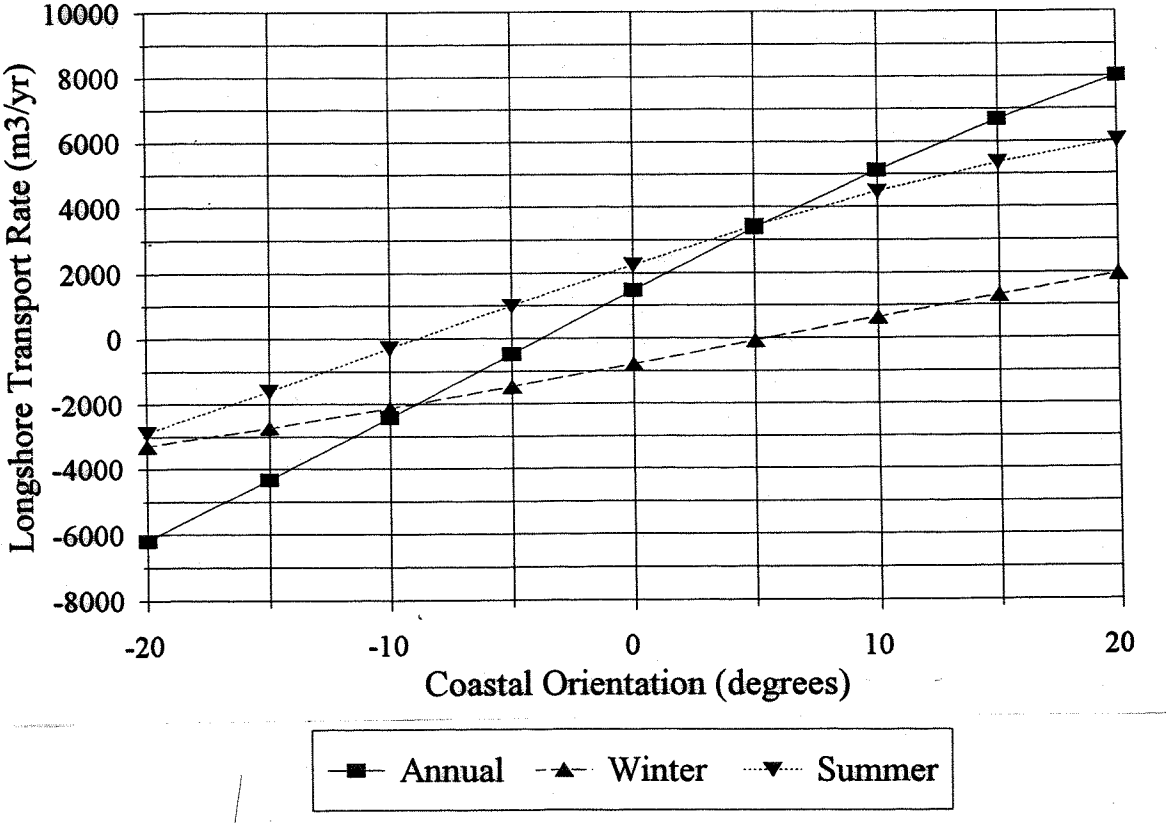

Figure 5.16. Seasonal variation in average annual potential net longshore transport rates at Long Beach, Whitstable

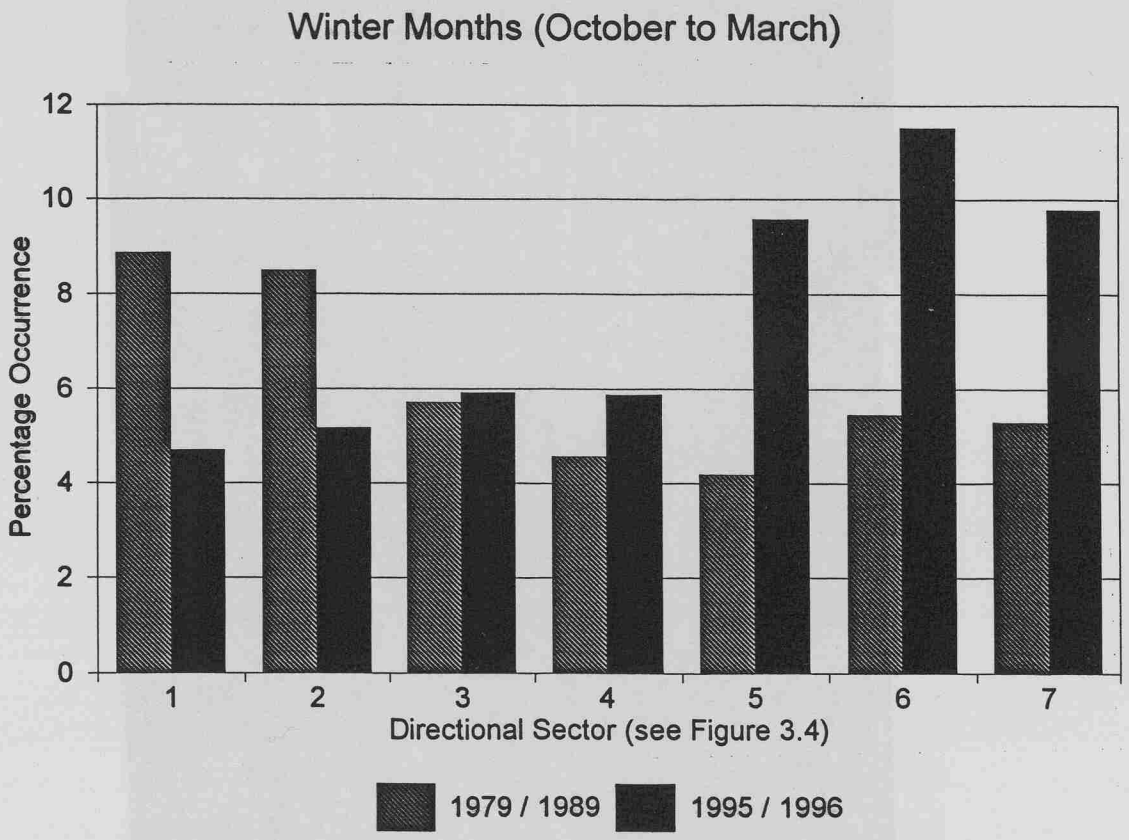

Figure 5.17. Comparison of wind speed and direction occurrences for the 'winter' period 1995/1996, and the average of 'winter' periods between 1979 to 1989: (data obtained from Manston Airport).

Plate 5.1. Aerial view of the field study site, Long Beach, Whitstable.

Plate 5.2. Movement of painted tracer pebbles across the 'sand run' under very low energy conditions at Long Beach, Whitstable: 16/03/92.

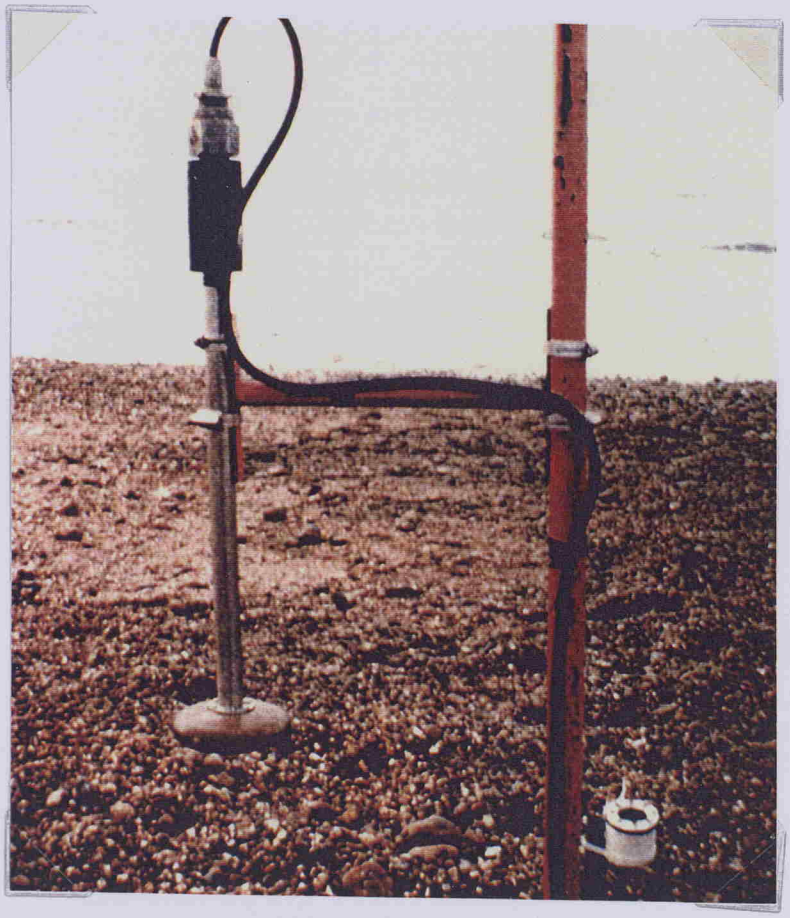

Plate 5.3. Pressure transducer and EM current meter, Long Beach, Whitstable: 23/01/93

Plate 5.4. Typical wave conditions, Long Beach, Whitstable: 25/01/93 (am).

Chapter 6: Results - Sediment Transport Studies

6.1. Introduction

In this Chapter the results of the coastal model (potential net annual longshore transport rates, as presented in Section 5.7) are used, in combination with the results of long-term (5 to 20 years) measurements of beach profiles, to develop an understanding of the patterns of stability of beaches in the study area.

Using the output from the coastal model, the potential net annual longshore transport rates have been determined for the whole of the study coastline; these are described in Section 6.2. Due to the presence of coastal structures, designed to restrict longshore movement, the actual transport rates will deviate from the calculated potentials in quantity and, in some cases, direction. A qualitative assessment can be made simply by estimating the relative efficiencies of the various sets of control structures along the coastline. In order to carry out a quantitative assessment of the impact of control structures, however, it is necessary to resort to measuring actual changes in the field.

As described in Chapter 3, the Coast Protection Authority have collected beach profile data from 72 beach monitoring stations located along this particular section of coastline. The majority of the data sets date from 1974, with changes at each location recorded on a quarterly basis. These data sets, together with details of changes undertaken to coastal defences, and the available information on the quantity of beach material added as beach replenishment, can be used to construct a sediment budget for the study area.

Because of the length of the study area and the extensive quantity of data which exists (and, therefore, requires validation), the analysis has not been carried out for the whole of the coastline; instead three representative examples of the application of the budgetary approach are included: Whitstable Central; Herne Bay West; and Tankerton, Figure 6.1. Details of these budget analyses are reproduced in section 6.3.

6. 2. Discussion of Results for Individual Coastal Sections.

Potential net annual longshore transport rates, obtained from the results presented in Section 5.7, are shown in Figure 6.2. It should be noted that these potential net annual longshore transport rates assume that there is an unrestricted supply of sediment, both within the section of coastline under consideration and between adjacent lengths of coastline. In addition to Figure 6.2, reference is made to aerial photographs of the coastline, Plates 2.1 (a-g).

All the transport rates are presented in cubic metres per year ($m^3 yr^{-1}$); positive values represent transport from east to west, whilst negative values represent transport from west to east. A coastal orientation of 0° represents an east - west aligned coastline. Positive angles represent a coastline which is orientated towards a northeast / southwest direction, with negative angles representing a coastline tending towards northwest / southeast.

6.2.1. Unit 1: Seasalter.

Seasalter is located at the western end of the study area and forms a sheltered embayment at the mouth of the Swale Estuary. The level of the beach toe is around +1.0m AOD, which is much higher than the typical toe levels over the remainder of the coastline. The foreshore at the east-end of Seasalter and at Whitstable have been subjected to high rates of erosion over the past 100 years. Based upon old Ordnance Survey maps (dated 1872 and 1896), the high water mark at Seasalter retreated to landward by some 150 m in 24 years, as the protective saltmarsh has been eroded (Canterbury City Council, 1993a). At present, the shoreline has been stabilised by the construction of seawalls and groynes. However, erosion of the alluvium and clay on the foreshore, beyond the toe of the shingle, is an on-going problem.

The potential net annual transport values predicted by the coastal model for Seasalter are shown on Figure 6.2. Net transport is from east to west, decreasing from 2500 m^3 at Seasalter slopes (v), to 1000 m^3 at the "Oaze" (iv) and 200 m^3 (iii) by the caravan and chalet site. This reduction in transport rate reflects the change in the orientation of the beaches along this particular section of coastline. Beyond the Red Mouth outfall (ii), there is a short section of coastline where the net transport rate reaches 2500 $m^3 yr^{-1}$. Further to the west, there is an accumulation of shingle (i), whose orientation is equal to the predicted equilibrium angle;

therefore it has zero net annual transport.

The model has not been extended further up into the Swale Estuary, due to the increased sheltering provided by the Isle of Sheppey.

6.2.2. Unit 1B: Whitstable.

The beaches located to the west of Whitstable Harbour (Figure 6.2) are orientated northeast to southwest (+50° - +55°). This orientation is largely a result of human interference, as defences have been erected in a somewhat 'haphazard' fashion since the 13th Century (Bowler, 1985). The result of this acute orientation in relation to the direction of wave approach, is that the whole coastline is heavily groyned.

The particular orientation of the coastline at Whitstable requires the model to be re-run; this was because the original model runs were undertaken with the assumption that the shoreline had an approximate east - west orientation. The results of the model re-run (Figure 6.3) demonstrate a revised equilibrium coastal orientation of +29°.

According to the coastal model, longshore transport along the Whitstable Central frontage (vii, viii) would be in the order of 5800 $m^3 yr^{-1}$, if no control structures were present. The transport rate decreases to 5200 $m^3 yr^{-1}$, by the Railway Wall (vi).

The sea defences at Whitstable were upgraded in 1989, with the construction of a large angled groyne system. The large size and narrow spacing of the new groynes is such that the actual longshore transport rates are much reduced. In Section 6.3.1, beach profile data is used to assess the impact of the new groynes on the predicted longshore transport rates.

To the east of Whitstable Harbour (ix) the harbour quay acts as a terminal groyne; against this, a stretch of lightly-groyned beach has accumulated. (This is Long Beach, Whitstable where the field experiments to determine "short-term" longshore transport rates were carried out (Chapter 5)).

The orientation of this particular beach is -4°; here the coastal model predicts a net potential

annual longshore transport rate of +2000 m^3. Based upon records of the volume of material dredged from the Harbour entrance, Canterbury City Council (1988) concluded that approximately 250 m^3 of shingle by-passed annually the eastern quay of the Harbour. This data suggests that the groynes at the western end of Long Beach reduce the annual longshore transport rate, by around 75 to 90%.

6.2.3. Unit 2: Tankerton.

The coastline at Tankerton (Figure 6.2) forms an embayment between the headlands of Long Rock (xv) and Tower Hill, Whitstable (x); the equilibrium coastline is -7°.

A strong easterly to westerly drift, of 8000 $m^3\ yr^{-1}$, is predicted to occur at the western end of the site, between Cliff Road and "The Street" (xi). To the east of Cliff Road (xii), the coastal orientation is such that zero net transport occurs. This result appears reasonable, since the orientation of the beach crests within the groyne bays is parallel to the seawall. To the east of St Annes Road (xiii), the coastal orientation again changes and results in a westerly transport, of around 6000 $m^3\ yr^{-1}$ to 7000 $m^3\ yr^{-1}$.

Beyond the Sailing Club (xiv), the coastline begins to turn towards the northeast. The coastal model suggests increased transport rate to the west; however, the sheltering effects of Long Rock have to be considered. To the west of the Sailing Club, the beaches are open to waves from the northeast. To the east of the Sailing Club however, the coast is partially sheltered from waves approaching from the northeast; this is related to the presence of Long Rock itself and the sediment banks lying offshore. Waves from the northeast, which reach the beach, have lost much of their energy; this is due to wave breaking over the banks and refraction such that the wave angles on the beach are less oblique than those predicted by the model. This results in a reduction in the amount of material transported to the west. Waves from the northwest, at the same site, do not suffer from sheltering; thus, the gross transport from west to east is not affected. Examination of the site itself has suggested that sheltering from the northeasterly wave action may be sufficient to cause a reversal in the direction of the net longshore transport.

In order to understand processes at East Tankerton, it is necessary to resort to a budgetary

analysis based upon recorded data (see Section 6.3.3).

6.2.4. Unit 3: Studd Hill.

The coastline at Studd Hill (Figure 6.2) forms another embayment between the headlands at Hampton Pier (xx) and Long Rock (xv). The beach at Swalecliffe (xvi) should, according to the model, show a small net transport from east to west of about 1000 $m^3 yr^{-1}$. In the central part of the bay the predicted net potential longshore transport varies from 2500 (xvii), to about 7000 $m^3 yr^{-1}$ (xviii), from east to west.

At the eastern end of the bay (xix) adjacent to Hampton Pier, a similar problem occurs to that at the eastern end of Tankerton, in that the beaches are sheltered from waves approaching from the northeast. The coastal model does not account for this sheltering and therefore, derivation of the transport potentials is not practical.

6.2.5. Unit 4B: Herne Bay.

Delft Hydraulics (1990) carried out a study at Herne Bay to determine the causes of beach erosion in Herne Bay Central Area (xxiii). This investigation identified that longshore transport was from east to west; it increased from 3000 $m^3 yr^{-1}$ to the east of the Neptune Jetty (xxiv), to 8000 $m^3 yr^{-1}$ along the seawall in the Central Area (xxiii). To the west of the pier (xxii) the transport rate was reduced to 3000 $m^3 yr^{-1}$. The variation in longshore transport rates was caused by a change in the orientation of the seawall from approximately east - west (0°) along the frontages from Lane End (xxii) to Hampton Pier (xx) and Coopers Hill to Neptune Jetty (xxiv) to an angle of +18°(northeast to southwest) in the central area. The equilibrium coastline for this particular region, as determined by Delft, using the UNIBEST model was -15° (northwest to southeast) (Delft Hydraulics, 1990b).

The model developed for this present investigation has been used also to determine transport rates in Herne Bay (Figure 6.2); these can be compared with the results of the Delft Hydraulics study.

The transport rate along Coopers Hill (xxiv) is predicted to be 4000 $m^3 yr^{-1}$, from east to west.

Along the central area frontage, the transport rate increases to 12000 $m^3 yr^{-1}$ (xxiii). West of the pier, between Lane End and Spa Esplanade (xxii), the model predicts a transport rate of 4000 $m^3 yr^{-1}$ (again from east to west); farther west (xxi), this reduces to 2000 $m^3 yr^{-1}$, with an eventual zero net annual transport at Hampton Pier itself.

The orientation of the beach at Hampton Pier is -6°, which corresponds to the equilibrium coastline predicted by the coastal model used in this study. Given that the beach at Hampton Pier is stable and is not accumulating (see Section 6.3.2), it is suggested that an equilibrium angle of -6° is more likely than the -15° (Delft Hydraulics, 1990), predicted by the UNIBEST model.

The section of coastline between Herne Bay Pier and Hampton Pier has been subjected to a budgetary analysis as part of the present study. The results are presented in Section 6.3.2.

6.2.6. Unit 5: East Cliff.

The East Cliff coastal section runs from around the Kings Hall Pumping Station (xxv), to the eastern end of the eroding cliffs near Reculver (xxix). At the western end of the section, a seawall protects slopes of graded London Clay. At the eastern end there is no seawall and the coastal cliffs are allowed to erode freely. These cliffs are composed of Tertiary sandstones overlain, by London Clay. Erosion of these cliffs releases approximately 4000 to 5000 m^3 of sediment into the coastal system on an annual basis. The bulk of this material is fine sand and silt. The pebble and cobble content is estimated to be less than 0.5% (Canterbury City Council, 1993a). On an annual basis, this equates to less than 25 m^3, which is not significant in the annual budget calculations.

The longshore transport model for East Cliff predicts an equilibrium coastline of 0°. The change to an east - west orientation over this section, compared with equilibrium coastlines in the sections to the west, is brought about by the increase in wave energy from the northwest; this, in turn, is due to the increase in fetch lengths and water depths available for the generation of waves. Additional energy losses of waves from the northeast as they pass over the Margate Sands (Figure 2.5), would also contribute to the change in the equilibrium orientation.

At the western end of East Cliff, between Kings Hall and the Hundred Steps (xxv), the potential net annual longshore transport rate has been calculated at 4000 $m^3 yr^{-1}$, from east to west. Farther to the east, at Bishopstone Glen (xxvi), this rate increases to 5000 $m^3 yr^{-1}$.

Beyond Bishopstone Glen, a dramatic change in the foreshore levels occurs from approximately -1.0 m AOD, to the west of Bishopstone Glen (xxvii), to a level of +1.7 m AOD adjacent to the Coastguard Lookout Post (xxviii). This rise in the foreshore levels is caused by the gentle east to west dip of the Tertiary sandstones. Within the Tertiary sandstones, there are bands of stiff silty clay which are more resistant to erosion than the sandstones. At the Coastguard Lookout, these more resistant layers form the foreshore; because they are more resistant than the overlying sandstones, they cause a local rise in the foreshore levels.

These changes in the foreshore levels affect the height and angle of waves which approach the shoreline. The net effect is to reduce longshore transport into the Bishopstone Glen (xvii) area; this results in a net loss of beach material at this latter location.

6.2.7. Unit 6(A to C): Reculver, Northern Sea Wall and Minnis Bay.

The coastline between Reculver and Minnis Bay (Figure 6.2) is a relatively recent feature (McFarland and Edwards, 1998). During Roman times this particular location was the site of the northern entrance to the Wantsum Channel; this linked the Outer Thames Estuary to the southern North Sea, via the east coast of Kent. Closure of the channel did not occur until the late 18th Century, when the original 'Northern Sea Wall' was completed. Reculver itself is the site of a Roman Fort (xxxi) of great archaeological importance; it is protected by a large stone apron, dating from late-Victorian times. The apron forms a prominent headland, which acts as a significant barrier to longshore transport.

To the west of Reculver Towers (xxx) the coastal model predicts a potential net annual longshore transport rate of 6000 $m^3 yr^{-1}$ along the seawall, in an east to west direction. This rate of transport combined with the effectiveness of the stone apron as a barrier to transport from the east, is consistent with the observation that there is no beach present on this section of the foreshore. Immediately to the east of Reculver (xxxii), the model predicts a longshore transport rate of 1500 $m^3 yr^{-1}$, also in a westerly direction.

Between 1km and 2km (xxxiii) to the east of Reculver, the coastal model predicts a reversal in the direction of shingle transport. Farther east (xxxiv) the net volume of transport is relatively low at -800 m^3 yr^{-1} (ie west to east). The beach along this length of the seawall is fairly stable as is shown by the large ungroyned shingle barrier at Cold Harbour Sluice (xxxv). However, some beach recycling is undertaken to maintain the shingle barrier.

At the eastern end of the Northern Sea Wall, at Plumpudding Island (xxxviii), a net annual longshore drift of 5000 m^3 yr^{-1} is predicted by the model. Farther to the east of Plumpudding Island, the shingle beach ends abruptly at Minnis Bay (xxxix) and sand beaches dominant. There have been problems of shingle "contaminating" the sand beaches here, which has led to the belief that the net shingle movement is from west to east. The shingle "contamination" is most likely a response to the action of northwesterly storms, which transport shingle east into Minnis Bay; this then becomes "trapped' on the sand beaches and is unable to move back towards the west during the dominant northeasterlies. Beach material from Plumpudding Island is lost, therefore, both to the west and, to a lesser extent, to the east. The result of this pattern of movement is an acute erosion on the beaches at Plumpudding Island; this has been confirmed by observations, and by the Environment Agency who are responsible for maintaining the beach.

Transport patterns of shingle are somewhat complicated along the Northern Sea Wall, as a result of the presence of the offshore banks (Figure 2.5). The large shingle beach at St Augustine's Bank (xxxvii) would appear to be an important sink for shingle, which is transported into the area from Plumpudding Island (and, probably, also from the beaches located to the east of Reculver).

Despite the uncertainties in the modelling of this particular length of the coastline, the patterns of shingle movement which are predicted are consistent with the observations in the field. For example, the model predicts strong beach erosion at two locations; at Plumpudding Island and a second approximately 1 km to the east of Reculver. Indeed the Environment Agency (Alder, pers comm) confirm that beach replenishment is undertaken at both of these sites, at regular intervals. The modelling undertaken predicts also an accumulation of shingle at St Augustine's Bank (xxxvii), which is supported by the presence of a large ungroyned beach.

6.3. Sediment Budget Analysis for Specific Coastal Sections

6.3.1. Whitstable, Central

Description of the Site

Whitstable Central (Figure 6.4) represents a section of coastline which relies entirely on the presence of a large groyne field to stabilise the shingle beach. Historically, Whitstable has suffered from serious flooding on a number of occasions (most recently, 1949 and 1953), as a result of beach levels being too low to accommodate extreme still water levels and wave conditions. As discussed previously (Section 6.2.2), the model predictions demonstrate that there is large potential net longshore transport of shingle towards the southwest.

The construction of the existing defences was completed in 1989, when 115,000 m^3 of replenishment material was placed in a new enlarged groyne field. The budgetary analysis for Whitstable covers the period 1989 to 1994 and, therefore, describes the behaviour of the beach replenishment following completion of the scheme.

The Whitstable Central Area is 1095 m in length. Based upon the orientation of the beach and the spacing of groynes, 4 beach management units (BMU) have been defined; these are shown in Figure 6.4.

Beach Monitoring Stations

Data from 8 BMS are available over the period of the investigation, with each station having been monitored 4 times a year. The location of the BMS are shown in Figure 6.4. A regression analysis has been carried out for the change in cross-sectional area of the beach profile, at each of the monitoring stations, over a 5 year period, to determine the average annual rate of change in cross-sectional area. The changes in cross-sectional area with time (trends) are presented in Table 6.1. Table 6.1 also shows the standard error in the trend, and the cross-sectional area immediately following the beach recharge (1989). Plots of the change in cross-sectional area, with time, are reproduced in Figure 6.5 (a-h).

Sediment Budget

Depending upon their location, each of the BMS has been allocated to one or more of the BMU. Each profile cross-sectional area is then multiplied by the length of coastline, of which it is representative. The process is repeated for other monitoring stations in the same management unit and the resulting volumes are summed, to provide the total volume of material present at any particular recording occasion. A regression analysis has then been undertaken for each of the BMU, to determine their erosional / depositional trends. The results of these calculations are presented in Table 6.2.

In Table 6.2., BMU are defined as 'stable' if the trend (having allowed for the standard error) is neither one of accretion or erosion. If there is a definite negative trend (trend + standard error is negative), then the beach management unit is defined as 'eroding'. A definite positive trend indicates a beach which is 'accreting'. On this basis the two central beach management units (B and C) are eroding whilst those at either end (A and D) are considered to be stable.

Combining the quantities of beach material in each of the management units provides an estimate of the total volume of beach material within Whitstable Central (Table 6.2). Regression analysis was applied to the variation of this total quantity, with time, to provide an overall trend. The results of this analysis are presented in Table 6.2.

Based upon the five years data used in the analysis, the overall volumetric change in Whitstable Central represents a loss of beach material at a rate of between 300 $m^3 yr^{-1}$ and 900 $m^3 yr^{-1}$. This figure represents a loss of total beach volume of approximately 0.5 $m^3 m^{-1} yr^{-1}$. It is likely that losses of this quantity can be attributed to the winnowing of fines from the replenishment material (CUR, 1987). The minimum recorded volume of beach material in Whitstable Central occurred during the latter part of 1990 (Figure 6.6). During the same period, there were a series of modest storms experienced on the North Kent coast (see Table 4.13). Most of these storms resulted from strong westerly winds; wave action during these events was typically of a high frequency (0.3 to 0.25Hz), with significant wave heights of around 1.0 m (Canterbury City Council, 1993b), ie steep waves. Vincent (1979) has described how steep waves result in the movement offshore of sand-sized sediment, at sites in East Anglia. It is possible that the reduction in beach volume during the latter part of 1990 was linked to a loss of fine-grained

material during these storm events, which were dominated by steep waves.

Examination of the beaches at Whitstable Central confirms that, due to the large size of the groynes, no shingle can be exchanged between the individual groyne bays. Likewise, no shingle can be transferred to the adjacent beach management units down-drift, ie towards the southwest. Therefore, the groynes have effectively halted all of the longshore transport (potentially, around 6000 $m^3 yr^{-1}$) (net) predicted by the model. Only transport of finer-beach material in an onshore / offshore direction is possible. The quantity of material lost from the beach equates to around 0.5 $m^3 m^{-1} yr^{-1}$.

6.3.2. Herne Bay, West

Description of the site

Herne Bay West extends from Hampton Pier to Neptune Jetty, (Figure 6.7). Within this area, there is known to be a net transport of coarse-grained sediment from east to west. This pattern is shown by the build-up of sediment on the eastern sides of Hampton Pier and Neptune Jetty. For this study, five beach management units (BMU's) have been defined, as shown in Figure 6.7.

In 1991-1992, a rock breakwater was constructed across (BMU E) to prevent flooding in the town of Herne Bay, during storms. The breakwater is attached to the shoreline at Neptune Jetty and forms an 'arm-like' structure, running across the central area; this approximately follows the orientation of the coastline, immediately to the east and west. The construction of the breakwater has affected the coarse sediment transport within the region, in various ways (as outlined below).

- A complete cessation of shingle-feeding into Herne Bay Central (BMU E) from the east. The quantity of shingle which would have passed Neptune Jetty prior, to construction of the breakwater, can be estimated by calculating the build-up of beach which is presently found on the seaward side of the breakwater. Based upon surveys undertaken following construction of the breakwater in 1991, approximately 150 m^3 of shingle by-passes the jetty on an annual basis.

• The protection provided to the new beach, by with the breakwater, is very effective; it has reduced significantly the mobility of the shingle beach which it protects. Prior to the construction of the breakwater, beach replenishment material supplied to this area was rapidly transported the west, feeding the beaches at Lane End and beyond. Such indirect replenishment of the beaches, between Lane End and Hampton Pier, was halted as a result of the breakwater construction. Details of beach replenishments carried out in Herne Bay West, since 1974, are shown in Table 6.3.

Coastal Model Results

The existence of a net easterly to westerly drift is supported by the findings of the coastal model (Section 6.2). At Herne Bay Central, the orientation of the coastline is such that, in the absence of control structures, 12000 m^3 of beach material would be lost from the area every year (less the small quantity of material which may be transported in from the east).

Towards Hampton Pier, there is a reduction in the longshore transport rates, as far as Hampton Pier itself (Figure 6.2.5). The coastal model predicts that the beach immediately to the east of Hampton is stable, ie the coastal orientation is equal to the equilibrium coastline. The consequences of a reduction in transport rate along the coast would be seen as erosion in BMU E, and a gradual accretion of beach in the each of the four other BMUs. Actual rates of beach volume changes would be lower than predicted in the coastal model due to the presence of groynes, along most of the frontage.

Beach Profile Changes

There are 5 beach monitoring stations (BMS) located within the Herne Bay West system (Figure 6.7), at which beach profiles have been levelled since 1975. A study of the changes in the beach profiles, at each of the locations, can provide valuable information; this includes whether the beach is stable, eroding or accreting.

The variation in cross-sectional areas for these stations are shown in Figures 6.8 (a-e). A regression analysis was carried out for each station for: (a) pre-breakwater construction (1975 - 1992); and (b) post-breakwater construction (1992 - 1995). The results of the regression

analysis are reproduced in Table 6.4. A description of the changes in cross-sectional area, with time for each of the beach monitoring stations is presented below.

BMS 33 (Figure 6.8(a)): the cross-sectional area varies between 154 m^2 and 192 m^2, over the 19 years when monitoring has been undertaken. Based upon the regression analysis, the beach is accreting at this point at the rate of approximately 0.5 $m^2 yr^{-1}$. However, this pattern masks a more complex profile development, in which the beach displays a strong accretionary tendency (between 1975 and 1980); this is followed by a sharp reduction in levels over a one year period. Further erosion of the profile occurs, albeit at a reduced rate, until 1985. Over the next decade, a very similar pattern emerges, with accretion followed by a period of erosion.

BMS 34 (Figure 6.8(b)): this shows a steady increase in the profile cross-sectional area (0.8 $m^2 yr^{-1}$), over the 20 year period. There is no indication in the data of the more irregular trend exhibited by BMS 33.

BMS 35 (Figure 6.8(c)): the beach profile at particular location shows an erosional tendency (up to 1985), although there is considerable variation from the general trend. Between 1985 and 1986, a large increase in the cross sectional area occurred, with these levels being maintained generally until 1995. The regression analysis suggests accretion at the rate of around 0.5 $m^2 yr^{-1}$, over the 20 year period; however, as was the case for BMS 33, this masks a more complex history of profile change.

BMS 36 (Figure 6.8(d)): following a severe storm in 1978, beach recharge was carried out at a number of locations along the North Kent coastline. The beach in the vicinity of the monitoring station received approximately 1600 m^3 of material; this recharge shows up (Figure 6.8(d)) as a sudden increase in the profile cross-sectional area, from 48 m^2 to 59 m^2. Between 1978 and 1992, the profile changes are erratic but remain mostly within the range of 45 m^2 to 60 m^2. The regression analysis shows that there was no overall change in beach levels, between 1978 and 1992.

Since 1992, the beach levels at BMS 36 display a strong erosional tendency. A regression analysis carried out on the data obtained between 1992 and 1994 shows an approximate rate of loss of 6 $m^2 yr^{-1}$ (Table 6.4).

Station 37 (Figure 6.8(e)): profile cross-sectional areas are highly erratic at this location. There have been four beach recharges here (excluding the major recharge carried out following construction of the breakwater), over the 16 year period between 1975 and 1991, (Table 6.3). The largest of the replenishments was carried out in June 1978, following the January 1978 storm. For approximately one year following this recharge, beach profile cross-sectional areas were maintained at around 35 m^2; after a further year, the cross-sectional area was halved to 18 m^2, by erosion.

Sediment Budget Analysis

Using the data derived from the beach profiles, the changes in the volume of beach within each BMU, over time, was determined. The results are shown in Table 6.5. It should be noted that no estimates were made for BMU E, for the reasons outlined below.

(a) The bulk of the beach material introduction at the monitoring station has been as the result of replenishment. Whilst the replenishments were successful in increasing the beach levels in the short-term, there has been no net gain in beach volume in the longer-term. It has been assumed, therefore, that material added to BMU E, eventually ends up along the coast, between BMU D and BMU A, due to longshore transport.

(b) Since the construction of the breakwater, BMU E can be considered as a separate sediment cell, which has no significant interchange of shingle with the adjacent units.

The average annual increase in beach volume in BMU A to D is calculated at 810 (+130) cubic metres per year, over the 18 year period. It is possible to balance this accumulation with beach replenishments carried out over the same period, the natural feed of material in or out of the area and offshore losses.

Hampton Pier forms an effective barrier to the westerly transport of shingle. Offshore losses of shingle are also considered to be negligible, as there is no evidence of offshore transport pathways during inspections of the site at low tide. With respect to the sand-sized fraction of the beach, onshore-offshore transport may occur; however, this is difficult to quantify.

A balanced sediment budget for Herne Bay West, prior to the breakwater construction is presented in Table 6.6(a). The budget compilation was constructed, on the basis of progressing easterly from Hampton Pier, by calculating the quantity of material required to be feed alongshore into each BMU to balance: (a) the feed of material out of the BMU; (b) volumetric changes in the BMU itself; and (c) onshore - offshore transport.

The onshore - offshore transport rates were determined retrospectively, by assuming that any net losses or gains to the area as a whole were the result of onshore - offshore transport. The budget shows net losses of 1091 m^3 offshore; this is equivalent to around 0.5 $m^3 m^{-1} yr^{-1}$, which is the same rate of loss as at Whitstable Central (Section 6.3.1).

The sediment budget can be used also to determine 'actual' longshore transport rates. Transport rates out of BMU E, are of the order of 1500 $m^3 yr^{-1}$, compared with the model predictions of 4000 to 12000 m3 yr^{-1}. Towards Hampton Pier, longshore transport rates based upon the budgetary analysis, decrease from 1300 to 100 $m^3 yr^{-1}$; these compared with 4000 $m^3 yr^{-1}$ to zero, predicted by the model. The differences can be attributed to the retarding effects of the groynes.

Effects of Breakwater Construction

Since the construction of the breakwater, no natural feed now enters the area. Further, the longshore feeding, from BMU E to the other units, has also been arrested. A second sediment budget has been compiled, assuming that the longshore and onshore - offshore transport patterns in the remaining four BMUs is unchanged (Table 6.6(b)).

This interpretation shows that to maintain existing patterns of transport and accumulation, estimated losses of 1465 m^3 of beach material needs to be compensated for by recharging at BMU D. Otherwise, erosion will occur at an average-annual rate equal to this particular replenishment requirement.

Examination of the actual changes in beach volumes, post-breakwater construction (Table 6.5), confirm generally the predicted budget presented in Table 6.6(b). Although the data set is somewhat limited with a high degree of uncertainty, there is a net loss of 700 $m^3 yr^{-1}$ from

BMU A to D; of this approximately 1800 ±300 $m^3 yr^{-1}$ occurs in BMU D. Therefore, it would appear that the budgetary analysis undertaken for Herne Bay West, provides a useful tool for predicting future coastal changes. This is discussed further in Chapter 7.

6.3.3. Tankerton

Description of the Site

Tankerton is the section of coastline between Whitstable Harbour and Long Rock (Figure 6.9). Timber groynes of various lengths, heights and ages have been constructed along the entire coastline, to reduce longshore shingle transport. Beach recharges have been carried out, on a more or less annual basis, along the whole 3 km length of coastline. Details of the recharges carried out between 1980 and 1994 are shown in Table 6.7.

In 1994, Tankerton was the subject of a study undertaken by Delft Hydraulics (1995), as part of planned upgrading of the sea defences. A sediment budgetary analysis was carried out by Delft Hydraulics, using the beach profile data supplied by the Coast Protection Authority; the results are shown in Figure 6.10. The beach management units adopted by Delft Hydraulics are shown in Figure 6.9.

Delft Hydraulics (op cit) conclude, from their budgetary analysis, that over the main part of the Tankerton frontage, net longshore transport of the beach material is from west to east. A drift divide is located towards the western end of the study area (BMU B), with east to west transport occurring west of the divide.

A study undertaken at East Tankerton (Canterbury City Council, 1992), to assess the performance of a small beach replenishment scheme, presented an hypothesis concerning the location of a drift divide (towards the eastern end of Tankerton, in the vicinity of beach monitoring BMS 24 to 25 (Figure 6.9). The coastline, at these two stations has been identified as being the most erosive section of the Tankerton coastline over the period 1977 and 1992 (Canterbury City Council, 1992). A volumetric analysis of the East Tankerton area concluded that there was a net "loss" of about 1000 $m^3 yr^{-1}$ of beach material, between BMS 23 and 27. It was proposed that this material was lost to both the east (onto Long Rock) and to the west.

It has been concluded previously (Canterbury City Council, 1992), that the reason for the drift divide was the sheltering from northeasterly waves, provided to the shoreline to the east of BMS 24, by the Long Rock headland. This explanation was supported by the observation that in the three months following the replenishment, aluminium pebbles placed at BMS 24 were found in groyne bays to the west only; in contrast, those pebbles placed at BMS 25 were found to have moved only towards the east.

Beach Profiles

For the budgetary analysis undertaken for Tankerton, data from 17 BMS were available between 1980 and 1995. The locations of these stations is shown in Figure 6.9. The results of the regression analysis for the change in beach cross-sectional area is reproduced in Table 6.8. On the basis of the data presented, it can be seen that most of the monitoring stations display erosive trends, since 1980.

Budgetary Analysis

The budgetary analysis for Tankerton (see above) has been re-examined in an attempt to determine whether a drift divide exists; if so, whether it is located to the east or west of Tankerton Bay. The data set used in this study is the same as that provided (by the author) to Delft Hydraulics, for their own budgetary analysis; however, there are some differences in the assumptions made (as outlined below).

Loss of fines from the replenishment material.

Delft Hydraulics (1995) carried out their budgetary calculations assuming that either: (i) there was a 15% loss of fine materials from the beach replenishment, "very soon" after the replenishment was undertaken; or (ii) that there was no loss of fines from the replenishment material. The results derived on the basis of both these assumptions are presented in Figure 6.10.

Beach replenishments carried out at Tankerton Bay, between 1980 and 1992, were subject to a grain-size specification distribution curve which did not allow for the grading of the

replenishment material from being finer than that of the natural beach. For this reason, it is assumed in the present study that there is no loss of fine material from any of the replenishment added to the beach. It should be noted that, in the case of the replenishment material added in 1992, a survey undertaken of the beach three months after replenishment showed that there was an actual increase in the beach volume. This increase was in spite of evidence (aluminium pebble displacement) to suggest that the only material transferred between the various groyne bays, by longshore transport, was a small quantity out of the area. The increase in volume was attributed to sorting of the upper layer of the beach, which led to a decrease in the placed density of the replenishment material area (Canterbury City Council, 1992).

(b) Definition of Beach Management Units.

The BMUs defined by Delft Hydraulics (1995) are considered adequate here, except that Delft's Unit D has been sub-divided into two separate BMUs, (D and E), for this study (Figure 6.9). There are two reasons for this division: firstly, the groynes in BMU E are much smaller than those in BMU D (Plate 6.1); and, secondly the shoreline in BMU E is sheltered from waves generated by northeasterly winds.

(c). Offshore Losses.

The budgetary analysis for both Whitstable and Herne Bay have demonstrated that a balanced budget required a net loss of material offshore. In both cases, this loss was estimated at 0.5 m^3 $m^{-1}yr^{-1}$. Because the Tankerton budget cannot be closed at each end, (see section (d) below), it is not possible to estimate these offshore losses. Delft Hydraulics (1995) made no allowance for such offshore losses in their analysis. The sediment budget analysis carried out in relation to the present study, presented in Table 6.9(a), assumes that offshore losses of the quantities estimated for Herne Bay and Whitstable will occur. Table 6.9(b) shows the effects of assuming that there will be no offshore losses, from the sedimentary budget system.

(d) Budget Closure

In the previous examples of sediment budgets carried out at Herne Bay and at Whitstable, longshore transport closure of the area under investigation was possible for both ends of the

system. Closure of the Tankerton study area cannot be undertaken so readily.

At the eastern end, Long Rock (Figure 6.9), consists of a stable accumulation of shingle; this is considered to receive a shingle feed from both Tankerton and Studd Hill (Section 6.2). No monitoring has been undertaken at Long Rock; it is therefore not possible to assess the volumetric changes at the site, with time. Further, as a result of the stream which exits from the bank, shingle-sized material is thought to be transported offshore during periods of high stream flows. This material forms a series of shingle banks located to the north of Long Rock; the shingle can also be seen to spread over the foreshore, beyond the toe of Long Rock itself, (Plate 2.1(c)).

Whilst complete closure of the Tankerton budget is not possible at the western end, it is known that 250 m^3 of shingle by-passes the harbour quay, on average, every year. Therefore, it is possible to utilise the harbour quay as a starting point for the budget compilation, on the basis of a knowledge of the quantity of material which is lost to the west.

Approximately 700m to the east of the Harbour, however, lies the "Street" (Figure 6.9). This is a narrow, approximately shore-normal sediment bank which extends for over 3km to seaward. The bank consists of a mixture of sand, shells and shingle, of up to 10mm (D_{50}) in diameter, (see Section 2.4; Canterbury City Council, 1993a). The Street is joined to the shingle beach at its toe. No studies have been undertaken to assess whether or not material is transferred from the shingle beach to the Street, or *vice-versa*. The likelihood of beach material being transported onshore - offshore means that the sediment budget cannot be effectively closed.

The budget analysis has been repeated, assuming that offshore losses increase to: (a) 1 $m^3\ m^{-1}\ yr^{-1}$; and (b) 2 $m^3\ m^{-1}\ yr^{-1}$ in BMU B, due to the presence of the Street. The results are presented in Table 6.9 (c) and 6.9 (d). The main impact upon the sediment budget of these additional offshore losses is to "shift" the position of the drift divide in an easterly direction. For example, if there are no additional losses to the offshore as a result of the Street, the drift divide is located in BMU B. The position of the drift divide shifts to BMU C (for losses of 1 $m^3\ m^{-1}\ yr^{-1}$ in BMU B), and to BMU D (for losses of 2 $m^3\ m^{-1}\ yr^{-1}$ in BMU B) as the assumed offshore losses to the Street increase. A second effect of the increased offshore losses at the

Street is to reduce the quantity of material fed to Long Rock, from Tankerton.

The sediment budget, based upon an assumed loss of 2 m^3 m^{-1} yr^{-1} in BMU B, is consistent with the findings of the studies at East Tankerton (Canterbury City Council, 1992). However, as the volume of beach lost to, or gained from, the Street and the Long Rock area cannot be quantified, it is not possible to balance the budget with any confidence. Further studies on sediment transport and additional monitoring at these two areas will be required, if the budgetary approach is to succeed at Tankerton.

BMS[a]	9.2	9.5	9.9	10.5	11.5	12.1	12.2	12.3
Distance to Harbour (m)	1080	940	800	630	385	195	165	135
BMU[b]	D	D	D	C	B	A,B	A	A
XSA[c] Recharge (m^2)	58	118	75	200	87	77	113	88
Trend ($m^2\ yr^{-1}$)	0.44	1.37	-0.22	-1.85	-1.62	-0.42	-0.42	0.58
Std Error in Trend	0.15	0.38	0.29	0.57	0.48	0.29	0.21	0.18
Beach Stability	A[d]	A	S[e]	E[f]	E	E	E	A

where: (a) Beach Monitoring Station; (b) Beach Management Unit; (c) cross-sectional area; (d) accreting; (e) stable; (f); eroding; see Figure 6.3 for locations.

Table 6.1 Details of Beach Monitoring Stations at Whitstable Central and results of regression analysis.

BMU	D	C	B	A	Total A to D
Length (m)	465	185	250	195	1095
Volume Recharge (m^3)	18070	20500	26548	52429	117547
Trend ($m^3\ yr^{-1}$)	4	-242	-316	-36	-591
Std Error in Trend	31	85	77	114	267
% Change in Volume per Annum	0.0 ±0.2	-1.2 ±0.4	-1.2 ±0.3	-0.1 ±0.2	-0.5 ±0.2
Beach Stability	S[b]	E[e]	E	S	E

where: (a) Beach Management Unit; (b) stable; (e); eroding; see Figure 6.3 for locations.

Table 6.2 Details of Beach Management Units at Whitstable Central and results of regression analysis.

Date	BMU[(a)]	Volume Added (m^3)
May 1978	E	7804
Jun 1978	D	1624
Jun 1978	E	11205
Jan 1985	E	2835
Jan 1986	E	3550
Feb 1987	E	1944

where: (a) Beach Management Unit; see Figure 6.7 for locations

Table 6.3 (a) Details of beach replenishments carried out at Herne Bay West: 1975 - 1994

BMU[(a)]	Volume Added	Net Added Annually
A	0	0
B	0	0
C	0	0
D	1624	98
E	27338	1657
Total	28962	1755

where: (a) Beach Management Unit; see Figure 6.7 for locations

Table 6.3 (b) Annually-averaged replenishment, added to each Beach Management Unit at Herne Bay West: 1975 - 1994

BLS[a]	33	34	35	36	37
Distance to Hampton Pier	130	300	735	1310	1705
BMU[b]	A,B	B	B,C	D	E
Pre-breakwater construction					
XSA[c] 1975 (m^2)	158	132	116	51	17
Trend (m^2 yr^{-1})	0.5	0.8	0.5	-0.1	0.2
Std Error in Trend	0	0	0	0	0
Beach Stability	A[d]	A	A	S[e]	S
Post-breakwater construction					
XSA 1992 (m^2)	158	145	129	52	na
Trend (m^2 yr^{-1})	0.7	-2.2	2.5	-5.9	na
Std Error in Trend	1.5	2.0	2.4	1.0	na

where: (a) Beach Monitoring Station; (b) Beach Management Unit; (c) cross-sectional area; (d) accreting; (e) stable; see Figure 6.7 for locations.

Table 6.4 Details of Beach Monitoring Stations at Herne Bay West and results of regression analysis for data collected between 1975 and 1994

BMU[a]	A	B	C	D	E	A to E
Length	125	455	580	300	605	2065
Pre-breakwater construction						
Volume 1975 (m^3)	19800	61300	67300	15300	10380	174080
Trend (m^3 yr^{-1})	62	326	310	108	na	813
Std Error in Trend	25	39	96	42	na	132
% Change in Volume per Annum	0.3 ±0.2	0.5 ±0.1	0.5 ±0.3	0.7 ±0.4	na	0.5 ±0.1
Beach Stability	A[b]	A	A	A	na	A
Post-breakwater construction						
Volume 1992 (m^2)	19750	66120	74820	15600	72000	248290
Trend (m^2 yr^{-1})	91	-471	1462	-1780	na	na
Std Error in Trend	191	675	1401	296	na	na

where: (a) Beach Management Unit; (b) accreting; see Figure 6.7 for locations.

Table 6.5 Details of Beach Management Units at Herne Bay West and results of regression analysis for data collected between 1975 and 1994

BMU	A		B		C		D		E	
Losses to offshore (m^3)	⇑ 66		⇑ 243		⇑ 294		⇑ 164		⇑ 324	
Beach Change / Longshore Feed (m^3)	**+62**	⇦*128*	**+326**	⇦*697*	**+310**	⇦*1301*	**+108**	⇦*1483*	**0**	⇦*150*
Feed from Recharge (m^3)	0		0		0		⇑ 90		⇑ 1657	

for location of BMU, see Figure 6.7

(a) Pre-Breakwater (1975-1992).

BMU	A		B		C		D		E	
Losses to offshore	⇑ 66		⇑ 243		⇑ 294		⇑ 164		0	
Beach Change / Longshore Feed	**+62**	⇦*128*	**+326**	⇦*697*	**+310**	⇦*1301*	**+0**	⇦*0*	**0**	⇦*0*
Feed from Recharge	0		0		0		⇑ 1465		0	

for location of BMU, see Figure 6.7

(b) Post-Breakwater (1992-1995).

Table 6.6 Annual-averaged sediment budget for Herne Bay Central showing situation: (a) pre-breakwater construction (1975 - 1991); and (b) post-breakwater construction (predicted)

Year	BMU[(a)]	Quantity (m^3)
1981	B	26
1981	C	1585
1981	D	13585
1982	E	1337
1984	D	3215
1985	B	2444
1985	C	4388
1985	D	360
1988	D	2347
1988	E	2347
1990	D	1697
1990	E	1448
1991	D	4444
Total	**All BMU**	**39223**

where: (a) Beach Management Unit; see Figure 6.9 for locations

Table 6.7 Beach Replenishments carried out at Tankerton: 1980 - 1994

BMS[a]	12.8	13	13.5	14	15	16	17	18	19	20	21	22	23	24	25	26	27
Representative length (m)	280	180	160	235	350	230	115	55	75	60	50	120	195	200	220	240	160
Trend ($m^2 yr^{-1}$)[c]	-0.2	-1.1	-1.1	-0.1	-1.4	0.2	-3.0	-1.1	-0.6	-0.7	0	0.5	-0.4	0.4	0.6	-0.3	1.6
Change (Rep. length), $m^3 yr^{-1}$	-56	-198	-176	-24	-490	46	-345	-61	-45	-42	0	60	-78	80	132	-72	256
BMU[b]	A			B			C				D				E		
Length, (m)	620			930			240				735				400		
Change(BMU) $m^3 yr^{-1}$	-430			-813			-148				+62				+184		
Est. Offshore Losses, ($m^3 yr^{-1}$)	-310			-465			-120				-368				-200		
Recharge, ($m^3 yr^{-1}$)	+2			+191			+458				+1496				+342		

where: (a) Beach Monitoring Station; (b) Beach Management Unit; (c) trend is based upon regression analysis of cross-sectional area; see Figure 6.9 for locations.

Table 6.8 Details of regression analysis (1980 to 1994) for: (a) profile data collected from Beach Monitoring Stations at Tankerton; and (b) Beach Management Units at Tankerton

Beach Management Unit		A		B		C		D		E	
Offshore loss (0.5 m^3 $m^{-1}yr^{-1}$)		⇑ 310		⇑ 465	•	⇑ 120		⇑ 368		⇑ 200	
Beach Change / Longshore Feed (m^3)	⇔250	**-430**	⇔*128*	**-813**	⇒ 411	**-148**	⇒ *897*	**+62**	⇒ *1963*	**+184**	⇒*1921*
Feed from Recharge (m^3)		⇑ 2		⇑ 191		⇑ 458		⇑ 1496		⇑ 342	

for location of BMU, see Figure 6.9

(a) 0.5$m^3m^{-1}yr^{-1}$ offshore losses.

BMU		A		B		C		D		E	
Offshore loss, (0 m^3 $m^{-1}yr^{-1}$		0		0		0		0		0	
Beach Change / Longshore Feed (m^3)	⇔250	**-430**	⇒*182*	**-813**	⇒ *1186*	**-148**	⇒*1792*	**+62**	⇒*3326*	**+184**	⇒*3384*
Feed from Recharge (m^3)		⇑ 2		⇑ 191		⇑ 458		⇑ 1496		⇑ 342	

for location of BMU, see Figure 6.9.

(b) no offshore losses.

Table 6.9 Sediment budget for Tankerton based upon beach profile data collected between 1980 and 1994, assuming: (a) offshore losses of 0.5 $m^3 m^{-1} yr^{-1}$; (b) no net offshore losses

Beach Management Unit		A		B		C		D		E	
Offshore loss, (1.0 m^3 $m^{-1}yr^{-1}$)		⇑ 310		*⇑ 930*		⇑ 120		⇑ 368		⇑ 200	
Beach Change / Longshore Feed (m^3)	⇔250	**-430**	*⇔ 128*	**-813**	*⇔ 54*	**-148**	*⇒ 432*	**+62**	*⇒ 1498*	**+184**	*⇒ 1456*
Feed from Recharge (m^3)		⇑ 2		⇑ 191		⇑ 458		⇑ 1496		⇑ 342	

for location of BMU, see Figure 6.9

(c) 0.5$m^3m^{-1}yr^{-1}$ offshore losses in A,C,D,E; 1.0$m^3m^{-1}yr^{-1}$ offshore losses in B

Beach Management Unit		A		B		C		D		E	
Offshore loss, (0.5 m^3 $m^{-1}yr^{-1}$)		⇑ 310		*⇑ 1860*		⇑ 120		⇑ 368		⇑ 200	
Beach Change / Longshore Feed (m^3)	⇔250	**-430**	*⇔ 128*	**-813**	*⇔ 984*	**-148**	*⇔ 498*	**+62**	*⇒ 568*	**+184**	*⇒ 526*
Feed from Recharge (m^3)		⇑ 2		⇑ 191		⇑ 458		⇑ 1496		⇑ 342	

for location of BMU, see Figure 6.9

(d) 0.5$m^3m^{-1}yr^{-1}$ offshore losses in A,C,D,E; 2.0$m^3m^{-1}yr^{-1}$ offshore losses in B

Table 6.9 (cont) Sediment budget for Tankerton based upon beach profile data collected between 1980 and 1994, assuming: (c) offshore losses of 0.5 $m^3 m^{-1} yr^{-1}$, and additional losses of 0.5 $m^3 m^{-1} yr^{-1}$ to the Street from BMU B; (d) offshore losses of 0.5 $m^3 m^{-1} yr^{-1}$ and additional losses of 1.5 $m^3 m^{-1} yr^{-1}$ to the Street from BMU B

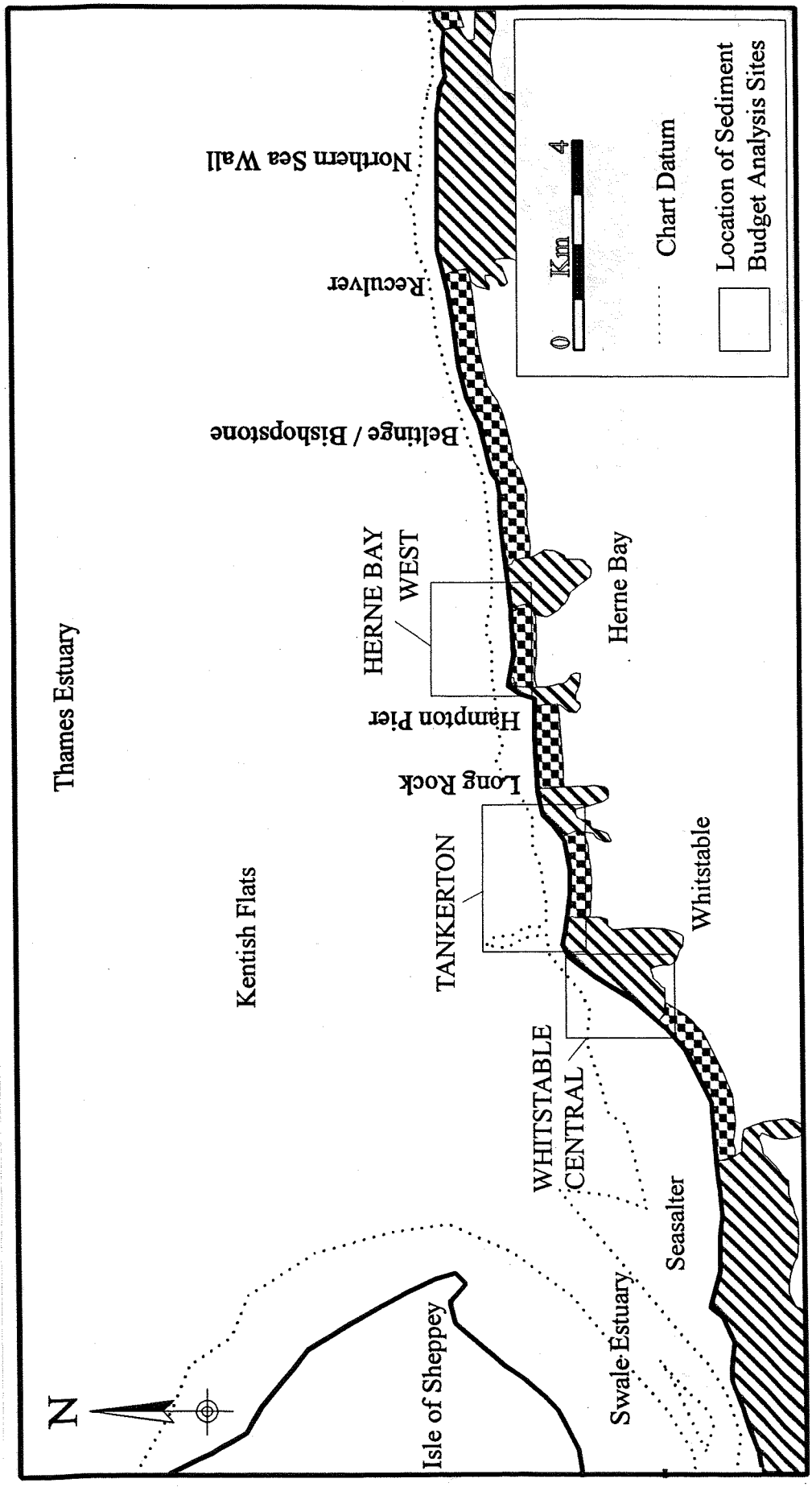

Figure 6.1. Location of sites where the sediment budget has been assessed

Figure 6.2. Net annual potential longshore transport rates for the study area

Figure 6.2 (cont) Net annual potential longshore transport rates for the study area

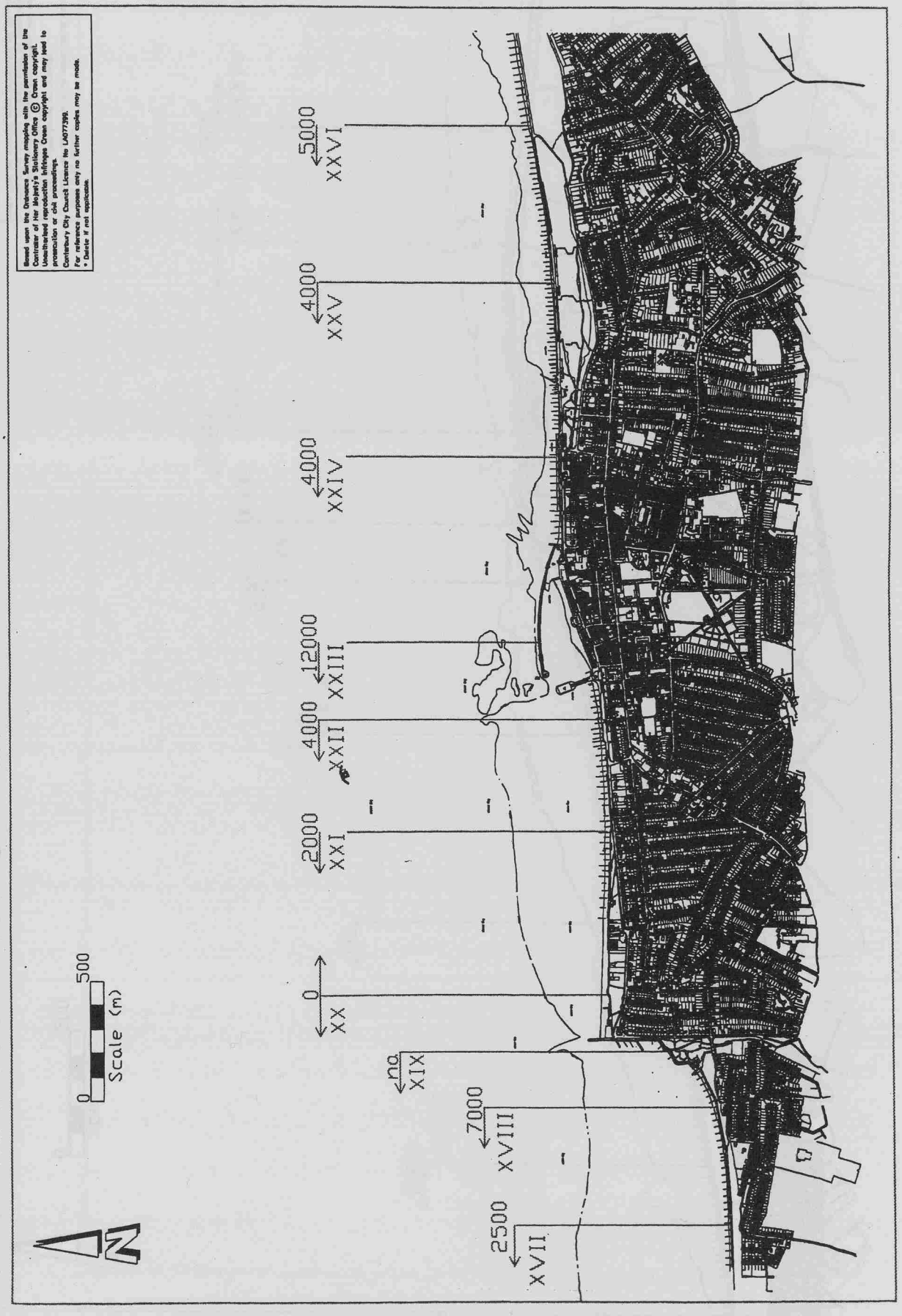

Figure 6.2 (cont) Net annual potential longshore transport rates for the study area

Figure 6.2 (cont) Net annual potential longshore transport rates for the study area

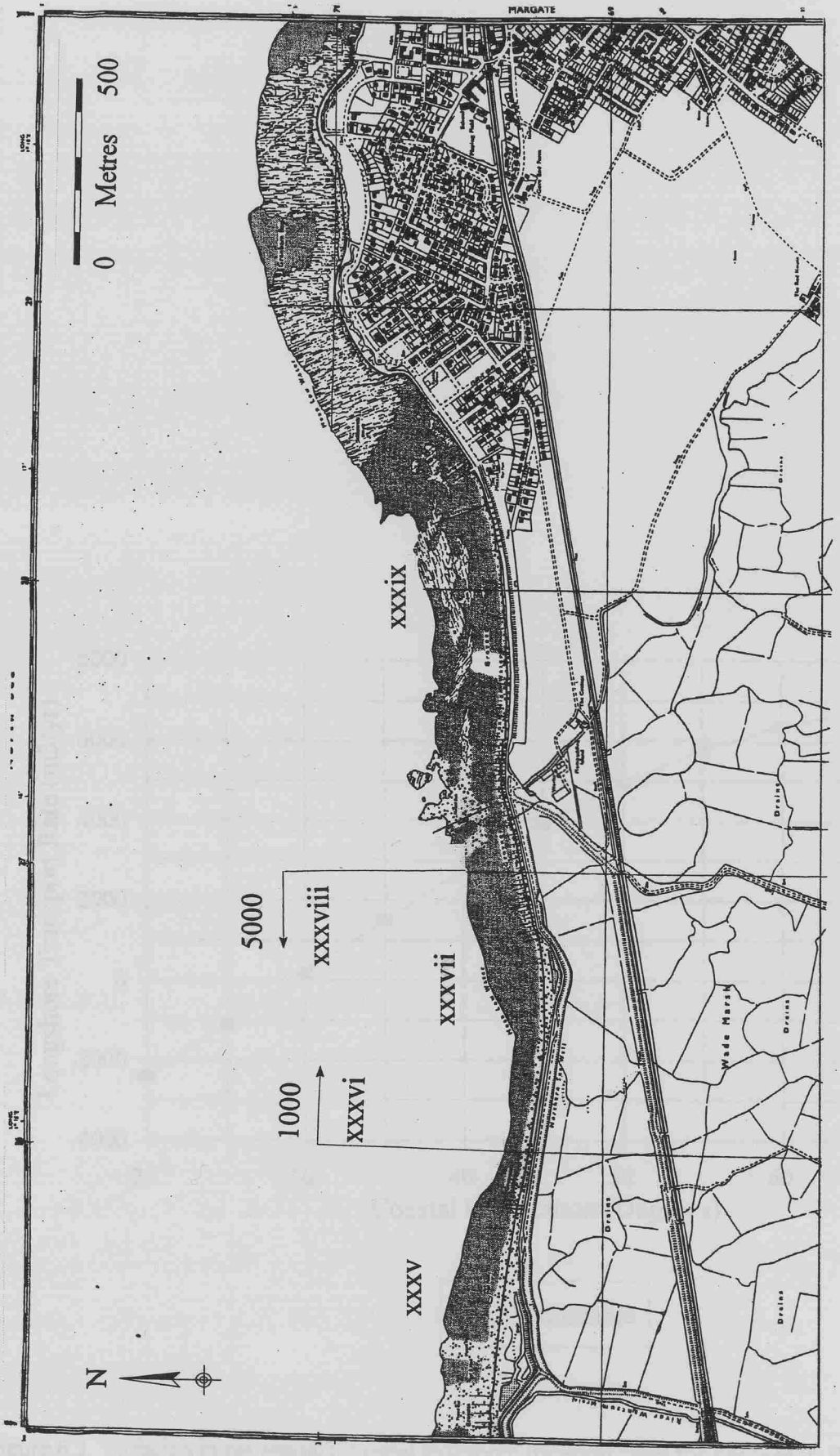

Figure 6.2 (cont) Net annual potential longshore transport rates for the study area

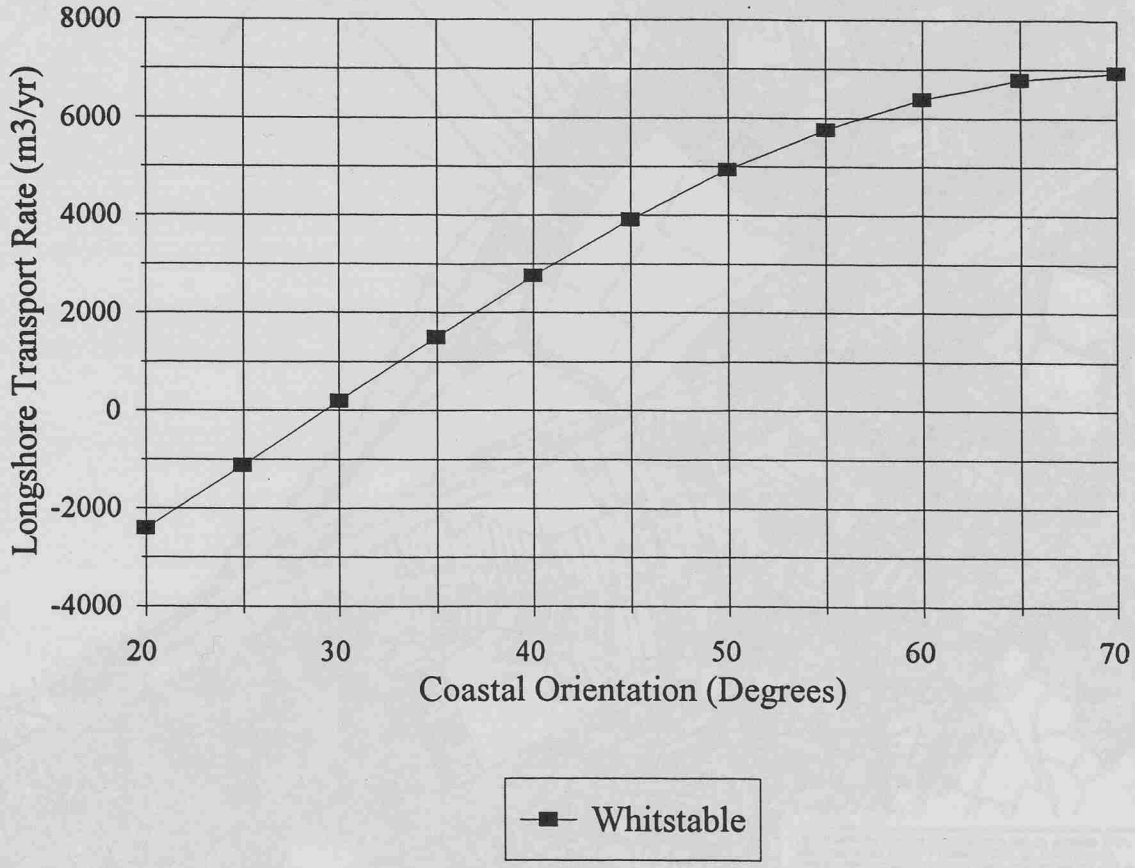

Figure 6.3. Variation in net annual potential longshore transport rates for beaches in Whitstable Central (based upon coastal model, see section 6.2.2).

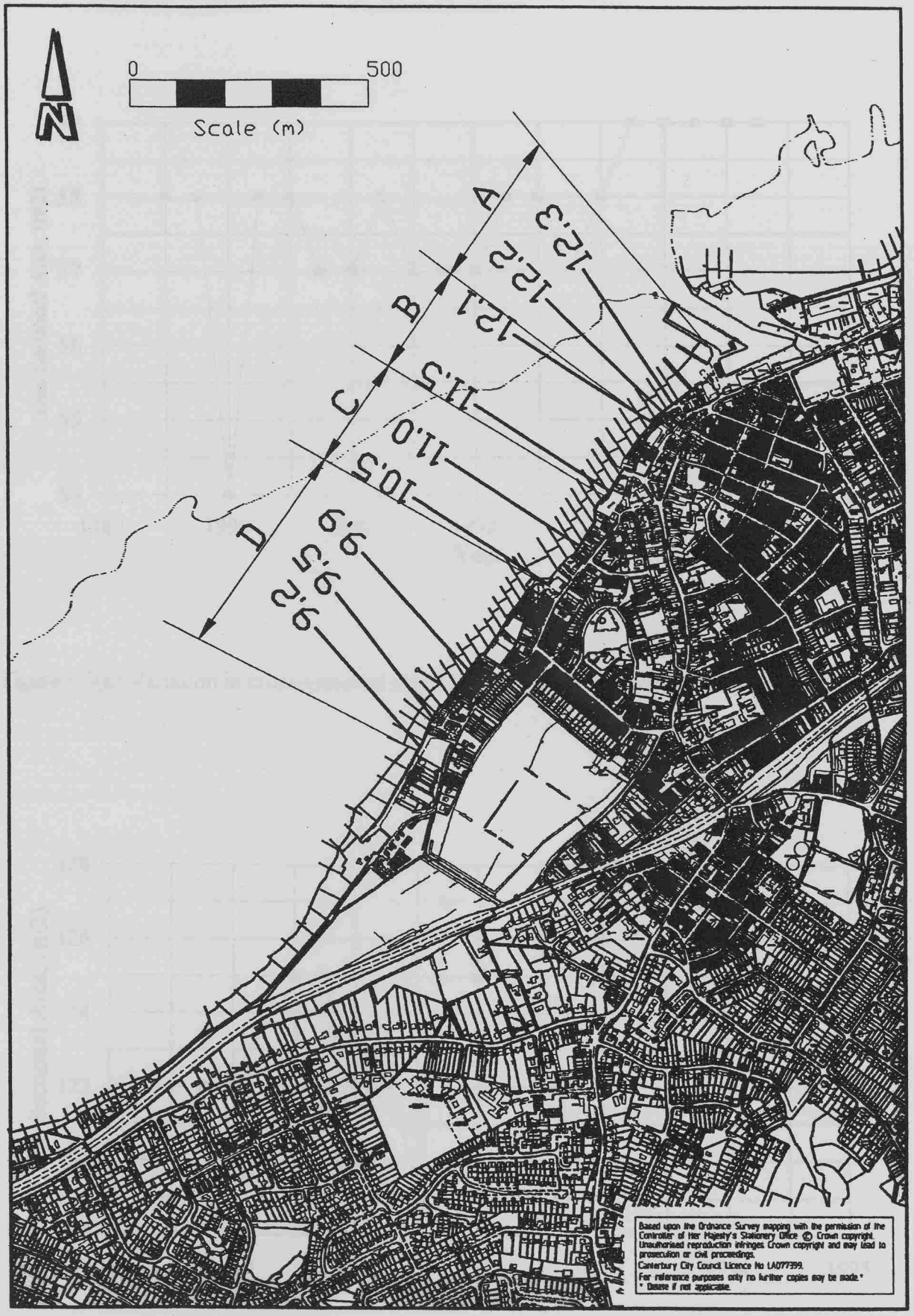

Figure 6.4 Extent of sediment budget study at Whitstable Central, showing location of Beach Monitoring Stations and Beach Management Units

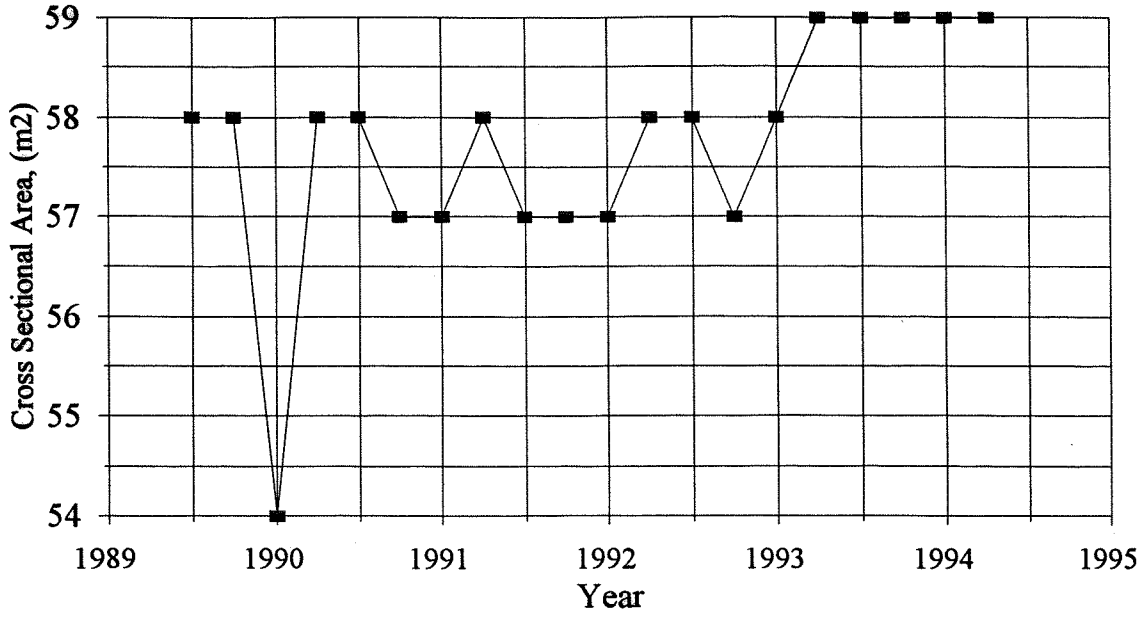

Figure 6.5(a) Variation in cross-sectional area of beach, BMS 9.2 (Whitstable): 1989 - 1994

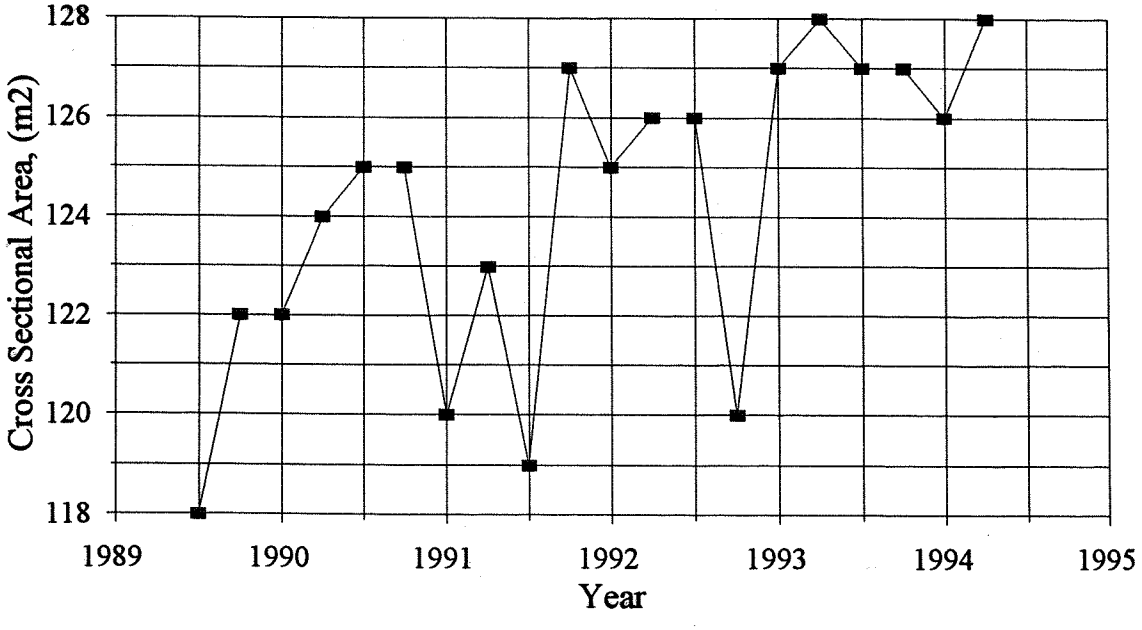

Figure 6.5(b) Variation in cross-sectional area of beach, BMS 9.5 (Whitstable): 1989 - 1994

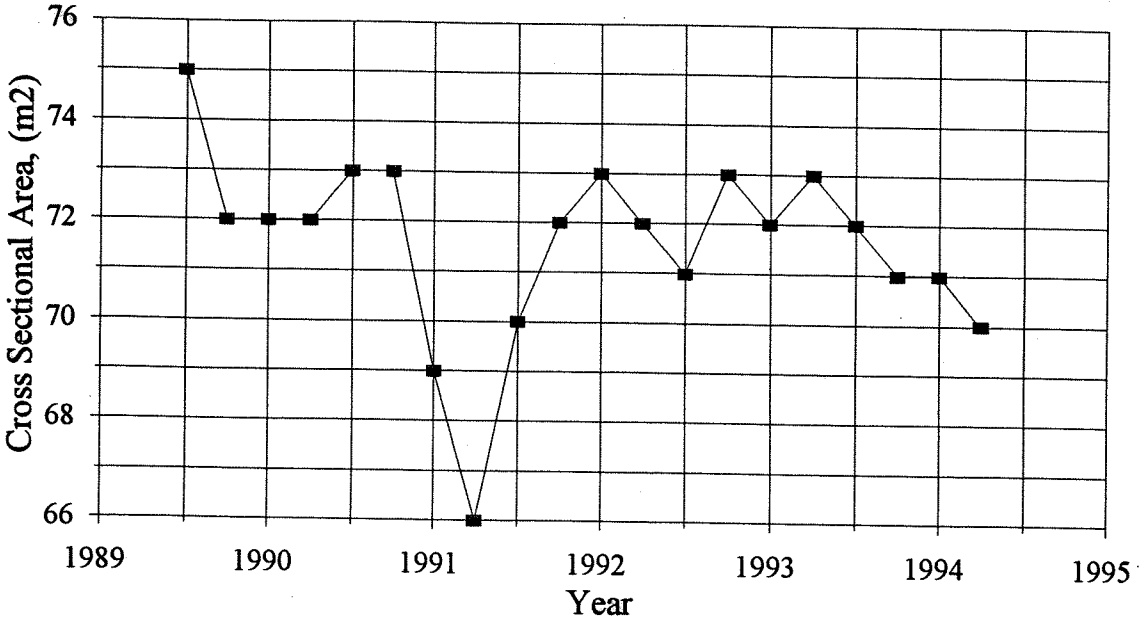

Figure 6.5(c) Variation in cross-sectional area of beach, BMS 9.9 (Whitstable): 1989 - 1994

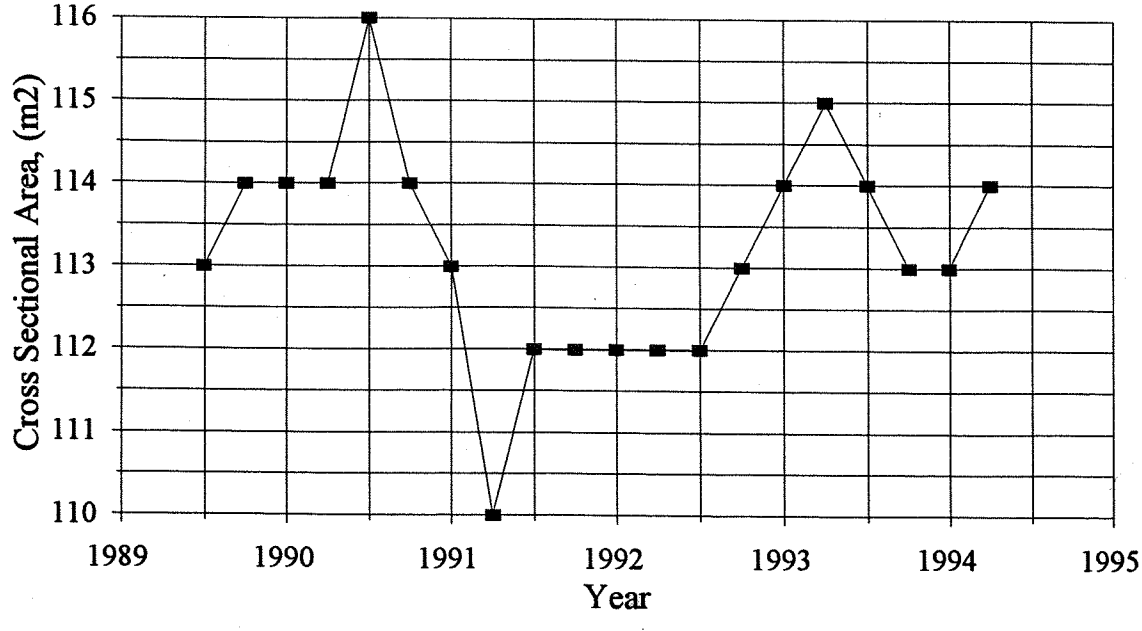

Figure 6.5(d) Variation in cross-sectional area of beach, BMS 10.5 (Whitstable): 1989 - 1994

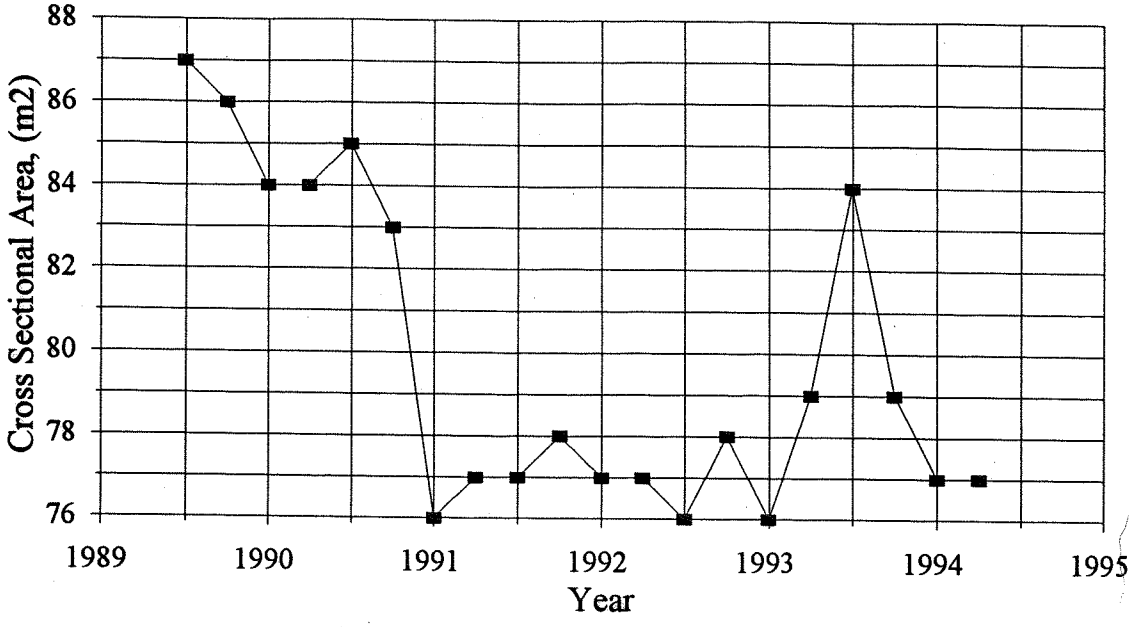

Figure 6.5(e) Variation in cross-sectional area of beach, BMS 11.5 (Whitstable): 1989 - 1994

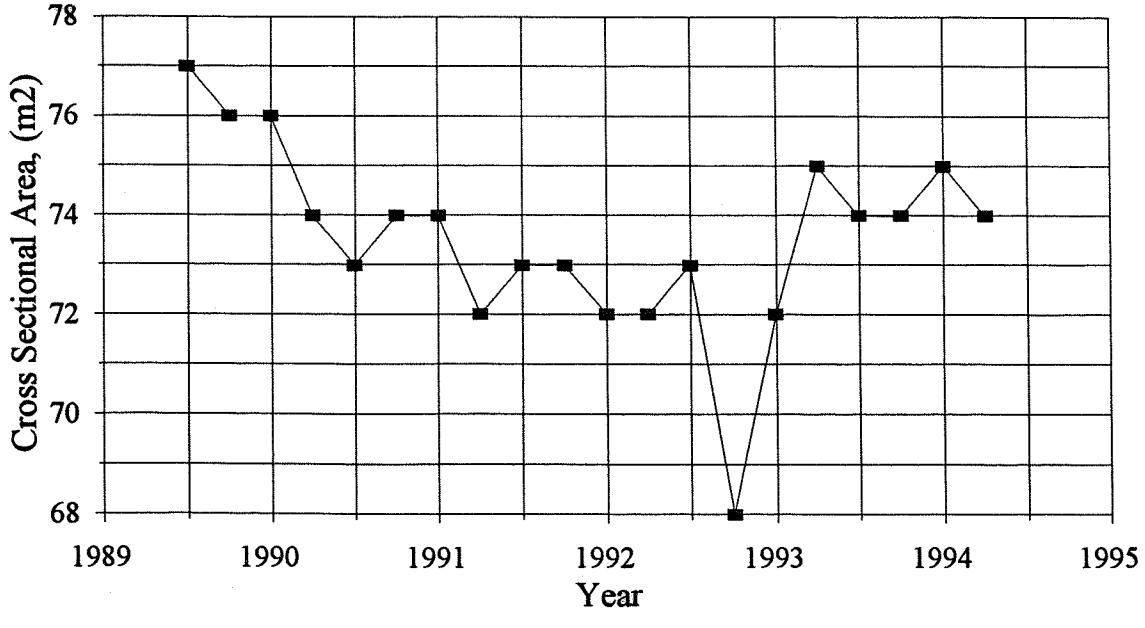

Figure 6.5(f) Variation in cross-sectional area of beach, BMS 12.1 (Whitstable): 1989 - 1994

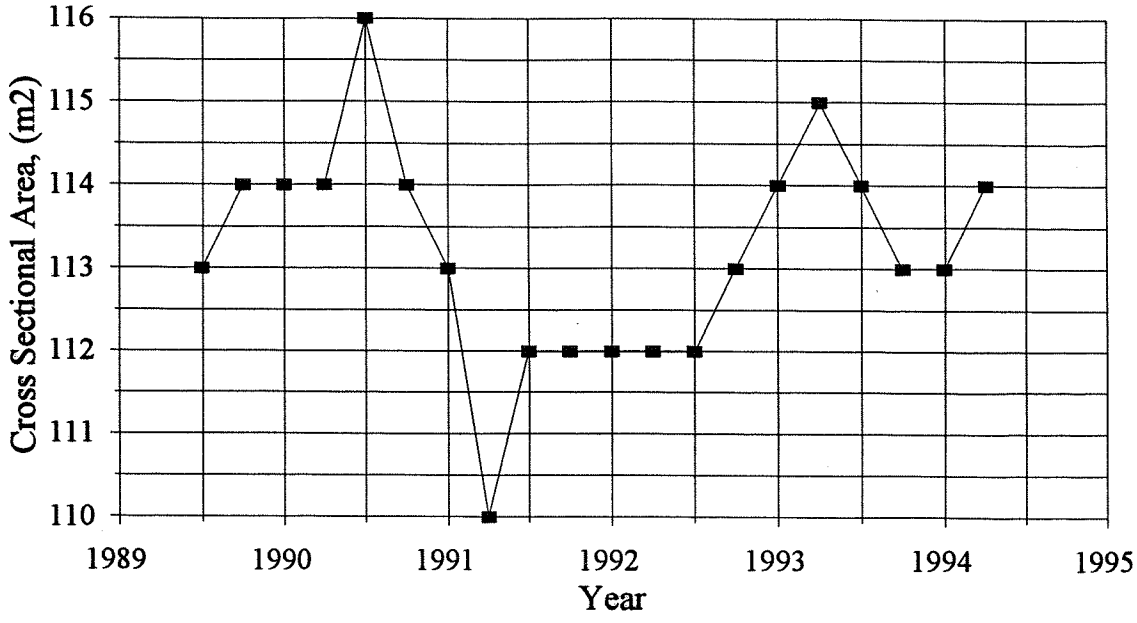

Figure 6.5(g) Variation in cross-sectional area of beach, BMS 12.2 (Whitstable): 1989 - 1994

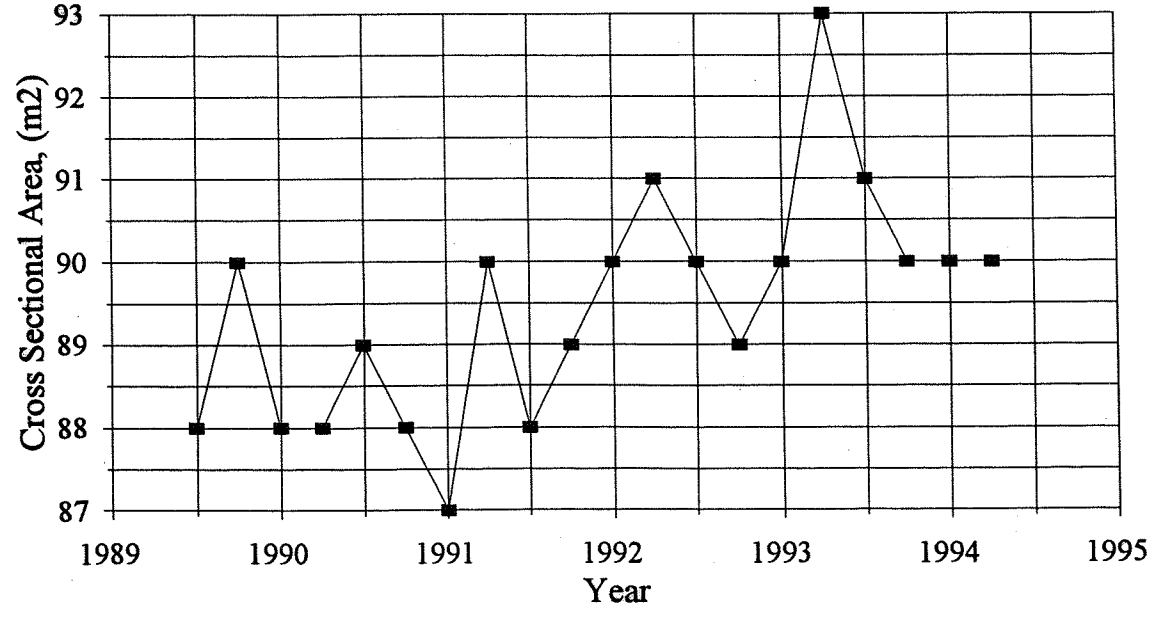

Figure 6.5(h) Variation in cross-sectional area of beach, BMS 12.3 (Whitstable): 1989 - 1994

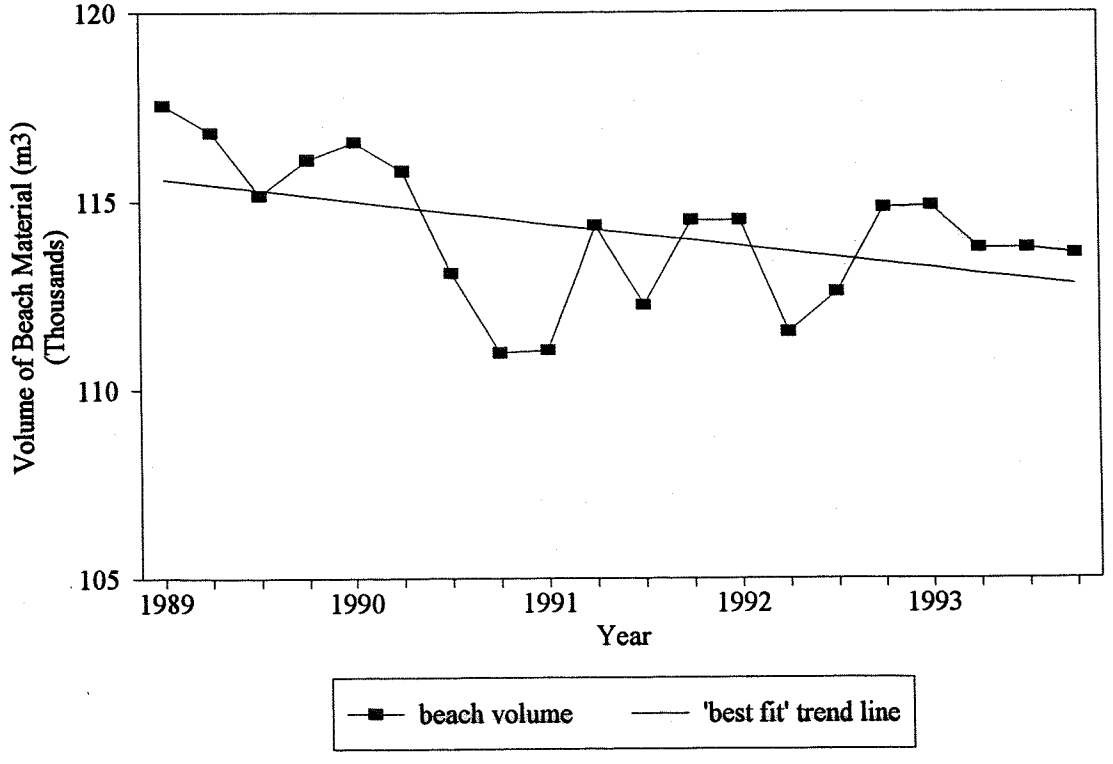

Figure 6.6 Variation in the total volume of beach material at Whitstable Central: 1989 - 1994

Figure 6.7 Extent of sediment budget study at Herne Bay West, showing location of Beach Monitoring Stations and Beach Management Units

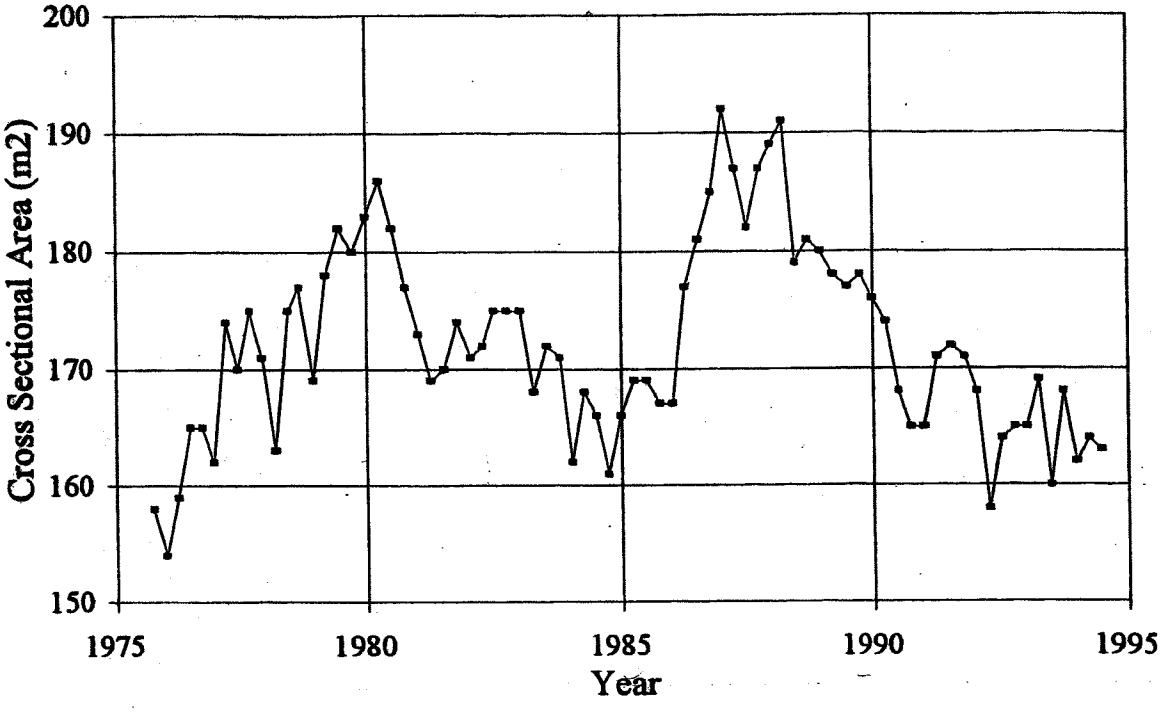

Figure 6.8(a) Variation in cross-sectional area of beach, BMS 33 (Herne Bay; 1975 - 1994)

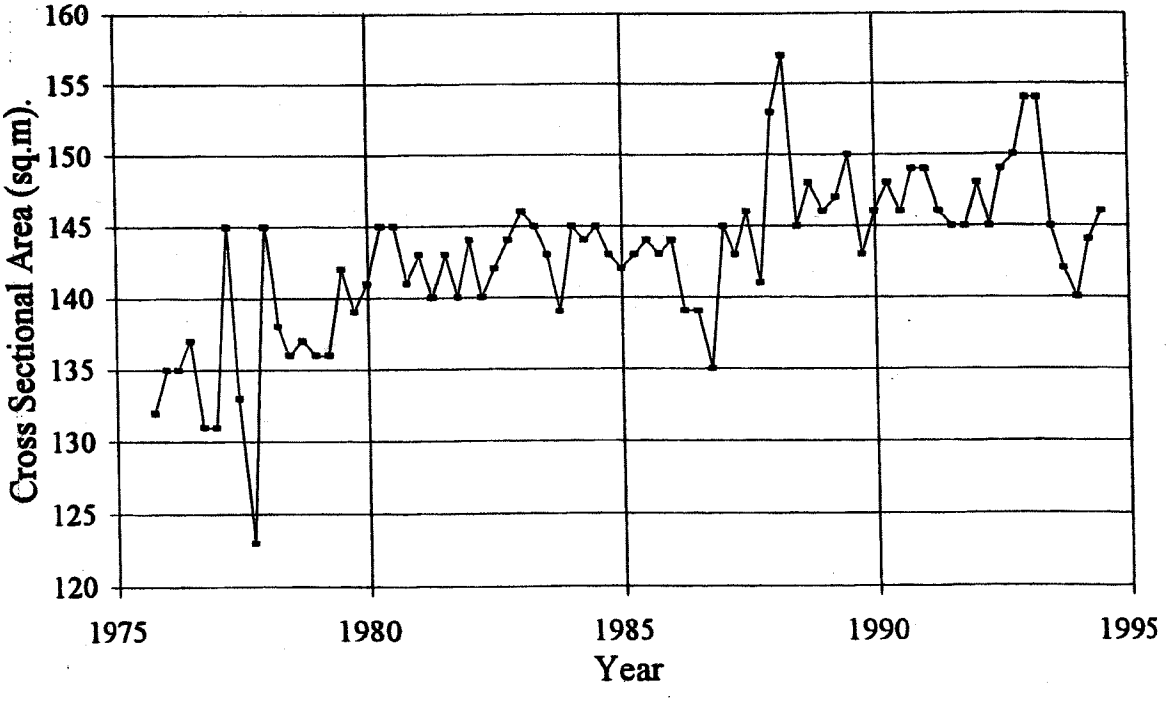

Figure 6.8(b) Variation in cross-sectional area of beach, BMS 34 (Herne Bay; 1975 - 1994)

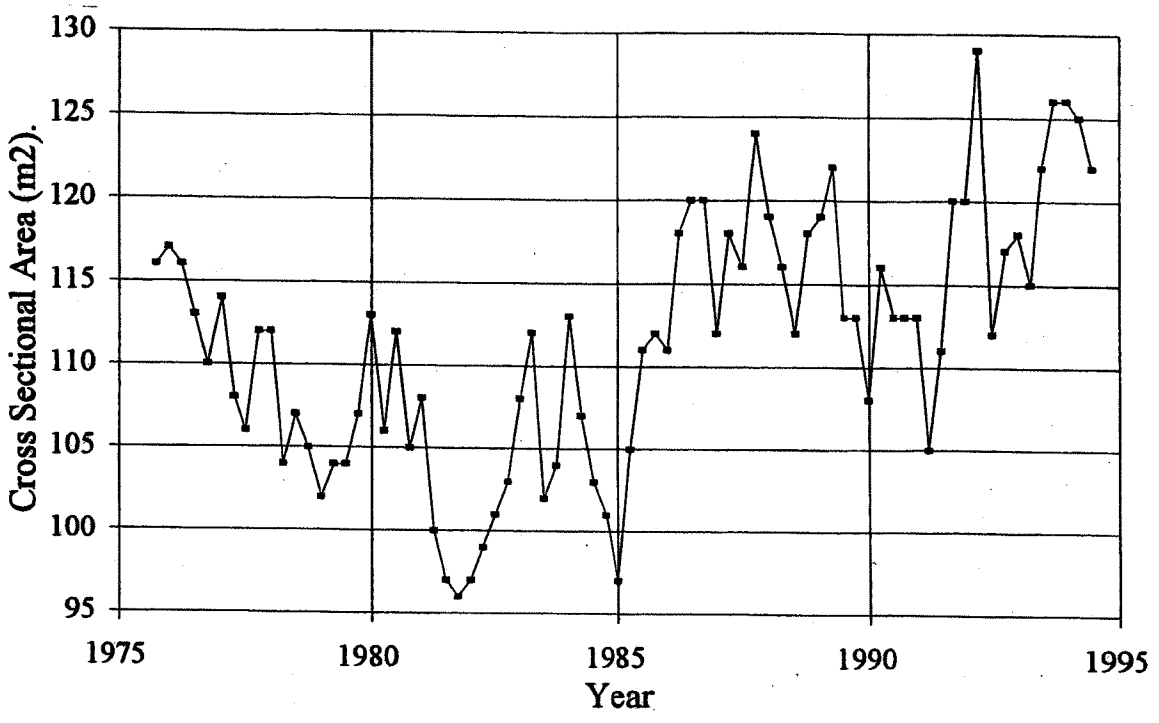

Figure 6.8(c) Variation in cross-sectional area of beach, BMS 35 (Herne Bay; 1975 - 1994)

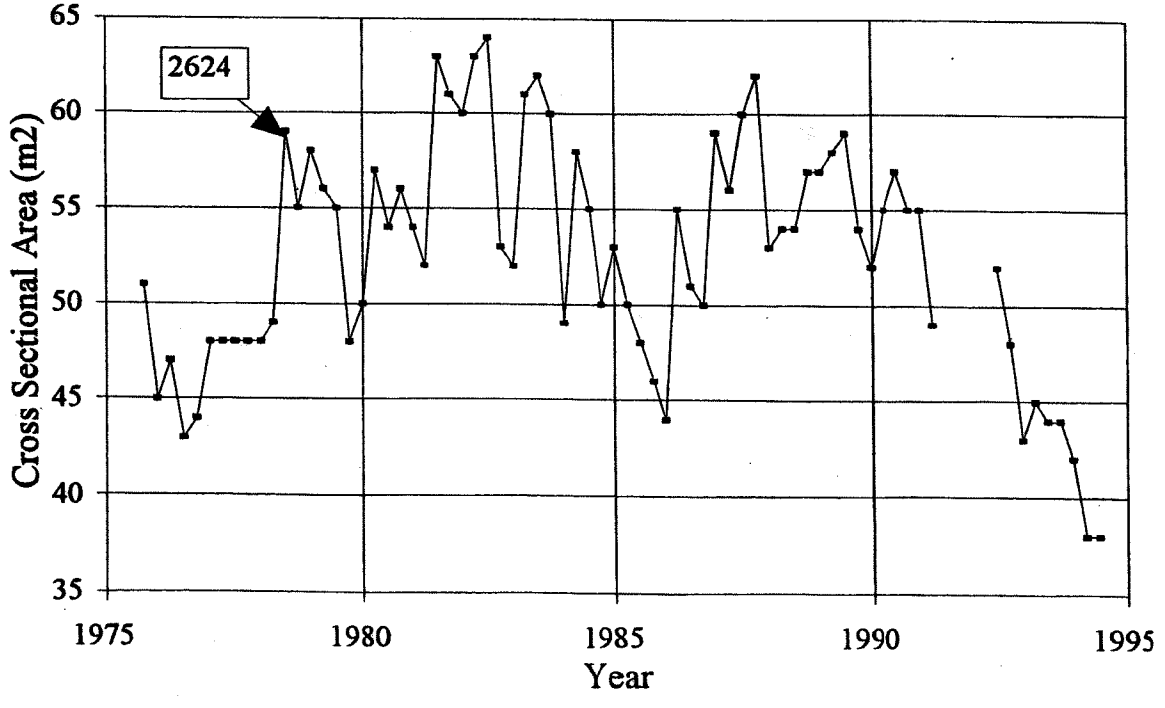

Figure 6.8(d) Variation in cross-sectional area of beach, BMS 36 (Herne Bay; 1975 - 1994)

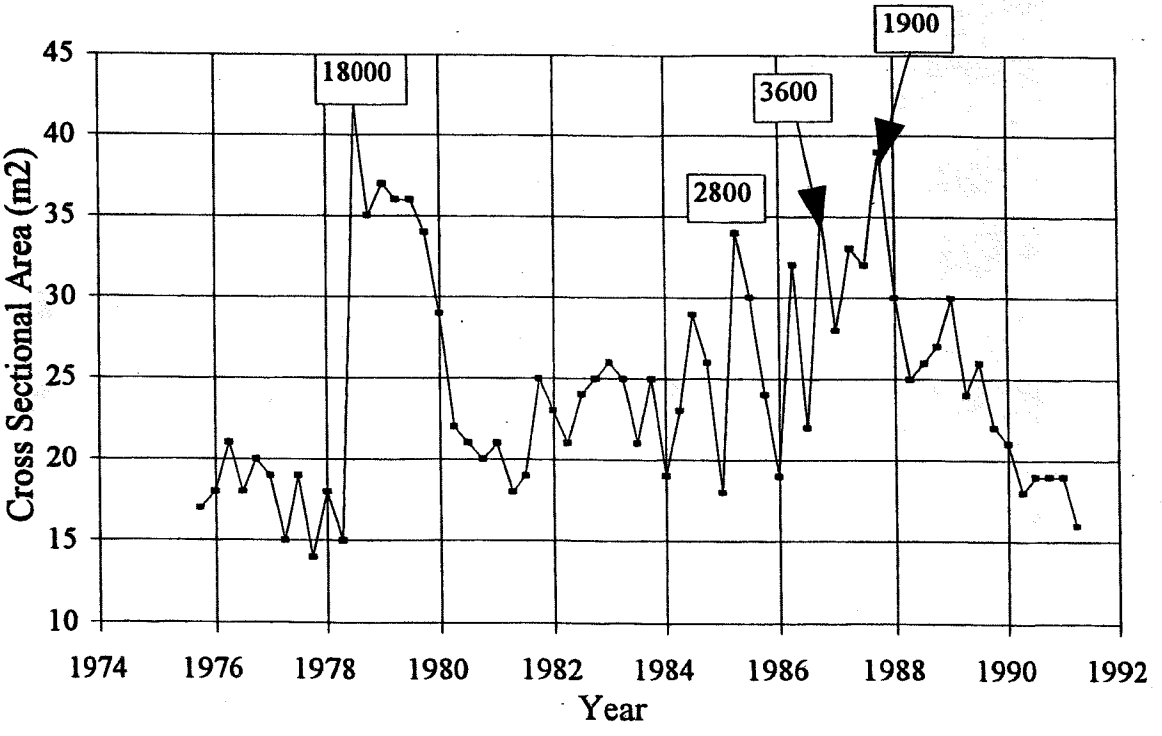

Figure 6.8(e) Variation in cross-sectional area of beach, BMS 37 (Herne Bay; 1975 - 1994)

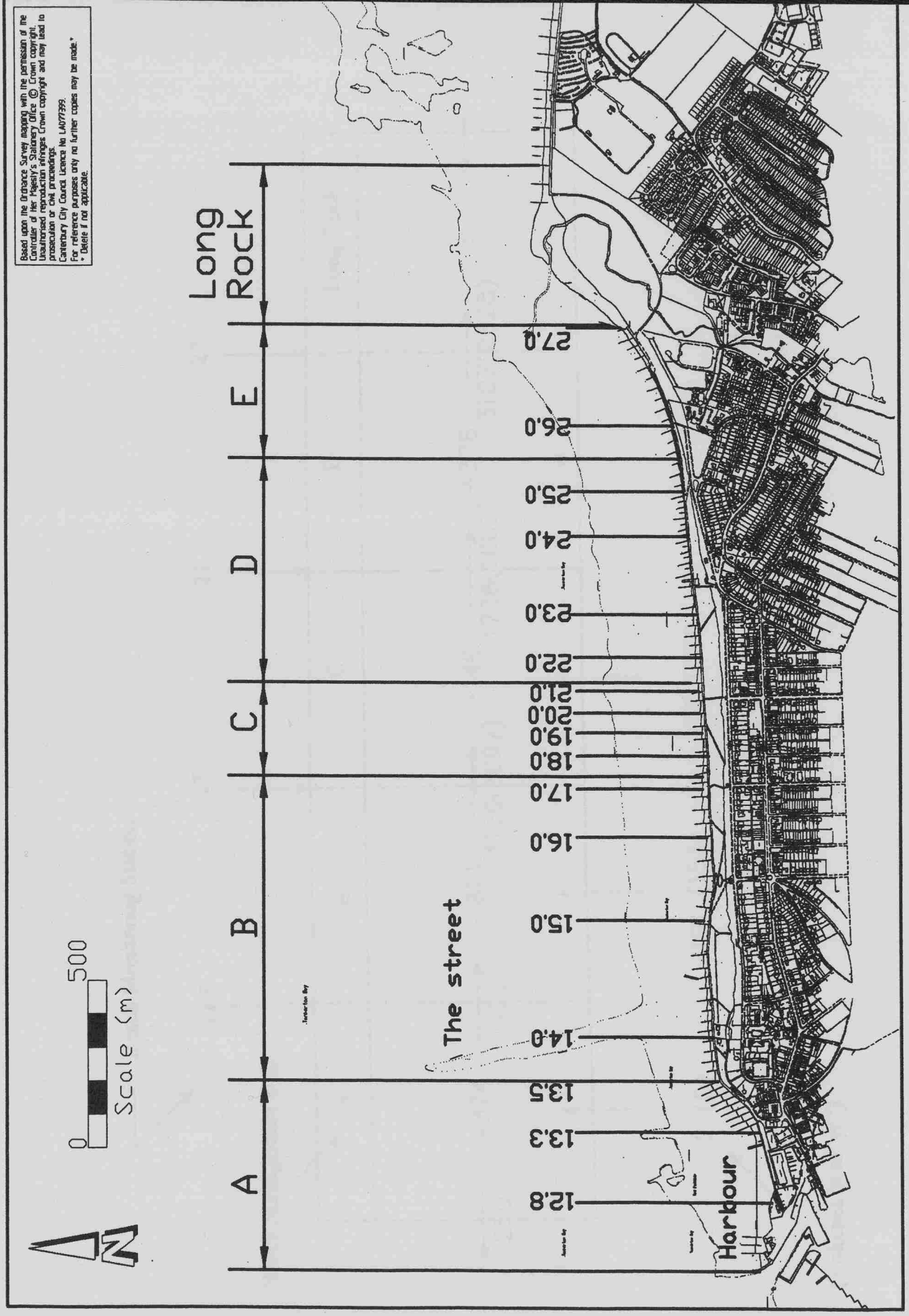

Figure 6.9 Extent of sediment budget study at Tankerton, showing location of Beach Monitoring Stations and Beach Management Units

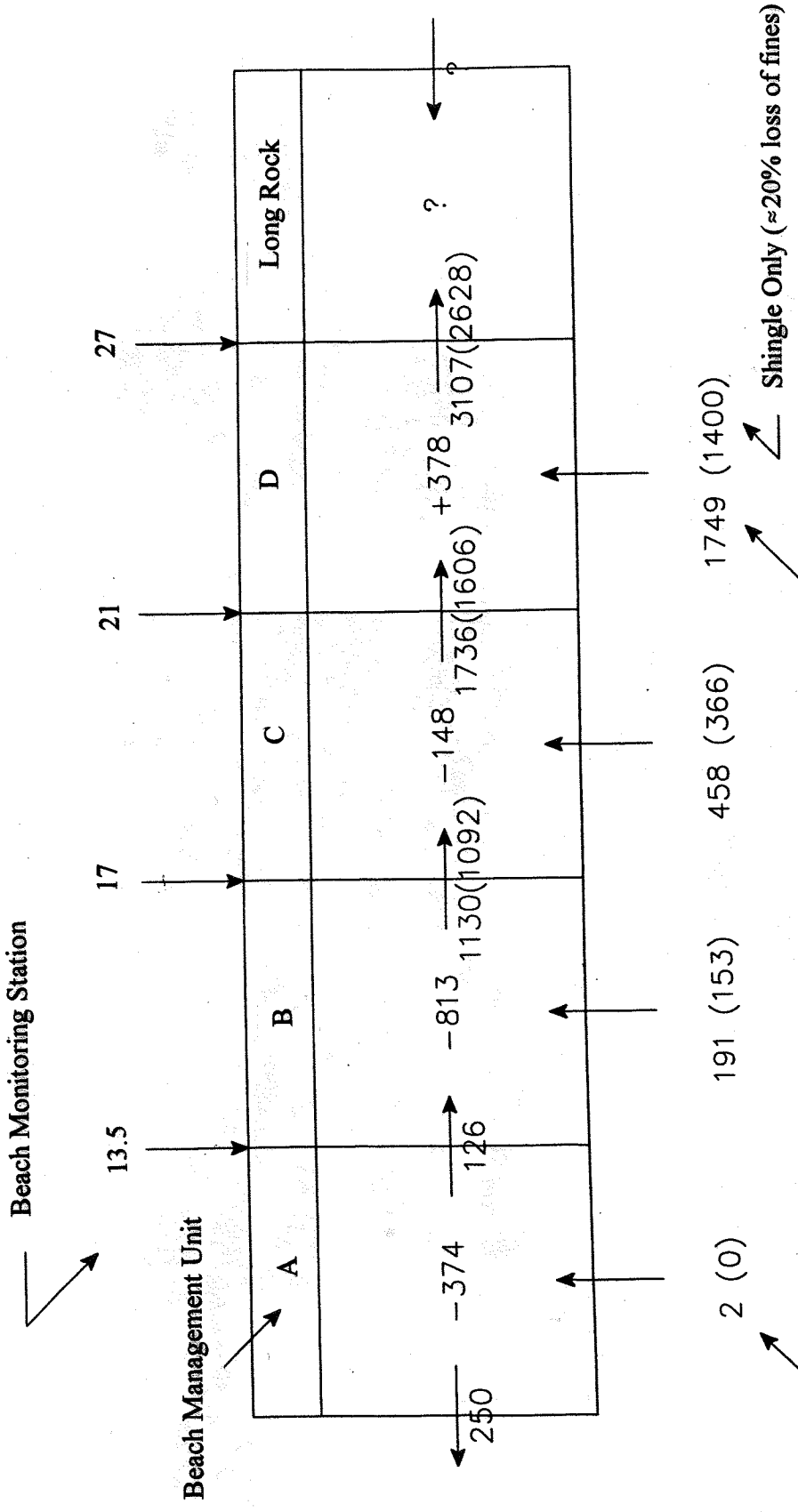

Figure 6.10 Sediment Budget for Tankerton based on beach profile data, 1980 - 1994, after Delft Hydraulics (1995)

Chapter 7: Discussion.

7.1. Introduction.

Within the UK, the emphasis on the management of the shoreline (for flood and coastal protection purposes) has shifted from addressing particular erosion problems on individual sites to a more strategic approach. This involves consideration of the whole coastal environment over longer time scales (typically 50 years) and upon a regional basis (for example, Shoreline Management Plans (MAFF, 1995) and Strategy Plans (MAFF, 1997). Within the context of such a strategic approach the importance of natural coastal processes cannot be overstated, (McFarland and Edwards 1998b).

The hydrodynamics of the shingle beaches along the North Kent coastline are not well understood, having failed to attract the same level of scientific interest, as their coarse clastic equivalents along the coastlines of Southern England, (Carr, 1983), Ireland (Carter and co-workers) and New Zealand (Kirk and co workers). Further, processes active on the North Kent beaches are likely to be distinct from those which are experienced at the locations noted earlier. This is due to the mixed sedimentological nature of the beaches and the particular wave climate which operate as a result of the presence of a wide and shallow nearshore region.

7.2. Hydrodynamics of the Study Area

7.2.1. General Points.

Wave conditions along the North Kent coast are characteristically low in amplitude. This is illustrated in the scattergraph compilation of over seven years of recorded wave data at the Whitstable Harbour site, (Figure 4.3(a)) and from the exceedence of recorded wave heights, Figure 4.4(a,b). Only 0.1% of waves recorded at Whitstable Harbour exceed 1.0m (Hs); 2.4% of the recorded waves exceed 0.5m (Hs). Interestingly, a significant wave height of 0.5m is equivalent to the threshold of movement for shingle beaches under wave action (Brampton and Motyka, 1987); this implies that beaches within the study area will be mobile for just over 2% of the time.

It was also noted from the wave records (Figure 4.3(a)), that for 56% of the time, significant wave heights recorded at Whitstable Harbour were less than 0.05m. Whilst this is partly a result of (tidal) water level variations (see section 7.2.2), it is also a reflection on the low wave energy nature of the site.

As well as being of low amplitude, the waves tend also to have short periods, (Figure 4.3(a)). For example, recorded waves with a significant wave height of greater than 0.15m are rarely associated with periods (Tz) greater than 6.5s. The mean wave period from the wave records is in the range 3.5 to 4.5 seconds; consequently, waves within the study area are steep.

The absence of a significant swell wave component (>0.15m) has already been noted. This is due to the high level of energy dissipation which occurs over (i) the numerous sediment banks located around the mouth of the Thames Estuary (Figure 2.5) combined with the wide area of shallow water (the Kentish Flats) which comprises the nearshore region.

The tidal range at Whitstable is approximately 6m. Over the duration of a tidal cycle, wave action takes various forms. Around low water, wave energy is expended in the shallow water of the Thames Estuary and over the extensive intertidal areas. Around high water, less wave energy is expended in the nearshore area and consequently is incident upon the beaches. A dramatic change in slope from the lower foreshore (typically 1 in 1000) to the steep shingle beaches (typically 1 in 8) results in plunging breakers. These waves expend high levels of wave energy over the narrow breaker and swash zones (Carter, 1990).

7.2.2. Coastal Hydrodynamics Model

The hydrodynamics in the study area have been investigated using a coastal hydrodynamics model (Chapter 4). The model comprises: (i) hindcasting of 'offshore' wave conditions from local wind data; (ii) transforming waves onto the beaches using a commercial wave propagation package (ENDEC) and; (iii) derivation of nearshore wave climates based upon the wave model results and the joint probability of occurrence of wind direction, wind speed and water level.

The wave propagation model used is one dimensional; it calculates wave modifications along

a pre-determined profile. The model was designed to operate in extensive areas of shallow water where wave breaking and frictional losses tend to be more important than wave refraction (Delft Hydraulics 1990b).

Whilst the model was found to perform well in general, there were difficulties associated with its application to those sections of the coastline which deviated from the general, uniform, east - west orientation. For example, at Long Rock (Plate 2.1(c)) refraction of waves is likely to be important in determining the patterns of wave energy which is incident along the beach in the local area.

The most sensitive parameters in the wave model were found to be the bottom friction factor and the overall depth of water. The friction factor can be varied to provide a better correlation with recorded data (Delft Hydraulics, 1990b) however, in the present investigation, it was not found to be necessary to adjust this from the initial value of 0.01 (typical of a sandy bottom).

Due to the shallow nature of the nearshore region, relatively small variations in the water level were found to have a major impact on the modelled waves, particularly under moderate to high wave energy conditions. The most dramatic example of this is around the time of low water when no wave action is able to reach the beaches. Because of the importance of water level on wave generation and propagation, a wide range of water levels were included at the offshore wave hindcasting stage. The water level was taken into account, at the wave propagation stage, by the inclusion of the water level distribution in the joint probability analysis to derive the nearshore wave climates.

Similar studies (Delft Hydraulics 1990a, 1995) have used just one or two water level scenarios to model the wave conditions and, ultimately sediment transport patterns, within the study area. Due to the sensitivity of the wave propagation to wave level, this approach would have lead to an over-simplification of the sediment transport processes.

Neither the offshore wave conditions nor the tidal currents were found to have a major influence on wave conditions ultimately experienced on the shoreline. Offshore waves tended to be modified by shoaling and wave breaking in the shallow water areas such that the final product of wave propagation was depth limited wave conditions. Tidal currents of greater than

1 to 2 ms^{-1} will have significant influence on wave heights and angles experienced at the coastline (Al-Mansi, 1990). Generally, tidal currents in the study area are below 1ms^{-1} in velocity.

The performance of the wave model was compared to actual recorded waves at Whitstable Harbour for a total of 840 "events". Overall the model performed well. For example, the percentage exceedence of significant wave heights of 1.0m (0.2%) and 0.5m (2.9%), derived from the coastal model were similar to those recorded at Whitstable Harbour (0.1% and 2.4% respectively).

A comparison between recorded and predicted wave conditions was also carried out for individual events when the recorded Hs exceeded 0.5m. The available data were subdivided into wind direction sub-sets and the relationship between recorded and predicted waves derived (Table 4.4). This shows that there is a tendency to over-predict the significant wave height of waves generated by winds from northerly and northeasterly directions, by about 15%.

For water levels below +1.0 m AOD, the comparison between predicted and recorded waves was less encouraging; the results for Sector 1 being particularly poor (Table 4.4; Figure 4.5(a)). This however was attributed to the difficulties in collecting wave data in shallow water when there was the likelihood of waves breaking over the recorder head. For water levels greater than 1.0m AOD the model results were more consistent with the recordings.

Comparison of the coastal hydrodynamics model with recorded wave data at Whitstable Harbour and at Long Beach, Whitstable was undertaken as a part of the field studies into longshore transport processes described in Chapter 5. Comparison of the coastal hydrodynamics model with the wave conditions recorded over the three day duration of the field trial demonstrated some variation between recorded and modelled wave conditions.

A reasonable correlation was obtained for the data sets collected during the day-time however, for the two evening recording periods, the model significantly underestimated the recorded wave conditions (by approximately 20 - 30%) in the evening. As these recordings were made in the winter-time, it is suggested (section 5.3.6) that the discrepancies may be due to the temperature effects on the relative viscosity between the surface of the sea and the air (Resio

and Vincent, 1977).

It was also noted during the field study that the local generation of waves within the Swale Estuary (Figure 2.5) may be important along the coastline to the west of Whitstable Harbour. Wave conditions recorded at Whitstable Harbour, during a period of west-southwesterly winds, were much larger (Hs ≈ 1.0m) than predicted. By contrast, at Long Beach, which is partly sheltered from the Swale Estuary by Whitstable Harbour, the predicted wave conditions were more accurate. The greater wave heights recorded by the Whitstable Harbour recorder are attributed to the local generation of waves within the Swale Estuary. The Harbour recorder is ideally suited to record these waves as it faces directly into the channel of the Swale Estuary; the impact of this wave action on the coastline is limited to area west of the Harbour.

Unfortunately, no instrumental recorded wave angle data is available for either the long term data set at the Harbour nor from the Long Beach arrays. It is not possible therefore to assess the performance of the wave model in this respect.

Typical uncertainties for recorded wave conditions are given by Soulsby (1997). For Hs and Tp, Soulsby (op cit) considers that the errors are in the order of 10%. For wave angle, a 15% error can be expected.

7.2.3. Hydrodynamic characteristics of the study area

A combination of extensive areas of shallow water over the whole of the nearshore region in the study area, combined with the limited fetch lengths and depths, leads to a wave climate within the study area which is characterised by relatively low significant wave heights and short periods. The wave climate is dominated by steep waves which are locally generated. This is in contrast to sites on the south coast of England, where 'low energy' swell waves have been found to dominate the coastal processes regime (Whitcombe 1995, Powell 1996).

Onshore winds in the study area are dominated by those which blow from the west or northwest however, due to the shorter fetches and shallower water to the northwest, waves which are generated by, the less common, northeasterly and easterly winds tend to have larger

wave heights and longer periods (Figure 4.8, Figure 4.9).

Wave heights and periods experienced on the beaches in the study area, generally, increase from west to east, reflecting the more open marine conditions which persist in the eastern part of the Thames Estuary. Whilst waves conditions generated by winds blowing from each of the onshore directional sectors increase towards the east, there is an indication that this increase in wave conditions is larger for westerly and northwesterly winds. This results in a reduction of the directional inequality in wave energy towards the east (Section 4.5.4). This has important consequences for the equilibrium angle of the coastline (Section 5.7).

Based upon 10 years of wind data at Manston Airport, there is evidence of a seasonal variation in the wind climate. During the winter months, the dominant onshore winds are from the west and north-west. By contrast in the summer months, winds from the north-east are more common (Figure 4.7(b&c)). Again, this has important implications for the equilibrium angle of the coastline (Section 5.8).

The winter months tend also to have more strong winds; this in turn leads to a increase in recorded wave activity over the same period (Figure 4.3(b&c)). The increase in wave energy experienced during the winter months may be enhanced by the (temperature-related) stability effect described earlier (Resio and Vincent, 1977).

Despite the relatively moderate wave climate experienced in the study area, the low-lying coastal regions have been subject to severe flooding in the past. The reason for the intensity of these flooding events can be attributed to the elevation of still water levels as a result of meteorological conditions - surges and seiches (section 4.6.2).

Examination of the these 'storm' events, demonstrates that the predicted (astronomical) high water levels may be exceeded by a considerable amount. For example, during the storm which occurred on 1st February 1953, still water levels were over 2m higher than expected, at the time of high tide. Examination of Table 4.13, which gives details of the storm events recorded at Whitstable between (1986 and 1993), shows that the Highest Astronomical Tide of +3.1m AOD is exceeded on a regular basis. These large deviations from the predicted tidal levels are a further consequence of the shallow water nature of the study area, as water level variations

occurring in the southern North Sea are enhanced up the estuary, (Pugh, 1980).

A tendency for extreme water levels to coincide with strong, northwesterly winds was noted by Ackers (1972), (Table 4.12(a,b)). Data recorded at Whitstable during storm events (Table 4.14) tends to confirm Ackers (op cit) findings. Based upon water level data obtained from Sheerness, and wind data from Shoeburyness, Hydraulics Research (1981, 1985) described also, the interdependency between water level and wind conditions which exist in the present area of investigation.

Figure 4.13, which is based on the data collected by Hydraulics Research (op cit) demonstrates clearly the dependency between the wind direction and the high water surge residual. For example, a high water surge residual of +0.8m is three times more likely to occur in conjunction with northwesterly winds than with any other wind direction. At lower levels of probability, the effect is more pronounced; a high water surge residual of +1.4m at Whitstable has a return period of 40 years, when in association with north-westerly winds, compared with a return period of 600 years for any other wind direction.

The impact of the elevated water levels upon the beaches is three-fold: (i) the wave breaker zone is pushed further inshore; (ii) due to the increased water depths, larger wave heights and angles can be sustained up to the point of breaking; (iii) the beach tends to be exposed to wave activity for a longer period of time. From a coastal processes point of view, the beach is exposed to a higher level of wave energy for a longer period of time. This increases the potential longshore transport rate and allows wave run-up to extend further up the beach; both of these factors could lead to enhanced erosion and beach destabilisation.

Enhanced erosion may also occur as a result of 'climatic anomalies' in which weather conditions deviate markedly from the 'normal' conditions. Comparison between the wind speed and direction occurrences for the winter of 1995 / 1996 (October 1995 to March 1996) and the average winter conditions for 1979 / 1989, is summarised in Figure 5.17. This demonstrates that during the winter of 1995 to 1996, a reversal in the average winter wind patterns occurred. Typically the winter period is dominated by westerly and northwesterly winds (as described earlier) however, during the winter of 1995 - 1996, northeasterly and easterly winds were dominant. The occurrence of deviations of this type and duration may

have major impacts on coastal sediment processes as described later.

7.3. Sediment Dynamics of the Study Area.

7.3.1. General.

Beaches in the study area are characteristically 'mixed' in nature, comprising sand and shingle-sized material in varying proportions; in this respect they are similar to the beaches described by Mason et al (1997). Sediment type on the surface layers of the beach varies both temporally and spatially. A typical variation in the distribution of sediments along a shore-normal profile is shown in Figure 5.2. Although the sediment distribution will deviate from this particular example, there is a distinct onshore - offshore zonation of the beach as follows: (i) coarse-grained beach ridges around the high water mark; (ii) a sandy strip of variable width immediately to seaward of the coarse-grained ridges; and (iii) a poorly-sorted mixture of sand and shingle extending to the beach toe.

Within the study area, the transport of shingle is dominated by bed-load transport under plunging waves. Due to the steepness of the beaches, wave energy is expended in a narrow band encompassing the breaker and swash zones (Carter, 1989); hence this is where the bulk of sediment transport tends to occur (Muir Wood, 1970). Intense bed-sheer stresses and turbulence occur within this zone leading to grain-grain collisions and often ejection of particles from the water (Carter and Orford, 1993).

Wave energy dissipation on shingle beaches occurs through wave breaking and frictional losses, Powell (1988). In this respect the roughness of the surface of the beach is important. Additional energy dissipation may occur within the body of the beach as a result of percolation. This mechanism is important in the swash zone, where the wave run up is attenuated by the percolation of water into the sediments, provided that the water table within the beach is not high.

The threshold of movement of coarse grained material was considered by Brampton and Motyka (1987) to occur when the significant wave height exceeded 0.5m. Within the present study, the movement of beach sediments has been noted under significantly lower wave heights

(≈0.2m) (see for example Plate 5.2).

Sediment transport on shingle beaches occurs in several modes depending upon factors such as wave conditions and the sediment grading. For example, Carter and Orford (1993) describe situations where shingle beaches develop transport resistant structures where groups of similarly-sized pebbles aggregate; interaction between the pebbles produces an armouring effect which resists movement.

In contrast, individual pebbles may be incompatible with the surrounding sediment and are left exposed on the surface of the beach; this process of clast rejection has been described by Moss (1963). Clasts which are rejected are subjected to current and wave action leading to potentially high transport rates. Once mobile, the pebble will continue to move rapidly until either it moves out of the area where it is subject to current and wave action, or until it reaches an area of beach where the particles are of a similar size and shape. In the latter case the pebble will be incorporated into the bed. Once rejected, larger clasts tend to be transported further as they are less likely to become trapped within a bed of finer material (Muir Wood, 1970).

The size / shape sorting mechanisms described above are responsible for: (i) the organisation of particles into alongshore facies assemblages; (Carter and Orford, 1993) and; overestimation of longshore transport rates derived from tracer pebbles, particularly if recovery depends upon visual recognition (Whitcombe, 1995). The transport of painted tracers across the sand run at Long Beach, Whitstable under low energy wave condition (Plate 5.2) is an example of particle rejection.

7.3.2. Longshore Transport Model.

The longshore transport model is based upon the modelled wave climate and the "Delft" longshore transport formula. The "Delft" formula was developed primarily from laboratory experiments and then relating the measured transport rates to the measured hydraulic parameters. The formula is derived by determining the mathematical relationship between groups of dimensionless variables. As the formula is derived empirically and is not processes based, the method of calculation of longshore transport ignores the different transport mechanisms which occur.

Further, as a result of scale effects, it has been suggested (Brampton and Motyka, 1987) that coarse-grained laboratory experiments provide an overestimate of the rate of longshore transport. This suggestion has been supported recently by van Wellan et al (1999), who found that the "Delft" formula overestimated longshore transport by a factor of 6 when calculating transport rates at Shoreham in southern England. In contrast, Schoonees and Theron (1996) assessed 52 longshore transport equations against a data base of field measurements from around the world and found that the "Delft" formula (along with the formula of Kamphius (1992)) provided the best estimate of longshore transport over a range of conditions.

Field studies have been carried out into longshore transport at Long Beach, Whitstable, as part of the present investigations (Chapter 5). It was found that predictions of longshore transport obtained using the "Delft" formula compared well to transport rates based upon beach plan surveys and the displacement of electronic tracer pebbles.

Over the three day period of the experiment at Long Beach, the "Delft" formula predicted a net longshore transport rate of $475m^3$, which is comparable to the rates obtained by the displacement of electronic tracer pebbles ($313m^3$ - over two days) and the analysis of volumetric changes in the beach plan surveys ($515m^3$). Whilst comparison between the transport rates summed over the three day period are in close agreement, this masks considerable variation in the daily transport rates. For example, longshore transport rates determined from the volumetric changes on 23/01/93 were greater than the rates determined from both the electronic tracer displacements by a factor of almost 3. For the two succeeding days, the rates determined from volumetric changes were lower than those determined by the two alternative methods.

Each method of determining the longshore transport rate is subject to limitations as described below.

longshore transport model

- calculations are based upon a mean grain size of 6mm. During the tidal cycle, different parts of the beach will be subjected to wave forces and hence the grain-size of material in transport will alter. Muir Wood (1970) noted that the bulk of transport occurs in the upper beach; hence

the grain-size used in calculations may be too small.

- the "Delft" formula was derived for 'gravel' beaches, not for mixtures of sand and shingle.

- longshore transport formula are very sensitive to variations in wave angle. The calculations used in the present investigation are based upon the output of the wave model which has not been calibrated against instrumentally recorded data.

- no account has been taken of the effect of currents on longshore transport. Mason (pers comm) has found that currents should be considered when calculating sediment transport on tidal beaches of mixed composition.

tracers

- although high recovery rates of the electronic pebbles were obtained, throughout the duration of the experiment, the small number of tracers used introduces a high level of uncertainty into the calculations.

- the calculation of the depth and width of the mobile layer over a tidal duration is suspect; this is because the depth of disturbance derived from measurement of tracers represents the maximum depth of disturbance which has occurred at some point during the tidal cycle; it does not represent the average depth of the mobile later over the duration of the experiment. Recent studies at Lancing, southern England suggest that transport rates calculated using tracer-derived mobile layer volumes may overestimate the transport rates by a factor of 2 (Stapelton et al, 1999).

- under the wave conditions experienced throughout the field trials at Long Beach, it is believed that mixing of tracers with the indigenous material occurred rapidly. However, those tracers located initially on the sand run may have been subjected to high transport rates before mixing occurred. Again this would lead to an overestimate of transport volumes.

- low recovery rates for aluminium tracers are attributed to the low efficiency of the search procedures due to the combined effects of a large number of items of trash, low depths of

detection and inability to cover the whole search area during a single tide. As a result, the aluminium tracers have not been used for transport calculations.

profiles

- whilst surveys undertaken using the EDM theodolite can be carried out to a high degree of accuracy, the extent of coverage of the survey and the profile lines in particular, may not be at a high enough resolution to accurately determine volumetric changes. Averaging of data over several surveys tends to reduce these errors.

- loss of the sand fraction to the offshore may occur during periods of moderate to strong wave activity. This leakage of sand-sized material would lead to underestimates of the longshore transport rates derived on the basis of volumetric changes.

general comments

Each of the three estimates of longshore transport described are based upon different assumptions of what material is being transported. The movement of the coarsest fraction of the sediment distribution is determined using the electronic tracers. Analysis of volumetric changes determines the transport of both sand and shingle-sized material present on the beach. As described earlier, the longshore transport model is based upon 6mm shingle, and may not accurately represent transport rates on a beach of mixed composition where the transport mechanisms are likely to be different.

7.3.3. Sediment Dynamic Characteristics of the Study Area

The wave climate was used in conjunction with the longshore transport formula, to assess the potential longshore transport rates at various locations in the study area. The wave model calibration factors (Table 4.4) were applied. The results are discussed, critically in Section 6.2.

A number of observations on the nature of processes in the study area can be made based upon the coastal model.

- towards the east, the increasing importance of the westerly / northwesterly component of the nearshore wave climate (Section 7.2.3) is manifest as an anticlockwise rotation of the predicted equilibrium coastal orientation towards an east - west alignment.

- the winter - summer variation in wind direction is reflected in the respective longshore transport potentials. At the Long Beach site, this was reflected in a reversal of the net transport direction between winter and summer seasons.

- storm events can result in large volumes of longshore transport over a single tidal cycle. For example, at Long Beach, Whitstable, the estimated longshore transport rate during one tidal cycle at the peak of the 1st February 1953 storm event was in the order of $1000m^3$. The net annual potential longshore transport rate at the same location is just $+320m^3$.

- the volume of material transported alongshore during a storm event depends more on the incident wave angle on the beach, than on the wave height, period or still water level.

- periods of time characterised by winds blowing from more or less the same direction have the ability to transport large quantities of beach material in one direction. For example the impact of the anomalous wind conditions experienced during the winter of 1995 / 1996 (Figure 4.17) resulted in failures of seawalls at Reculver and undermining of sea defences at Tankerton.

- the averaging of transport rates over a period of several years can mask the dramatic impacts of events which occur over shorter time periods.

- the averaging of transport rates over a period of several years will not account for longer-term variations in the wind directions. Such variations can lead to shifts in the 'annual' wave climate and hence equilibrium orientation of the coastline.

An assessment of the sediment budget based upon archived beach profile data can provide important information on the longshore and on-offshore transport processes. Provided that losses and gains from longshore transport and beach replenishment are known, the budget can be balanced by exchanges to the offshore area.

At Whitstable Central, no longshore transport was possible as a result of the large closely spaced groynes. A net reduction in the volume of beach within this area was attributed to offshore loss of fines in the order of 0.5 $m^3 m^{-1} yr^{-1}$.

At Herne Bay West, closure of the budget at both ends of the beach management unit was possible. Net losses of fines to the offshore at the rate of around 0.5 $m^3 m^{-1} yr^{-1}$ was similar to that obtained at Whitstable. The sediment budget at Herne Bay West was used to: (i) estimate actual (average annual) longshore transport rates in the BMU; (ii) based upon (i), estimate the impact of the existing groynes on the potential net annual potential longshore transport rates obtained from the model; (iii) assess the impact of the construction of the Herne Bay breakwater on patterns of erosion within the BMU and (iv) assess the requirements for future beach recharge and recycling projects in the BMU.

In the case of the Tankerton budget, closure to longshore transport was possible at the west end only. Attempts to balance the budget at this location, lead to uncertainties as to the actual transport patterns in the area, in particular: (i) the quantity of beach material which is transported into the Long Rock area from Tankerton; (ii) the extent of offshore losses/gains with particular respect to the Street and; (iii) the location of the sediment drift divide,

Chapter 8: Conclusions and Recommendations for Further Research

8.1. Conclusions

The following conclusions can be ascertained from the present investigation:

- wave action in the study area is characterised by low amplitude, short period waves;
- the beaches are macrotidal and water level variations impose a major control on the wave climate and hence patterns of shingle mobility;
- output from the wave model provides a reasonable comparison with recorded wave data collected over a 10 year period;
- there is an inequality in the wave energy incident on the beaches, in which waves generated by northeasterly and easterly winds dominate. The inequality in wave conditions decreases towards the east;
- significant elevation of water levels in the study area occurs as a result of storm surges - this allows larger waves with greater wave angles to reach the beaches;
- there is an interdependency between extreme water levels, wind speed and wind direction which means that wave action generated by northwesterly winds is more likely to accompany the elevated water levels;
- the 'Delft' formulae for longshore transport of gravel was found to give a good estimation of the longshore transport rates in the study area;
- shingle is mobile under low energy wave conditions (Hs $\approx$ 0.2m) perhaps as a result of the inclusion of a significant proportion of sand in the beaches;
- net annual longshore transport of shingle is generally from east to west along the coastline although variations occur due to geomorphological features eg Long Rock;
- extreme events can led to large volumes of beach material being transported alongshore in a short time scale. Under storm conditions, the angle of wave incidence on the beach is more important than wave height in transporting the maximum volume of beach material alongshore;
- climatic anomalies such as periods of time during which winds are dominant from one direction can led to severe erosion problems;
- sediment budgets, based on archived beach profile data can provide an effective tool for assessing transport patterns, provided adequate closure can be obtained.

8.2. Recommendations for Further Research

With respect to the numerical modelling:

- development of the model to account for wave refraction patterns around minor coastal features such as Long Rock;
- development of the model to take into account the effects of currents on sediment transport processes.

With respect to coastal monitoring:

- update the coastal environmental instrumentation to allow digital logging of wind, water level and wave conditions;
- obtain measurements of wave conditions, in particular wave angles, at several locations along the coastline;
- extend the existing beach monitoring programme to include Long Rock and the beaches at Reculver to Minnis Bay and at Seasalter;
- monitor lower foreshore levels since it appears that a high level of erosion is occurring at some localities. This will led to deeper water at the toe of the shingle beaches, and subsequently, higher mobility of beach material due to increased wave activity;

With respect to the mixed composition of the beaches, in particular those which have been recharged with marine-dredged sediments:

- investigate the impact of an increase in the quantity of fine-grained material on the beaches in terms of wave energy dissipation and the formation of 'cliffing';
- determine how the fine-grained fraction in the beaches will impact upon beach slope under the influence of storms.

Finally, with respect to the regional coastal processes:

- assess the potential for coarse-grained material to move between the beaches and nearshore features at the Street and at Long Rock;
- determine the extent to which finer sand-sized material is exchanged between the beaches, the nearshore area and the offshore sediment banks (eg Margate Sands).

References

Ackers P., (1972). Extreme levels arising from meteorological surges. Coastal Engineering 1. p69 - 86.

Admiralty Tide Tables, (1991). Hydrographer of the Navy, Taunton Somerset; vol. 1, 440 p.

Airy, G.B., (1845). On tide and waves. Encycl.Metropolitana, 5. p 241-396.

Al-Mansi, A.M.A., (1990). Wave refraction patterns and sediment transport in Monifieth Bay, Tay Estuary, Scotland. Marine Geology, 91. p299 - 312.

Bagnold, R.A. (1940). Beach formation by waves; some model experiments in a wave tank. Journal Institution of Civil Engineers, 15. p27 - 52.

Bascom, W.N. (1952). The relationship between sand size and beach face slope. Trans. American Geophysical Union 32. p866-874.

Bird, E.C.F., (1996). Beach Management. Wiley: 218p.

Blackman and Graff, (1978). The analysis of annual extreme sea levels at certain ports in southern England. Proceedings Institution of Civil Engineers, 65. p339-357.

Bland, T., (1993). A comparison of the transmitting and aluminium tracing technique. University of Southampton, Department of Oceanography, Bsc. dissertation.

Bluck, B.J., (1967). Sedimentation of beach gravels: Examples from South Wales. Journal of Sedimentary Petrology, 37. pp 128-156.

Bowler, E. (1985). Coastal erosion and sea defence work in the Whitstable Area - A Report. Unpublished 34p

Brampton A.H. and Motyka J.M. (1987). Modelling the plan shape of shingle beaches. Lecture

notes on coastal and estuarine studies, (12), p219-234.

Bray, M., (1990). A geomorphological investigation of the southwest Dorset Coast. A report to Dorset County Council, January 1990, 942 pages.

Bretschneider, C.L. and Reid, R.O., (1953). Change in wave height due to bottom friction, percolation and refraction, 34th Annual Meeting of the American Geophysical Union, 1953.

British Geological Survey, (1990). Sea Bed Sediments and Quaternary Geology, Thames Estuary. (Map).

Caldwell, J.M., (1956). Wave action and sand movement near Anaheim Bay, California, TM-68, U.S. Army, Corps of Engineers, Beach Erosion Board, Washington.

Caldwell, N.E., (1983). Relationship between tracers and background beach material. Journal of Sedimentary Petrology, 51. pp. 1163-1168.

Canterbury City Council, (1984). Report on the Stability of the Coastal Slopes. Unpublished Report, 72p.

Canterbury City Council, (1988). Coastal Management Study. Unpublished Report, 205p.

Canterbury City Council, (1990). Report on Wave Activity at Whitstable Harbour, 1979 - 1990. Unpublished, 108p

Canterbury City Council, (1991). Observations of a newly replenished beach at Tankerton, N. Kent. Unpublished, 38p.

Canterbury City Council, (1992a). Coastal Management Study 2, Research Objectives and Current Progress, Unpublished, 119p

Canterbury City Council, (1992b). Hydraulic investigations for coast protection works - Hampton Pier Avenue. Unpublished, 59p.

Canterbury City Council, (1993a). Coastal Management Study 2, Part 1. Background to the Study. Unpublished, 82p.

Canterbury City Council, (1993b). Coastal Management Study 2, Part 2. Hydraulic Consideration; Wind, Water Levels and Waves. Unpublished, 90p.

Canterbury City Council, (1994a). Coastal Management Study 2, Part 3. Model Validation, Extreme Events and Longshore Transport. Unpublished, 76p

Canterbury City Council, (1994b). Hydraulic investigations for coast protection works - Lane End. Unpublished, 68p.

Canterbury City Council, (1995). Feasibility of shingle beach recycling - Lane End to Hampton Pier. Unpublished, 30p.

Canterbury City Council, (1997). Reculver to Minnis Bay Scheme Strategy Plan. Unpublished, 607p

Carr, A.P., (1971). Experiments on longshore transport and sorting of pebbles: Chesil Beach, England. Journal of Sedimentary Petrology, 41. p1084-1104.

Carr, A.P., (1983). Shingle Beaches: Aspects of their structure and stability. In Shoreline Protection, Proceedings of a conference organised by the Institution of Civil Engineers, London. Thomas Telford Ltd. London, p69 - 76.

Carrier G.F. and Greenspan, H.P., (1958). Water waves of finite amplitude on a sloping beach. Journal Fluid Mechanics, 4. p.97-109.

Carter, R.W.G., (1989). Coastal Environments. Academic Press, London, 617p.

Carter, R.W.G. and Orford, J.D. (1993). Coarse clastic beaches: a discussion of the distinct dynamic and morphosedimentary features. Marine Geology, 60: p377-389.

CERC, (1984). Shore Protection Manual. US Army Corps of Engineers, Visksburg. 2 vols.

Chadwick, A.J., (1987). Sediment dynamics on open shingle beaches. Report on Shoreham Beach Field Measurement Programme. Department of Civil Engineering, Brighton Poly.

Chadwick, A.J., (1989). Field measurements and numerical model verification of coastal shingle transport. BHRA, The Fluid Engineering Centre, Cranfield. Chapter 27, p381-402.

Chadwick, A.J. and Morfett, J., (1993). Hydraulics in Civil and Environmental Engineering, 2nd ed. E & FN Spoon, London. 557pp.

Chao, Y.Y., (1970). An asymptotic evaluation of the wave field near a smooth caustic. Journal Geophysical Research 76. p7401-7408.

Crickmore, M.J., (1976). Tracer techniques for sediment studies. Reprint of paper presented at the Central Water and Power Research Station Diamond Jubilee Symposium, Poona, India. HR Wallingford

CUR, (1987). Manual on artificial beach nourishment. Report no 130, Centre for Civil Engineering Research, Codes and Specifications, The Netherlands. pp195.

Darbyshire, J., (1963). The one-dimensional wave spectrum in the Atlantic Ocean and coastal waters. Ocean Wave Spectra, Report of Conference, Englewood Cliffs: Prentice-Hall, p27-31.

Davidson, M.A., Bird, P.A.D., Bullock, G.N. and Huntley, D.A. (1994). Wave reflection: field measurements, analysis and theoretical developments. Proceedings of Coastal Dynamics, '94. ASCE p642-655.

Dean, R.G., (1974). Evaluation and development of water wave theories for engineering application, Special Report No. 1, CERC. Vicksburg.

del Valle, R., Medina, R. and Losada, M.A., (1993). Dependence of coefficient k on grain size. Journal of Waterway Port Coastal and Ocean Engineering, v119, no. 5, 568-574.

Delft Hydraulics, (1990a). Herne Bay Sea Defences. Unpublished 102pp

Delft Hydraulics, (1990b). Description of Endec Model.(User Manual). Unpublished 78pp

Delft Hydraulics, (1995). Tankerton Foreshore Management Study, Unpublished. 156pp

Diserens, A.P. and Coates, T.T. (1993). UK South Coast Shingle Beach Study: Storm Response of Shingle Beaches. HR Wallingford Report: SR323.

Dobkins and Folk, (1970). Shape Development on Tahiti-Nui. Journal Sedimentary Petrology 40. 1167-1203.

D'Olier, B., (1975). Some Aspects of Late Pliestocene-Holocene drainage of the River Thames in the eastern part of the London Basin. Phil. Transactions of the Royal Society London, p269-277.

Draper, L. (1967) The analysis and presentation of wave data - a plea for uniformity. Proceedings 10th Conference on Coastal Engineering. ASCE. p1-11

Driver, J. (1992). Pressure Type Wave Recorder, User Manual, Unpublished, 26pp.

Dyer, K.R., (1986). Coastal and Estuarine Sediment Dynamics. Wiley-Interscience, Chichester. 342pp.

Evans, A.W. and Hardisty, J., (1989). An experimental investigation of the effect of bedslope and grain pivot angle on the threshold of marine gravel transport. Marine Geology, 89. p163-167.

Fairgrieve, I., (1994). Beach Recharge Specification: A Contractors Opinion. Proceedings of MAFF conference of river and coastal engineers, Loughborough.

Folk, R.L. and Ward, W.C., (1957). Brazos River Bar: A study in the significance of grain size parameters. Journal of Sedimentary Petrology, 27, p3-26.

Frihy, O.E., Fanos, A.M., Khafagy, A.A. and Komar, P.D (1991). Patterns of nearshore sediment transport along the Nile Delta, Egypt. Coastal Engineering, 15. p409-429.

Fuller, R.M. & Randall, R.E., (1988). The Orford Shingles, Suffolk, UK. Classic conflicts in coastline management. Biological Conservation.

Galvin, C.J. (1972). Wave Breaking in Shallow Water. In waves on beaches and resulting sediment transport, Ed. by R.E. Meyer. Academic Press, London, p413 - 465.

Gleason, R., Blackley, M.L. and Carr, A.P., (1975). Beach stability and particle size distribution, Start Bay. Journal of the Geological Society of London, 131, p83-101.

Greensmith, J.T. and Tucker, E.V., (1973). Holocene transgressions and regressions on the Essex coast Outer Thames Estuary. Geologie en Mijnbouw, 52. p193-202.

Greer, M.N. and Madison, O.S., (1978). Longshore sediment transport data: a review. Proceedings of the 16th International Conference on Coastal Engineering, Hamburg, ASCE: p1563-1576.

Guza, R.T. and Inman, D.L., (1975). Edge waves and beach cusps. Journal Geophysical Research. 80. p2997-3012.

Halcrow, (1996). North Kent Shoreline Management Plan, Unpublished. p1006

Harlow D.A., (1980). Sediment Processes, Selsey Bill to Portsmouth and a Coast Protection Strategy for Hayling Island. Ph.D. Thesis. University of Southampton, Department of Civil Engineering. 772p.

Hart, B.S. and Plint, A.G., (1989). Conglomerate shoreface deposits from the Cretaceous Cardium Formation, Alberta, Canada. Proc Coastal Sediments '91. ASCE p949-959

Hasselmann K. et al, (1973). Measurements of wind wave growth and swell decay during the joint North Sea Project (JONSWAP). Deutsch. Hydrogr. Z. Suppl. A, nr. 12. p1-96.

Henderson, G. and Webber, N.B., (1978). Wind-wave relationships for a coastal site in the central English Channel. Estuarine and Coastal Marine Science 9. p29-39

Hjulstrom, F., (1935). Studies of the morphological activity of rivers as illustrated by the river Fyris. Geological Institute of the University of Uppsala 25. p221-528.

Holmes, S.C.A., (1981). Geology of the country around Faversham. Memoirs Geological Survey of Great Britain, Sheet 273. 117pp

Hotta, S. and Mizuguchi, M., (1980). A field study of waves in the surf zone, Coastal Engineering in Japan, 23.

Hurdle D.P. and Stive R.J.H., (1989). Revision of SPM (1984) wave hindcast model to avoid inconsistencies in engineering applications; Coastal Engineering, 12. p 339-351

Hydraulics Research (1981). Sheerness Sea Defence Study, HR Wallingford, 59pp

Hydraulics Research, (1986). Whitstable Sea Defences; Joint Probability and Refraction Studies. HR Wallingford, 86pp

Hydraulics Research, (1993). South coast sea bed mobility study, Technical Report. Ex 2827, 56pp.

Inman, D.L., (1949). Sorting of sediment in light of fluid mechanics. Journal Sedimentary Petrology, 19, p51-70.

Inman, D.L. and Bagnold, R.A., (1963). Littoral processes, The Sea. The earth beneath the sea, Hill, M.N. (ed) Interscience Publ., New York, Vol 3: p529-551

Inman D.L., and Frautschy, J.D., (1966). Littoral processes and the development of shorelines. Proceedings 10th Coastal Engineering Conference, American Society of Civil Engineers p511-536.

Kamphius, J.W., Davis, M.H., Nairn, R.B. and Sayao, O.J., (1986). Calculation of littoral sand transport rate. Coastal Engineering, 10, p1-21.

Kamphius, J.W., (1992). Basics of coastal sediment transport: Basic shore processes: One-dimensional modelling of coastal morphology and 2-D and quasi 3-D modelling of coastal morphology. Lecture notes, Design and Reliability of Coastal Structures, Proceedings of the Short Course attached to 23rd ICCE.

Kemp P.H., (1963). A field study of wave action on natural beaches. 10th IAHR Congress, London.

Kidson, C. and Carr, A.P., (1959). The movement of shingle over the sea bed close inshore. Geophysical Journal, 125. p380-389.

Kidson, C. and Carr, A.P., (1971). Marking beach materials for tracer experiments. In Introduction to coastline development, Ed J.A. Steers. McMillan, London, p69 - 93.

Kidson, C. and Smith, D.B., (1956). Drift experiments with radioactive pebbles. Nature 178. p257.

King, C.A.M., (1961). Depth of disturbance of sand on sea beaches by waves. Journal of Sedimentary Petrology, 21. p131-140.

King, C.A.M., (1972). Beaches and Coasts, Edward Arnold Ltd. London, 570p.

Kirk, R.M., (1980). Mixed sand and gravel beaches: morphology, processes and sediments. Progress in Physical Geography 4. p189-210.

Kobayshi, N., Cox, D.T. and Wurjanto A. (1992). Permeability effects on irregular wave run-up and reflection. Journal of Coastal Research, 7. p127 - 136.

Komar, P.D., (1975). In Nearshore Sediment Dynamics and Sedimentation, Ed. J.R.Hails and A.P. Carr. Wiley, London.

Komar, P.D. (1989). Environmental controls on littoral sand transport. Proceedings of 21st Coastal Engineering Conference ASCE, 1238-1252.

Kraus, N.C. (1985) Field Measurements on vertical mixing of sand in the surf zone. Journal of Sedimentary Petrology, 55. p3-14.

Krumbein, W.C. (1934) Size frequency distribution of sediments. Journal of Sedimentary Petrology, 4. p65-77.

Le Mehaute, B. and Wang, S., (1984) Effects of measurement error on long-term wave statistics. Proceedings 19th Coastal Engineering Conference ASCE. p345-361

Litizin, E. (1974). Sea level Changes. Elsevier, Amsterdam.

Longuet-Higgins, M.S., (1970). Longshore currents generated by oblique incident sea waves. Journal of Geophysical Research, 75. p6790 - 6801.

MAFF, (1993). Flood and Coastal Defence April 1993, Issue 3.

MAFF, (1995). Shoreline Management Plans - A guide for coastal defence authorities. 24pp

MAFF, (1997). Interim Guidance for the Strategic Planning and Appraisal of Flood and Coastal Defence Schemes. 22pp.

Mason, T., Volgaris, G., Simmonds, D.J. and Collins, M.B., (1997). Hydrodynamics and sediment transport on composite (mixed sand / shingle) and sand beaches: a comparison. Proceedings of Coastal Dynamics '97, American Society of Civil Engineers. p48-57.

McDowell, D.M., (1989). A general formula for estimation of the rate of transport of non-cohesive bed-load. Journal Hydraulic Research 27. p355-361.

McFarland, S.M., Whitcombe, L.J. and Collins, M.B. (1994). Recent shingle beach renourishment schemes in the U.K; some preliminary observations. Ocean and Coastal

Management 25: p143 - 149.

McFarland, SM., and Edwards, E.R., (1998a). Development and Implementation of a Coastal Defence Strategy for Reculver, N. Kent. Proceedings International Conference on Coastlines, Structures and Breakwaters '98: p211-222

McFarland, SM., and Edwards, E.R., (1998b). A Scheme strategy plan for Reculver, North Kent. Proceedings 33rd MAFF Conference of river and coastal engineers p 4.2.1-4.2.14.

McLean, R.F. and Kirk, R.M., (1969). Relationships between grain-size, size-sorting, and foreshore slope on mixed sand and shingle beaches. New Zealand Jour. of Geology and Geophysics, 12. p138-155.

Meyers, R.D., (1933). A model of wave action on beaches. University of California: Unpub. MSc. Thesis.

Miles, J.W., (1965). A note on the interaction between surface waves and wind profiles. Journal of Fluid Mechanics. 22. p823-827.

Miles, J.W., (1967). On the generation of surface waves by shear flows. Journal of Fluid Mechanics. 30 p163-175.

Morfett, (1989). The development and calibration of an alongshore shingle transport formula. Journal Hydraulic Research 27. p717-729.

Moss A.J., (1963). The physical nature of sandy and pebbly deposits, Part II. American Journal of Science, 261. p297-343.

Muir-Wood, A.M., (1970). Characteristics of shingle beaches: the solution to some practical problems. Proc. 12th Conf. on Coastal Engineering. p1059-1075.

Muir-Wood, A.M. and Fleming, C.A., (1981). Coastal Hydraulics, 2nd edition., MacMillan Press, London.

Nicholls, R.J., (1985). The stability of the shingle beaches in the eastern half of Christchurch Bay. PhD. Thesis, University of Southampton, Department of Civil Engineering.

Nicholls R.J. and Webber, N.B., (1987). Aluminium Pebble Tracer Experiments on Hurst Castle Spit. Proceedings of Coastal Sediments '87. ASCE.

Nicholls R.J. and Webber, N.B., (1988). Characteristics of shingle beaches with reference to Christchurch Bay, S. England. Proceedings of 21st International Conference on Coastal Engineering. ASCE, p1922-1936.

Nicholls, R.J., and Wright, P., (1991). Longshore transport of pebbles: Experimental estimates of K. Coastal Sediments '91, p920-933.

Open University, (1994). Course text - Waves, Tides and Shallow Water Processes. Pergamon 187pp.

Petrov, A. (1989). The differentiation of material on gravel beaches. Oceanology 29, p208-212

Philips, O.M., (1957). On the generation of waves by turbulent wind. Journal of Fluid Mechanics. 2. p417-445.

Powell, K.A., (1990). Predicting short term profile response for shingle beaches. HR Report SR 219. Wallingford. pp197.

Powell, K.A., (1996).Study of complex coastal processes for a shoreline management plan. Proceedings Institution of Civil Engineers, Municipal Engineer, 115. p28-36.

Prettijohn, C., (1992). Transmitting Pebbles: A new technique for sediment tracer on shingle beaches. Univ. of Southampton, Department of Oceanography, B.Sc. dissertation.

Pugh, D.T. (1987). Tides, Surges and Mean Sea Level. John Wiley.

Pugh and Faull, (1982). Tides, Surges and Mean Sea Level Trends. In Shoreline Protection.

Thomas Telford Ltd, London, p45-55

Pugh, D.T. and Vassie, J.M. (1979). Extreme sea levels from tide and surge probability. Proceedings 16th Coastal Engineering Conference, ASCE. p911-930

Quick, M.C. (1991). Onshore-offshore sediment transport on beaches. Coastal Engineering, 15, p313-332.

Reid, W.J. and Jolliffe, I.P., (1961). Coastal experiments with fluorescent tracers, Dock and Harbour Authority, 41. p341-345.

Resio, D.T. and Vincent, C.L., (1977) Estimation of winds over the Great Lakes. Jour. Waterway, Port, Coastal and Ocean Division, Proc. ASCE, 103. p265.

Reynolds, W.J., (1987). Sediment budget analysis and interpretation. Coastal Sediments '87, p113-124

Richardson, N.M., (1902). An experiment on the movement of a load of brickbats deposited on the Chesil Beach: Proceedings Dorset Natural History and Antiquarian Field. Club. 23. p123-133.

Robert West and Partners, (1993). Sea Defence Works, Minnis Bay to Reculver. Unpublished 145p

Roberts, A.G. and McGown, A., (1987). A coastal area management system as developed for Seasalter-Reculver, North Kent. Proceedings of Institution Civil Engineers, 82. p777 - 797.

Seymore, R.J. and Castel, D., (1990). Episodicity in longshore transport. ASCE. Journal of Waterway, Port, Coastal and Ocean Engineering, 3. p542-5 1

Shiels, A., (1936). Application of similarity principles and turbulence research to bed-load movement. Trans. by Ott, W. and von Uchelen, J.C. Published by Californian Institute of Technology Hydrodynamic Lab. No. 167, 36p.

Schoones, J.S. and Theron, A.K., (1996) Improvement of the most accurate longshore transport formula. Proceedings 25th International Conference on Coastal Engineering, Orlando, ASCE. p3652-3665.

Silvester, R., (1974) Coastal Engineering. Elsevier, Amsterdam, 2 vols, 786p.

Smith, (1988). Bypassing of sand over sand waves and through a sand wave field in the central region of the southern North Sea. In Tide-Influenced Sedimentary Environments and Facies. D.Reidel.

So, C.L. (1967). Some coastal changes between Whitstable and Reculver, Kent. Proceedings Geological Association, 77. 475-490

Soulsby, R. (1997). Dynamics of Marine Sands. Thomas Telford London. p249

Stapelton, K.R., Mason, T. and Coates, T.T., (1999). Sub-tidal resolution of beach profiles on a macro-tidal shingle beach. Proceedings Coastal Sediments '99. p885-893.

Stapor, F.W., (1971). Sediment budgets on a comparatively low-to-moderate energy coast in northwest Florida. Marine Geology, 10. pM1-M7.

Stapor, F.W., (1983). The cellular nature of littoral drift along the northeast Florida Coast. Marine Geology, 51. p217-37.

Summers, D., (1978). The East Coast Floods. David and Charles, Publishers Ltd., Newton Abbot, 176p.

Sunamura T. and Horikawa, K., (1974). Two Dimensional Beach transformation due to waves, Proceedings 14th Conference on Coastal Engineering, 2.

Suthons, C.T., (1963). Frequency and occurrence of abnormally high sea levels on the east and south coasts of England. Proceedings of the Institution of Civil Engineers, p443 - 449.

Sverdrup, H.U. and Munk, W.H., (1947). Wind, sea and swell theory of relationships in forecasting. Hydrogical. Office Publication 601. Hydrogical Office U.S. Navy.

Teukolsky (1992). Fourier analysis. In Numerical Recipes, The Art of Scientific Computing (Fortran Version), William H. Press, Brian P. Flannery, Saula A. Teukolsky William T.Vetterling, 1992 702pp

Thompson, E.F. and Seelig, W.N., (1984). High wave grouping in shallow water. Journal Waterway, Port, Coastal and Ocean Division, ASCE.

Thorne, P.D., Williams, J.J. and Heathershaw, A.D., (1989). Measurements of turbulence in the benthic boundary layer over a gravel bed. Sedimentology 36. p959-971.

Tucker, M.J., (1963). Analysis of records of sea waves. Proceedings Institution of Civil Engineers, 26. p305- 316.

van der Meer, J.W., (1988). Rock slopes and gravel beaches under wave attack. Delft Hydraulics Communication No. 396.

van der Meer, J.W., (1990). Static and dynamic stability of loose material. Coastal Protection, Balkema. p157-195.

van Hijum, E. and Pilarczyk, K.W. (1982). Equilibrium profile and longshore transport of coarse material under regular and irregular wave attack. Delft Hydraulics Laboratory, Publication No. 274.

van Hijum, E. (1974). Equilibrium profiles of coarse material under wave attack. Proceedings 14th Conf on Coastal Engineering, 2.

Van Wellen, E., Chadwick, A.J. and Mason, T. (1999). A review and assessment of longshore sediment transport equations for coarse-grained beaches. (submitted to Coastal Engineering)

Vincent, C.E., (1979). Longshore sand transport rates - a simple model for the East Anglian

Coast. Coastal Engineering, 3. p113-136.

Wentworth, C.K., (1922). A scale of grade and class terms for clastic sediments. Journal Geology, 30. p377-392.

Whitcombe, L.J. (1995). Sediment Transport Processes with particular reference to Hayling Island. Unpublished PhD Thesis, University of Southampton, 370p.

Williams, J., Thorne, P.D. and Heathershaw, A.D., (1989). Comparisons between acoustic measurements and predictions of the bedload transport of marine gravels. Sedimentology 36. p973-979.

WMO (World Meteorological Organisation), (1988). Guide to Wave Analysis and Forecasting, WMO, No. 702, 178p.

Workman, M., (1993). The practical use of transmitting pebbles as tracers for the calculation of littoral drift rates - An assessment: Whitstable, Kent. University of Southampton, Department of Oceanography, B.Sc. dissertation.

Wright, P., (1982). Aspects of the Coastal Dynamics of Poole and Christchurch Bays. Ph.D. thesis, Department of Civil Engineering University of Southampton.

Wright P., Cross J.S. and Webber, N.B., (1978). Shingle tracing by a new technique. Proceedings 16th International Conference on Coastal Engineering.

Wright L.D. and Short, A.D. (1983). In Handbook of Coastal Processes and Erosion, Ed P.D. Komar. p35-64. CRC Press, Boca Raton.

Zenkovich, V.P., (1967). Processes of coastal development. Edinburgh: Oliver and Boyd.

SOUTHAMPTON UNIVERSITY LIBRARY

USER'S DECLARATION

AUTHOR: McFARLAND, STEPHEN M. TITLE: FACTORS CONTROLLING THE MOBILITY OF SHINGLE BEACHES, WITH PARTICULAR REFERENCE TO THE NORTH KENT COAST DATE: 1999

I undertake not to reproduce this thesis, or any substantial portion of it, or to quote extensively from it without first obtaining the permission, in writing, of the Librarian of the University of Southampton.

To be signed by each user of this thesis

DATE	SIGNATURE	ADDRESS